

Characterization of mutualistic plant-fungus interactions and the participating fungal chemical mediators

Dissertation

zur Erlangung des akademischen Grades
„doctor rerum naturalium“ (Dr. rer. nat.)



seit 1558

vorgelegt dem
Rat der Fakultät für Biowissenschaften
der Friedrich-Schiller-Universität Jena

von Master of Science Yu-Heng Tseng
geboren am 15.10.1991 in Kaohsiung, Taiwan

Gutachter:

1. Prof. Dr. Ralf Oelmüller, Friedrich-Schiller-Universität Jena, Jena, Germany
2. Prof. Dr. Jan Schirawski, Friedrich-Schiller-Universität Jena, Jena, Germany
3. Prof. Dr. Thorsten Hamann, Norwegian University of Science and Technology, Gløshaugen, Norway

Datum der Verteidigung: 26.09.2022

Table of Contents

Abbreviations	i
Summary	1
Zusammenfassung	3
1. General introduction	5
1.1 Beneficial effects of plant growth-promoting microbes	5
1.1.1 Nitrogen nutrition	6
1.1.2 Phosphorus nutrition	7
1.1.3. Sulfur nutrition.....	7
1.1.4 Phytohormone regulation.....	8
1.1.5 Antioxidant	9
1.1.6 Osmoregulators.....	10
1.1.7 Biotic stress.....	10
1.2 Chemical mediators in plant-microbe interaction	11
1.2.1 Microbial-associated molecular patterns	11
1.2.2 Effectors.....	11
1.2.3 Damage-associated molecular patterns.....	12
1.2.4 Volatile organic compounds	13
2. Objectives	15
3. Manuscript overview	17
3.1 Manuscript 1	17
3.2 Manuscript 2	21
3.3 Manuscript 3	25
3.4 Manuscript 4	28
3.5 Manuscript 5	31
4. Manuscripts	34
4.1 Manuscript 1	34
4.2 Manuscript 2	61
4.3 Manuscript 3	79
4.4 Manuscript 4	94
4.5 Manuscript 5	128
5. Unpublished Results	180
5.1 Supplemental experiment for Manuscript 1	180
6. General discussion	183
6.1 The new <i>Trichoderma</i> strain promoted plant fitness against pathogens	183
6.2 Novel elicitors from the fungal cell wall material triggered calcium response	184
6.3 Environmental factors affected the growth-promotion effect by <i>Trichoderma</i>	184
6.4 Secretome provided new insight into the dynamics of symbiosis under different salt concentrations	185
6.5 Environmental factors shape the plant- <i>Trichoderma</i> interaction	186
6.6 Effect of <i>M. hyalina</i> VOCs on plant	187
6.7 Incorporation pathway of S-containing VOCs into plant metabolism	188
6.8 Synthetic pathway of S-containing VOCs in microbes.....	188
6.9 Receptor perception of chemical mediators.....	189

6.10 Lectin receptor-like kinases (LecRLKs)	190
6.11 Malectin/malectin-like domain receptor kinases (MD-/MLD-RLKs)	190
6.12 Conclusion and future perspectives	192
7. References	194
8. Curriculum Vitae	217
9. Acknowledgenemt	220
10. Eigenständigkeitserklärung	221

Abbreviations

[Ca ²⁺] _{cyt}	cytoplasmic calcium
ABA	abscisic acid
ACC	1-aminocyclopropane-1-carboxylate
AM	arbuscular mycorrhiza
AMF	arbuscular mycorrhiza fungi
APX	ascorbate peroxidase
ATP	adenosine triphosphate
BCA	biological control agent
BNF	biological nitrogen fixation
CAT	catalase
CBM	carbohydrate-binding modules
CDPKs	calcium-dependent protein kinases
COM	cellooligomer
CORK1	cellooligomer receptor kinase 1
CSC	cellulose synthase complex
CT	cellotriase
CWDEs	cell-wall degrading enzymes
CWI	cell wall integrity
CWP	cell wall preparation
DADS	diallyl disulfide
DMDS	dimethyl disulfide
DMS	dimethyl sulfide
DP	degree of polymerization
EF-Tu	elongation factor Tu
EGF	epidermal growth factor
EMS	ethyl methanesulfonate
ER	endoplasmic reticulum
ET	ethylene
ETI	effector-triggered immunity
GA	gibberellin
GC-MS	gas chromatography-mass spectrometry
GSH	glutathione
GSLs	glucosinolates

GSSG	glutathione disulfide
GST	glutathione transferase
GWAS	genome-wide association study
HG	homogalacturonan
HR	hypersensitive response
IAA	indole-acetic acid
IMPRS	International Max Planck Research School
ISR	induced systemic resistance
ITC	isothermal titration calorimetry
JA	jasmonic acid
JA-Ile	JA-isoleucine
K	potassium
LCOs	lipo-chitooligosaccharides
LecRLKs	lectin receptor-like kinases
LPS	lipopolysaccharides
LRRs	leucine-rich repeats
LYKs	LysM-RLKs
LysM	lysine motif
MAMPs	microbial-associated molecular patterns
MAPKs	mitogen-activated protein kinases
MD-RLKs	malectin domain receptor kinases
MeJA	methyl jasmonate
MeSA	methysalicylate
MLD-RLKs	malectin-like domain receptor kinases
MPI-CE	Max Planck Institute for Chemical Ecology
N	nitrogen
NFRs	nod factor receptors
NLR	nucleotide binding, leucine-rich repeat
Nod factors	nodulation factors
NSAPs	non-specific acid phosphatases
OASTLs	O-acetylserine(thiol)lyases
OBPs	odorant-binding proteins
OGs	oligogalacturonides
P	phosphate
PAMPs	pathogen-associated molecular patterns

PGN	peptidoglycan
PGPF	plant growth-promoting fungus
PGPMs	plant growth-promoting microbes
PRRs	pattern recognition receptors
PTI	pattern-triggered immunity
R proteins	resistance proteins
RALF	rapid alkalization factor
RG-I	rhamnose-containing rhamnogalacturonan I
RG-II	rhamnogalacturonan II
RLKs	receptor-like kinases
RLPs	receptor-like proteins
ROS	reactive oxygen species
S	sulfur
SA	salicylic acid
SAR	systemic acquired resistance
SOD	superoxide dismutase
SPR	surface plasmon resonance
SYMRK	symbiosis receptor-like kinase
TMTM	tris(methylthio)methane
TMV	tobacco mosaic virus
VOCs	volatile organic compounds

Summary

Beneficial microbes are indispensable for environment and agriculture. They provide plants with more accessible nutrients and protect them from pathogen infection. To understand how plants and microbes communicate, it is important to identify the chemical mediators and to characterize their physiological functions. This knowledge will provide us with better strategies for modern agriculture. In this thesis, the interaction between *Arabidopsis thaliana* plants and a *Trichoderma* species, *Mortierella hyalina*, and *Piriformospora indica* was investigated.

Trichoderma species are widely applied as biological control agent (BCA) to enhance plant resistance to pathogens. I characterized a novel *Trichoderma* strain and showed that it protects *A. thaliana* and *Nicotiana attenuata* seedlings from infection by the pathogenic fungus *Alternaria brassicicola*, by restricting root colonization and hyphal spread. Arbuscular mycorrhiza (AM) formation was not affected in *N. attenuata* roots. Furthermore, the *Trichoderma* strain promoted growth of its hosts in soil and media with sufficient nutrients. Under phosphate (P) deficiency condition, it initially provided P to *Arabidopsis* seedlings which diminished their P stress. During later stages, I observed a massive propagation of the fungus in the entire seedling under P, and salt stress indicating a transition from a beneficial to a more saprophytic lifestyle. To restrict sugar loss from the apoplastic root space to the fungus under P stress, the host down-regulates the genes for the phloem sucrose exporters SWEET11 and -12, and up-regulates those for SUC1 and SWEET2 which transports sucrose from the apoplast to the cytoplasm and vacuole of the root cells. Under salt stress, the antioxidant enzyme activities in the host were reduced in the presence of the fungus. Analyses of the fungal and plant secretomes demonstrated that the host has to invest more in defense to restrict hyphal propagation with increasing salt stress. From the fungal cell wall, potential novel chemical elicitors were found to induce these responses *via* cytoplasmic calcium ($[Ca^{2+}]_{\text{cyt}}$) elevation in the host cells. In conclusion, I characterized a novel *Trichoderma* strain with novel features in its interaction with host plants. The results will be helpful for its potential agricultural application.

The plant growth-promoting fungus *Mortierella hyalina* produced a garlic-like smell. Gas chromatography-mass spectrometry (GC-MS) analysis of the headspace identified the sulfur (S)-containing compound tris(methylthio)methane (TMTM) as the major component (>95%). TMTM was incorporated into plant S metabolism, reduced the expression of genes for sulfur deficiency response (*SDI1* and *SDI2*), prevented breakdown of sulfur-containing metabolites such as glucosinolates (GSLs) and glutathione (GSH), and sustained plant growth under S limitation.

Piriformospora indica, a well-studied plant growth-promoting fungus (PGPF), releases cellotriose (CT) from the hyphae. CT is a celooligomer (COM), which is also generated during cellulose degradation in the plant cell wall. COMs (n= 2-7) trigger $[Ca^{2+}]_{\text{cyt}}$ elevation in root cells,

which informs the cell about the integrity of its wall. To identify COM perception or signalling compounds, an ethyl methanesulfonate (EMS) population with the calcium sensor aequorin in pMAQ background was screened for mutants impaired in their $[Ca^{2+}]_{cyt}$ response. I discovered CORK1 (CelloOligomer Receptor Kinase 1), a putative COM receptor in *Arabidopsis*, which contains leucine-rich repeats (LRRs), a malectin and a receptor kinase domain. The *cork1* mutants did not show $[Ca^{2+}]_{cyt}$ elevation, reactive oxygen species (ROS) production and *WRKY30/WRKY40* up-regulation upon COM application, other malectin-domain containing proteins in *Arabidopsis* do not compensate the *cork1* mutation. With a protoplast luciferase assay, I identified two conserved phenylalanine residues in the malectin domain which are essential for COM-induced signaling. Through transcriptomic and phosphoproteomic analysis, I unveiled the COM-regulated genes involved in tryptophan and secondary metabolite biosynthesis, as well as early phosphorylation targets including proteins belonging to the cell wall synthesis complex.

Zusammenfassung

Nützliche Mikroben sind für Umwelt und Landwirtschaft unverzichtbar. Sie versorgen die Pflanzen mit besser zugänglichen Nährstoffen und schützen sie vor einer Infektion mit Krankheitserregern. Um zu verstehen, wie Pflanzen und Mikroben kommunizieren, ist es wichtig chemische Mediatoren zu identifizieren und ihre physiologischen Funktionen in der Interaktion zu charakterisieren. Dieses Wissen wird uns bessere Strategien für die moderne ökologische Landwirtschaft liefern. In dieser Arbeit wurde die Interaktion zwischen der Pflanze *Arabidopsis thaliana* und freundlichen Pilzen, einer *Trichoderma*-Species, *Mortierella hyalina* und *Piriformospora indica* untersucht.

Trichoderma-Species werden häufig als biologisches Kontrollmittel verwendet, um die Pflanzenresistenz gegen Krankheitserreger zu erhöhen. In meiner Arbeit habe ich einen neu isolierten *Trichoderma*-Stamm charakterisiert und gezeigt, dass er *A. thaliana*- und *Nicotiana attenuata*-Keimlinge vor einer Infektion durch den pathogenen Pilz *Alternaria brassicicola* schützt, indem er die Wurzelbesiedelung und Hyphenausbreitung einschränkt. Die Ausbildung der arbuskulären Mykorrhiza (AM) war bei *N. attenuata* Wurzeln nicht negativ beeinflusst. Darüber hinaus förderte der *Trichoderma*-Stamm das Wachstum seiner Wirte in Böden und Medien mit ausreichend Nährstoffen. Unter Phosphat (P)-Mangelbedingung lieferte es zunächst P an *Arabidopsis*-Keimlinge, was ihren P-Stress verringerte. In späteren Stadien beobachtete ich eine massive Vermehrung des Pilzes im gesamten Keimling unter P- und Salzstress, was auf einen Übergang von einer symbiotischen zu einer eher saprophytischen Lebensweise hindeutete. Es zeigte sich, dass der Wirt die Gene für die Phloem-Saccharose-Exporter SWEET11 und -12 herunterreguliert, um den Zuckerverlust aus dem apoplastischen Wurzelraum an den Pilz unter P-Stress zu begrenzen. Die Gene für SUC1 und SWEET2 werden dabei gleichzeitig hochreguliert, um Saccharose vom Apoplasten zum Zytoplasma und in die Vakuole der Wurzelzellen zu transportieren. Unter Salzstress waren auch die antioxidativen Enzymaktivitäten im Wirt in Gegenwart des Pilzes reduziert. Analysen der Pilz- und Pflanzensekretome zeigten, dass der Wirt bei zunehmendem Salzstress mehr in die Abwehr investieren muss, um die Hyphenvermehrung einzuschränken. Die Pilzzellwand enthält potenzielle neue chemische Mediatoren, die diese Reaktionen über eine Erhöhung des zytoplasmatischen Calciumlevels ($[Ca^{2+}]_{cyt}$) in den Wirtszellen induzieren können. Zusammenfassend habe ich einen neuen *Trichoderma*-Stamm mit neuartigen Eigenschaften in seiner Interaktion mit Wirtspflanzen charakterisiert. Die Ergebnisse werden für eine potenzielle landwirtschaftliche Anwendung hilfreich sein.

Der pflanzenwachstumsfördernde Pilz *Mortierella hyalina* produzierte einen Knoblauch-ähnlichen Geruch. Analysen mit Hilfe der Gaschromatographie-Massenspektrometrie (GC-MS) identifizierten

die Schwefel (S)-enthaltende Verbindung Tris(methylthio)methan (TMTM) als Hauptkomponente (>95%) des Geruchsstoffprofils. Ich konnte zeigen, dass TMTM in den S-Stoffwechsel der Pflanze eingebaut wurde und die Expression von Genen für die Reaktion auf Schwefelmangel (*SDI1* und *SDI2*) reduzieren konnte, gleichzeitig verhinderte TMTM Applikation den Abbau von schwefelhaltigen Metaboliten wie Glucosinolaten und Glutathion und unterstützte das Pflanzenwachstum unter S-Limitierung.

Piriformospora indica, ein gut untersuchter pflanzenwachstumsfördernder Pilz, setzt Cellotriose (CT) aus den Hyphen frei. CT ist ein Cellooligomer (COM), das auch beim Celluloseabbau in der Pflanzenzellwand entsteht. COMs (n= 2-7) lösen eine $[Ca^{2+}]_{cyt}$ -Erhöhung in Wurzelzellen aus, die die Zelle über die Integrität ihrer Wand informiert. Um COM-Wahrnehmungs- oder Signalkomponenten zu identifizieren, wurde eine Ethylmethansulfonat-Population mit dem cytosolischen Calciumsensor Aequorin nach Mutanten gescreent, die in ihrer $[Ca^{2+}]_{cyt}$ -Antwort beeinträchtigt sind. Ich entdeckte CORK1 (CelloOligomer Receptor Kinase 1), einen mutmaßlichen COM-Rezeptor in *Arabidopsis*, der leucinreiche Wiederholungssequenzen (LRRs), eine Malectin- und eine Rezeptor-Kinase-Domäne enthält. Da die *cork1*-Mutanten keine $[Ca^{2+}]_{cyt}$ -Erhöhung, Produktion reaktiver Sauerstoffspezies und *WRKY30/WRKY40*-Hochregulierung nach COM-Applikation zeigten, kompensieren andere Malectin-Domänen enthaltende Proteine in *Arabidopsis* die *cork1*-Mutation nicht. Mit einem Protoplasten-Luciferase-Assay konnte ich zwei konservierte Phenylalaninreste in der Malecindomäne identifizieren, die für die COM-induzierte Signalübertragung essentiell sind. Durch transskriptomische und phosphoproteomische Analysen identifizierte ich COM-regulierten Gene, die an der Biosynthese von Tryptophan und sekundären Metaboliten beteiligt sind, sowie frühe Phosphorylierungsziele, einschließlich Proteine, die zum Zellwandsynthesekomplex gehören.

1. General introduction

Over the past decades, the production of chemical fertilizers, pesticides and antimicrobial products by agricultural companies has dramatically increased. However, this strategy may no longer support the ever-growing population. Therefore, it is necessary to develop a more sustainable way to provide food.

In their natural habitat, plants interact with microbes in the soil. A straight forward method is to look at microorganisms which form mutualistic interactions with plants, as they offer novel tools to optimize crop production in various environments. For example, by analyzing the microbial communities of crop plant roots in local soil samples, we can gain a better understanding on how crop growth can be promoted by microbes in the rhizosphere. Isolation of plant growth-promoting microbes (PGPMs) from soil sample and characterization of their physiological effects on plants provide an alternative strategy to optimize crops yield and food production under different environmental conditions. Besides physical interaction of the symbionts and exchange of nutrients and water, the communication between the partners is based on chemical mediators, which affect the physiology and development of the two symbionts and fine-tune the symbiosis. Understanding the mechanism behind this communication system can identify key targets or signaling compounds which could be the basis to design new or more sustainable chemical compounds for agricultural applications.

As sessile organisms, plants developed a plethora of methods to interact with other plants, animals and microorganisms in their neighborhood to adapt to changing environmental conditions and stress factors. In the following paragraphs, I will first describe the key features of PGPMs, how they promote plant growth and reduce biotic and abiotic stress. In the second part, the chemical mediators establishing/shaping the interaction will be described, focusing on plant perception systems of these elicitors and their physiological effects on plant growth, development and defense.

1.1 Beneficial effects of plant growth-promoting microbes

Modern agriculture relies heavily on fertilizers, pesticides and antimicrobial chemicals. They provide plants with essential nutrients for proper growth and development, and protect them from pathogen infection or feeding by insects. However, in the long run, the excessive use of fertilizers will contaminate the soil and alter the rhizosphere communities with detrimental environmental impact (Horrigan et al., 2002; Savcı, 2012). Likewise, the use of pesticides and antimicrobial chemicals may decrease the biodiversity in the environment, and increases resistance against the applied chemicals (Meena et al., 2020). As a result, the soil may not be suitable for sufficient crop growth any more, causing drastic problems for local and worldwide food production.

In the rhizosphere, plant growth-promoting microbes (PGPMs) are important symbionts which enhance plant growth, and protect them against biotic and abiotic stress. They possess the ability to fix nitrogen from the atmosphere, and are able to solubilize soil minerals and provide essential nutrients such as nitrogen (N), phosphate (P) and sulfur (S) to their hosts (Lopes et al., 2021). PGPMs can increase plant growth by influencing the phytohormone levels in plants, such as increasing auxin or gibberellin (GA) and decreasing the ethylene (ET) levels (Khan et al., 2020). PGPMs can also induce systemic defense responses in plants by modulating salicylic acid (SA) and jasmonic acid (JA) levels, or directly combat pathogens in the rhizosphere (Khan et al., 2020; Woo et al., 2014). In some cases, PGPMs can configure osmoprotectants and antioxidants in their host plants, thereby helping plants to resist stress (Lopes et al., 2021). Establishment of such interactions has important impact on agriculture, and understanding of the molecular and chemical basis of these interactions might contribute to the goal to replace chemical fertilizers in agriculture.

1.1.1 Nitrogen nutrition

Although the atmosphere is abundant in nitrogen gas (N_2), it must be converted to ammonia (NH_3) for incorporation into plants. Diazotrophs are microbes which can perform biological nitrogen fixation (BNF), converting N_2 into NH_3 (Gupta et al., 2019; Raymond et al., 2004). They possess nitrogenases to carry out the fixation reaction, which provide plants with nitrogen from the unlimited air N_2 source (Shin et al., 2016). Nitrogenases are comprised of a larger heterotetrameric molybdenum-iron (MoFe) co-factor, and a smaller homodimeric iron (Fe) protein. Apart from the canonical FeMo co-factor, there exist nitrogenases with vanadium-iron (VFe) and iron-iron (FeFe) co-factors (Bellenger et al., 2020; Harris et al., 2019). The Fe protein functions as an ATP-dependent electron donor, providing the MoFe protein with electrons for N_2 reduction (Seefeldt et al., 2009). This process is very sensitive to oxygen, thus proper sequestration is necessary for optimal nitrogen fixation (Bellenger et al., 2020; Seefeldt et al., 2009).

Several PGPMs improve N nutrition in their host plants. *Azospirillum* is a genus of aerobic, gram-negative bacteria. Inoculation of *A. brasilense* increases potassium (K) and N accumulation in shoot, and the bacterium also increases grain yield in different crops (Garcia de Salamone et al., 1996; Boleta et al., 2020; Bashan and de-Bashan, 2010; Filho et al., 2017). Rhizobia are also extensively studied due to their nitrogen-fixation capacity (Lindström and Mousavi, 2020). They interact with legumes (*Fabaceae*), such as common beans (Hailu Gunnabo et al., 2021; Wekesa et al., 2021). Once the symbiosis is initiated, the infected tissue develops a specialized organ called nodules. In this scenario, rhizobia are well-supplied with carbon in an oxygen-controlled environment, allowing them to efficiently fix N by the nitrogenase, and supply it to their hosts (Rutten and Poole, 2019; Herridge et al., 2008; Day et al., 2001). Colonization of roots by beneficial fungi such as arbuscular mycorrhiza

fungi (AMF) and nitrogen-fixing bacteria exerts synergistic growth-promoting effect on host plants (Mikola, 1986; Bauer et al., 2012; Júnior et al., 2017), although the mechanism is unknown at present.

1.1.2 Phosphorus nutrition

Phosphorus (P) is an essential building block for cellular components such as nucleic acids and cell membranes, and is involved in various cellular processes, including photosynthesis and the energy carrier adenosine triphosphate (ATP). In soil, most of the P is insoluble, which renders it unavailable for plant assimilation. However, microbes, including PGPMs, can enrich the soluble P source accessible for plants by releasing PO_4^{3-} , HPO_4^{2-} , and H_2PO_4^- ions from insoluble PO_4^{3-} (Tian et al., 2021). One strategy is to secrete organic acids to reduce soil pH (Zhao et al., 2014). Acidification by proton release in exchange of the cations from the insoluble P is another strategy (Sharma et al., 2013). To remobilize P from organic compounds, microbes utilize the non-specific acid phosphatases (NSAPs) to dephosphorylate the phosphorester or phosphoanhydride bonds (Nannipieri et al., 2011).

Phosphate solubilization often results in plant growth promotion. *Bacillus* sp., *Pseudomonas* sp. and *Rhizobium* sp., are known bacteria to solubilize phosphate, although the capability varies across species (Wekesa et al., 2021; Zaidi et al., 2010; Turan et al., 2006). Many fungal species also exhibit phosphate solubilization ability, including *Trichoderma* sp., *Penicillium* sp., *Aspergillus* sp., *Mucor* sp., *Rhizopus* sp and *Serendipita (Piriformospora) indica* (abbreviated as *P. indica* in the following text; Kumar et al., 2011; Bakshi et al., 2015; Bononi et al., 2020; Jiang et al., 2020). Notable examples are AMF. They can not only solubilize P, but also enhance P uptake into plants by releasing organic anions or proton, which contributes to the promotion of plant growth and yield (Kobae, 2019; Gao et al., 2020; Zaidi et al., 2010). In addition, AMF colonized roots recruit phosphatase-producing bacteria, which further improves P nutrition in the host plant (Zhang et al., 2018b).

1.1.3. Sulfur nutrition

After nitrogen, phosphorus and potassium, sulfur (S) is the fourth major macromolecule for plant nutrition. It can be found not only in primary metabolites such as proteins and Fe-S co-factors necessary for electron transport and nutrient assimilation (Raven et al., 1999; Lancaster et al., 1979; Krueger and Siegel, 1982), but also in secondary metabolites important for pathogen and herbivore defence, such as glucosinolates (Bakhtiari and Rasmann, 2020; Halkier and Gershenzon, 2006; Ting et al., 2020; Wittstock et al., 2016).

Although plants are able to incorporate SO_2 gas from the atmosphere, the major source of S remains in the soil in the form of sulfate (SO_4^{2-}). Microbial oxidation of elemental sulfur was first described in 1877, and the first S-oxidizing bacteria *Thiobacillus denitrificans* and *T. thioparus* were

later isolated (Beijerinck, 1904; Lipman et al., 1916; Waksman and Joffe, 1922). Besides bacteria, fungi are also able to produce sulfate by activating arylsulfatase activity, especially under S-limiting conditions (Fitzgerald, 1976; Marzluf, 1997; Omar and Abd-Alla, 2000; Baum and Hryniewicz, 2006). AMF also increase S uptake in maize, clover and tomato (Gray and Gerdemann, 1973; Cavagnaro et al., 2006). They enhance the expression of sulfate transporter genes in plants, which leads to improved S nutrition under S deficient condition (Giovannetti et al., 2014).

Another route for S uptake is through volatile organic compounds (VOCs) released by microorganisms. *Bacillus* spp. B55 is capable of producing dimethyl disulfide (DMDS). This compound can sustain plant growth and increase root branching under S deficiency (Meldau et al., 2013). Various fungi also produce S-containing volatiles that may influence S nutrition in plants (Splivallo et al., 2007; Seifert and King, 1982; Nemcovic et al., 2008; Schalchli et al., 2011; Larsen, 1998; Dickschat, 2017; Citron et al., 2012; Birkinshaw and Chaplen, 1955; Brock et al., 2011). However, the molecular mechanism of their incorporation into plant metabolism is not yet clear.

1.1.4 Phytohormone regulation

Distribution of phytohormones plays an important role in plant development and growth regulation. For instance, auxin and GA promote plant growth, while JA, SA and ET are primarily involved in pathogen defense (Kamiya, 2009). The distribution of phytohormones differs in different growth stages, plant organs and tissues, responses to environmental conditions and interactions with microbes (Saidi and Hajibarat, 2021; Pozo et al., 2015).

One mechanism PGPMs enhance plant growth is by depositing auxin or auxin precursors to colonized roots. Rhizobia, AMF and *P. indica* are all able to produce auxin precursors, which promote root growth (Nadzieja et al., 2018; Wang et al., 2021; Meents et al., 2019; Sirrenberg et al., 2007). In case of drought stress, AMF-produced auxin can maintain trifoliolate orange (*Poncirus trifoliata*) growth (Liu et al., 2018). Under moderate soil drying, treatment of *P. indica* enhanced auxin level in rice roots and recruited more growth-promoting bacteria *Bacillus cereus* in the rice rhizosphere (Xu et al., 2021). Interestingly, beneficial fungi possess higher amount of IAA and lower or undetectable amount of abscisic acid (ABA) in their mycelium, while pathogenic fungi such as *Alternaria brassicicola* and *Verticillium dahliae* contain undetectable IAA and high ABA levels (Meents et al., 2019).

GAs are tetracyclic diterpenoid acids which are required to break seed dormancy, and involved in root growth (Ubeda-Tomás et al., 2008; Ogawa et al., 2003; Shu et al., 2016). Rhizobia have been reported to stimulate root elongation by GA production (Dobert et al., 1992). In rice, a native *Rhizobium* strain was found to produce both GA and auxin, improving plant growth and yield (Yanni et al., 2001). For beneficial fungi, the endophytic fungus *P. indica* induces the growth and

early flowering on the medical plant *Coleus forskohlii* by up-regulating core flowering genes and GA-related genes, including *RGAI*, *AGL24*, *GA3*, and *MYB5* (Pan et al., 2017; Kim et al., 2017). Likewise, AMF induce GA biosynthetic genes upon colonization in rice (Gümil et al., 2005). However, there are reports showing that GAs also act as negative regulator for AMF colonization (Yu et al., 2014; Floss et al., 2013). This demonstrates the importance of GA for AMF-mediated plant growth is difficult to evaluate.

JA and SA are involved in the systemic acquired resistance (SAR) and induced systemic resistance (ISR). While SAR is generally induced by pathogens and requires SA, ISR is triggered by beneficial microbes and is mediated by JA (Métraux et al., 1990; Gaffney et al., 1993; Vlot et al., 2021; Pieterse et al., 2009). Several reports have shown that root colonization by rhizobia up-regulates ISR through JA signaling, and enhances pathogen resistance of its host plant (Poza et al., 2008; Cartieaux et al., 2003). Colonization by *Trichoderma* species also induces ISR, providing their host plant higher resistance against pathogens (Brotman et al., 2008; Singh et al., 2019).

ET governs various aspects of plant development. Particularly, high ethylene levels result in chlorosis and senescence in leaves, reduced fruit yield, photosynthesis and root development (de Souza et al., 2015; Koukounaras et al., 2006; Özgen et al., 2005). Ethylene production is also observed upon salinity stress and heavy metal stress (Gharbi et al., 2017; Keunen et al., 2016). PGPMs possess ACC-deaminase activity, which converts the ethylene precursor 1-aminocyclopropane-1-carboxylate (ACC) to ammonia and α -ketobutyrate, thereby reducing stress level (Honma and Shimomura, 1978). It has been reported that *Pseudomonas* sp., *Aneurinibacillus aneurinilyticus* and *Paenibacillus* sp. can reduce salinity stress in tomato and beans by applying this strategy (Orozco-Mosqueda et al., 2019; Gupta and Pandey, 2019). Rhizobacteria can also use ACC deaminase to reduce drought stress (Saikia et al., 2018). *Trichoderma longibrachiatum* up-regulates its ACC deaminase activity and, in combination of IAA production, enhances resistant to salinity stress in wheat (Zhang et al., 2019).

1.1.5 Antioxidant

Abiotic stress, such as heat, salinity and heavy metal stress, are the primary cause of crop yield loss (Godoy et al., 2021). The adverse effect from abiotic stress comes from the increase in ROS, including hydrogen peroxide (H_2O_2) and superoxide anion (O_2^- ; Thorpe et al., 2013; Nadarajah, 2020). These ROS species are harmful to plants, as they cause lipid oxidation, damage to proteins and nuclear acids and may eventually lead to cell death (Nouman et al., 2014). To scavenge these ROS species, plants rely on detoxification enzymes such as catalase (CAT), superoxide dismutase (SOD), ascorbate peroxidase (APX) and glutathione transferase (GST), or metabolites such as GSH, ascorbate/dehydroascorbate, carotenoids and phenolic compounds (Gouda et al., 2018; Arora et al., 2020). PGPMs reduce abiotic stress of their host plants by releasing these enzymes or compounds,

and enhance SOD and CAT activity to alleviate salinity and drought stress (Mitra et al., 2021; Li et al., 2019; Kumar Arora et al., 2020).

1.1.6 Osmoregulators

An additional strategy for PGPMs to reduce abiotic stress is to release osmoregulators. Rhizobia are known to produce exopolysaccharides, which form a protective layer of biofilms along the root surface. This layer can retain water for plants, protect them from water or ion loss (Hashem et al., 2019). Other beneficial microbes can produce carbohydrates, lipids, proline and trehalose to regulate the osmotic pressure in the rhizosphere (Van Oosten et al., 2017).

1.1.7 Biotic stress

As mentioned, PGPM colonization often has strong influence on the distribution of JA and SA levels in plants, which make them more resistant to pathogens. *Trichoderma* species are of particular interest due to their strong propensity to protect plants against pathogenic fungi (Grosch et al., 2007; Sánchez-Montesinos et al., 2021). Another mechanism they protect their host plants is by mycoparasitism. They are able to physically penetrate fungal cells or produce metabolites to the pathogens in their surrounding (Brotman et al., 2010; Baiyee et al., 2019). Besides pathogenic fungi, *Trichoderma* species can also target pathogenic nematodes (Poveda et al., 2020). With this outstanding trait against broad spectrum of pathogens, there are more than 200 commercial strains world-wide serving as BCA (Woo et al., 2014).

1.2 Chemical mediators in plant-microbe interaction

To pose an effect on host plants, PGPMs must either possess or release bio-active molecules which directly affect plant growth and development, e.g. phytohormones, enzymes or antioxidants. However, there are numerous metabolites which can indirectly induce physiological responses in plants. For example, the mycellium of some fungal strains does not contain JA or SA, but releases metabolites regulating JA and SA production in root and shoot tissues of the hosts (Vahabi et al., 2013; Meents et al., 2019). In this chapter, the physiological functions of signaling molecules and how they are perceived by plants will be discussed.

1.2.1 Microbial-associated molecular patterns

Detection of the presence of microbes by the host starts with the recognition of conserved microbial molecules. These molecules are known as microbe- (pathogen-) associated molecular patterns (MAMPs/PAMPs). They are usually essential components of the microbes, such as lipochitooligosaccharides (LCOs, component of nodulation (Nod) factors) produced by rhizobia (Schauser et al., 1999; Pan et al., 2018), chitin (Felix et al., 1993; Miya et al., 2007), flagellin (Felix et al., 1999; Gómez-Gómez et al., 2001), elongation factor Tu (EF-Tu; Kunze et al., 2004), peptidoglycan (PGN; Gust et al., 2007; Willmann et al., 2011) and lipopolysaccharides (LPS; Ranf et al., 2015; Newman et al., 1995). Their perception occurs through membrane-localized pattern recognition receptors (PRRs). These PRRs are either receptor-like kinases (RLKs) or receptor-like proteins (RLPs). Both consist of a functional extracellular domain for ligand binding, and single-pass transmembrane domain. While RLKs have an intracellular kinase domain, RLPs often have only a short cytosolic domain (Jamieson et al., 2018).

These PRRs serve as the first-line defense perception system (PTI, Pattern-Triggered Immunity). Upon ligand binding, plant cells experience a fast elevation of $[Ca^{2+}]_{cyt}$ and high level of ROS production (Yu et al., 2017), followed by phosphorylation of mitogen-activated protein kinases (MAPKs) and calcium-dependent protein kinases (CDPKs; Huang et al., 2020; Asai et al., 2002). Depolarization of membrane potential transfers an electric signal from the perception site to neighboring cells or distal tissues for systematic signaling (Yu et al., 2017). Finally, the signaling cascades result in up-regulations of genes such as *WRKY* transcription factors, leading to defense response and restricts the spread of microbes (Huang et al., 2020; Asai et al., 2002).

1.2.2 Effectors

Throughout the evolution of the plant-microbe interaction, microbes have gained the ability to secrete effectors to evade plant immunity for more efficient infection or colonization (Tanaka and Kahmann, 2021; Zhao et al., 2019). Effectors from pathogens have been extensively studied, since

they cause severe crop loss (Xue et al., 2020; Fones et al., 2020). These effectors may affect plant metabolism, or target the host's phytohormone pathways (Plett et al., 2014; Lv et al., 2021; Xian et al., 2020). Beneficial microbes also release effector protein which optimize the symbiosis. Besides promotion of host's growth and strengthening its immune system, this also creates a suitable habitat for the microbe (Akum et al., 2015; Lucke et al., 2020).

Conversely, plants have evolved a system to detect these effectors as a secondary line of defense (ETI, Effector-Triggered Immunity). The gene-for-gene hypothesis was first proposed in the 1940s, which states that individual effector gene products from pathogens interact with R (resistance) proteins in plants (Flor, 1942). The guard model, zig-zag model and decor model were later proposed to explain the complicated interaction between effectors and R proteins (Zipfel and Rathjen, 2008; Zhou and Chai, 2008; Jones and Dangl, 2006; Dangl and Jones, 2001). In any case, the R proteins are known as nucleotide binding, leucine-rich repeat (NLR) proteins, since they possess two conserved domains: nucleotide-binding (NB) and leucine-rich-repeat (LRR) domains, and either a Toll-interleukin 1-like receptor (TIR) or a coiled-coil (CC) domain at the N terminus (Richard et al., 2018; van Wersch and Li, 2019).

ETI usually leads to hypersensitive response (HR), causing programmed cell death (Gao et al., 2017; Zavaliev et al., 2020; Dangl and Jones, 2001). The downstream response by ETI is often similar to PTI, although the magnitude is somehow greater (Peng et al., 2018). ETI is triggered only after perception of effectors, and PTI may trigger higher ROS production during ETI, while transcription of PTI-responsive genes and MAPK3/6 phosphorylation can be enhanced by ETI (Yuan et al., 2021; Ngou et al., 2021). The individual response and cross-talk between PTI and ETI provide immunity to a broad range of microbes.

1.2.3 Damage-associated molecular patterns

Plant cell wall is composed of numerous sugar polymers. The major component is cellulose, which consists of unbranched fiber made of D-glucose with β -(1,4) glycosidic bonds. Hemicellulose, on the other hand, is made of various polysaccharides, containing short branches (Scheller and Ulvskov, 2010; Gibson, 2012). The third component in the cell wall are pectins. They can be categorized into unbranched homogalacturonan (HG), branching rhamnase (Rha)-containing rhamnogalacturonan I (RG-I), and rhamnogalacturonan II (RG-II) with complex composition (Mohnen, 2008; Atmodjo et al., 2013).

These cell wall forms a rigid physical barrier to protect the plant from microbe invasion. Therefore, microbe colonization is initiated by cell-wall degrading enzymes (CWDEs), which cause plant cell damage and release of cellular components (Yang et al., 2021a). These components act as signaling molecules, triggering immune response, and are so-called damage-associated molecular

patterns (DAMPs). Recent studies have shown that fragments from cellulose (cellooligomers), hemicellulose (xyloglucans) and pectins (oligogalacturonides, OGs) can induce immune response in plants. Similar to PTI by MAMPs/PAMPs, DAMPs induce calcium elevation, ROS production and MAPK phosphorylation, though in lower intensity (Johnson et al., 2018; Souza et al., 2017; Claverie et al., 2018; Mérida et al., 2020; Rebaque et al., 2021; Yang et al., 2021a; Hu et al., 2004; Galletti et al., 2011). Up until now, only the receptor for OGs and pectins were discovered (Brutus et al., 2010; Tang et al., 2022). While in rice, β -1,3/1,4-glucans from hemicellulose were shown to bind to OsCERK1 inducing the dimerization of OsCERK1 and the chitin receptor OsCEBiP (Yang et al., 2021a).

1.2.4 Volatile organic compounds

VOCs present another path for plant-microbe interaction. They are small molecules which can diffuse easily throughout the airspace, or permeate through cell membrane (Schulz-Bohm et al., 2017). VOCs produced by microbes belong to different classes of molecules, and their effects range from promoting photosynthesis, adjusting hormone distribution, providing plant nutrition, enhancing abiotic stress to activating systematic resistance against pathogens (Zhang et al., 2007, 2008, 2009). Among the microbial VOCs, DMDS has been extensively studied due to its growth-promoting function by providing plants with sulfur and increasing auxin production (Meldau et al., 2013; Vasseur-Coronado et al., 2021). These characteristics make them a potential candidate for agriculture application (Thomas et al., 2020).

However, the molecular pathway and components for VOC perception are still not completely clear. This is partially due to the fact that the physiological effect from VOCs may be caused by receptor binding at the plasma membrane or in the nucleus, or simply by reacting with other components in the cell. A prominent example of a volatile compound is CO₂. Although it is not strictly defined as VOC, it regulates stomata closure in *Arabidopsis* guard cells through the Slow Anion Channel 1 (SLAC1; Yamamoto et al., 2016; Zhang et al., 2018a). In the nucleus, it was found that the transcriptional co-repressor Topless-like (TPL) protein is able to bind volatile sesquiterpenes (Nagashima et al., 2019).

Another well-known signaling volatile methylsalicylate (MeSA) is produced upon tobacco mosaic virus (TMV) infection. MeSA then can travel to other non-infected leaves and be converted back to SA through salicylic acid-binding protein 2 (SABP2) and MeSA esterase, achieving systematic resistance (Park et al., 2007).

These lead to the new hypothesis proposing the presence of putative odorant-binding proteins (OBPs; Loreto and D'Auria, 2021; Giordano et al., 2021), as shown for the binding proteins for MeSA, methyl jasmonate (MeJA) and sesquiterpenes (Nagashima et al., 2019; Park et al., 2007; Sheard et

al., 2010; Cheong and Choi, 2003). However, more experimental evidence is needed to demonstrate the presence of these OBPs.

2. Objectives

The aim of this study was to investigate the role of chemical mediators from three beneficial fungi in their symbiotic interaction with the model plants *Arabidopsis thaliana* or *Nicotiana attenuata* (cf. **Manuscript 1**).

In the first part of the thesis, I characterized a new *Trichoderma* strain from India by rRNA sequencing and phylogenetic analysis (**Manuscript 1**). The symbiotic interaction of this strain with *A. thaliana* and *N. attenuata* plants was carried out in established co-cultivation systems and assayed at the phytohormone and gene expression levels, by physiological parameters as well as fungal colonisation strategies. Furthermore, we tested whether *Trichoderma* can distinguish between beneficial and pathogenic fungi. Therefore, we analyzed *N. attenuata* plants colonized by the new *Trichoderma* strain after additional exposure to the pathogenic fungus *Alternaria brassicicola*, or arbuscular mycorrhiza fungi, or both. Finally, a chemical compound from the fungal cell wall was investigated for its potential elicitor function. The new strain promoted plant growth in the initial stage. This trait was greatly influenced by different salt concentration and nutrient availability. This led to two more studies in **Manuscript 2** and **Manuscript 3**, in which I investigated whether the benefits for the host were affected by salt and nutrient.

In **Manuscript 2**, we exposed *Trichoderma*-colonized *Arabidopsis* seedlings to extreme P stress. We investigated whether the stress affects root colonisation, the mode of interaction between the two symbionts, and the distribution of photoassimilates between the fungus and the host.

Manuscript 3 compared the secretomes of the *Trichoderma* strain and *Arabidopsis* roots alone or in symbiotic interaction under increasing salt stress conditions. We aimed to identify plant and fungal proteins which are specific for the symbiotic interaction, salt stress and salt concentrations which promote a beneficial interaction between both partners.

The second part of the study focused on the physiological effect of VOCs from the plant growth-promoting fungus (PGPF) *Mortierella hyalina* (Johnson et al., 2019) on *Arabidopsis* (**Manuscript 4**). I investigated whether the fungal VOC promoted growth of *Arabidopsis* seedlings, in particular under S limitation. GC-MS analysis was carried out to determine the major components in the fungal headspace. I investigated whether the volatile participates in the plant S nutrition and how it interferes with the plant S metabolism.

In the third part of this study (**Manuscript 5**), I aimed to understand how celotriose (CT), a cellooligomer (COM) released by *P. indica*, is perceived by root cells. COMs were recently described as novel invasion patterns, which are released by fungi but also generated during the breakdown of cellulose of the plant cell. COMs with 2-7 glucose moieties trigger calcium elevation, ROS production and defence responses in plant (Souza et al., 2017; Johnson et al., 2018). To identify their perception components, a newly-generated EMS population of *Arabidopsis* with the cytosolic calcium sensor

aequorin was screened based on $[Ca^{2+}]_{\text{cyt}}$ elevation upon CT treatment. I identified a mutant with a point mutation in a LRR-malectin receptor kinase, which was further characterized in this thesis. I wanted to confirm its specificity for COM perception, analyze the role of the malectin domain for sugar sensing, investigate whether the receptor kinase induces downstream responses which respond to COM, identify COM-regulated genes and find out the phosphorylation target proteins for CORK1.

3. Manuscript overview

3.1 Manuscript 1

An Endophytic *Trichoderma* Strain Promotes Growth of Its Hosts and Defends Against Pathogen Attack

Authors: Yu-Heng Tseng, Hamid Rouina, Karin Groten, Pijakala Rajani, Alexandra C. U. Furch, Michael Reichelt, Ian T. Baldwin, Karaba N. Nataraja, Ramanan Uma Shaanker, Ralf Oelmüller (2020).

Status: published, *Frontiers in Plant Science*, 11:573670. doi: 10.3389/fpls.2020.573670.

Summary:

The aim of this study was to characterize a *Trichoderma* strain isolated from leaves of *Leuceas aspera*, which stimulated growth and biomass production of several crop species in field studies. Morphological and phylogenetic analysis suggested that it is a new *Trichoderma* strain. It survived on high NaCl and mannitol, and could feed on the pathogenic fungus *Alternaria brassicicola*. The strain colonized the root of *Arabidopsis thaliana* and *Nicotiana attenuata*, and promoted their growth. Moreover, colonized *Arabidopsis* plants were more salt tolerant and better protected against *A. brassicicola* infection. However, the *Trichoderma* strain did not affect arbuscular mycorrhiza formation in *N. attenuata*. These characteristics are important for future agricultural applications.

Y-HT organized the project, performed the experiments, collected the samples and data, analyzed the results, plotted the figures, and wrote up the study. **HR** performed the soil and salt experiments with *Arabidopsis*. **KG** performed the experiments with *Nicotiana*. **PR** isolated the *Trichoderma* strain. **AF** assisted in the microscopy. **MR** measured the phytohormones. **IB**, **KNN**, **RUS**, and **RO** edited the manuscript. **RO** designed the project and revised the manuscript.

Angaben zum Eigenanteil

Formular 1

Manuskript Nr. 1

Titel des Manuskriptes: An Endophytic *Trichoderma* Strain Promotes Growth of Its Hosts and Defends Against Pathogen Attack

Autoren: Yu-Heng Tseng, Hamid Rouina, Karin Groten, Pijakala Rajani, Alexandra C. U. Furch, Michael Reichelt, Ian T. Baldwin, Karaba N. Nataraja, Ramanan Uma Shaanker, Ralf Oelmüller

Bibliographische Informationen: Tseng Y-H, Rouina H, Groten K, Rajani P, Furch ACU, Reichelt M, Baldwin IT, Nataraja KN, Uma Shaanker R and Oelmüller R (2020) An Endophytic *Trichoderma* Strain Promotes Growth of Its Hosts and Defends Against Pathogen Attack. *Front. Plant Sci.* 11:573670. doi: 10.3389/fpls.2020.573670

Der Kandidat / Die Kandidatin ist

Erstautor, Ko-Erstautor, Korresp. Autor, Koautor.

Status: veröffentlicht in „Frontiers in Plant Science“

Anteile (in %) der Autoren / der Autorinnen an der Publikation

Autor/-in	Konzeptionell	Datenanalyse	Experimentell	Verfassen des Manuskriptes	Bereitstellung von Material
Yu-Heng Tseng	40%	60%	70%	75%	0%
Hamid Rouina	5%	15%	10%	5%	0%
Karin Groten	5%	15%	10%	5%	10%
Michael Reichelt	0%	10%	10%	0%	10%
Ralf Oelmüller	50%	0%	0%	15%	80%
Summe	100%	100%	100%	100%	100%

Formular 2

Manuskript Nr. 1

Kurzreferenz: Tseng et al (2020), Front. Plant Sci.

Beitrag des Doktoranden / der Doktorandin

Beitrag des Doktoranden / der Doktorandin zu Abbildungen, die experimentelle Daten wiedergeben (nur für Originalartikel):

Abbildung(en) # 1, 2, 4, 7, S1, S3, S5, Table S1	<input checked="" type="checkbox"/>	100 % (die in dieser Abbildung wiedergegebenen Daten entstammen vollständig experimentellen Arbeiten, die der Kandidat/die Kandidatin durchgeführt hat)
	<input type="checkbox"/>	0 % (die in dieser Abbildung wiedergegebenen Daten basieren ausschließlich auf Arbeiten anderer Koautoren)
	<input type="checkbox"/>	Etwaiger Beitrag des Doktoranden / der Doktorandin zur Abbildung: Kurzbeschreibung des Beitrages:

Abbildung(en) # 3, 5	<input type="checkbox"/>	100 % (die in dieser Abbildung wiedergegebenen Daten entstammen vollständig experimentellen Arbeiten, die der Kandidat/die Kandidatin durchgeführt hat)
	<input type="checkbox"/>	0 % (die in dieser Abbildung wiedergegebenen Daten basieren ausschließlich auf Arbeiten anderer Koautoren)
	<input checked="" type="checkbox"/>	Etwaiger Beitrag des Doktoranden / der Doktorandin zur Abbildung: 30 % Kurzbeschreibung des Beitrages: Plotting data, Statistical analysis

Abbildung(en) # 6	<input type="checkbox"/>	100 % (die in dieser Abbildung wiedergegebenen Daten entstammen vollständig experimentellen Arbeiten, die der Kandidat/die Kandidatin durchgeführt hat)
	<input type="checkbox"/>	0 % (die in dieser Abbildung wiedergegebenen Daten basieren ausschließlich auf Arbeiten anderer Koautoren)
	<input checked="" type="checkbox"/>	Etwaiger Beitrag des Doktoranden / der Doktorandin zur Abbildung: 90 % Kurzbeschreibung des Beitrages: Performing Experiments, Plotting data, Statistical analysis

Abbildung(en) # 8	<input type="checkbox"/>	100 % (die in dieser Abbildung wiedergegebenen Daten entstammen vollständig experimentellen Arbeiten, die der Kandidat/die Kandidatin durchgeführt hat)
	<input type="checkbox"/>	0 % (die in dieser Abbildung wiedergegebenen Daten basieren ausschließlich auf Arbeiten anderer Koautoren)
	<input checked="" type="checkbox"/>	Etwaiger Beitrag des Doktoranden / der Doktorandin zur Abbildung: 10 % Kurzbeschreibung des Beitrages: Plotting data

Abbildung(en) # 9, S6, Table S3, Video S1	<input type="checkbox"/>	100 % (die in dieser Abbildung wiedergegebenen Daten entstammen vollständig experimentellen Arbeiten, die der Kandidat/die Kandidatin durchgeführt hat)
	<input type="checkbox"/>	0 % (die in dieser Abbildung wiedergegebenen Daten basieren ausschließlich auf Arbeiten anderer Koautoren)
	<input checked="" type="checkbox"/>	Etwaiger Beitrag des Doktoranden / der Doktorandin zur Abbildung: 80 % Kurzbeschreibung des Beitrages: Performing Experiments, Plotting data, Statistical analysis

Abbildung(en) # S2, S4	<input type="checkbox"/>	100 % (die in dieser Abbildung wiedergegebenen Daten entstammen vollständig experimentellen Arbeiten, die der Kandidat/die Kandidatin durchgeführt hat)
	<input type="checkbox"/>	0 % (die in dieser Abbildung wiedergegebenen Daten basieren ausschließlich auf Arbeiten anderer Koautoren)
	<input checked="" type="checkbox"/>	Etwaiger Beitrag des Doktoranden / der Doktorandin zur Abbildung: 20 % Kurzbeschreibung des Beitrages: Plotting data

Abbildung(en) # Table S2	<input type="checkbox"/>	100 % (die in dieser Abbildung wiedergegebenen Daten entstammen vollständig experimentellen Arbeiten, die der Kandidat/die Kandidatin durchgeführt hat)
	<input checked="" type="checkbox"/>	0 % (die in dieser Abbildung wiedergegebenen Daten basieren ausschließlich auf Arbeiten anderer Koautoren)
	<input type="checkbox"/>	Etwaiger Beitrag des Doktoranden / der Doktorandin zur Abbildung: Kurzbeschreibung des Beitrages:

***Arabidopsis* Restricts Sugar Loss to a Colonizing *Trichoderma harzianum* Strain by Downregulating *SWEET11* and *-12* and Upregulation of *SUC1* and *SWEET2* in the Roots**

Authors: Hamid Rouina, Yu-Heng Tseng, Karaba N. Nataraja, Ramanan Uma Shaanker, Ralf Oelmüller (2021).

Status: published, *Microorganisms*, 9(6), 1246. doi:10.3390/microorganisms9061246.

Summary:

The aim of this study was to understand how phosphate availability affects plant-fungus symbiosis. Using the newly characterized *Trichoderma* strain and the model plant *Arabidopsis thaliana*, we showed that, on medium with insoluble phosphate, *Trichoderma* alleviated the phosphate starvation responses of its host, and sustained plant growth in the early stage. However, under phosphate deficiency, the colonized plants died earlier compared to the non-colonized controls. Microscopic studies suggested a transition from a beneficial to a saprotrophic relationship with increase in stress. We monitored this transition by analyzing gene expression changes for the sugar transporters in *Arabidopsis*. The genes for the sucrose transporters *SWEET11* and *SWEET12*, which regulate the sucrose flow from the phloem parenchyma cells to the apoplast, were down-regulated and those of *SUC1* and *SWEET2*, which govern sucrose uptake into the parenchyma cells and sucrose sequestration in vacuoles, respectively, were upregulated in colonized roots exposed to phosphate starvation. We propose that under phosphate deficiency, plants restricted sucrose outflow to the fungus to maintain their growth, and restrict fungal propagation in the plant tissue.

Conceptualization: **RO**, **KNN** and **RUS**; methodology, **HR** and **Y-HT**; software, **HR** and **Y-HT**; validation, **HR**, **Y-HT** and **RO**; formal analysis, **HR**; investigation, **HR**; resources, **KNN**, **RUS**, data curation, **HR**; original draft preparation, **HR** and **Y-HT**; review and editing, **RO**; visualization and supervision, **RO**; project administration, **Y-HT** and **R.O.**; funding acquisition, **RO**.

Angaben zum Eigenanteil

Formular 1

Manuskript Nr. 2

Titel des Manuskriptes: *Arabidopsis* Restricts Sugar Loss to a Colonizing *Trichoderma harzianum* Strain by Downregulating SWEET11 and -12 and Upregulation of SUC1 and SWEET2 in the Roots

Autoren: Hamid Rouina, Yu-Heng Tseng, Karaba N. Nataraja, Ramanan Uma Shaanker, Ralf Oelmüller

Bibliographische Informationen: Rouina, H.; Tseng, Y.-H.; Nataraja, K.N.; Uma Shaanker, R.; Oelmüller, R. *Arabidopsis* Restricts Sugar Loss to a Colonizing *Trichoderma harzianum* Strain by Downregulating SWEET11 and -12 and Upregulation of SUC1 and SWEET2 in the Roots. *Microorganisms* 2021, 9, 1246. doi: 10.3390/microorganisms9061246

Der Kandidat / Die Kandidatin ist

Erstautor, Ko-Erstautor, Korresp. Autor, Koautor.

Status: veröffentlicht in „Microorganisms“

Anteile (in %) der Autoren / der Autorinnen an der Publikation

Autor/-in	Konzeptionell	Datenanalyse	Experimentell	Verfassen des Manuskriptes	Bereitstellung von Material
Hamid Rouina	35%	70%	80%	20%	30%
Yu-Heng Tseng	20%	30%	20%	10%	20%
Ralf Oelmüller	45%	0%	0%	70%	50%
Summe	100%	100%	100%	100%	100%

Formular 2

Manuskript Nr. 2

Kurzreferenz: Rouina et al (2021), Microorganisms

Beitrag des Doktoranden / der Doktorandin

Beitrag des Doktoranden / der Doktorandin zu Abbildungen, die experimentelle Daten wiedergeben (nur für Originalartikel):

Abbildung(en) # 1, 3, Table S1	<input type="checkbox"/> 100 % (die in dieser Abbildung wiedergegebenen Daten entstammen vollständig experimentellen Arbeiten, die der Kandidat/die Kandidatin durchgeführt hat)
	<input type="checkbox"/> 0 % (die in dieser Abbildung wiedergegebenen Daten basieren ausschließlich auf Arbeiten anderer Koautoren)
	<input checked="" type="checkbox"/> Etwaiger Beitrag des Doktoranden / der Doktorandin zur Abbildung: 30 % Kurzbeschreibung des Beitrages: Formatting figure, Providing material

Abbildung(en) # 2	<input type="checkbox"/> 100 % (die in dieser Abbildung wiedergegebenen Daten entstammen vollständig experimentellen Arbeiten, die der Kandidat/die Kandidatin durchgeführt hat)
	<input type="checkbox"/> 0 % (die in dieser Abbildung wiedergegebenen Daten basieren ausschließlich auf Arbeiten anderer Koautoren)
	<input checked="" type="checkbox"/> Etwaiger Beitrag des Doktoranden / der Doktorandin zur Abbildung: 50 % Kurzbeschreibung des Beitrages: Plotting data, Performing experiments

Abbildung(en) # 4, 5, 6, 7, S1, S2	<input type="checkbox"/> 100 % (die in dieser Abbildung wiedergegebenen Daten entstammen vollständig experimentellen Arbeiten, die der Kandidat/die Kandidatin durchgeführt hat)
	<input type="checkbox"/> 0 % (die in dieser Abbildung wiedergegebenen Daten basieren ausschließlich auf Arbeiten anderer Koautoren)
	<input checked="" type="checkbox"/> Etwaiger Beitrag des Doktoranden / der Doktorandin zur Abbildung: 10 % Kurzbeschreibung des Beitrages: Assisting on experimental procedures

Abbildung(en)
8

- 100 % (die in dieser Abbildung wiedergegebenen Daten entstammen vollständig experimentellen Arbeiten, die der Kandidat/die Kandidatin durchgeführt hat)
- 0 % (die in dieser Abbildung wiedergegebenen Daten basieren ausschließlich auf Arbeiten anderer Koautoren)
- Etwaiger Beitrag des Doktoranden / der Doktorandin zur Abbildung:
Kurzbeschreibung des Beitrages:

Comparative Secretome Analyses of *Trichoderma/Arabidopsis* Co-Cultures Identify Proteins for Salt Stress, Plant Growth Promotion, and Root Colonization

Authors: Hamid Rouina, Yu-Heng Tseng, Karaba N. Nataraja, Ramanan Uma Shaanker, Thomas Krüger, Olaf Kniemeyer, Axel Brakhage, Ralf Oelmüller (2021).

Status: published, *Frontiers in Ecology and Evolution*, 9:808430. doi: 10.3389/fevo.2021.808430.

Summary:

A recently described *Trichoderma* strain was shown to promote *Arabidopsis* growth with 50 mM NaCl, while 150 mM NaCl did not. Since secretome from both sides of the interaction partners has been shown to be involved in the balance of the interactions, we analyzed the secretome under different salt concentrations to understand the dynamic of symbiosis. Under high salt concentration, stress-related proteins and cell-wall modifying enzymes disappeared during co-cultivation, while the plant antioxidant proteins decreased. Under low salt concentration, only the *Arabidopsis* PYK10 and a fungal prenylcysteine lyase were found during co-cultivation. In combination with antioxidant enzyme assays, the results suggest that both partners profited from the interaction under low salt stress but have to invest more in balancing the symbiosis when the salt concentration increases. The study also sheds light on secreted proteins which could be important for studying symbiotic interaction under various conditions.

HR and **Y-HT** designed and performed the experiments, **TK**, **OK** and **AB** performed the LC-MS/MS analysis and **KNN**, **RUS** and **RO** supervised and coordinated the experiments.

Angaben zum Eigenanteil

Formular 1

Manuskript Nr. 3

Titel des Manuskriptes: Comparative Secretome Analyses of *Trichoderma/Arabidopsis* Co-Cultures Identify Proteins for Salt Stress, Plant Growth Promotion, and Root Colonization

Autoren: Hamid Rouina, Yu-Heng Tseng, Karaba N. Nataraja, Ramanan Uma Shaanker, Thomas Krüger, Olaf Kniemeyer, Axel Brakhage, Ralf Oelmüller

Bibliographische Informationen: Rouina H, Tseng Y-H, Nataraja KN, Uma Shaanker R, Krüger T, Kniemeyer O, Brakhage A and Oelmüller R (2022) Comparative Secretome Analyses of *Trichoderma/Arabidopsis* Co-cultures Identify Proteins for Salt Stress, Plant Growth Promotion, and Root Colonization. *Front. Ecol. Evol.* 9:808430. doi: 10.3389/fevo.2021.808430

Der Kandidat / Die Kandidatin ist

Erstautor, Ko-Erstautor, Korresp. Autor, Koautor.

Status: veröffentlicht in „Frontiers in Ecology and Evolution“

Anteile (in %) der Autoren / der Autorinnen an der Publikation

Autor/-in	Konzeptionell	Datenanalyse	Experimentell	Verfassen des Manuskriptes	Bereitstellung von Material
Hamid Rouina	30%	15%	50%	20%	15%
Yu-Heng Tseng	20%	15%	20%	20%	30%
Thomas Krüger	0%	20%	30%	0%	15%
Ralf Oelmüller	50%	50%	0%	60%	40%
Summe	100%	100%	100%	100%	100%

Formular 2

Manuskript Nr. 3

Kurzreferenz: Rouina et al (2021), Front. Ecol. Evol.

Beitrag des Doktoranden / der Doktorandin

Beitrag des Doktoranden / der Doktorandin zu Abbildungen, die experimentelle Daten wiedergeben (nur für Originalartikel):

Abbildung(en) # 1, 2, 3, 4, Table 1, Table 2, Table 3	<input type="checkbox"/>	100 % (die in dieser Abbildung wiedergegebenen Daten entstammen vollständig experimentellen Arbeiten, die der Kandidat/die Kandidatin durchgeführt hat)
	<input type="checkbox"/>	0 % (die in dieser Abbildung wiedergegebenen Daten basieren ausschließlich auf Arbeiten anderer Koautoren)
	<input checked="" type="checkbox"/>	Etwaiger Beitrag des Doktoranden / der Doktorandin zur Abbildung: 30 % Kurzbeschreibung des Beitrages: Optimizing experimental procedures

Abbildung(en) # 5	<input type="checkbox"/>	100 % (die in dieser Abbildung wiedergegebenen Daten entstammen vollständig experimentellen Arbeiten, die der Kandidat/die Kandidatin durchgeführt hat)
	<input type="checkbox"/>	0 % (die in dieser Abbildung wiedergegebenen Daten basieren ausschließlich auf Arbeiten anderer Koautoren)
	<input checked="" type="checkbox"/>	Etwaiger Beitrag des Doktoranden / der Doktorandin zur Abbildung: 30 % Kurzbeschreibung des Beitrages: Providing experimental protocols

Tris(methylthio)methane Produced by *Mortierella hyalina* Affects Sulfur Homeostasis in *Arabidopsis*

Authors: Yu-Heng Tseng, Stefan Bartram, Sandra S. Scholz, Michael Reichelt, Anja K. Meents, Anatoli Ludwig, Axel Mithöfer, Ralf Oelmüller (2021).

Status: submitted, 14.09.2021, Scientific Reports. Preprint: Authorea. July 06, 2021. doi: 10.22541/au.162428733.37123941/v2.

Summary:

The aim of this study was to investigate the physiological effect of a fungal volatile from *Mortierella hyalina* on its host plant *Arabidopsis thaliana*. *M. hyalina* was shown to promote *Arabidopsis* growth, even when both species were not in physical contact. Analysis of the fungal headspace with GC-MS unveiled the sulfur-containing volatile tris(methylthio)methane (TMTM) to be the major compound. The incorporation of TMTM could be detected in plant tissue by ³⁴S labeling experiment. Under sulfur deficiency condition, TMTM reduced the expression of genes for sulfur deficiency response, prevented breakdown of sulfur-containing metabolites such as glucosinolate (GSL) and glutathione (GSH), and sustained plant growth. However, high amount of TMTM caused accumulation of GSH and GSL, and reduced plant growth, indicating stress to the volatile-exposed plants. Therefore, TMTM affects sulfur homeostasis in plant. Finally, unlike free sulfide, incorporation of TMTM was not directly into cysteine, thus there exists another pathway for organosulfide metabolism in plants.

Y-HT, AM, RO organized the project. **Y-HT**, performed the physiological experiments on *Arabidopsis*, collected the samples and data, analyzed the results and plotted the figures. **SB** identified the natural compound and assisted in the sulfur labeling experiment. **MR** performed the LC-MS analysis, established the method to quantify the isotope ratio, and analyzed the data. **SB** and **AKM** performed the GC-MS analysis. **SSS** and **SB** extracted the fungal volatile for chemical analysis. **AL** established the desiccator assay. **Y-HT** and **RO** wrote up the study. All authors contributed to the manuscript.

Angaben zum Eigenanteil

Formular 1

Manuskript Nr. 4

Titel des Manuskriptes: Tris(methylthio)methane Produced by *Mortierella hyalina* Affects Sulfur Homeostasis in *Arabidopsis*

Autoren: Yu-Heng Tseng, Stefan Bartram, Sandra S. Scholz, Michael Reichelt, Anja K. Meents, Anatoli Ludwig, Axel Mithöfer, Ralf Oelmüller

Bibliographische Informationen:

Der Kandidat / Die Kandidatin ist

Erstautor, Ko-Erstautor, Korresp. Autor, Koautor.

Status: zur Publikation eingereicht in „Scientific Reports“

Anteile (in %) der Autoren / der Autorinnen an der Publikation

Autor/-in	Konzeptionell	Datenanalyse	Experimentell	Verfassen des Manuskriptes	Bereitstellung von Material
Yu-Heng Tseng	80%	60%	55%	70%	40%
Stefan Bartram	5%	20%	20%	5%	10%
Sandra S. Scholz	0%	0%	5%	5%	10%
Michael Reichelt	5%	20%	20%	5%	10%
Ralf Oelmüller	10%	0%	0%	15%	30%
Summe	100%	100%	100%	100%	100%

Formular 2

Manuskript Nr. 4

Kurzreferenz: Tseng et al (2021)

Beitrag des Doktoranden / der Doktorandin

Beitrag des Doktoranden / der Doktorandin zu Abbildungen, die experimentelle Daten wiedergeben (nur für Originalartikel):

Abbildung(en) # 1, Table 1, S3, S4, S5, S6, Table S2	<input type="checkbox"/> 100 % (die in dieser Abbildung wiedergegebenen Daten entstammen vollständig experimentellen Arbeiten, die der Kandidat/die Kandidatin durchgeführt hat)
	<input type="checkbox"/> 0 % (die in dieser Abbildung wiedergegebenen Daten basieren ausschließlich auf Arbeiten anderer Koautoren)
	<input checked="" type="checkbox"/> Etwaiger Beitrag des Doktoranden / der Doktorandin zur Abbildung: 10 % Kurzbeschreibung des Beitrages: Organizing figure and table
Abbildung(en) # 2, 6	<input type="checkbox"/> 100 % (die in dieser Abbildung wiedergegebenen Daten entstammen vollständig experimentellen Arbeiten, die der Kandidat/die Kandidatin durchgeführt hat)
	<input type="checkbox"/> 0 % (die in dieser Abbildung wiedergegebenen Daten basieren ausschließlich auf Arbeiten anderer Koautoren)
	<input checked="" type="checkbox"/> Etwaiger Beitrag des Doktoranden / der Doktorandin zur Abbildung: 70 % Kurzbeschreibung des Beitrages: Performing experiments, Plotting data, Statical analysis
Abbildung(en) # 3, 4, 5, 7, S1, S2, Table S1	<input checked="" type="checkbox"/> 100 % (die in dieser Abbildung wiedergegebenen Daten entstammen vollständig experimentellen Arbeiten, die der Kandidat/die Kandidatin durchgeführt hat)
	<input type="checkbox"/> 0 % (die in dieser Abbildung wiedergegebenen Daten basieren ausschließlich auf Arbeiten anderer Koautoren)
	<input type="checkbox"/> Etwaiger Beitrag des Doktoranden / der Doktorandin zur Abbildung: Kurzbeschreibung des Beitrages:

CORK1, a LRR-Malectin Receptor Kinase for Cellooligomer Perception in *Arabidopsis thaliana*

Authors: Yu-Heng Tseng, Sandra S. Scholz, Judith Fliegmann, Thomas Krüger, Akanksha Gandhi, Olaf Kniemeyer, Axel A. Brakhage, Ralf Oelmüller (2022).

Status: submitted, 26.04.2022, Plant Physiology.

Summary:

The aim of this study was to identify the signaling component of cellooligomers. They inform the cells about the integrity of their cell wall and, among others, induce plant immune responses, including cytoplasmic calcium elevation, up-regulation and phosphorylation of MAP kinases, and ROS production. In this study, I started by screening an EMS mutant population. Using cellobiose as elicitor and cytoplasmic calcium elevation as read out, I isolated and characterized an EMS mutant which did not respond to the stimulus. Through back-cross, genome-wide association study (GWAS) and complementation, I identified CORK1 (CelloOligomer Receptor Kinase 1), the putative receptor for cellooligomers. It possesses a leucine-rich repeat domain, followed by a malectin domain and a functional cytoplasmic kinase domain. The EMS mutant and two independent T-DNA insertion lines exhibited no cytoplasmic calcium elevation, no ROS production, nor up-regulation of *WRKY30* and *WRKY40* upon cellobiose treatment. With protoplast luciferase assay, we showed that two conserved phenylalanine residues in the malectin domain are important for cellooligomer signaling. To further understand the signaling events upon cellooligomer perception, transcriptomic and phosphoproteomic study were carried out. From them, I discovered the cellooligomer-regulated genes related to tryptophan and secondary metabolite metabolism, and early phosphorylation target proteins for CORK1, such as proteins within the cellulose synthase complex.

Y-HT and **RO** developed the idea and organized the project. **Y-HT**, performed the experiments, collected the samples and data, analyzed the results and plotted the figures. **SSS** generated the EMS mutant population. **JF** performed the protoplast assay and analyzed the data. **TK** carried out the phosphopeptide measurement and data analysis. **AG** assisted on sample collection and protein extraction. **AAB** and **OK** provided the materials and equipment for protein extraction. **Y-HT** and **RO** wrote up the study. All authors contributed to the manuscript.

Angaben zum Eigenanteil

Formular 1

Manuskript Nr. 5

Titel des Manuskriptes: CORK1, a LRR-Malectin Receptor Kinase for Celooligomer Perception in *Arabidopsis thaliana*

Autoren: Yu-Heng Tseng, Sandra S. Scholz, Judith Fliegmann, Thomas Krüger, Akanksha Gandhi, Olaf Kniemeyer, Axel A. Brakhage, Ralf Oelmüller

Bibliographische Informationen:

Der Kandidat / Die Kandidatin ist

Erstautor, Ko-Erstautor, Korresp. Autor, Koautor.

Status: zur Publikation eingereicht in „Plant Physiology“

Anteile (in %) der Autoren / der Autorinnen an der Publikation

Autor/-in	Konzeptionell	Datenanalyse	Experimentell	Verfassen des Manuskriptes	Bereitstellung von Material
Yu-Heng Tseng	60%	65%	65%	40%	30%
Sandra S. Scholz	5%	0%	5%	10%	0%
Judith Fliegmann	5%	5%	10%	10%	10%
Thomas Krüger	5%	15%	10%	5%	10%
Akanksha Gandhi	5%	0%	10%	5%	0%
Olaf Kniemeyer	0%	0%	0%	0%	10%
Axel A. Brakhage	0%	0%	0%	0%	10%
Ralf Oelmüller	20%	15%	0%	30%	30%
Summe	100%	100%	100%	100%	100%

Formular 2

Manuskript Nr. 5

Kurzreferenz: Tseng et al (2022)

Beitrag des Doktoranden / der Doktorandin

Beitrag des Doktoranden / der Doktorandin zu Abbildungen, die experimentelle Daten wiedergeben (nur für Originalartikel):

Abbildung(en) # 1, 2, 3, 4, 5, 7, Table 1, S1, S2, S3, S4, S5, Table S1, Table S2, Dataset S1	<input checked="" type="checkbox"/>	100 % (die in dieser Abbildung wiedergegebenen Daten entstammen vollständig experimentellen Arbeiten, die der Kandidat/die Kandidatin durchgeführt hat)
	<input type="checkbox"/>	0 % (die in dieser Abbildung wiedergegebenen Daten basieren ausschließlich auf Arbeiten anderer Koautoren)
	<input type="checkbox"/>	Etwaiger Beitrag des Doktoranden / der Doktorandin zur Abbildung:

Abbildung(en) # 6	<input type="checkbox"/>	100 % (die in dieser Abbildung wiedergegebenen Daten entstammen vollständig experimentellen Arbeiten, die der Kandidat/die Kandidatin durchgeführt hat)
	<input type="checkbox"/>	0 % (die in dieser Abbildung wiedergegebenen Daten basieren ausschließlich auf Arbeiten anderer Koautoren)
	<input checked="" type="checkbox"/>	Etwaiger Beitrag des Doktoranden / der Doktorandin zur Abbildung: 80 % Kurzbeschreibung des Beitrages: Performing experiments, Plotting data, Statical anaysis

Abbildung(en) # Table 2, Dataset S2	<input type="checkbox"/>	100 % (die in dieser Abbildung wiedergegebenen Daten entstammen vollständig experimentellen Arbeiten, die der Kandidat/die Kandidatin durchgeführt hat)
	<input type="checkbox"/>	0 % (die in dieser Abbildung wiedergegebenen Daten basieren ausschließlich auf Arbeiten anderer Koautoren)
	<input checked="" type="checkbox"/>	Etwaiger Beitrag des Doktoranden / der Doktorandin zur Abbildung: 50 % Kurzbeschreibung des Beitrages: Performing experiments, Organizing data

4. Manuscripts

4.1 Manuscript 1

An Endophytic *Trichoderma* Strain Promotes Growth of Its Hosts and Defends Against Pathogen Attack

Yu-Heng Tseng, Hamid Rouina, Karin Groten, Pijakala Rajani, Alexandra C. U. Furch, Michael Reichelt, Ian T. Baldwin, Karaba N. Nataraja, Ramanan Uma Shaanker, Ralf Oelmüller

Published in *Frontiers in Plant Science* (2020)

Front. Plant Sci. 11:573670. doi: 10.3389/fpls.2020.573670



An Endophytic *Trichoderma* Strain Promotes Growth of Its Hosts and Defends Against Pathogen Attack

Yu-Heng Tseng¹, Hamid Rouina¹, Karin Groten², Pijakala Rajani³,
Alexandra C. U. Furch¹, Michael Reichelt², Ian T. Baldwin², Karaba N. Nataraja⁴,
Ramanan Uma Shaanker³ and Ralf Oelmüller^{1,3*}

¹ Department of Plant Physiology, Matthias Schleiden Institute of Genetics, Bioinformatics and Molecular Botany, Friedrich-Schiller-University Jena, Jena, Germany, ² Department of Molecular Ecology, Max-Planck-Institute for Chemical Ecology, Jena, Germany, ³ School of Ecology and Conservation, University of Agricultural Sciences, Gandhi Krishi Vigyana Kendra (GKVK), Bengaluru, India, ⁴ Department of Crop Physiology, University of Agricultural Sciences, Gandhi Krishi Vigyana Kendra (GKVK), Bengaluru, India

OPEN ACCESS

Edited by:

Sabine Dagmar Zimmermann,
Délégation Languedoc Roussillon
(CNRS), France

Reviewed by:

Marc Knight,
Durham University, United Kingdom
Justin Lee,
Leibniz-Institut für Pflanzenbiochemie
(IPB), Germany

*Correspondence:

Ralf Oelmüller
b7oera@uni-jena.de

Specialty section:

This article was submitted to
Plant Symbiotic Interactions,
a section of the journal
Frontiers in Plant Science

Received: 17 June 2020

Accepted: 02 November 2020

Published: 03 December 2020

Citation:

Tseng Y-H, Rouina H, Groten K,
Rajani P, Furch ACU, Reichelt M,
Baldwin IT, Nataraja KN,
Uma Shaanker R and Oelmüller R
(2020) An Endophytic *Trichoderma*
Strain Promotes Growth of Its Hosts
and Defends Against Pathogen
Attack. *Front. Plant Sci.* 11:573670.
doi: 10.3389/fpls.2020.573670

Plants host numerous endophytic microbes which promote plant performance, in particular under stress. A new endophytic fungus was isolated from the leaves of a deciduous wood tree *Leucas aspera*. Morphological inspection and multilocus phylogeny identified the fungus as a new *Trichoderma* strain. If applied to *Arabidopsis thaliana* and *Nicotiana attenuata*, it mainly colonizes their roots and strongly promotes initial growth of the plants on soil. The fungus grows on high NaCl or mannitol concentrations, and shows predatory capability on the pathogenic fungus *Alternaria brassicicola*. Colonized *Arabidopsis* plants tolerate higher salt stress and show lower *A. brassicicola* spread in roots and shoots, while arbuscular mycorrhiza formation in *N. attenuata* is not affected by the *Trichoderma* strain. These beneficial features of the novel *Trichoderma* strain are important prerequisites for agricultural applications.

Keywords: *Trichoderma*, plant beneficial endophyte, growth promotion, pathogen protection, hormone induction

INTRODUCTION

Trichoderma species are versatile filamentous ascomycetes which are found in nearly all environments. They live in soil, grow on wood as saprophytes, or feed on fungi, plants, animals and insects as parasites (Carsolio et al., 1994; Gautheret et al., 1995; Furukawa et al., 1998; El-Katatny et al., 2000; Rocha-Ramirez et al., 2002; Druzhinina et al., 2011; Li et al., 2013; Mukherjee et al., 2014; Li Destri Nicosia et al., 2015; Berini et al., 2016; Druzhinina and Kubicek, 2016; Rosmana et al., 2016; Karlsson et al., 2017). Various *Trichoderma* species were shown to protect plants against pathogenic fungi, such as *Rhizoctonia solani* (Grosch et al., 2007; Zhang and Zhuang, 2020). Therefore, they are commonly used as bio-control agents in agriculture, with more than 250 commercial *Trichoderma*-based bio-fungicides registered world-wide (Woo et al., 2014). Apart from being used as bio-fungicide, *Trichoderma* species also stimulate plant growth (Lee et al., 2016)

and nutrient uptake under nutrient deficient conditions (Li et al., 2015), often in combination with better stress tolerance of crop plants (Studholme et al., 2013). Other species, such as *T. pleuroti* (CBS124387) and *T. pleuroticola* (CBS124383) cause green mold disease in oyster mushroom (*Pleurotus ostreatus*) farms (Park et al., 2006).

Most of the investigated *Trichoderma* species colonize either the root surface, or live as endophytes inside root tissues (Samolski et al., 2012; Ruano-Rosa et al., 2016). However, some species were also isolated from the aerial parts of the plants (Bailey and Melnick, 2013). In response, plants often activate defense mechanisms including the biosynthesis of the defense-related phytohormones salicylic acid (SA), jasmonic acid (JA), ethylene (ET) or abscisic acid (ABA) (Contreras-Cornejo et al., 2009; Hermosa et al., 2012; Sivakumaran et al., 2016; Checker et al., 2018). The phytohormones regulate two types of induced resistance in plants, namely, SA-dependent systemic acquired resistance (SAR) and JA/ET-dependent induced systemic resistance (ISR). The signaling events induced by *Trichoderma* species often result in elevated SA and JA levels in different parts of the plant (Martínez-Medina et al., 2013; Leonetti et al., 2017).

In this study, we wanted to find out if the novel endophytic *Trichoderma* strain isolated from the leaves of *Leucas aspera* also interacts with other plant species (*Arabidopsis*, *Nicotiana attenuata*) and has beneficial effects in terms of plant growth and alleviation of abiotic and biotic stress. We could show that, although the strain is phylogenetically related to mushroom-infecting *T. pleuroti* and *T. pleuroticola*, it efficiently colonizes the roots of the two plant species, strongly promotes their growth on soil during early development and protects them against systemic *A. brassicicola* spread, while mycorrhiza formation in *N. attenuata* appears not to be affected. We also evaluated if phytohormones might be involved in the plant-fungus interaction.

MATERIALS AND METHODS

Growth Medium and Conditions for Seedlings

Seeds of wild-type *A. thaliana* (ecotype Columbia-0) were surface-sterilized for 8 min in sterilizing solution containing lauryl sarcosine (1%) and Clorix cleaner (23%). Surface-sterilized seeds were washed with sterilized water eight times and placed on Petri dishes with MS medium supplemented with 0.3% gelrite (Murashige and Skoog, 1962). After cold treatment at 4°C for 48–72 h, plates were incubated at 22°C under long day conditions (16 h light/8 h dark; 80 $\mu\text{mol m}^{-2} \text{s}^{-1}$).

Nicotiana attenuata Torr. ex S. Watson seeds of the 31st generation of an inbred accession originally collected from southwestern Utah were used for all experiments mentioned for this species. Seeds were germinated after surface sterilization and treatment with liquid smoke (1:50 dilution; House of Herbs, Passaic, NY, United States) and 1 mM of gibberellic acid (GA₃; Duchefa-Biochemie, The Netherlands) on agar plates containing Gamborg's B5 medium as previously described in

Krügel et al. (2002). Seeds were kept in a growth chamber under a day/night cycle of 16 h (26–28°C)/8 h (24–26°C).

Growth of Fungi and Spore Collection

Based on our previous screen for plant growth-promoting fungi in a field station in India, the new *Trichoderma* strain was selected for detailed characterization. It was isolated from the leaves of *Leucas aspera* (Wild.) Link (family: *Lamiaceae*), a widely distributed medicinal plant reported for its antifungal, antioxidant, antimicrobial and cytotoxic activities (Prajapati et al., 2010; Rajani et al., 2020). The *Trichoderma* strain was grown on Petri dishes with Kaefer medium (KM) or Potato-Dextrose-Agar (PDA) medium, pH 6.5, at 23°C in the dark (Bains and Tewari, 1987; Hill and Käfer, 2001). *Alternaria brassicicola* was grown on Potato-Dextrose-Agar (PDA) medium, pH 6.5, 23°C in the dark (Bains and Tewari, 1987). We did not observe any difference of the fungal performance on the two media. Two additional pathogens, *Fusarium brachygibbosum* and *Alternaria* spp. isolate Utah 10, native to the natural habitat of *N. attenuata* isolated in a previous study (Luu et al., 2015), were grown on PDA medium at 26°C in the dark.

For spore collection, sterilized 0.01% Tween 20 solution was poured onto plates with fungi which were grown for less than 2 weeks. Spores were scratched from the agar surface and dispersed in 0.01% Tween 20. The resulting spore suspension was filtered through two layers of nylon membrane (75 μm pore size, Sefar AG, Switzerland), pelleted and washed with sterile distilled water. The *A. brassicicola* spore concentration was determined in a hemocytometer, while the *Trichoderma* spore concentration was determined by O.D._{600 nm} measurements using a spectrometer (BioSpectrometer® basic, Eppendorf, Germany).

For co-cultivation experiments with *N. attenuata*, the *Trichoderma* strain was cultivated on PDA plates. Spores of 7–14 day-old cultures were dislodged from the surface with sterile distilled water containing 0.01% Triton X-100. The resulting solution was diluted with distilled water to an O.D._{600 nm} of 0.250–0.350.

Co-cultivation of *A. thaliana* and *N. attenuata* With *Trichoderma*

Co-cultivation of *A. thaliana* and fungi was performed according to Johnson et al. (2011) with modifications. A plug (5 mm diameter) from a KM plate containing the fungus or a control plug without the fungus was put on a fresh plate with solid plant nutrient medium (PNM), which contained a layer of a nylon membrane (pore size 75 μm) on the agar surface. The plates were incubated at 23°C for 7 days. Unless specified, four 10 day-old *A. thaliana* seedlings of equal size were transferred to the plates. They were incubated at 22°C under long day conditions (16 h light/8 h dark; 80 $\mu\text{mol m}^{-2} \text{s}^{-1}$).

For co-cultivation of *A. thaliana* with *Trichoderma* on soil, 1 kg of soil was suspended in 5 L of distilled water overnight. The liquid was removed by filtration and the soil was autoclaved twice. 200 g of the soil was transferred to magenta boxes for co-cultivation assays. The soil was inoculated with a 5 mm plug of KM medium with or without *Trichoderma* 3 cm below the soil

surface in the center of the box. 10 day-old *Arabidopsis* seedlings were transferred to the soil, and the boxes were kept at 22°C under long day conditions (16 h light/8 h dark; 80 $\mu\text{mol m}^{-2} \text{s}^{-1}$) for 4 weeks.

Co-cultivation of *N. attenuata* with *Trichoderma* was performed in Petri dishes and on soil. For experiments in Petri dishes, sterilized seeds treated with liquid smoke (1:50 dilution; House of Herbs, Passaic, NY, United States) and GA (1 mM GA₃; Duchefa-Biochemie, The Netherlands) were incubated for 1 h with a highly diluted spore and hyphae solution before transfer to GB5 medium (see Santhanam et al., 2019 for experimental details). In a second set-up, liquid smoke-and GA-treated seeds were germinated on GB5 medium for 7 days before they were transferred in a circle with 10 seedlings to a new plate. Immediately after transfer roots either received 10 μL sterile distilled water or the same amount of spore solution (O.D._{600 nm} = 0.2653). One day later an Agar plug of *Alternaria* spp. Utah 10 was placed in the middle of the plate. Inoculated seedlings were kept at 26°C and 14 h light and 10 h dark cycle for 16 days.

For pot experiments on soil, *Trichoderma* treated seedlings and controls were transferred to pots and cultivated in a Snijders Chamber with a 16 h light/8 h dark cycle at 65% relative humidity.

To study the effect of *Trichoderma* strain on arbuscular mycorrhizal fungi (AMF), *N. attenuata* seedlings were transferred to Teku pots with sand 10 days after germination, and transferred to 10% of the commercial inoculum (BiomycVital, which contains AMF spores and tiny pieces of roots/hyphae in expanded clay)¹ after another 12 days. Upon transfer, half of the plants received a *Trichoderma* spore solution, while control plants received the same amount of distilled water. Plants were watered with hydroponics solution containing 0.05 mM P. Roots were collected for further analysis 8 weeks after transfer.

Nucleic Acid Isolation, Primers, and PCR and Sequencing

Arabidopsis root and fungal tissue were ground in liquid nitrogen, and DNA extraction was performed according to Doyle (1990). RNA from AMF-colonized *N. attenuata* roots was extracted with the LiCl method according to Kistner and Matamoros (2005). RNA samples were treated with DNase removal kit (Ambion, Thermo Fisher Scientific, Germany) according to the manufacturer's instructions and reverse transcribed with Superscript II (Invitrogen, Thermo Fisher Scientific, Germany) and Oligo-dT.

The primer pairs for amplifying the *TEF1* (translation elongation factor 1-alpha) and *RPB2* (RNA polymerase II subunit 2) genes from *Trichoderma* are: *TEF1*-F: 5'-CATCGAGAAGTTCGAGAAGG-3'; *TEF1*-R: 5'-AACTTGCAGGCAATGTGG-3'; *RPB2*-F: 5'-TGGGGWGAYCARAARAAGG-3'; *RPB2*-R: 5'-CATRATGACSGAATCTTCCTGGT-3'. Each 20 μL PCR reaction contains 2 μL of 10 \times DreamTaq Buffer (Thermo Fisher Scientific, Germany), 0.2 mM dNTP, 1.0 μM forward/reverse primer, 100 ng genomic DNA template and 1U of DreamTaq DNA Polymerase (Thermo Fisher Scientific,

Germany). The reaction was performed in a thermal cycler (Applied Biosystems SimpliAmp Thermal Cycler, Thermo Fischer Scientific, Germany). The initial denaturation step was set at 95°C for 3 min, followed by 30 cycles of denaturation at 95°C for 30 s, annealing at 55°C (*TEF1*) or 62°C (*RPB2*) for 30 s, and extension at 72°C for 30 s. The final extension step was set at 72°C for 10 min. The PCR products from at least two independent PCR runs were purified by NucleoSpin Gel and PCR Clean-up kit (Macherey-Nagel, Germany). Purified PCR products were sent to Eurofins Genomics for Sanger sequencing. Consensus sequence of *TEF1* and *RPB2* was deposited to Genbank with accession numbers MT591352 and MT602550, respectively.

To quantify the colonization of *Trichoderma* under various salt concentrations, *Trichoderma TEF1* and *A. thaliana RPS* (AT1G34030) were detected by qPCR with the following primers: *TEF*-qF: 5'-TCAAGTCCGTTGAGATGCAC-3'; *TEF*-qR: 5'-CGTTCTTGACGTTGAAACCA-3'; *RPS*-qF: 5'-GTCTCCAATGCCCTTGACAT-3'; *RPS*-qR: 5'-TCTTTCCTGCGACCAAGT-3'.

For qPCR analysis of AMF colonization of *N. attenuata* roots, qPCR reactions were performed on Mx3005P qPCR system (Stratagene, Santa Clara, CA, United States) with Takyon Sybr Green No ROX kit (Eurogentec, Belgium). Primers for *NaRAM1*, *NaPT4*, and *Rhizophagus irregularis tubulin* are from Wang et al. (2018a). Primers for *NaEF1* are from Wang et al. (2018b). Primers for *RPB2* of *Trichoderma* are: *RPB2*-qF: 5'-AGACGTCCATGATCTGCATGAC-3'; *RPB2*-qR: 5'-TGTCTTGGTCTTGAGTCGCTTG-3'

The genes for *A. thaliana Ubiquitin 5*, *N. attenuata Elongation Factor 1 alpha (NaEF1)*, Wang et al., 2018b) and *A. brassicicola Cutinase 1* were used to monitor *A. brassicicola* infection in root tissue. The primer pairs for qPCR analysis are: *AtUBQ5*-qF: 5'-GACGCTTCATCTCGTCC-3'; *AtUBQ5*-qR: 5'-GTAAACGTAGGTGAGTCCA-3'; *AbCUT1*-qF: 5'-GACCGAGGAAGCTCAGATGC-3'; *AbCUT1*-qR: 5'-GCCTGGGATCTTGAATGC-3'.

Multilocus Phylogenetic Analysis

The nucleotide sequences of *TEF1* and *RPB2* from 55 *Trichoderma* species and an outgroup species, *Nectria eustromatica*, were retrieved from the NCBI Nucleotide public database. The *TEF1* and *RPB2* sequences of the new *Trichoderma* strain were obtained from the PCR products. *TEF1* and *RPB2* genes from the same species were concatenated for combined analysis. In total, 56 concatenated sequences were subjected to alignment using MAFFT v7 online at <https://mafft.cbrc.jp/alignment/server> (Katoh et al., 2019), with G-INS-i parameters and a scoring matrix of "1PAM/ $\kappa = 2$ " for nucleotide sequences. The resulting alignment was inspected and selected for conserved blocks using Gblocks version 0.91b (Castresana, 2000).

Maximum likelihood analysis was conducted using RaxML-NG v.0.9.0 through web service at <https://raxml-ng.vital-it.ch> (Kozlov et al., 2019). Using the GTR+FO+G4m model, 2000 distinct ML tree were searched and bootstrapped with 100 replicates. For maximum parsimony analysis,

¹www.biomyc.de

PAUP 4.0a166 was utilized (Swofford, 2002). Heuristic search of 100 replicates was performed with random addition of sequence, and tree bisection-reconnection (TBR) as the branch-swapping algorithm (steepest decent and MulTrees option not in effect). All characters were weighted equally, and gaps were treated as missing character. Bootstrap of 1,000 replicates was undertaken with Maxtrees set as 5,000.

The Bayesian analysis was conducted using MrBayes v3.2.7a (Huelsenbeck and Ronquist, 2001; Ronquist and Huelsenbeck, 2003). The evolutionary model was set to the general time-reversible model (GTR; Tavare, 1986), and the nucleotide variation rate set to inverse gamma distribution (Yang, 1993). Two simultaneous and independent Markov chain Monte Carlo (mcmc) analyses was run to generate 1 million generations each, while they were sampled for every 10 generations to determine the posterior probability (Geyer, 1991). From the resulting 100,000 sampled trees, the first 25% of them were discarded, and the remaining 75,000 trees were summarized to produce the consensus tree.

The Maximum likelihood bootstrap proportions (MLBP), Maximum parsimony bootstrap proportions (MPBP), as well as the Bayesian inference posterior probability (BIPP) from each analysis were combined to the phylogenetic tree from the RAxML analysis using TreeGraph2.15.0-887 beta (Stöver and Müller, 2010). The final tree was created with FigTree v1.4.4 (Rambaut, 2018). The accession numbers of the individual genes are provided in **Supplementary Table 1**.

Histological Staining and Microscopy

Roots of *A. thaliana* co-cultivated with the *Trichoderma* strain for 2 or 7 days were collected and immersed in Wheat Germ Agglutinin, Alexa Fluor™ 488 Conjugate (Thermo Fisher Scientific, Germany) for 10 min in dark. Immersed samples were taken out from the staining solution and placed on a glass slide. Water was applied to the slide to wash away excess staining solution and the slide was covered with a cover slip for microscopic inspection with Axio Imager.M2 (Zeiss Microscopy GmbH, Germany). The bright field and fluorescent images were recorded with a monochromatic camera AxioCam 503 mono (Zeiss Microscopy GmbH, Germany). Digital images were processed with the ZEN software (Zeiss Microscopy GmbH, Germany).

For confocal imaging of root colonization, *A. thaliana* roots co-cultivated with *Trichoderma* for 2 days were stained with Wheat Germ Agglutinin, Alexa Fluor™ 488 Conjugate and RH414 [N-(3-Triethylammoniumpropyl)-4-(4-(Diethylamino)phenyl)Butadienyl]Pyridinium Dibromide; Thermo Fischer Scientific, Germany] with the method described above. Samples were imaged using an LSM 880 microscope (Zeiss Microscopy GmbH, Germany) with the 488 nm laser line of an argon multiline laser (11.5 mW). Images were taken with a 40× objective (Plan-Apochromat 40×/0.8). Lambda stacks were created using the 32 channel GaAsP detector followed by Linear Unmixing with the ZEN software. Z-stacks were taken from specific areas of the sample and Maximum Intensity Projections were produced with the ZEN software.

Phytohormone Analyses by LC-MS/MS

Sixteen seedlings from control and co-cultured plates were harvested and separated into root and shoot samples. Mycelium of the *Trichoderma* strain grown on KM plates was harvested for phytohormone analysis.

Fifty to one hundred thirty milligrams of fresh tissue were extracted and homogenized in 1.5 mL methanol containing 60 ng D4-SA (Santa Cruz Biotechnology, United States), 60 ng D6-JA (HPC Standards GmbH, Germany), 60 ng D6-ABA (Santa Cruz Biotechnology, United States), 12 ng D6-JA-Ile (HPC Standards GmbH), and D5-indole-acetic acid (D5-IAA, OlChemIm s.r.o., Olomouc, Czech Republic) as internal standards. Samples were agitated on a horizontal shaker at room temperature for 10 min. The homogenate was mixed for 30 min and centrifuged at 13,000 rpm for 20 min at 4°C and the supernatant was collected. The homogenate was re-extracted with 500 µL methanol, mixed and centrifuged and the supernatants were pooled. The combined extracts were evaporated under reduced pressure at 30°C and dissolved in 500 µL methanol.

Phytohormone analysis was performed by LC-MS/MS as in Heyer et al. (2018) on an Agilent 1260 series HPLC system (Agilent Technologies) with the modification that a tandem mass spectrometer QTRAP 6500 (SCIEX, Darmstadt, Germany) was used. Since we observed that both the D6-labeled JA and D6-labeled JA-Ile standards (HPC Standards GmbH, Cunnersdorf, Germany) contained 40% of the corresponding D5-labeled compounds, the sum of the peak areas of the D5- and D6-compounds was used for quantification. Details of the instrument parameters and response factors for quantification can be found in **Supplementary Table 2**.

Indole-acetic acid was quantified using the same LC-MS/MS system with the same chromatographic conditions but with positive mode ionization with an ion spray voltage at 5,500 eV. Multiple reaction monitoring (MRM) was used to monitor analyte parent ion → product ion fragmentations as follows: m/z 176 → 130 [collision energy (CE) 19 V; declustering potential (DP) 31 V] for indole-acetic acid (IAA); m/z 181 → 133 + m/z 181 → 134 + m/z 181 → 135 (CE 19 V; DP 31 V) for D5-indole-acetic acid.

Quantification of Mycelial Growth, AMF Colonization, and 11-Carboxyblumenol Levels

Plates with mycelia were scanned with an Epson scanner (Perfection V600 Photo, Epson, Germany), and the files imported into ImageJ (Schindelin et al., 2012). Mycelial coverage on each plate was delineated using a free-hand selection tool and measured with the built-in “Measure” function.

AMF colonization was determined by the “magnified intersections method” described in detail by McGonigle et al. (1990). In brief, roots were cut in about 1 cm pieces and we counted the fungal structures of 150 intersections per sample after staining with Trypan Blue.

For determination of AMF colonization marker 11-carboxyblumenol, three leaf disks per AMF inoculated of the first and second stem leaf were harvested 6 and 8 weeks after

AMF inoculation. 11-Carboxyblumenol levels were determined as markers of arbuscule colonization and quantified following the protocol of Wang et al. (2018a).

Statistical Tests

Statistical tests were performed using R studio version 1.1.463 with R version 3.4.4. Figures were plotted using Python 3.7.4 and arranged with LibreOffice Draw 5.1.6.2.

RESULTS

Morphological and Phylogenetic Analysis of the New *Trichoderma* Strain

The *Trichoderma* strain was isolated from leaves of *Leucas aspera* (Wild.) Link. We selected this strain for further analysis because we observed in preliminary field experiments that it promotes growth of several crop species. Its morphology shows typical characteristics of *Trichoderma* species of the *harzianum* clade. On KM plates, the hyphae cover the entire Petri dish from a single plug (5 mm in diameter) in 3–4 days (Supplementary Figure 1A). During the first 3 days after transfer to a new plate, the hyphae extended and formed conidiophores at the tip of hyphal branches. The conidia grew, replicated, and aggregated at the tip of a conidiophore (Supplementary Figure 1B). After 7 days, mature conidia developed as sphere-like structure composed of numerous individual conidia (Supplementary Figure 1C). The hyphal cell shrank after the conidia were fully developed. This allowed them to detach from the hyphae (Supplementary Figure 1D). The fully matured conidia displayed a green color (Supplementary Figure 1E).

Phylogenetic analysis based on Maximum likelihood, Maximum Parsimony and Bayesian Inference of phylogeny uncovered that the isolated *Trichoderma* strain belongs to the *harzianum* clade (Figure 1), closely related to *T. confertum* TC62 and *T. confertum* TC139, two strains recently isolated from the soil 2,000 m above sea level in Tibet (Chen and Zhuang, 2017). The multilocus sequence analysis also indicated that the strain is closely related to *T. pleuroti* and *T. pleuroticola*, but less compared to *T. confertum*. In summary, according to the three different analysis methods, the isolated fungus is most probably a new *Trichoderma* strain closely related to *T. confertum*.

The New *Trichoderma* Strain Colonizes *Arabidopsis* and *Nicotiana* Roots and Promotes Plant Growth

To characterize the endophytic lifestyle of the new strain, and to check which organ of the plant can be colonized by the fungus, it was co-cultivated with the model species, *Arabidopsis thaliana*. Two days after co-cultivation, hyphae were already detectable on the surface of the roots (Figures 2A,C). Light and confocal microscopy showed that hyphae also invaded into the root hair (Figures 2B,D–G and Supplementary Movie 1). Seven days after co-cultivation, the *Arabidopsis* roots were highly colonized, and conidiophores were found at the tip of the root hair, although not every root hair contained hyphae or

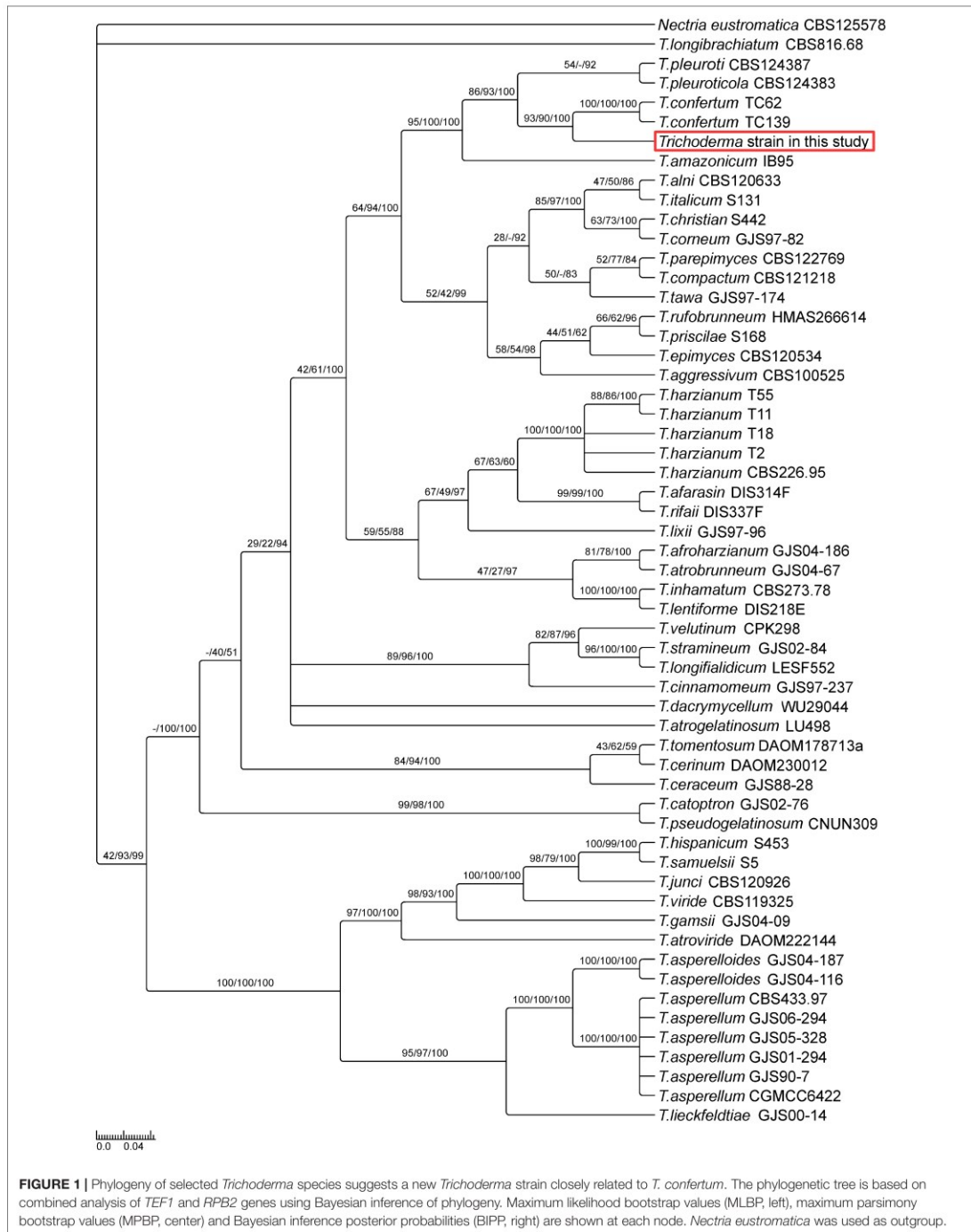
conidiophore (Figures 2H–K). Close inspections revealed that the conidiophores derived from the hyphae in the root hairs. Under these co-cultivation conditions without stress, the aerial parts of the plant were not colonized.

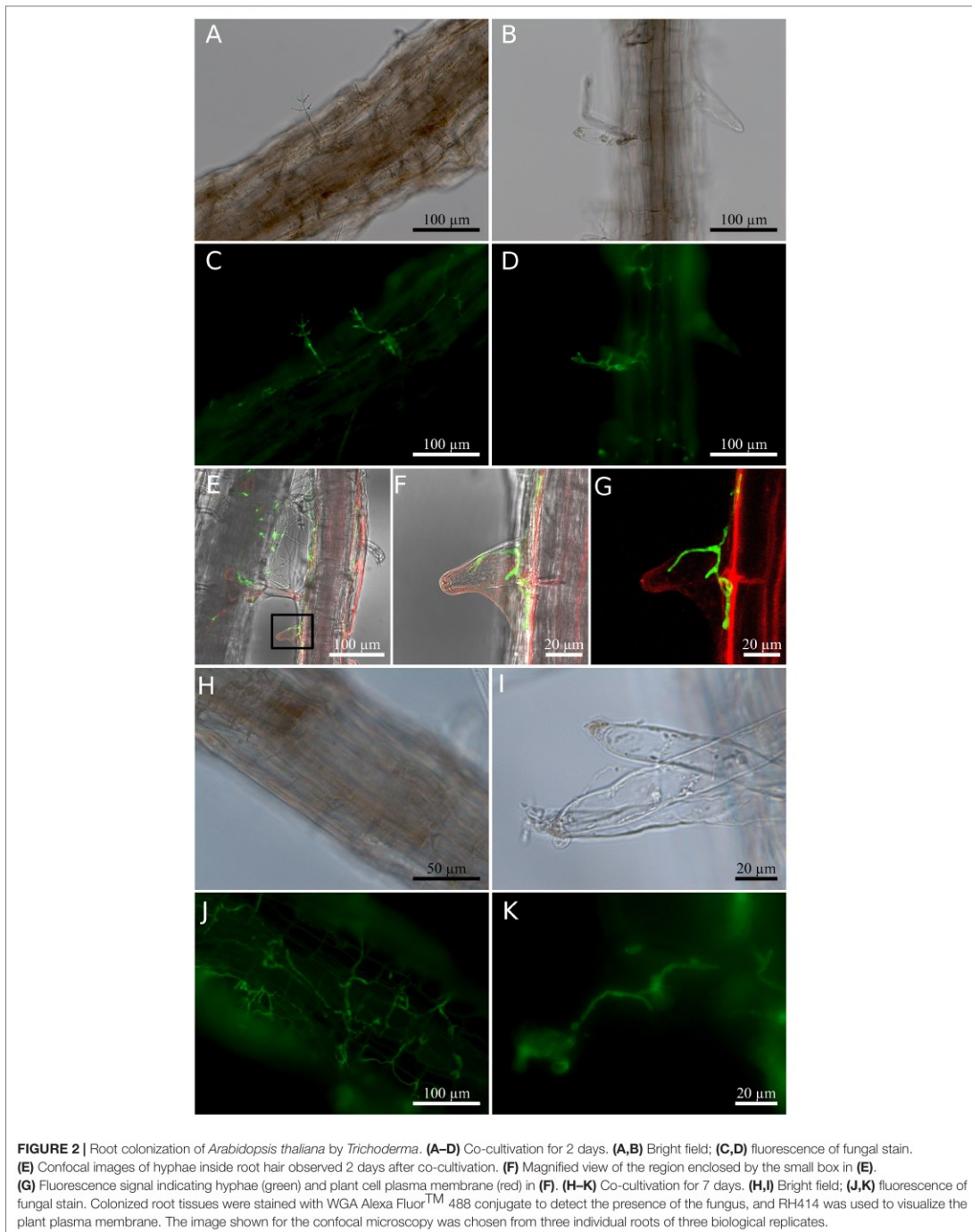
When *Arabidopsis* plants were co-cultivated on soil in the greenhouse, the germination rate and the performance of the young seedlings were not affected by the fungus. However, we observed a strong initial growth-promoting effect of the fungus on 4-week old *Arabidopsis* plants, since colonized plants were almost twice as large as the uncolonized controls (Figures 3A,B). Root colonization by the *Trichoderma* strain was confirmed by microscopy (Supplementary Figure 2). During later stages, the growth difference between colonized and uncolonized plants became less and during flowering time, the growth-stimulating effect of the fungus was barely visible. The number and size of seeds was not significantly different for plants grown with or without the fungus (data not shown). This indicates that the fungus promotes plant growth during early stages of development.

Growth promotion was also observed for the model plant *N. attenuata* (cf. also below). We observed the same colonization efficiencies as described above for *Arabidopsis* seedlings. Also, the germination rates were similar for inoculated and non-inoculated seeds, and all seedlings were healthy. Similar to *Arabidopsis*, we observed a stimulatory effect of the fungus on *N. attenuata* growth after 4 weeks on soil, when both the rosette diameter and root biomass were larger (Figures 3C,D). Comparable to *Arabidopsis*, the growth-stimulating effect disappeared during later stages of development. However, we observed a clear difference in the response of the two hosts on agar plates during early seedling's development, where root and shoot development can be monitored in more details. With fungal inoculation, the shoots and roots of 12-day-old *Arabidopsis* seedlings were bigger in the presence of the fungus (see Figure 5), while 12-day-old colonized *N. attenuata* had significantly shorter shoots and roots than the uncolonized controls (Figure 3E). We also observed more root hairs beneath the root-shoot junction, where roots are in contact with the fungus (Figure 3F). These effects were not observed for the roots of *Arabidopsis* seedlings. In conclusion, the fungus has different effects on the early development of the seedlings on agar medium.

The New *Trichoderma* Strain Is Tolerant Against 100 mM Salt and Mild Salt Conditions Promote the Interaction With the Host on Synthetic Medium

Plant growth promoting fungi and bacteria often also improve the stress tolerance of plants (Qin et al., 2016). Therefore, we first tested if the fungus itself is tolerant against salt and mannitol (osmotic) stress. Fungal growth was not altered on 100 mM NaCl compared to control plates without salt. At 300 mM NaCl, the mycelial growth was reduced by about 50%. At 1 M NaCl, only slowly growing mycelia could be detected after 10 days, and no growth was detectable on 3 M NaCl (Figure 4A and Supplementary Figures 3A–G). Increasing mannitol concentrations did not inhibit mycelial





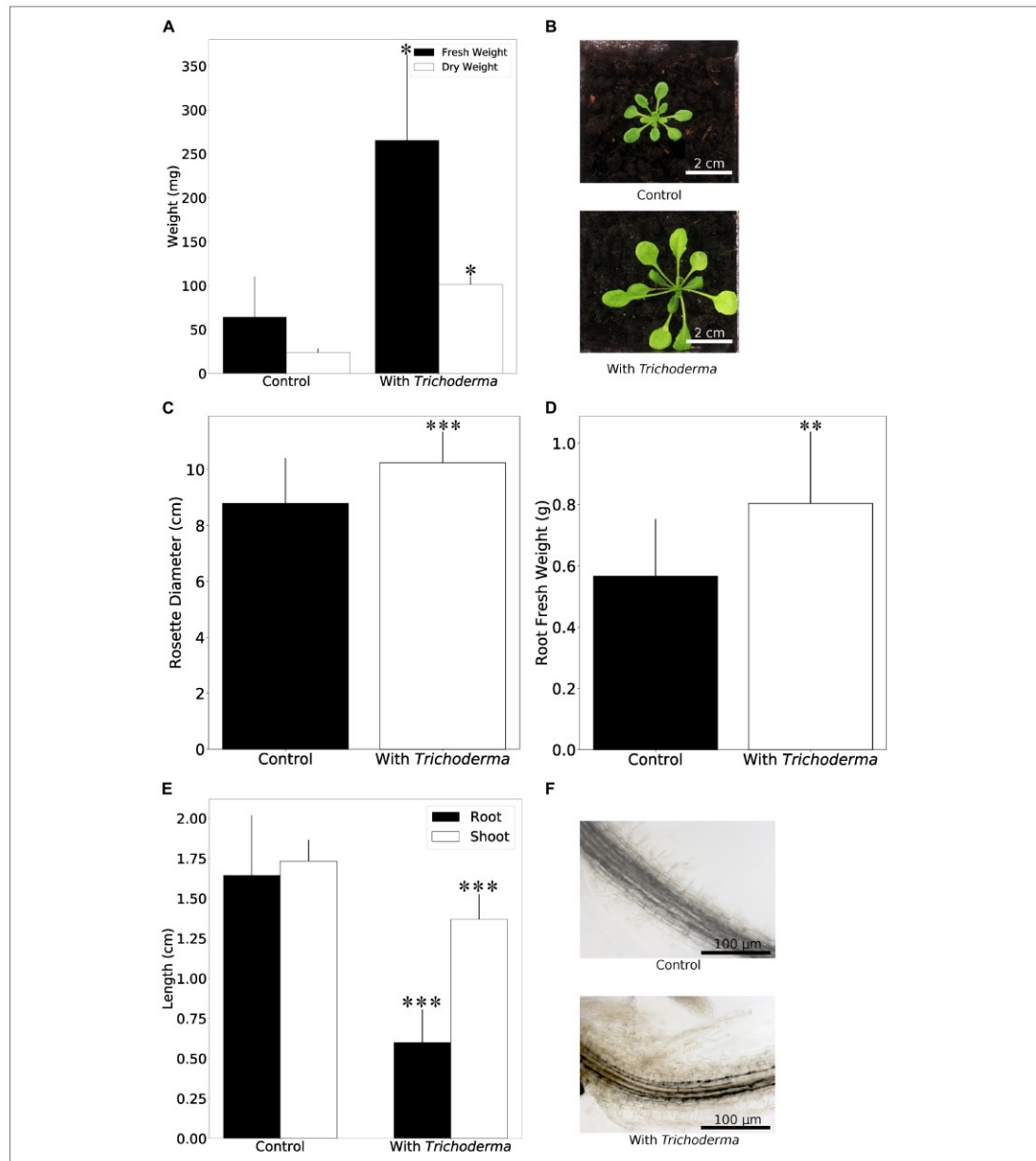
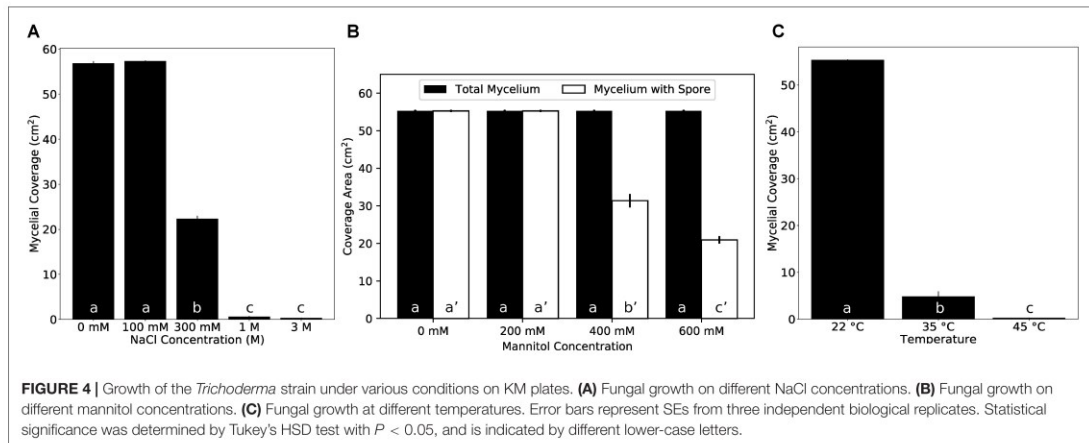


FIGURE 3 | Plant growth performance is influenced by *Trichoderma* colonization. **(A)** Fresh and dry weights of *A. thaliana* grown on soil with or without *Trichoderma* after 4 weeks. Error bars represent SEs from three independent biological replicates, each with four seedlings. Statistical significance was determined by Welch Two Sample *t*-test ($*P < 0.05$). **(B)** Growth promotion on *A. thaliana* on soil after 4 weeks. **(C,D)** Rosette diameter **(C)** and root fresh weight **(D)** of *N. attenuata* inoculated with or without *Trichoderma* on soil after 4 weeks. Error bars represent SDs from 39 independent biological replicates for shoots and 18 replicates for roots. Statistical significance was determined by Welch Two Sample *t*-test ($**P < 0.01$; $***P < 0.001$). **(E)** Shoot and root lengths of *N. attenuata* 12 days after co-cultivation with *Trichoderma* (spore solution O.D._{600 nm} = 0.0135) or without *Trichoderma* on Petri dishes. Error bars represent SDs from 10 biological replicates. Statistical significance was determined by Welch Two Sample *t*-test ($***P < 0.001$). **(F)** Microscopy of *N. attenuata* roots 12 days on Petri dishes with or without *Trichoderma*.



growth, although the production of conidia was reduced on media with >400 mM mannitol (Figure 4B and Supplementary Figures 3H–K). Also high temperature strongly impaired growth of the fungus (Figure 4C and Supplementary Figures 3L–N).

The ability of the fungus to survive 1 M NaCl intrigued us to find out if salt influences the growth stimulating effect of its host. Unlike on soil, when seedlings were grown on solid PNM medium without addition of NaCl for 5 days, we observed only a small increase in growth and biomass production of the *Arabidopsis* seedlings in the presence of the fungus. However, application of 50 mM NaCl to the medium strongly promoted growth and biomass production (Figures 5A,B; supported by *post-hoc* analysis shown in Supplementary Table 3). This was accompanied by a stronger root colonization (Figure 5C). In particular, the lateral roots of the host were massively colonized and the fungus produced large amounts of conidiospores, compared to those on medium without NaCl. On 100 mM and higher NaCl concentrations, the growth of the uncolonized plants was gradually reduced, and growth of *Trichoderma*-colonized roots was not stimulated any more (Figure 5A and Supplementary Figure 4). Closer inspections uncovered that roots were even more colonized, and the hyphae also appeared on the surface of the areal parts. They were not only detectable at and around the hypocotyl (Supplementary Figure 4) but also on the leaf surface (data not shown). In summary, apparently, the fungus colonizes preferentially the roots. Low NaCl concentrations promoted root colonization and stimulated plant growth, while higher salt concentrations forced the fungus to invade the aerial parts which was associated with a loss of the benefits to the host.

The New *Trichoderma* Strain Inhibits Growth of *Alternaria* and Protects *Arabidopsis* and *Nicotiana* Against *Alternaria* Infection

One of the prominent traits of *Trichoderma* species in the *harzianum* clade is their potential to act as bio-control agent. After 8 days of co-cultivation of *Alternaria brassicicola* with

the *Trichoderma* strain on PDA plates, the mycelial coverage of *A. brassicicola* was reduced by 73% and *Trichoderma* hyphae grew on top of the *A. brassicicola* mycelial lawn (Figures 6A–C). To rule out that faster growth of *Trichoderma* restricts *A. brassicicola* growth, *Trichoderma* was added to an agar plate with a 7-day old *A. brassicicola* culture (Figure 6D). After additional 7 days of co-cultivation, *Trichoderma* hyphae and spores were again observed on top of the *A. brassicicola* mycelial lawn (Figure 6E). This supports active predation of *A. brassicicola* by the new *Trichoderma* strain (Druzhinina et al., 2018).

We further tested *Fusarium brachygibbosum* and *Alternaria* spp. *Utah isolate 10*, two fungal species previously characterized as a native pathogen for *N. attenuata* (Luu et al., 2015), and co-cultivated them with *Trichoderma*. Growth of *Trichoderma* was much faster than that of the two other species, but *F. brachygibbosum* clearly stopped further growth of *Trichoderma* when hyphae of the two fungi met, while *Alternaria* spp. was overgrown by *Trichoderma* after 3½ weeks of co-cultivation (Figures 6F,G).

To test if the *Trichoderma* strain also protects plants from *Alternaria* infection, *Arabidopsis* seedlings were first exposed to *A. brassicicola* (A) or *Trichoderma* (T) or were mock-treated (C) and then transferred to plates with either *A. brassicicola* or *Trichoderma* for additional 7 days. As expected, the highest amount of *A. brassicicola* DNA was detected in seedlings which were exposed to *A. brassicicola* only (Figure 7A). Roots which were exposed to *Trichoderma* either before or after *A. brassicicola* treatment (A-T) contained less DNA of the fungal pathogen. Furthermore, the seedlings were better protected against *A. brassicicola* when they were already colonized by *Trichoderma* before pathogen infection (Figure 7A and Supplementary Figure 5A). Similar results were observed for *N. attenuata* and *Alternaria* (Supplementary Figure 5B). This demonstrates that the *Trichoderma* strain restricts growth of the pathogen in roots of its host plant.

To investigate whether *Trichoderma* also protects the leaves against *A. brassicicola* infection, 500 colony forming units (CFU)

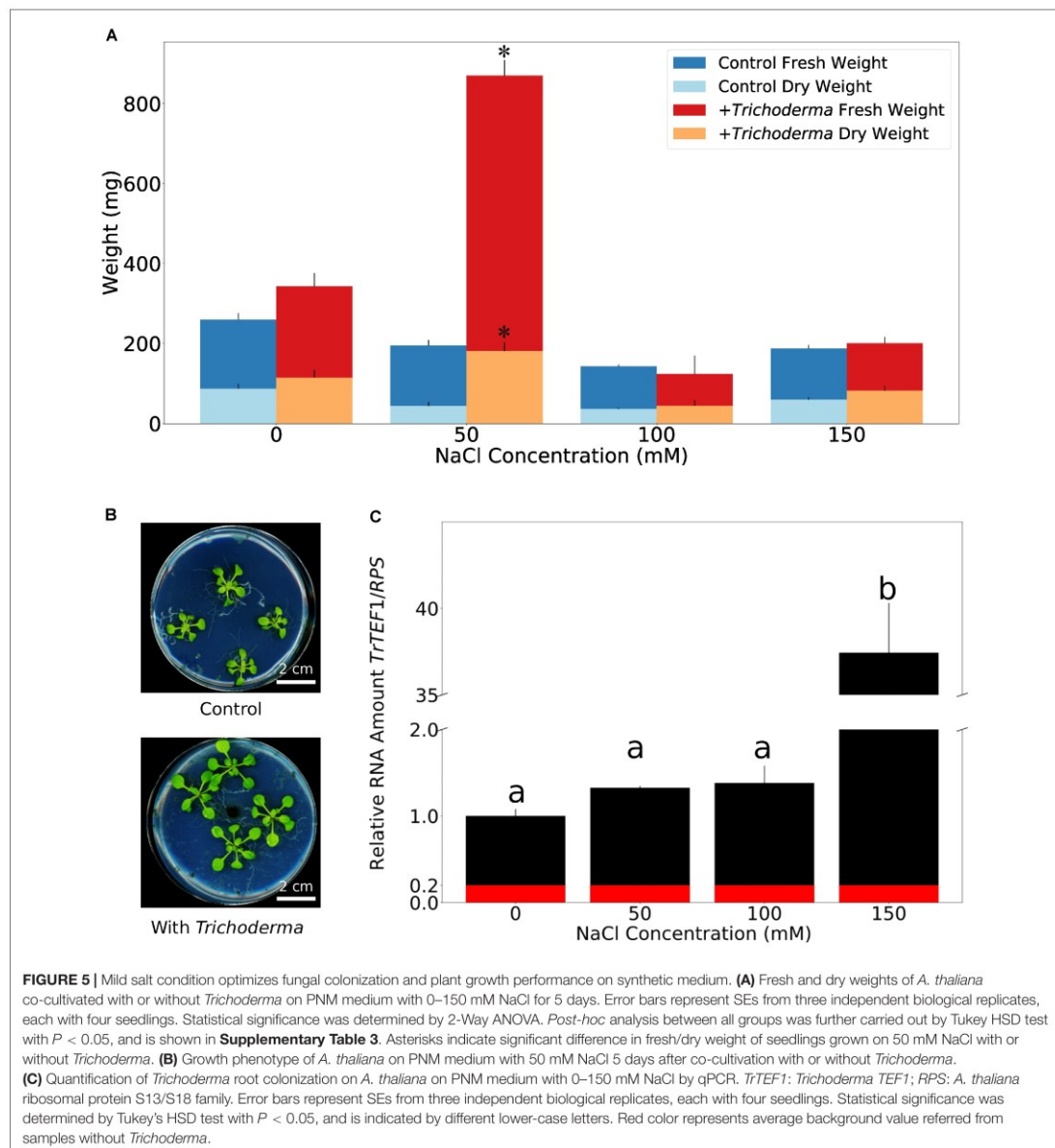
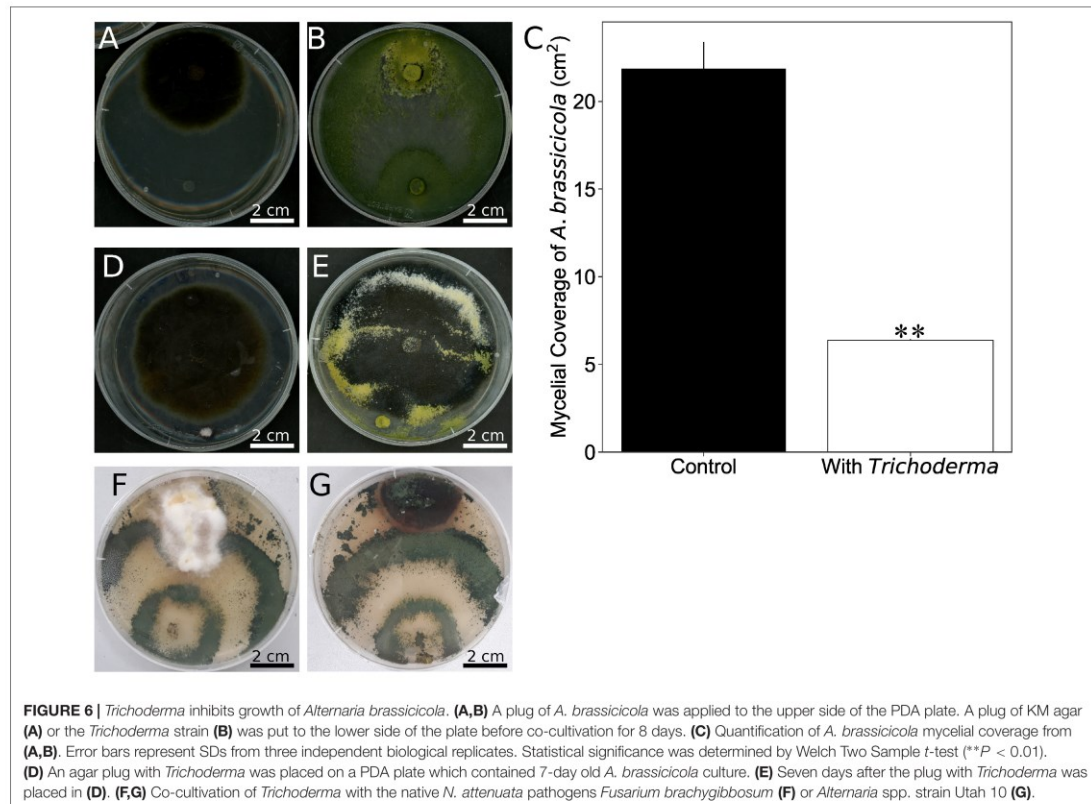


FIGURE 5 | Mild salt condition optimizes fungal colonization and plant growth performance on synthetic medium. **(A)** Fresh and dry weights of *A. thaliana* co-cultivated with or without *Trichoderma* on PNM medium with 0–150 mM NaCl for 5 days. Error bars represent SEs from three independent biological replicates, each with four seedlings. Statistical significance was determined by 2-Way ANOVA. *Post-hoc* analysis between all groups was further carried out by Tukey HSD test with $P < 0.05$, and is shown in **Supplementary Table 3**. Asterisks indicate significant difference in fresh/dry weight of seedlings grown on 50 mM NaCl with or without *Trichoderma*. **(B)** Growth phenotype of *A. thaliana* on PNM medium with 50 mM NaCl 5 days after co-cultivation with or without *Trichoderma*. **(C)** Quantification of *Trichoderma* root colonization on *A. thaliana* on PNM medium with 0–150 mM NaCl by qPCR. *TrTEF1*: *Trichoderma TEF1*; *RPS*: *A. thaliana* ribosomal protein S13/S18 family. Error bars represent SEs from three independent biological replicates, each with four seedlings. Statistical significance was determined by Tukey's HSD test with $P < 0.05$, and is indicated by different lower-case letters. Red color represents average background value referred from samples without *Trichoderma*.

of an *A. brassicicola* spore suspension were applied to the leaves of *Arabidopsis* seedlings which were either co-cultivated with the symbiont or mock-treated for 7 days. Four days later, the necrotic zone on the leaves of co-cultivated plants was significantly smaller compared to the non-colonized controls (**Figure 7B**). Taken together, *Trichoderma* restricts spread of *Alternaria* in both roots and shoots.

Mycorrhiza Formation Is Not Affected by the New *Trichoderma* Strain in *N. attenuata*

Restriction of *Alternaria* growth by the new *Trichoderma* strain indicated a putative use for bioprotection. However, agricultural application requires that other beneficial fungi, such as arbuscular mycorrhizal fungi (AMF) are not affected by the



Trichoderma strain. As *Arabidopsis* is a non-mycorrhizal species, we used the well-established *N. attenuata* system (Groten et al., 2015). *N. attenuata* plants grown on soil in the greenhouse were simultaneously inoculated with AMF and *Trichoderma*. Microscopic observations of the roots and qPCR analyses with fungus-specific markers clearly indicate that AMF and *Trichoderma* colonize the roots and propagate, without inhibiting each other (Figures 8A,B). In addition, the amounts of 11-carboxyblumenol, a marker for AMF root colonization (Wang et al., 2018a), did not differ between *Trichoderma*-inoculated and non-inoculated samples (Figure 8C). 11-Carboxyblumenol levels were also similar when plants were pre-inoculated with AMF and after 6 weeks co-cultured with *Trichoderma* (data not shown). These results suggest that AMF colonization is not affected by the new *Trichoderma* strain in *N. attenuata*.

The *Trichoderma* Strain Alters Phytohormone Levels in *Arabidopsis* Roots and Shoots

Beneficial plant-microbe interactions often result in altered phytohormone levels, which may lead to better fitness of the host upon pathogen attack but can also influence root colonization

due to an altered plant immune system (Jacobs et al., 2011). In mycelial cultures, we detected only trace amounts of auxin (indole-acetic acid, IAA) and SA (Figure 9A). However, SA in *Trichoderma*-colonized seedlings were significantly reduced in roots and increased in shoots compared to controls (Figure 9B). Metabolites related to the biosynthesis and degradation of JA as well as ABA and IAA also showed some minor changes after *Trichoderma* colonization, but compared to SA, these changes were rather weak (Figures 9C,D and Supplementary Figure 6). Overall, it appears that the fungus does not produce high hormone levels itself influencing plant performance, but the fungus may activate SA-dependent resistance responses in the plant.

DISCUSSION

In this study, a new endophytic *Trichoderma* strain is described. It belongs to the *harzianum* clade, closely related to *T. confertum*, *T. pleuroti* and *T. pleuroticola*. It survives under salt and osmotic stress, and possesses a strong capability to reduce *A. brassicicola* growth. The hyphae colonize the root surface and are found in root hairs of *A. thaliana*. Infection assays showed reduced

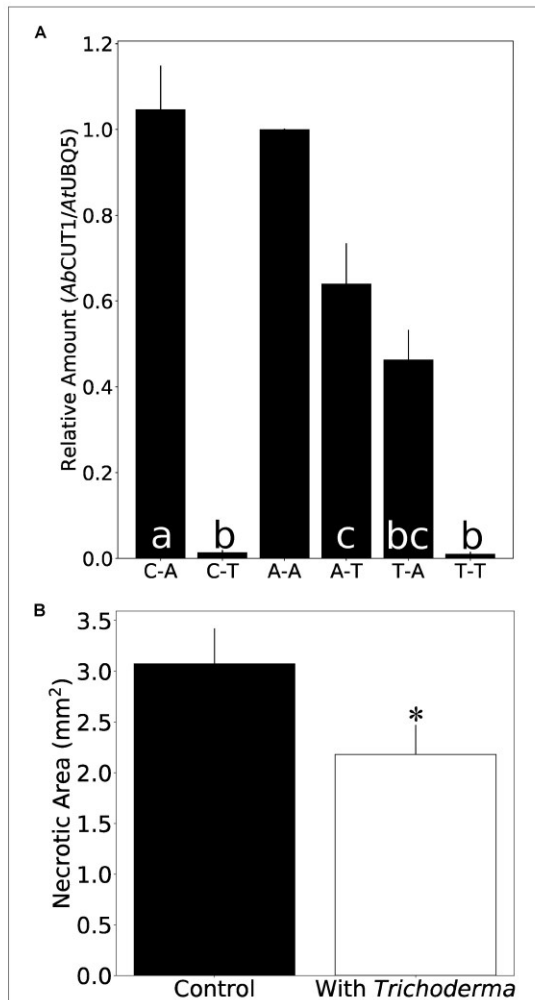


FIGURE 7 | *Trichoderma* protects *Arabidopsis* seedlings against *A. brassicicola* infection. **(A)** Amount of *A. brassicicola* *CUT1* DNA relative to *A. thaliana* *UBQ5* DNA in root tissue. C-A: co-cultivation with control plug for 7 days, then co-cultivation with *A. brassicicola* for another 7 days. C-T: co-cultivation with control plug for 7 days, then co-cultivation with *Trichoderma* for another 7 days. A-A: co-cultivation with *A. brassicicola* for 7 days, then co-cultivation with *A. brassicicola* for another 7 days. A-T: co-cultivation with *A. brassicicola* for 7 days, then co-cultivation with *Trichoderma* for another 7 days. T-A: co-cultivation with *Trichoderma* for 7 days, then co-cultivation with *A. brassicicola* for another 7 days. T-T: co-cultivation with *Trichoderma* for 7 days, then co-cultivation with *Trichoderma* for another 7 days. Values from qPCR experiment were normalized to A-A. Error bars represent SEs from three independent biological replicates, each with 6–9 seedlings. Statistical significance was determined by Tukey’s HSD test with $P < 0.05$, and is indicated by different lower-case letters. **(B)** Necrosis area on leaflets infected by *A. brassicicola*. Error bars represent SEs from 35 independent biological replicates. Statistical significance was determined by Welch Two Sample *t*-test (* $P < 0.05$).

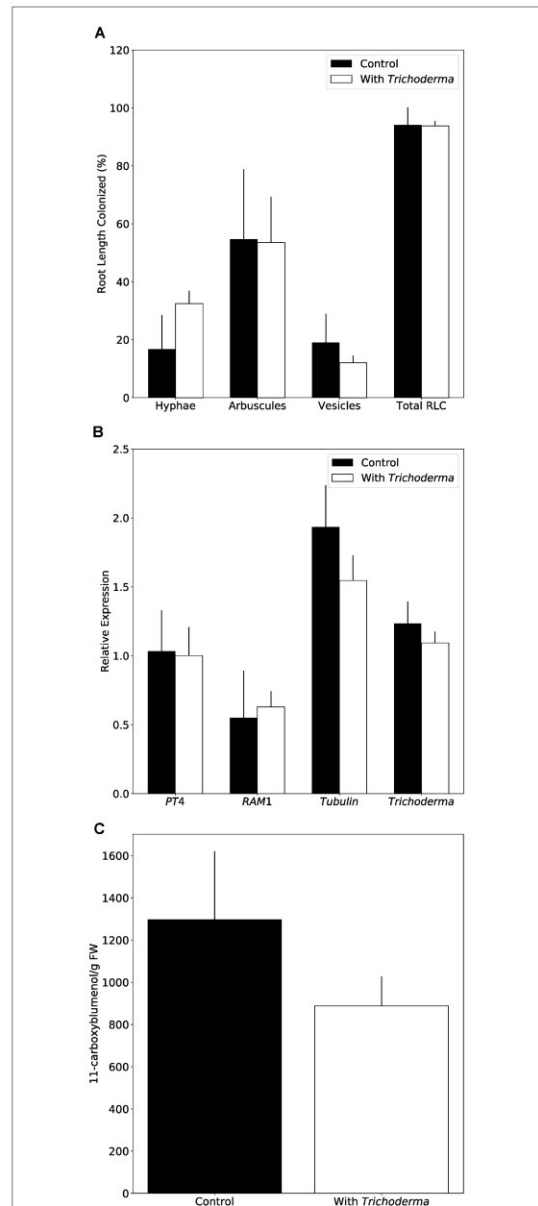


FIGURE 8 | *Trichoderma* does not interfere with mycorrhiza formation on *N. attenuata*. **(A)** AMF colonization 8 weeks after inoculation with or without *Trichoderma* and AMF simultaneously. Error bars represent SEs from three independent biological replicates. Statistical significance was determined by Welch Two Sample *t*-test between control and co-culture treatments and was not significantly different. RLC, Root length colonization. **(B)** AMF marker gene expression determined by qPCR. *PT4*, Phosphate transporter 4; *RAM1*, (Continued)

FIGURE 8 | Continued

Reduced Arbuscular Mycorrhization 1; *Tubulin*, *Tubulin* gene of *R. irregularis*; *Trichoderma*, *FPB2* of *Trichoderma*. Relative expression was normalized to *N. attenuata* elongation factor 1- α . Error bars represent SEs from three to five independent biological replicates. Statistical significance was determined by Welch Two Sample *t*-test between control and co-culture treatments, and was not significantly different. **(C)** 11-Carboxyblumenol level in *N. attenuata* roots 8 weeks after inoculation of AMF, with or without *Trichoderma*. Error bars represent SEs from five to six independent biological replicates. Statistical significance was determined by Welch Two Sample *t*-test between control and co-culture treatments; no significant differences were found.

A. brassicicola spread in roots and shoots of *Trichoderma*-colonized *Arabidopsis* plants, while mycorrhiza formation is not affected in *N. attenuata*. These observations are important for potential application of the endophyte as bio-control agent, and for the development of more effective and versatile bio-control agents.

Numerous *Trichoderma* species have been reported to stimulate plant growth (Contreras-Cornejo et al., 2009; González-Pérez et al., 2018), and *T. atroviride* and *T. virens* have been shown to promote root hair development (Contreras-Cornejo et al., 2015; González-Pérez et al., 2018). Our results highlight the importance of the growth conditions for the investigations of the symbiotic interactions with the new *Trichoderma* strain. Most importantly, as long as the symbionts grow in soil, we observe growth promotion during early phases of the development in the two tested host species. However, the growth stimulating effect of the fungus was barely or not detectable at all on agar plates, as long as no NaCl is added. A possible scenario could be that the fungus requires low concentrations of NaCl for growth and thus root colonization. If the salt concentration in the medium is too high, the fungus helps the plant by stimulating osmolyte production and Na⁺ elimination through root exudates (Contreras-Cornejo et al., 2014). We demonstrate that the fungus also tries to escape from the stress by growing on the plant material, since the roots become more colonized with increased salt concentrations. Ultimately, hyphae can also be detected in the aerial parts of the plant, which occurs only when the stress around the roots is high. We assume that the extensive fungal propagation triggers the plant defense machinery to restrict fungal growth and consequently may reduce the host's investment into growth. While our experiment focusses on the role of NaCl for the symbiosis, there are apparently other growth-stimulating factors in soil. A comparative analysis of the different growth conditions established in this study may help to elucidate critical parameters with agricultural relevance.

Root Colonization Alters Root Architecture

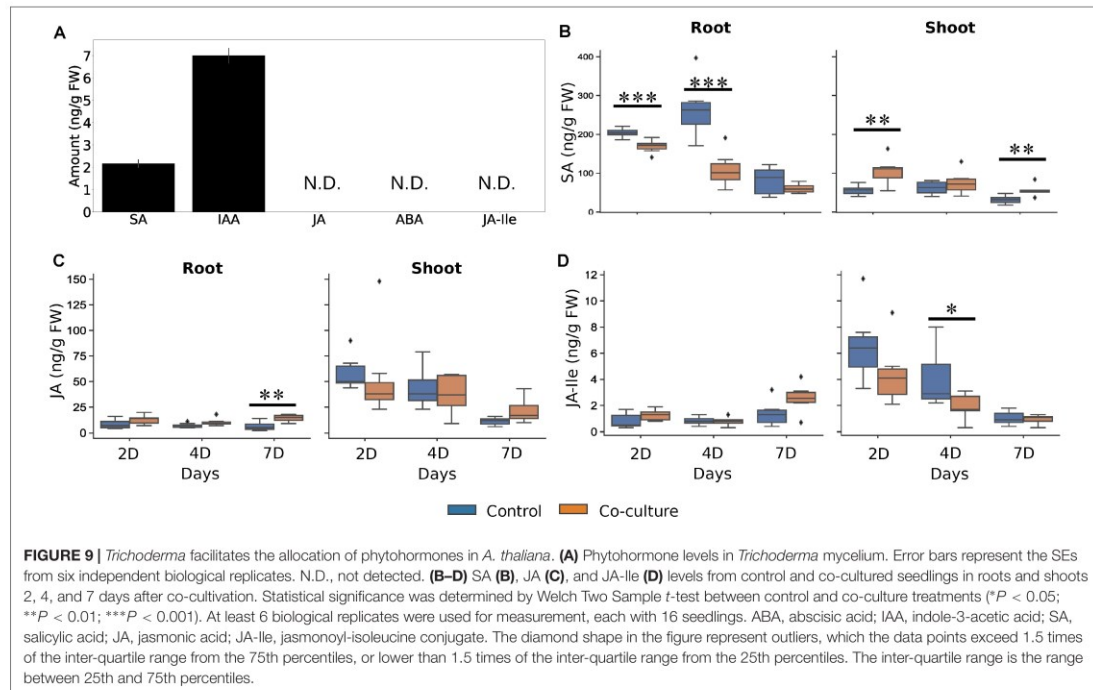
The new *Trichoderma* strain not only colonizes the root surface, but also penetrates into the root epidermis and resides in the root hairs (Figures 2E–G and Supplementary Movie 1). To the best of our knowledge, this is a new colonization strategy for *Trichoderma* species and demonstrates that the fungus can also live as endophyte. This finding is further

supported by the fact that the fungus was originally isolated from the leaf cells of a tree. Although *Trichoderma* species have been often reported to colonize plant roots (López-Bucio et al., 2015; Ruano-Rosa et al., 2016), the invasion of hyphae into root cells might indicate a closer symbiosis compared to other *Trichoderma* strains and species. Reprogramming of root development, inhibition of root growth and stimulating root branching is a typical feature of AMF (Bonfante and Genre, 2010), but also observed for *Trichoderma*-colonized *Arabidopsis* roots (e.g., Contreras-Cornejo et al., 2015). Similar to AMF associations, the endophyte might contribute to nutrient and water uptake and allow the plants to reduce their root sizes. Further studies are needed to support this hypothesis. Additionally, an increase in the number of root hairs may lead to a larger surface area for fungal attachment. Its close phylogenetic relationship to *Trichoderma* species which grow preferentially on mushrooms also demonstrates that minor changes in the *Trichoderma* genomes allow major changes, enlargements or alterations in their host range or preference.

The New *Trichoderma* Strain Has Potential as New Bio-Control Agent

The infection assays with *A. brassicicola* show effective protection of *Arabidopsis* roots and shoots by *Trichoderma*. Interestingly, the beneficial fungus also restricted growth of *A. brassicicola* in the roots, when the roots were already infected by the pathogen (Figure 7A, A-T vs. C-T). This is consistent with the plate experiments in which *Trichoderma* actively predated *A. brassicicola*. Propagation of the pathogen in the leaves is also restricted when the roots are colonized by *Trichoderma*. Different local and systemic plant immune responses against various pathogens in *Alternaria*-colonized hosts have been reported, however, a general strategy for *Trichoderma* species is not apparent (Busby et al., 2016; Rai and Agarkar, 2016). Apparently, systemic signals travel from the roots to the leaves, and this is reflected by elevated SA levels in the leaves of *Trichoderma*-colonized seedlings even before they are exposed to the pathogen (Figure 9B). The higher SA levels in the leaves might indicate that the new *Trichoderma* strain has the ability to induce SAR. The low or undetectable levels of the defense-related hormones in the mycelium suggest that they are not of fungal origin.

Another feature of this new strain is its ability to sustain beneficial microbe interaction with plants. Although pathogen progression in root tissue is hindered by the new *Trichoderma* strain, the presence of the fungus does not interfere with AMF colonization. Recently, Metwally and Al-Amri (2020) showed an interactive role of *Trichoderma viride* and AMF on growth and pigment content of onion plants, however, due to the small number of AMF–*Trichoderma*–host plant combinations that have been investigated so far, general conclusions on those tripartite interactions are not possible (cf. Szczalba et al., 2019). Those studies are important for a successful bio-control agent, as *Trichoderma* species are also competitors of beneficial microbes (Sood et al., 2020), which could impair plant growth or yield.



CONCLUSION

In conclusion, the new *Trichoderma* strain might be a useful tool as bio-control agent, since it stimulates the plant immune system against pathogen infection, but at the same time does not interfere with other beneficial microbial interactions, such as mycorrhizal formation. Its growth promoting ability in soil provides additional benefit in agricultural application. Furthermore, the experimental set-up allows us to address further questions to understand the role of this fungus on plant performance, especially why the fungus is successful in promoting plant growth in soil but not on minimal medium, and how it influences the balance between growth and stress responses under different environmental conditions.

DATA AVAILABILITY STATEMENT

The datasets generated for this study can be found in the online repositories. The names of the repository/repositories and accession number(s) can be found in the article/Supplementary Material.

AUTHOR CONTRIBUTIONS

Y-HT organized the project, performed the experiments, collected the samples and data, analyzed the results, plotted

the figures, and wrote up the study. HR performed the soil and salt experiments on *Arabidopsis*. KG performed the experiments on *Nicotiana*. PR isolated the *Trichoderma* strain. AF assisted in the microscopy. MR measured the phytohormones. IB, KN, RU, and RO edited the manuscript. RO organized the project and wrote up the study. All authors contributed to the article and approved the submitted version.

FUNDING

The work was supported by the CRC1127.

ACKNOWLEDGMENTS

We thank Veit Grabe from the Max Planck Institute for Chemical Ecology, Jena, for his assistance on confocal microscopy.

SUPPLEMENTARY MATERIAL

The Supplementary Material for this article can be found online at: <https://www.frontiersin.org/articles/10.3389/fpls.2020.573670/full#supplementary-material>

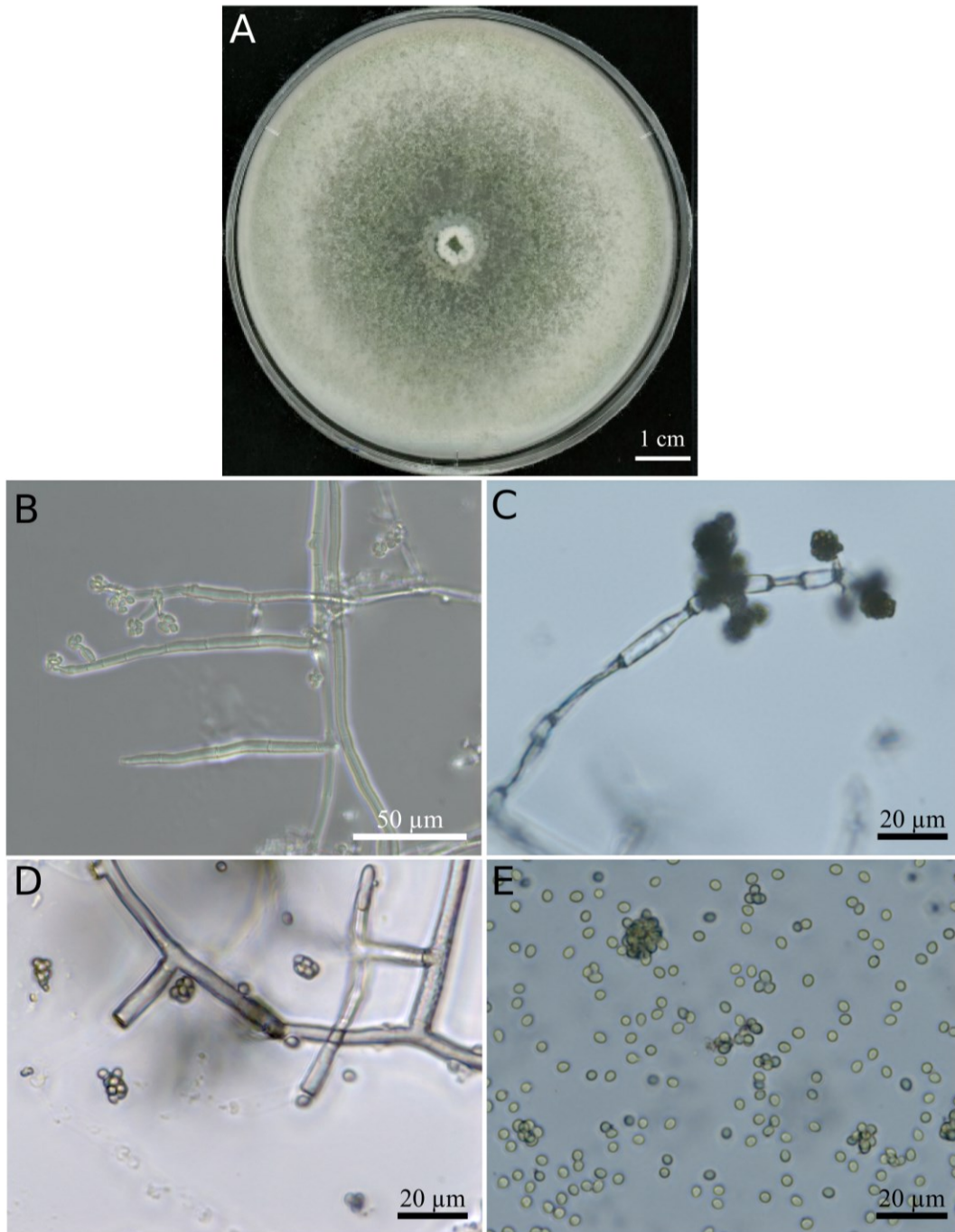
REFERENCES

- Bailey, B. A., and Melnick, R. L. (2013). "The endophytic *Trichoderma*," in *Trichoderma: Biology and Applications*, eds P. K. Mukherjee, B. K. Horwitz, U. S. Singh, M. Mukherjee, and M. Schmoll (Wallingford: CAB International), 152–172. doi: 10.1079/9781780642475.0000
- Bains, P. S., and Tewari, J. P. (1987). Purification, chemical characterization and host-specificity of the toxin produced by *Alternaria brassicae*. *Physiol. Mol. Plant Pathol.* 30, 259–271. doi: 10.1016/0885-5765(87)90039-7
- Berini, F., Caccia, S., Franzetti, E., Congiu, T., Marinelli, F., Casartelli, M., et al. (2016). Effects of *Trichoderma viride* chitinases on the peritrophic matrix of *Lepidoptera*. *Pest Manag. Sci.* 72, 980–989. doi: 10.1002/ps.4078
- Bonfante, P., and Genre, A. (2010). Mechanisms underlying beneficial plant–fungus interactions in mycorrhizal symbiosis. *Nat. Commun.* 1, 1–11. doi: 10.1038/ncomms1046
- Busby, P. E., Ridout, M., and Newcombe, G. (2016). Fungal endophytes: modifiers of plant disease. *Plant Mol. Biol.* 90, 645–655. doi: 10.1007/s11103-015-0412-0
- Carsolio, C., Gutiérrez, A., Jiménez, B., Van Montagu, M., and Herrera-Estrella, A. (1994). Characterization of ech-42, a *Trichoderma harzianum* endochitinase gene expressed during mycoparasitism. *Proc. Natl. Acad. Sci. U. S. A.* 91, 10903–10907. doi: 10.1073/pnas.91.23.10903
- Castresana, J. (2000). Selection of conserved blocks from multiple alignments for their use in phylogenetic analysis. *Mol. Biol. Evol.* 17, 540–552. doi: 10.1093/oxfordjournals.molbev.a026334
- Checker, V. G., Kushwaha, H. R., Kumari, P., and Yadav, S. (2018). "Role of phytohormones in plant defense: signaling and cross talk," in *Molecular Aspects of Plant-Pathogen Interaction*, eds A. Singh, and I. K. Singh (Singapore: Springer), 159–184. doi: 10.1007/978-981-10-7371-7_7
- Chen, K., and Zhuang, W.-Y. (2017). Seven new species of *Trichoderma* from soil in China. *Mycosystema* 36, 1441–1462. doi: 10.13346/j.mycosystema.170134
- Contreras-Cornejo, H. A., López-Bucio, J. S., Méndez-Bravo, A., Macías-Rodríguez, L., Ramos-Vega, M., Guevara-García, Á.A., et al. (2015). Mitogen-activated protein kinase 6 and ethylene and auxin signaling pathways are involved in *Arabidopsis* root-system architecture alterations by *Trichoderma atroviride*. *Mol. Plant-Microbe Interact.* 28, 701–710. doi: 10.1094/MPMI-01-15-0005-R
- Contreras-Cornejo, H. A., Macías-Rodríguez, L., Alfaro-Cuevas, R., and López-Bucio, J. (2014). *Trichoderma* spp. improve growth of *Arabidopsis* seedlings under salt stress through enhanced root development, osmolyte production, and Na⁺ elimination through root exudates. *Mol. Plant-Microbe Interact. MPMI* 27, 503–514. doi: 10.1094/MPMI-09-13-0265-R
- Contreras-Cornejo, H. A., Macías-Rodríguez, L., Cortés-Penagos, C., and López-Bucio, J. (2009). *Trichoderma virens*, a plant beneficial fungus, enhances biomass production and promotes lateral root growth through an auxin-dependent mechanism in *Arabidopsis*. *Plant Physiol.* 149, 1579–1592. doi: 10.1104/pp.108.130369
- Doyle, J. J. (1990). Isolation of plant DNA from fresh tissue. *Focus* 12, 13–15.
- Druzhinina, I. S., Chenthamara, K., Zhang, J., Atanasova, L., Yang, D., Miao, Y., et al. (2018). Massive lateral transfer of genes encoding plant cell wall-degrading enzymes to the mycoparasitic fungus *Trichoderma* from its plant-associated hosts. *PLoS Genet.* 14:e1007322. doi: 10.1371/journal.pgen.1007322
- Druzhinina, I. S., and Kubicek, C. P. (eds) (2016). *Environmental and Microbial Relationships*, 3rd Edn. Berlin: Springer International Publishing, doi: 10.1007/978-3-319-29532-9
- Druzhinina, I. S., Seidl-Seiboth, V., Herrera-Estrella, A., Horwitz, B. A., Kenerley, C. M., Monte, E., et al. (2011). *Trichoderma*: the genomics of opportunistic success. *Nat. Rev. Microbiol.* 9, 749–759. doi: 10.1038/nrmicro2637
- El-Katatny, M., Somitsch, W., Robra, K., El-Katatny, M., and Gubit, G. (2000). Production of chitinase and β -1,3-glucanase by *Trichoderma harzianum* for control of the phytopathogenic fungus *Sclerotium rolfsii*. *Food Technol. Biotechnol.* 38, 173–180.
- Furukawa, H., Kusne, S., Sutton, D. A., Manez, R., Carrau, R., Nichols, L., et al. (1998). Acute invasive sinusitis due to *Trichoderma longibrachiatum* in a liver and small bowel transplant recipient. *Clin. Infect. Dis. Off. Publ. Infect. Dis. Soc. Am.* 26, 487–489. doi: 10.1086/516317
- Gautheret, A., Dromer, F., Bourhis, J. H., and Andremont, A. (1995). *Trichoderma pseudokoningii* as a cause of fatal infection in a bone marrow transplant recipient. *Clin. Infect. Dis. Off. Publ. Infect. Dis. Soc. Am.* 20, 1063–1064. doi: 10.1093/clindis/20.4.1063
- Geyer, C. J. (1991). "Markov chain monte carlo maximum likelihood," in *Computing Science and Statistics: Proceedings of the 23rd Symposium on the Interface*, ed. E. M. Keramidas (Fairfax, VA: Interface Foundation), 156–163.
- González-Pérez, E., Ortega-Amaro, M. A., Salazar-Badillo, F. B., Bautista, E., Douterlungne, D., and Jiménez-Bremont, J. F. (2018). The *Arabidopsis*-*Trichoderma* interaction reveals that the fungal growth medium is an important factor in plant growth induction. *Sci. Rep.* 8:16427. doi: 10.1038/s41598-018-34500-w
- Grosch, R., Lottmann, J., Rehn, V. N. C., Rehn, K. G., Mendonça-Hagler, L., Smalla, K., et al. (2007). Analysis of antagonistic interactions between *Trichoderma* isolates from Brazilian weeds and the soil-borne pathogen *Rhizoctonia solani*. *J. Plant Dis. Prot.* 114, 167–175. doi: 10.1007/BF03356213
- Groten, K., Nawaz, A., Nguyen, N. H. T., Santhanam, R., and Baldwin, I. T. (2015). Silencing a key gene of the common symbiosis pathway in *Nicotiana attenuata* specifically impairs arbuscular mycorrhizal infection without influencing the root-associated microbiome or plant growth. *Plant Cell Environ.* 38, 2398–2416. doi: 10.1111/pce.12561
- Hermosa, R., Viterbo, A., Chet, I., and Monte, E. (2012). Plant-beneficial effects of *Trichoderma* and of its genes. *Microbiol. Read. Engl.* 158, 17–25. doi: 10.1099/mic.0.052274-0
- Heyer, M., Reichelt, M., and Mithöfer, A. (2018). A holistic approach to analyze systemic jasmonate accumulation in individual leaves of *Arabidopsis* rosettes upon wounding. *Front. Plant Sci.* 9:1569. doi: 10.3389/fpls.2018.01569
- Hill, T., and Käfer, E. (2001). Improved protocols for *Aspergillus* minimal medium: trace element and minimal medium salt stock solutions. *Fungal Genet Newslett.* 48, 20–21. doi: 10.4148/1941-4765.1173
- Huelsenbeck, J. P., and Ronquist, F. (2001). MRBAYES: bayesian inference of phylogenetic trees. *Bioinforma. Oxf. Engl.* 17, 754–755. doi: 10.1093/bioinformatics/17.8.754
- Jacobs, S., Zechmann, B., Molitor, A., Trujillo, M., Petutschnig, E., Lipka, V., et al. (2011). Broad-spectrum suppression of innate immunity is required for colonization of *Arabidopsis* roots by the Fungus *Piriformospora indica*. *Plant Physiol.* 156, 726–740. doi: 10.1104/pp.111.176446
- Johnson, J. M., Sherameti, I., Ludwig, A., Nongbri, P., Sun, C., Lou, B., et al. (2011). Protocols for *Arabidopsis thaliana* and *Piriformospora indica* co-cultivation – A model system to study plant beneficial traits. *Endocytobiosis Cell Res.* 21, 101–113.
- Karlsson, M., Atanasova, L., Jensen, D., and Zeilinger, S. (2017). "Necrotrophic mycoparasites and their genomes," in *The Fungal Kingdom*, eds J. Heitman, B. Howlett, P. Crous, E. Stukenbrock, T. James, and N. Gow (Washington, DC: ASM Press), 1005–1026. doi: 10.1128/microbiolspec.FUNK-0016-2016
- Katoh, K., Rozewicki, J., and Yamada, K. D. (2019). MAFFT online service: multiple sequence alignment, interactive sequence choice and visualization. *Brief. Bioinform.* 20, 1160–1166. doi: 10.1093/bib/bbx108
- Kistner, C., and Matamoros, M. (2005). "RNA isolation using phase extraction and LiCl precipitation," in *Lotus Japonicus Handbook*, ed. A. J. Márquez (Berlin: Springer-Verlag), 123–124. doi: 10.1007/1-4020-3735-X_9
- Kozlov, A. M., Darriba, D., Flouri, T., Morel, B., and Stamatakis, A. (2019). RAxML-NG: a fast, scalable and user-friendly tool for maximum likelihood phylogenetic inference. *Bioinforma. Oxf. Engl.* 35, 4453–4455. doi: 10.1093/bioinformatics/btz305
- Krügel, T., Lim, M., Gase, K., Halitschke, R., and Baldwin, I. T. (2002). Agrobacterium-mediated transformation of *Nicotiana attenuata*, a model ecological expression system. *Chemoecology* 12, 177–183. doi: 10.1007/PL00012666
- Lee, S., Yap, M., Behringer, G., Hung, R., and Bennett, J. W. (2016). Volatile organic compounds emitted by *Trichoderma* species mediate plant growth. *Fungal Biol. Biotechnol.* 3:7. doi: 10.1186/s40694-016-0025-7
- Leonetti, P., Zonno, M. C., Molinari, S., and Altomare, C. (2017). Induction of SA-signaling pathway and ethylene biosynthesis in *Trichoderma harzianum*-treated tomato plants after infection of the root-knot nematode *Meloidogyne incognita*. *Plant Cell Rep.* 36, 621–631. doi: 10.1007/s00299-017-2109-0
- Li, R.-X., Cai, F., Pang, G., Shen, Q.-R., Li, R., and Chen, W. (2015). Solubilisation of phosphate and micronutrients by *Trichoderma harzianum* and its relationship with the promotion of tomato plant growth. *PLoS One* 10:e0130081. doi: 10.1371/journal.pone.0130081

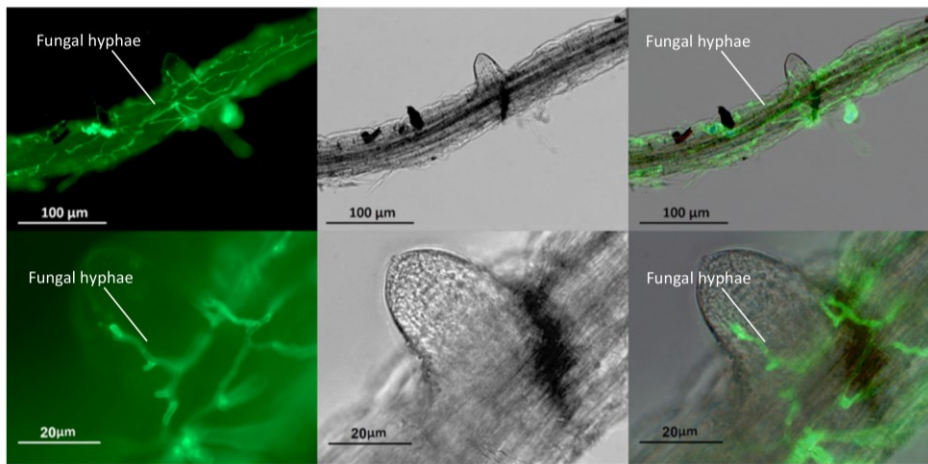
- Li, Y., Fu, K., Gao, S., Wu, Q., Fan, L., Li, Y., et al. (2013). Impact on bacterial community in midguts of the Asian corn borer larvae by transgenic *Trichoderma* strain overexpressing a heterologous chit42 gene with chitin-binding domain. *PLoS One* 8:e55555. doi: 10.1371/journal.pone.0055555
- Li Destri Nicosia, M. G., Mosca, S., Mercurio, R., and Schena, L. (2015). Dieback of *Pinus nigra* seedlings caused by a strain of *Trichoderma viride*. *Plant Dis.* 99, 44–49. doi: 10.1094/PDIS-04-14-0433-RE
- López-Bucio, J., Pelagio-Flores, R., and Herrera-Estrella, A. (2015). *Trichoderma* as biostimulant: exploiting the multilevel properties of a plant beneficial fungus. *Sci. Hort.* 196, 109–123. doi: 10.1016/j.scienta.2015.08.043
- Luu, V. T., Schuck, S., Kim, S.-G., Weinhold, A., and Baldwin, I. T. (2015). Jasmonic acid signalling mediates resistance of the wild tobacco *Nicotiana attenuata* to its native *Fusarium*, but not *Alternaria*, fungal pathogens. *Plant Cell Environ.* 38, 572–584. doi: 10.1111/pce.12416
- Martínez-Medina, A., Fernández, I., Sánchez-Guzmán, M. J., Jung, S. C., Pascual, J. A., and Pozo, M. J. (2013). Deciphering the hormonal signalling network behind the systemic resistance induced by *Trichoderma harzianum* in tomato. *Front. Plant Sci.* 4:206. doi: 10.3389/fpls.2013.00206
- McGonigle, T. P., Miller, M. H., Evans, D. G., Fairchild, G. L., and Swan, J. A. (1990). A new method which gives an objective measure of colonization of roots by vesicular–arbuscular mycorrhizal fungi. *New Phytol.* 115, 495–501. doi: 10.1111/j.1469-8137.1990.tb00476.x
- Metwally, R. A., and Al-Amri, S. M. (2020). Individual and interactive role of *Trichoderma viride* and arbuscular mycorrhizal fungi on growth and pigment content of onion plants. *Lett. Appl. Microbiol.* 70, 79–86. doi: 10.1111/lam.13246
- Mukherjee, A. K., Sampath Kumar, A., Kranthi, S., and Mukherjee, P. K. (2014). Biocontrol potential of three novel *Trichoderma* strains: isolation, evaluation and formulation. *3 Biotech* 4, 275–281. doi: 10.1007/s13205-013-0150-4
- Murashige, T., and Skoog, F. (1962). A revised medium for rapid growth and bioassays with tobacco tissue cultures. *Physiol. Plant.* 15, 473–497. doi: 10.1111/j.1399-3054.1962.tb08052.x
- Park, M. S., Bae, K. S., and Yu, S. H. (2006). Two new species of *Trichoderma* associated with green mold of oyster mushroom cultivation in Korea. *Mycobiology* 34, 111–113. doi: 10.4489/MYCO.2006.34.3.111
- Prajapati, M. S., Patel, J. B., Modi, K., and Shah, M. B. (2010). *Leucas aspera*: a review. *Pharmacogn. Rev.* 4, 85–87. doi: 10.4103/0973-7847.65330
- Qin, Y., Druzhinina, I. S., Pan, X., and Yuan, Z. (2016). Microbially mediated plant salt tolerance and microbiome-based solutions for saline agriculture. *Biotechnol. Adv.* 34, 1245–1259. doi: 10.1016/j.biotechadv.2016.08.005
- Rai, M., and Agarkar, G. (2016). Plant–fungal interactions: what triggers the fungi to switch among lifestyles? *Crit. Rev. Microbiol.* 42, 428–438. doi: 10.3109/1040841X.2014.958052
- Rajani, P., Rajasekaran, C., Vasanthakumari, M. M., Olsson, S. B., Ravikanth, G., Uma Shaanker, R., et al. (2020). Inhibition of plant pathogenic fungi by endophytic *Trichoderma* spp. through mycoparasitism and volatile organic compounds. *Microbiol. Res.* 242:126595. doi: 10.1016/j.micres.2020.126595
- Rambaut, A. (2018). *FigTree*. Available at: <http://tree.bio.ed.ac.uk/software/figtree/> (accessed June 11, 2020).
- Rocha-Ramirez, V., Omero, C., Chet, I., Horwitz, B. A., and Herrera-Estrella, A. (2002). *Trichoderma atroviride* G-protein alpha-subunit gene *tgal* is involved in mycoparasitic coiling and conidiation. *Eukaryot. Cell* 1, 594–605. doi: 10.1128/ec.1.4.594-605.2002
- Ronquist, F., and Huelsenbeck, J. (2003). MRBAYES 3: bayesian phylogenetic inference under mixed models. *Bioinform. Oxf. Engl.* 19, 1572–1574. doi: 10.1093/bioinformatics/btg180
- Rosmana, A., Nasaruddin, N., Hendarto, H., Hakkar, A. A., and Agriansyah, N. (2016). Endophytic association of *Trichoderma asperellum* within *Theobroma cacao* suppresses vascular streak dieback incidence and promotes side graft growth. *Mycobiology* 44, 180–186. doi: 10.5941/MYCO.2016.44.3.180
- Ruano-Rosa, D., Prieto, P., Rincón, A., Gómez Rodríguez, M. V., Valderrama, R., Barroso, J., et al. (2016). Fate of *Trichoderma harzianum* in the olive rhizosphere: time course of the root colonization process and interaction with the fungal pathogen *Verticillium dahliae*. *BioControl* 61, 269–282. doi: 10.1007/s10526-015-9706-z
- Samolski, I., Rincón, A. M., Pinzón, L. M., Viterbo, A., and Monte, E. (2012). The *qid74* gene from *Trichoderma harzianum* has a role in root architecture and plant biofertilization. *Microbiol. Read. Engl.* 158, 129–138. doi: 10.1099/mic.0.053140-0
- Santhanam, R., Menezes, R. C., Grabe, V., Li, D., Baldwin, I. T., and Groten, K. (2019). A suite of complementary biocontrol traits allows a native consortium of root-associated bacteria to protect their host plant from a fungal sudden-wilt disease. *Mol. Ecol.* 28, 1154–1169. doi: 10.1111/mec.15012
- Schindelin, J., Arganda-Carreras, I., Frise, E., Kaynig, V., Longair, M., Pietzsch, T., et al. (2012). Fiji: an open-source platform for biological-image analysis. *Nat. Methods* 9, 676–682. doi: 10.1038/nmeth.2019
- Sivakumaran, A., Akinyemi, A., Mandon, J., Cristescu, S. M., Hall, M. A., Harren, F. J. M., et al. (2016). ABA suppresses *Botrytis cinerea* elicited NO production in tomato to influence H₂O₂ generation and increase host susceptibility. *Front. Plant Sci.* 7:709. doi: 10.3389/fpls.2016.00709
- Sood, M., Kapoor, D., Kumar, V., Sheteiwy, M. S., Ramakrishnan, M., Landi, M., et al. (2020). *Trichoderma*: the “secrets” of a multitailed biocontrol agent. *Plants Basel Switz.* 9:762. doi: 10.3390/plants9060762
- Stöver, B. C., and Müller, K. F. (2010). TreeGraph 2: combining and visualizing evidence from different phylogenetic analyses. *BMC Bioinformatics* 11:7. doi: 10.1186/1471-2105-11-7
- Studholme, D. J., Harris, B., Le Cocq, K., Winsbury, R., Perera, V., Ryder, L., et al. (2013). Investigating the beneficial traits of *Trichoderma hamatum* GD12 for sustainable agriculture—insights from genomics. *Front. Plant Sci.* 4:258. doi: 10.3389/fpls.2013.00258
- Swofford, D. (2002). *PAUP*. Phylogenetic Analysis Using Parsimony (*and Other Methods). Version 4.0b10*. doi: 10.1111/j.0014-3820.2002.tb00191.x
- Szczalba, M., Kopta, T., Gęstoł, M., and Sękara, A. (2019). Comprehensive insight into arbuscular mycorrhizal fungi, *Trichoderma* spp. and plant multilevel interactions with emphasis on biostimulation of horticultural crops. *J. Appl. Microbiol.* 127, 630–647. doi: 10.1111/jam.14247
- Tavare, S. (1986). Some probabilistic and statistical problems on the analysis of DNA sequences. *Lect. Math. Life Sci.* 17, 57–86.
- Wang, M., Schäfer, M., Li, D., Halitschke, R., Dong, C., McGale, E., et al. (2018a). Blumenols as shoot markers of root symbiosis with arbuscular mycorrhizal fungi. *eLife* 7:e37093. doi: 10.7554/eLife.37093
- Wang, M., Wilde, J., Baldwin, I. T., and Groten, K. (2018b). *Nicotiana attenuata*'s capacity to interact with arbuscular mycorrhiza alters its competitive ability and elicits major changes in the leaf transcriptome. *J. Integr. Plant Biol.* 60, 242–261. doi: 10.1111/jipb.12609
- Woo, S. L., Ruocco, M., Vinale, F., Nigro, M., Marra, R., Lombardi, N., et al. (2014). *Trichoderma*-based products and their widespread use in agriculture. *Open Mycol. J.* 8, 71–126. doi: 10.2174/1874437001408010071
- Yang, Z. (1993). Maximum-likelihood estimation of phylogeny from DNA sequences when substitution rates differ over sites. *Mol. Biol. Evol.* 10, 1396–1401. doi: 10.1093/oxfordjournals.molbev.a040082
- Zhang, Y., and Zhuang, W.-Y. (2020). *Trichoderma brevicrassum* strain TC967 with capacities of diminishing cucumber disease caused by *Rhizoctonia solani* and promoting plant growth. *Biol. Control* 142:104151. doi: 10.1016/j.biocontrol.2019.104151

Conflict of Interest: The authors declare that the research was conducted in the absence of any commercial or financial relationships that could be construed as a potential conflict of interest.

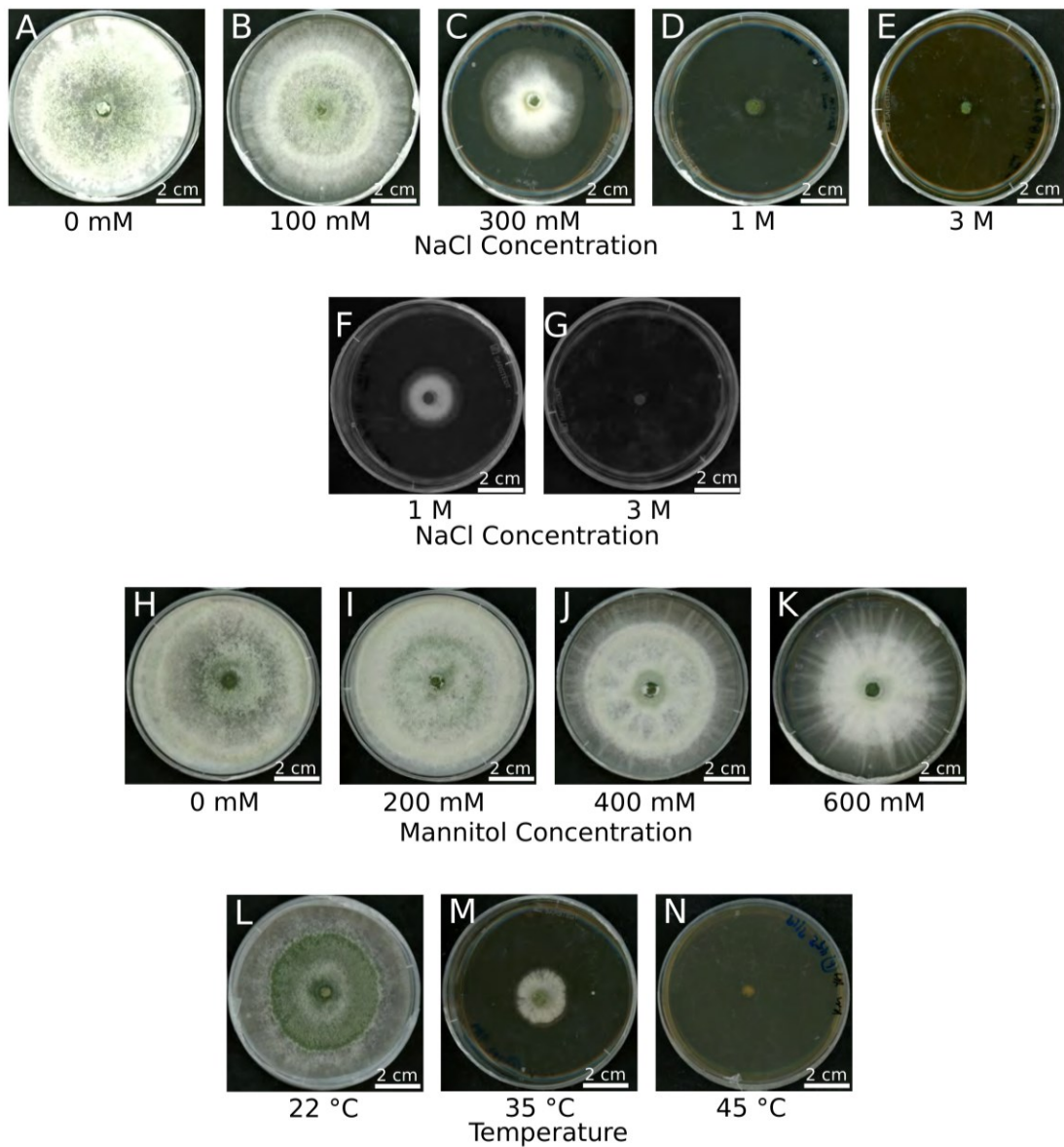
Copyright © 2020 Tseng, Rouina, Groten, Rajani, Furch, Reichelt, Baldwin, Nataraja, Uma Shaanker and Oelmüller. This is an open-access article distributed under the terms of the Creative Commons Attribution License (CC BY). The use, distribution or reproduction in other forums is permitted, provided the original author(s) and the copyright owner(s) are credited and that the original publication in this journal is cited, in accordance with accepted academic practice. No use, distribution or reproduction is permitted which does not comply with these terms.



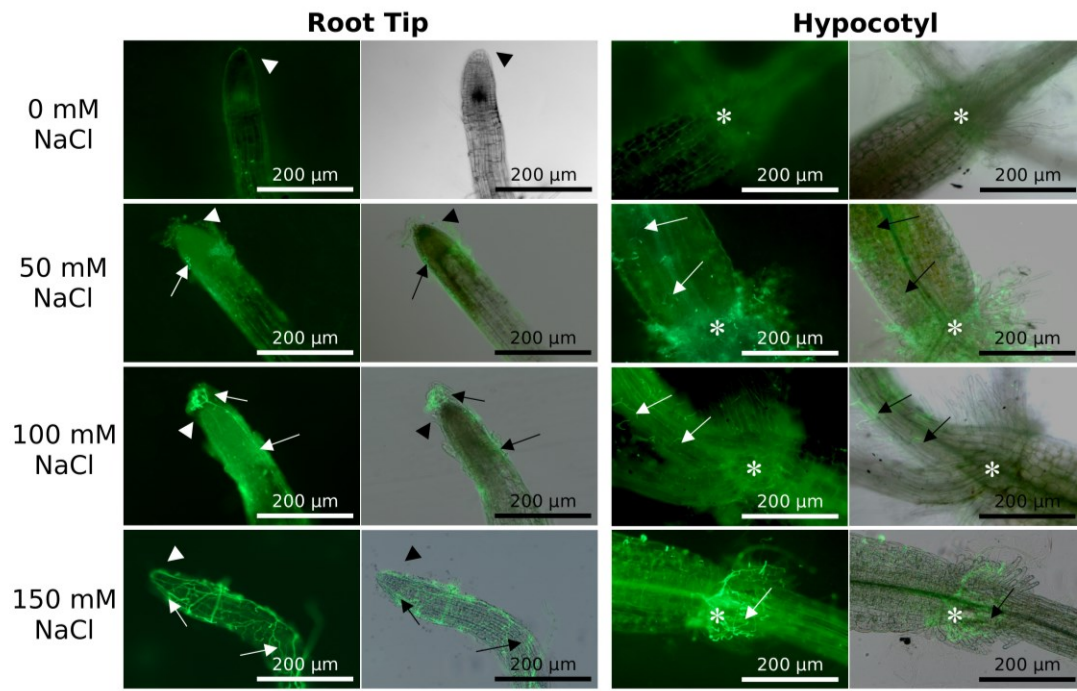
Supplementary Figure 1. Morphology of the new *Trichoderma* strain. **(A):** The strain on KM plates after 4 days. **(B) - (D):** Developing conidia 3 **(B)** and 7 **(C - D)** days after incubation. **(E):** Released conidia.



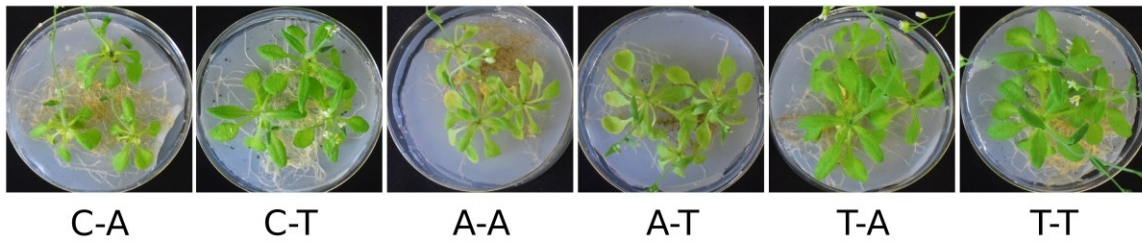
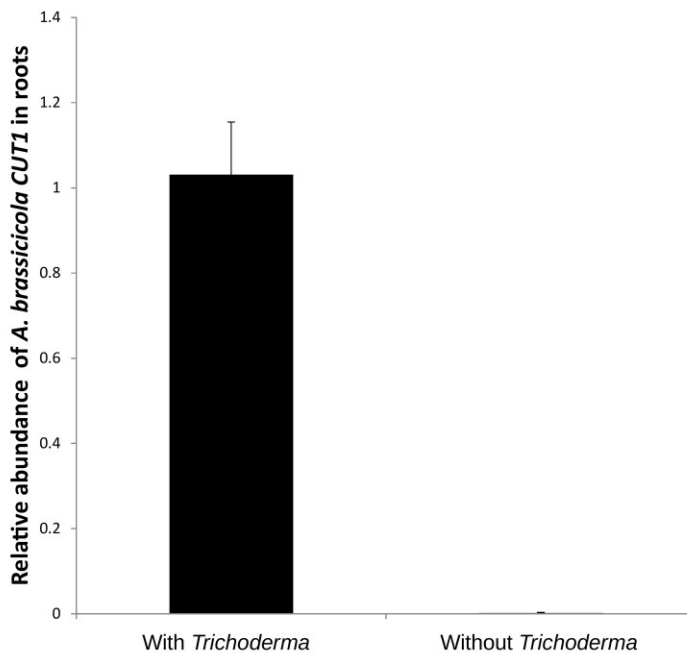
Supplementary Figure 2. Colonization of *Trichoderma* on *Arabidopsis* roots on soil. Left: Fluorescence of fungal stain; Center: bright field; Right: overlay. Fungal hyphae was stained by WGA Alexa Fluor™ 488 conjugate and visualized by fluorescence.



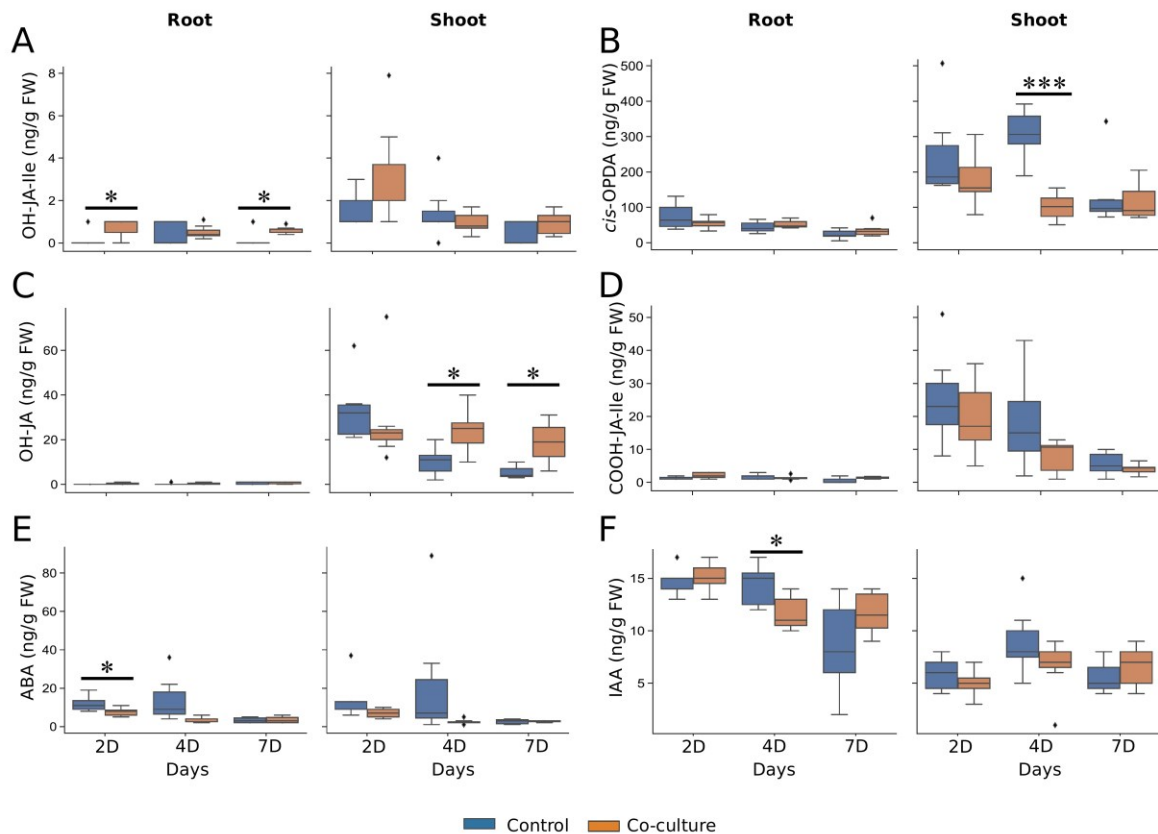
Supplementary Figure 3. Growth phenotype of the *Trichoderma* strain under various conditions on KM plates. **(A) - (E):** Fungal growth on different NaCl concentrations for 4 days. **(F) and (G):** Mycelial growth on KM plates with 1 M **(F)** or 3 M **(G)** NaCl for 10 days. **(H) - (K):** Fungal growth on different mannitol concentrations for 4 days. **(L) - (N):** Fungal growth at different temperatures for 4 days.



Supplementary Figure 4. Root colonization on *A. thaliana* on PNM medium with 0 - 150 mM NaCl. Root tips, hypocotyls and fungal hyphae are indicated by filled triangles, asterisks and arrows, respectively.

A**B**

Supplementary Figure 5. *Trichoderma* strain prevents *A. brassicicola* spread in root. **(A):** Growth of *Arabidopsis* seedlings infected by *A. brassicicola* or cultivated with the *Trichoderma* strain. C-A: co-cultivation with control plug for 7 days, then co-cultivation with *A. brassicicola* for another 7 days. C-T: co-cultivation with control plug for 7 days, then co-cultivation with *Trichoderma* for another 7 days. A-A: co-cultivation with *A. brassicicola* for 7 days, then co-cultivation with *A. brassicicola* for another 7 days. A-T: co-cultivation with *A. brassicicola* for 7 days, then co-cultivation with *Trichoderma* for another 7 days. T-A: co-cultivation with *Trichoderma* for 7 days, then co-cultivation with *A. brassicicola* for another 7 days. T-T: co-cultivation with *Trichoderma* for 7 days, then co-cultivation with *Trichoderma* for another 7 days. **(B):** Relative DNA Amount of *A. brassicicola* CUT1 to *N. attenuata* TEF1.



Supplementary Figure 6. Phytohormone redistribution in *A. thaliana* facilitated by *Trichoderma*. **(A):** OH-JA-Ile **(B):** *cis*-OPDA **(C):** OH-JA **(D):** COOH-JA-Ile **(E):** ABA and **(F):** IAA levels from control and co-cultured seedlings in roots and shoots 2, 4 and 7 days after co-cultivation. Statistical significance was determined by Welch Two Sample t-test between control and co-culture treatments (* $P < 0.05$; *** $P < 0.001$). At least 6 biological replicates were used for measurement, each with 16 seedlings. ABA: abscisic acid; IAA: indole-3-acetic acid; *cis*-OPDA: *cis*-12-oxo-phytodienoic acid; OH-JA: 12-hydroxyl jasmonic acid; OH-JA-Ile: 12-hydroxyl-jasmonyl-isoleucine; COOH-JA-Ile: 12-carboxyl-jasmonyl-isoleucine. The diamond shape in the figure represent outliers, which the data points exceed 1.5 times of the inter-quartile range from the 75th percentiles, or lower than 1.5 times of the inter-quartile range from the 25th percentiles. The inter-quartile range is the range between 25th and 75th percentiles.

Supplementary Table 1. Sequence accessions used in the multilocus phylogenetic analysis.

Name	Strain	GenBank Accession Number	
		<i>TEF1</i>	<i>RPB2</i>
<i>Trichoderma</i> sp. in this study		MT591352	MT602550
<i>T. pleuroti</i>	CBS 124387	HM142382	HM142372
<i>T. pleurotica</i>	CBS 124383	HM142381	HM142371
<i>T. afroharzianum</i>	GJS 04-186	FJ463301	FJ442691
<i>T. afarasin</i>	Dis341F	FJ463400	FJ442778
<i>T. asperelloides</i>	GJS 04-187	JN133571	JN133560
	GJS 04-116	GU248412	GU248411
<i>T. asperellum</i>	CBS 433.97	AY376058.1	EU248617.1
	GJS 90-7	EU338333	EU338337
	GJS 01-294	EU856323	FJ150788
	GJS 06-294	GU198235	GU198266
	CGMCC 6422	KF425756	KF425755
	GJS 05-328	EU248627	EU248614
<i>T. atrobrunneum</i>	GJS 04-67	FJ463360	FJ442724
<i>T. atroviride</i>	DAOM 222144	AF456889	FJ442754
<i>T. gamsii</i>	GJS 04-09	DQ307541	JN133561
<i>T. harzianum</i>	T55	KX632625	KX632568
	T18	KX632606	KX632549
	T2	KX632591	KX632534
	CBS 226.95	AF348101	AF545549
	T11	KX632486	KX632543
<i>T. hispanicum</i>	S453	JN715659	JN715600
<i>T. inhamatum</i>	CBS 273.78	AF348099	FJ442725
<i>T. junci</i>	CBS 120926	FJ860641	FJ860540
<i>T. lentiforme</i>	Dis 218E	FJ463310	FJ442793

<i>T. lieckfeldtia</i>	GJS 00-14	EU856326	EU883562
<i>T. lixii</i>	GJS 97-96	AF443938	KJ665290
<i>T. rifaii</i>	Dis 337F	FJ463321	FJ442720
<i>T. samuelsii</i>	S5	JN715651	JN715599
<i>T. viride</i>	CBS 119325	DQ672615	EU711362
<i>T. longibrachiatum</i>	CBS 816.68	AY865640.1	DQ087242.1
<i>T. confertum</i>	TC62	MF371218	MF371203
	TC139	MF371220	MF371205
<i>T. aggressivum</i>	CBS 100525	AF534614	AF545541
<i>T. alni</i>	CBS 120633	EU498312	EU498349
<i>T. amazonicum</i>	IB 95	HM142377	HM142368
<i>T. atrogelatinosum</i>	LU 498	KJ871087	KJ842176
<i>T. velutinum</i>	CPK 298	KJ665769	KF134794
<i>T. tomentosum</i>	DAOM 178713a	AF534630	AF545557
<i>T. tawa</i>	GJS 97-174	AY392004	AY391956
<i>T. stramineum</i>	GJS 02-84	AY391999	AY391945
<i>T. rufobrunneum</i>	HMAS 266614	KF729989	KF730010
<i>T. catoptron</i>	GJS 02-76	AY391963	AY391900
<i>T. pseudogelatinosum</i>	CNUN 309	HM920202	HM920173
<i>T. priscilae</i>	S168	KJ665691	KJ665333
<i>T. parepimyces</i>	CBS 122769	FJ860664	FJ860562
<i>T. longifialidicum</i>	LESF 552	KT279020	KT278955
<i>T. ceraceum</i>	GJS 88-28	AY391964	AY391901
<i>T. cerinum</i>	DAOM 230012	AY605802	KJ842184
<i>T. christiani</i>	S442	KJ665439	KJ665244
<i>T. cinnamomeum</i>	GJS 97-237	AY391979	AY391920
<i>T. compactum</i>	CBS 121218	KF134798	KF134789
<i>T. corneum</i>	GJS 97-82	KJ665455	KJ665252

<i>T. dacrymycellum</i>	WU 29044	FJ860633	FJ860533
<i>T. epimyces</i>	CBS 120534	EU498320	EU498360
<i>T. italicum</i>	S131	KJ665525	KJ665282
<i>Nectria eustromatica</i>	CBS 125578	HM534876	HM534887

Supplementary Table 2. Details of phytohormone analysis by LC-MS/MS [HPLC 1260 (Agilent Technologies)-QTRAP6500 (SCIEX)] in negative ionization mode.

Q1	Q3	RT (min)	Compound	Internal standard	RF	DP	EP	CE	CXP
136.93	93	3.3	SA	D4-SA	1.0	-20	-8	-24	-7
263	153.2	3.4	ABA	D6-ABA	1.0	-20	-12	-22	-2
209.07	59	3.6	JA	D6-JA	1.0	-20	-9	-24	-2
322.19	130.1	3.9	JA-Ile	D6-JA-Ile	1.0	-50	-4.5	-30	-4
290.9	165.1	4.6	OPDA	D6-JA	1.0	-20	-12	-24	-2
338.1	130.1	3	OH-JA-Ile	D6-JA-Ile	1.0	-50	-4.5	-30	-4
225.1	59	2.6	OH-JA	D6-JA	1.0	-20	-9	-24	-2
352.1	130.1	3	COOH-JA-Ile	D6-JA-Ile	1.0	-50	-4.5	-30	-4
140.93	97	3.3	D4-SA			-20	-8	-24	-7
269	159.2	3.4	D6-ABA			-20	-12	-22	-2
215	59	3.6	D6-JA			-20	-9	-24	-2
214	59	3.6	D5-JA			-20	-9	-24	-2
328.19	130.1	3.9	D6-JA-Ile			-50	-4.5	-30	-4
327.19	130.1	3.9	D5-JA-Ile			-50	-4.5	-30	-4

Supplementary Table 3. Post-hoc analysis of *Arabidopsis* fresh/dry weight with (Y) or without (N) *Trichoderma* under different salt concentrations by Tukey HSD.

Fresh Weight	Difference (mg)	p adj.
Y:0mM-N:0mM	83.3333	0.3986
N:50mM-N:0mM	-66.6667	0.6509
Y:50mM-N:0mM	613.3333	0.0000
N:100mM-N:0mM	-116.6667	0.0997
Y:100mM-N:0mM	-136.6667	0.0376
N:150mM-N:0mM	-70.0000	0.5986
Y:150mM-N:0mM	-60.0000	0.7516
N:50mM-Y:0mM	-150.0000	0.0191
Y:50mM-Y:0mM	530.0000	0.0000
N:100mM-Y:0mM	-200.0000	0.0015
Y:100mM-Y:0mM	-220.0000	0.0005
N:150mM-Y:0mM	-153.3333	0.0161
Y:150mM-Y:0mM	-143.3333	0.0269
Y:50mM-N:50mM	680.0000	0.0000
N:100mM-N:50mM	-50.0000	0.8776
Y:100mM-N:50mM	-70.0000	0.5986
N:150mM-N:50mM	-3.3333	1.0000
Y:150mM-N:50mM	6.6667	1.0000
N:100mM-Y:50mM	-730.0000	0.0000
Y:100mM-Y:50mM	-750.0000	0.0000
N:150mM-Y:50mM	-683.3333	0.0000
Y:150mM-Y:50mM	-673.3333	0.0000
Y:100mM-N:100mM	-20.0000	0.9993
N:150mM-N:100mM	46.6667	0.9097
Y:150mM-N:100mM	56.6667	0.7979
N:150mM-Y:100mM	66.6667	0.6509
Y:150mM-Y:100mM	76.6667	0.4952
Y:150mM-N:150mM	10.0000	1.0000
Dry Weight	Difference (mg)	p adj.
Y:0mM-N:0mM	26.6667	0.7569
N:50mM-N:0mM	-43.3333	0.2387
Y:50mM-N:0mM	96.6667	0.0007
N:100mM-N:0mM	-53.3333	0.0882
Y:100mM-N:0mM	-43.3333	0.2387
N:150mM-N:0mM	-30.0000	0.6444
Y:150mM-N:0mM	-6.6667	0.9999
N:50mM-Y:0mM	-70.0000	0.0137
Y:50mM-Y:0mM	70.0000	0.0137
N:100mM-Y:0mM	-80.0000	0.0043
Y:100mM-Y:0mM	-70.0000	0.0137

N:150mM-Y:0mM	-56.6667	0.0616
Y:150mM-Y:0mM	-33.3333	0.5278
Y:50mM-N:50mM	140.0000	0.0000
N:100mM-N:50mM	-10.0000	0.9985
Y:100mM-N:50mM	0.0000	1.0000
N:150mM-N:50mM	13.3333	0.9914
Y:150mM-N:50mM	36.6667	0.4173
N:100mM-Y:50mM	-150.0000	0.0000
Y:100mM-Y:50mM	-140.0000	0.0000
N:150mM-Y:50mM	-126.6667	0.0000
Y:150mM-Y:50mM	-103.3333	0.0003
Y:100mM-N:100mM	10.0000	0.9985
N:150mM-N:100mM	23.3333	0.8538
Y:150mM-N:100mM	46.6667	0.1743
N:150mM-Y:100mM	13.3333	0.9914
Y:150mM-Y:100mM	36.6667	0.4173
Y:150mM-N:150mM	23.3333	0.8538

4.2 Manuscript 2

***Arabidopsis* Restricts Sugar Loss to a Colonizing *Trichoderma harzianum* Strain by Downregulating *SWEET11* and *-12* and Upregulation of *SUC1* and *SWEET2* in the Roots**

Hamid Rouina, Yu-Heng Tseng, Karaba N. Nataraja, Ramanan Uma Shaanker, Ralf Oelmüller

Published in *Microorganisms* (2021)

Microorganisms 9(6), 1246. doi: 10.3390/microorganisms9061246



Article

Arabidopsis Restricts Sugar Loss to a Colonizing *Trichoderma harzianum* Strain by Downregulating *SWEET11* and *-12* and Upregulation of *SUC1* and *SWEET2* in the Roots

Hamid Rouina¹, Yu-Heng Tseng¹, Karaba N. Nataraja², Ramanan Uma Shaanker³ and Ralf Oelmüller^{1,2,*}

¹ Department of Plant Physiology, Matthias Schleiden Institute of Genetics, Bioinformatics and Molecular Botany, Friedrich-Schiller-University Jena, 07743 Jena, Germany; a.h.rouina@gmail.com (H.R.); yu.tseng@uni-jena.de (Y.-H.T.)

² Department of Crop Physiology, University of Agricultural Sciences, GKVK, Bangalore 560065, Karnataka, India; nataraja_karaba@yahoo.com

³ School of Ecology and Conservation, University of Agricultural Sciences, GKVK, Bangalore 560065, Karnataka, India; umashaanker@gmail.com

* Correspondence: b7oera@uni-jena.de



Citation: Rouina, H.; Tseng, Y.-H.; Nataraja, K.N.; Uma Shaanker, R.; Oelmüller, R. *Arabidopsis* Restricts Sugar Loss to a Colonizing *Trichoderma harzianum* Strain by Downregulating *SWEET11* and *-12* and Upregulation of *SUC1* and *SWEET2* in the Roots. *Microorganisms* **2021**, *9*, 1246. <https://doi.org/10.3390/microorganisms9061246>

Academic Editors: Kerstin Voigt and Mohamed I. Abdelwahab Hassan

Received: 18 May 2021

Accepted: 4 June 2021

Published: 8 June 2021

Publisher's Note: MDPI stays neutral with regard to jurisdictional claims in published maps and institutional affiliations.



Copyright: © 2021 by the authors. Licensee MDPI, Basel, Switzerland. This article is an open access article distributed under the terms and conditions of the Creative Commons Attribution (CC BY) license (<https://creativecommons.org/licenses/by/4.0/>).

Abstract: Phosphate (Pi) availability has a strong influence on the symbiotic interaction between *Arabidopsis* and a recently described root-colonizing beneficial *Trichoderma harzianum* strain. When transferred to media with insoluble $\text{Ca}_3(\text{PO}_4)_2$ as a sole Pi source, *Arabidopsis* seedlings died after 10 days. *Trichoderma* grew on the medium containing $\text{Ca}_3(\text{PO}_4)_2$ and the fungus did colonize in roots, stems, and shoots of the host. The efficiency of the photosynthetic electron transport of the colonized seedlings grown on $\text{Ca}_3(\text{PO}_4)_2$ medium was reduced and the seedlings died earlier, indicating that the fungus exerts an additional stress to the plant. Interestingly, the fungus initially alleviated the Pi starvation response and did not activate defense responses against the hyphal propagation. However, in colonized roots, the sucrose transporter genes *SWEET11* and *-12* were strongly down-regulated, restricting the unloading of sucrose from the phloem parenchyma cells to the apoplast. Simultaneously, up-regulation of *SUC1* promoted sucrose uptake from the apoplast into the parenchyma cells and of *SWEET2* sequestration of sucrose in the vacuole of the root cells. We propose that the fungus tries to escape from the $\text{Ca}_3(\text{PO}_4)_2$ medium and colonizes the entire host. To prevent excessive sugar consumption by the propagating hyphae, the host restricts sugar availability in its apoplastic root space by downregulating sugar transporter genes for phloem unloading, and by upregulating transporter genes which maintain the sugar in the root cells.

Keywords: *Trichoderma*; *SWEET11*; *SWEET12*; *SWEET2*; *SUC1*; sucrose/sugar transporter; endophyte; symbiosis; *Arabidopsis*; phosphate starvation; *Trichoderma harzianum*

1. Introduction

Beneficial interactions between fungi and host plant roots rely on the exchange of nutrients between the symbiotic partners. Well investigated examples are mycorrhizal symbioses, where the plant delivers photo-assimilates to the fungi and fungi inorganic ions, in particular phosphate (Pi), and water to their hosts [1]. Quite similar exchanges might occur in beneficial symbiotic endophyte/plant interactions, although the molecular, cellular, and physiological bases are less understood [2,3] and ref. therein. All these beneficial symbioses are fragile and can shift to neutral, saprophytic, or even pathogenic interactions when stress conditions impair the exchange balance, and the survival of one of the symbiotic partners is compromised [4].

Upon Pi limitation, roots respond with the upregulation of Pi transporter genes and some Pi starvation regulators. The high affinity Pi transporters *Pht1;1* and *Pht1;4* play a major role in Pi acquisition under low Pi conditions [5]. *Pht1;1* and *-1;4* are induced by

Pi starvation, and the transporter activities are controlled by additional mechanisms, including protein trafficking, localization, and degradation [6]. Furthermore, PHOSPHATE1 (PHO1) is the main Pi transporter into the xylem and *PHO1* is preferentially expressed in the root vascular system under low Pi [7]. Chen et al. [8] demonstrated that WRKY6 regulates *PHO1* expression, whereas low Pi reduced WRKY6-binding to the *PHO1* promoter, thereby stimulating the expression of the gene. In addition, expression of many Pi transporter genes is controlled by Pi starvation response (PHR) transcription factors [9–13]. Castrillo et al. [14] showed that PHR1 is a central regulator in balancing the Pi starvation response and plant immune regulation, which occurs mainly post-transcriptionally and is only weakly regulated at the transcriptional level.

Restriction of fungal growth due to nutrient limitations in the environment promotes colonization of the host plants by suppressing the host's immune system. On the other hand, the increased demand of the fungus for photosynthates forces the plant to control its sucrose distribution to prevent loss to the microbes. Under Pi limitation, the plants transport more sugar from the leaves to the roots through the phloem to support root growth [15]. However, this also has tremendous effects on the growth of the root-associated fungi. They obtain the sugar either through direct transport from host cell to microbial cell [16], from the host apoplast, which contains the secreted sugar after release from the phloem cells, or from the rhizosphere, which contains secreted sugar from different root cells. Several transporter families have been proposed to transport sugars to the symbiotic partners [16]. Loading and unloading of the root phloem parenchyma cells with sugar involves the SWEET transporters [17,18] and ref. therein. The unloaded sucrose in the root apoplast is mainly transported into the mesophyll or epidermal root cells by SUC1 [2] and further transported into the vacuole of these cells by SWEET2, where it is stored [19]. Most of the hyphae of beneficial root-colonizing endophytic fungi grow in the root apoplastic space, which makes it likely that they also use the sugar from this plant compartment.

We studied the symbiotic interaction of *Arabidopsis* with a recently characterized *Trichoderma harzianum* strain [20]. The fungus strongly promotes plant growth on soil and full culture medium [20]. However, under Pi limitation, the fungus colonizes *Arabidopsis* aggressively, shifting the beneficial relationship towards an interaction with no or fewer benefits for the host. By analyzing genes for sugar and Pi transporters, as well as for defense, we were able to dissect the influence of Pi limitation on the symbiosis and propose a model for the shift in this interaction.

2. Methods and Materials

2.1. Growth Conditions of Plants and Fungus

Arabidopsis thaliana (ecotype Columbia-0) was used for this study. The seeds were surface-sterilized with a solution containing sterile distilled water (dH₂O), sodium lauroyl sarcosinate, and DanKlorix (GP GABA GmbH Hamburg, Germany; 64%, 4%, 32%; v/v/v) for eight minutes under constant shaking, followed by six rinses with dH₂O. Surface-sterile seeds were sown on MS media supplemented with 0.3% gelrite [21]. After cold treatment at 4 °C for 48 h, plates were incubated for 10 days at 22 °C under continuous illumination (100 μmol m⁻² sec⁻¹). The *Trichoderma* strain was propagated on KM medium (pH 6.5) for a week at 25 °C in the dark, as described previously, and pH changes were monitored by adding 0.004% (w/v) bromocresol purple pH indicator [20]. All experiments with insoluble Pi were performed on National Botanical Research Institute's Pi growth medium (NBRIP) (glucose, 10 g/L; Ca₃(PO₄)₂, 2.5 g/L; MgCl₂ × 6 H₂O, 5 g/L; MgSO₄ × 7 H₂O, 0.25 g/L; KCl, 0.2 g/L; and (NH₄)₂SO₄, 0.1 g/L), either on plates with 0.3% gelrite or in liquid medium for fungal growth. The medium with soluble Pi, which was used as a control, contained the same molar Pi concentration of K₃PO₄ instead of Ca₃(PO₄)₂.

2.2. *Trichoderma*-*Arabidopsis* Co-Cultivation

Cocultivation of *A. thaliana* and *Trichoderma* strain was performed under in vitro culture conditions. Ten-day-old *A. thaliana* seedlings of equal sizes were directly transferred

from MS medium to NBRIP medium. The fungus was grown on NBRIP plates. The cocultivation of *Arabidopsis* plants and *Trichoderma* strain were performed on NBRIP medium. A 5 mm plug of the *Trichoderma* strain was placed at the center of the cocultivation's plate. Cocultivation was monitored over a period of 10 days at 22 °C under continuous illumination ($100 \mu\text{mol m}^{-2} \text{s}^{-1}$) [20,22].

2.3. RNA Extraction and cDNA Synthesis

RNA was isolated from the roots of colonized and uncolonized *Arabidopsis* seedlings with an RNA isolation kit (RNeasy, Qiagen, Hilden, Germany) and used for quantitative RT-PCR. Reverse transcription of 1 μg of total RNA was performed with an oligo(dT) primer. First strand synthesis was performed with a kit from Qiagen (Omniscript RT Kit, Qiagen, Hilden, Germany).

2.4. Real-Time PCR

Real-time quantitative RT-PCR was performed using the iCycler iQ real-time PCR detection system and iCycler software version 2.2 (Bio-Rad, Munich, Germany). For the amplification of the PCR products, iQ SYBR Supermix from Bio-Rad was used according to the manufacturer's instructions in a final volume of 23 μL . The iCycler was programmed to 95 °C 3 min, $40 \times (94 \text{ }^\circ\text{C 30 s, 57 }^\circ\text{C 30 s, 72 }^\circ\text{C 40 s})$, 72 °C 10 min, followed by a melting curve program (50–85 °C in increasing steps of 0.5 °C). All reactions were repeated at least 3 times. The mRNA levels for each cDNA probe were normalized with respect to the *Arabidopsis glyceraldehyde-3-phosphate dehydrogenase 2 (GAPC2)* and/or *ACTIN2* mRNA level. Fold induction values for the *tefl* mRNA levels (Genbank accession number: MT591352) from the *Trichoderma* cDNA were calculated with the ΔCt equation. Root colonization was determined relative to the plant *GAPC2* cDNA levels. The primer pairs for the *Arabidopsis* genes are given in the Supplementary Table S1.

2.5. Fluorescence Microscopy

The entire *Arabidopsis* roots, root tips, hypocotyls, and leaves were imaged using an AXIO Imager.M2 (Zeiss Microscopy GmbH, Jena, Germany) equipped with a 10 \times objective (N-Achroplan 10 \times /0.3). The bright field and fluorescence images (EX 545/25 and EM 605/70) were recorded with a color camera (AXIOCAM 503 color Zeiss, Jena, Germany) by use of an EGFP (EM 525/50 nm) and DsRED filter (EM 605/70 nm). Digital images were processed with the ZEN software (Zeiss, Jena, Germany), treated with Adobe R PhotoShop to optimize brightness, contrast, and coloring, and to overlay the photomicrographs to confirm fluorescence information.

2.6. Measurement of Photosynthesis Parameters

The *Arabidopsis* seedlings were dark-adapted for 15 min and the chlorophyll fluorescence was measured using a FluorCam 700F (Photon System Instruments, Czech Republic). Program parameters of FluorCam were set according to Wagner et al. [23]. The maximum quantum yield of the photosystem II (Fv/Fm) was calculated according to Maxwell and Johnson [24].

2.7. Acid Phosphatase (AcP) Assay

Extraction for the AcPase activity assays was carried out using 50 mL of sterilized NBRIP broth in a 100 mL conical flask. The flasks were inoculated with 1 mL of *Trichoderma* spore solution. The inoculated flasks were incubated at 25 °C for three days. The samples were centrifuged at 10,000 rpm for 10 min at 4 °C. The cell-free supernatant was assayed for crude AcP activity according to the method outlined by Tabatabai and Bremner [25]. One mL of the supernatant was mixed with 4 mL of modified universal buffer (pH 6.5). Further to this, 0.025 mM disodium p-nitrophenyl Pi (tetrahydrate) was mixed with the culture supernatant and incubated at 37 °C for 1 h. After 1 h of incubation, the reaction was stopped by adding 4 mL of 0.5 M NaOH and 1 mL of 0.5 M CaCl_2 . The concentration

of p-nitrophenol was measured in triplicate by measuring the absorbance at 420 nm using a UV-Vis spectrophotometer, and the amount was quantified based on a standard curve with serially diluted solutions of p-nitrophenol. One unit (U) of phosphatase activity was defined as the amount of enzyme required to release 1 mol of p-nitrophenol/mL/min from di-Na p-nitrophenyl Pi (tetrahydrate) under the assay condition.

2.8. Quantitative Estimation of Soluble Pi

Erlenmeyer flasks containing 100 mL of NBRIP broth without bromophenol were inoculated with 1 mL spore solution of 5-day-old fungal cultures. Non-inoculated medium served as a control. The flasks were incubated in the dark at 25 °C for three days. The pH of the culture medium was measured 72 h after inoculation. A volume of 5 mL of the fungal culture was collected and centrifuged at 10,000 rpm for 10 min. The supernatant used to estimate the released Pi was determined spectrophotometrically (880 nm) according to Murphy and Riley [26].

3. Results

3.1. Pi Limitation Promotes Plant Colonisation

We have previously shown that cocultivation of *Arabidopsis* seedlings with the *Trichoderma* strain resulted in the colonization of the roots and the establishment of a beneficial symbiotic interaction. The fungus promoted growth of the host and defended it against pathogen attack [20]. Without stress, the fungal colonization was restricted to the roots, and hyphae were never detected in the aerial parts of the *Arabidopsis* seedlings [20]. To test how nutrient limitation influences the symbiotic interaction, we co-cultivated *Trichoderma* and *Arabidopsis* seedlings on NBRIP medium with insoluble $\text{Ca}_3(\text{PO}_4)_2$ as sole Pi source.

As expected, when 10-day-old *Arabidopsis* seedlings were transferred from MS medium to the NBRIP medium, they started to die after an additional 10 days (Figure 1A). If these seedlings were transferred to soil, none of them recovered ($n = 3$ with 100 seedlings each; data not shown). Compared to control media with soluble Pi, the *Trichoderma* strain could only slowly grow in liquid NBRIP medium and on solid NBRIP agar plates (Figure 1B), since the fungus had AcP activity (Figure 1C) and can solubilize $\text{Ca}_3(\text{PO}_4)_2$. The AcP activity, as well as solubilized Pi in the medium, is shown in .

When *Arabidopsis* seedlings and the fungus were cocultured on NBRIP plates, we observed a fast root colonization (Figure 1D). After 2 days, hyphae can also be detected on the stem and, ultimately, leaves (Figure 2). Figure 2B shows the presence of hyphae at the stem/leaf junction 5 days after exposure to the fungus on insoluble Pi medium. At the same time, on soluble Pi medium, hyphae can only be detected in the roots (Figure 2B). The seedlings did not benefit from the interaction (Figure 1E). This can be shown by a recovery assay after transfer to soil. If the colonized seedlings were transferred to soil 8 days after colonization, $4.2 \pm 0.6\%$ ($n = 3$) survived, while $29.0 \pm 3.7\%$ ($n = 3$) survived when they were not exposed to the fungus.

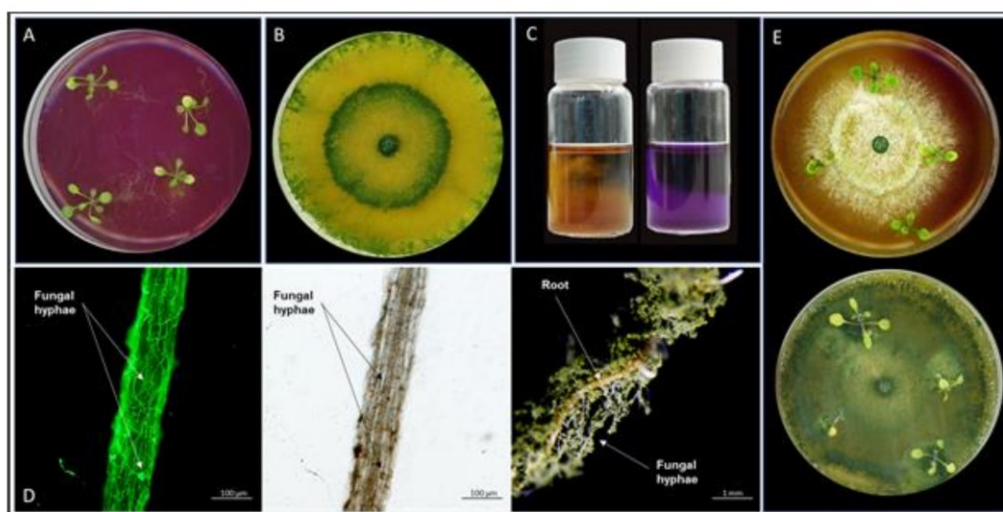


Figure 1. *Arabidopsis* and *Trichoderma* growth performance on NBRIP medium containing 0.004% (*w/v*) bromocresol purple as pH indicator (bright yellow indicates pH 5.2 and deep purple pH 7.0). (A) *Arabidopsis* seedlings started to die 10 days after cultivation on NBRIP medium. (B) Pi solubilization by *Trichoderma* 10 days after cultivation. (C) pH change induced by the fungus in insoluble Pi liquid medium. Left: directly after inoculation; right: 10 days later. (D) WGA Alexa 488 fluorescence staining of fungal hyphae after 10 days of coculture with *Arabidopsis* roots on NBRIP medium. Bright field confocal (left) and dissection (right) images. (E) Cocultivation of *Arabidopsis* and *Trichoderma* for 5 days (top) and 10 days (bottom).

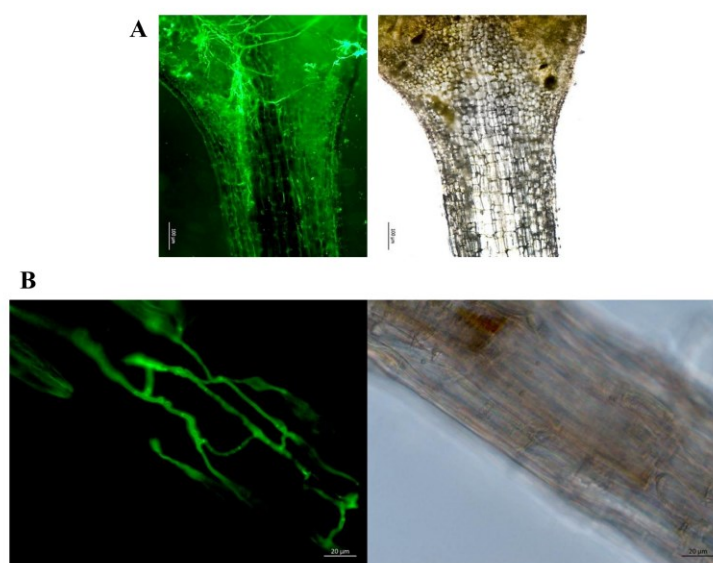


Figure 2. (A) WGA Alexa 488 fluorescence staining of *Trichoderma* hyphae at the stem/leaf junction of *Arabidopsis* seedlings, five days after cocultivation and transfer to NBRIP medium. (B) At the same time, after transfer to the medium with soluble phosphate, hyphae can only be detected in the roots, but never in the stems or leaves. Bright field confocal (left) and dissection (right) images of roots. For experimental details, cf. Methods and Materials.

The (*Thtef1*RNA)/(*AtGAPC2* RNA) ratio can be utilized to quantify fungal colonization. A full 24 h after cocultivation, *Thtef1* transcripts can be detected in the roots, but not in the shoots. Between 24 h and 72 h, we observed a greater than sixfold increase in root colonization (Figure 3). Between 72 and 96 h, leaf colonization increased strongly. This indicates that 72 h after the cocultivation, the root tissue is fully colonized, and additional colonization of the host requires propagation of the hyphae towards the aerial parts of the seedlings. Propagation of the hyphae to the aerial parts of the seedlings does not occur when the cocultivation was performed on media with soluble Pi (Figure 2B, cf. also [20]).

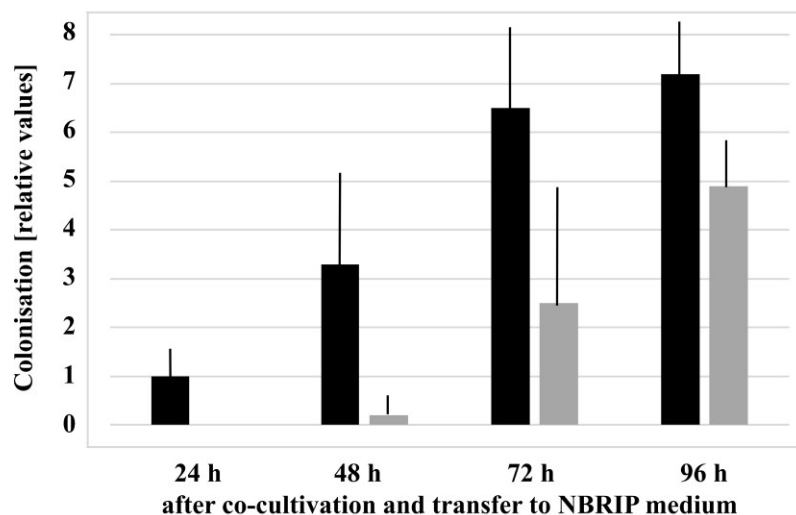


Figure 3. Colonization of *Arabidopsis* roots (black) and shoots (grey) by *Trichoderma* between 24 and 96 h after cocultivation on NBRIP medium. The amount of the fungus in the plant tissue was determined as the mRNA ratio (*Thtef1/AtGAPC2*) (cf. Methods and Materials). For better comparison, the value for the colonization of the roots 24 h after the onset of the experiment was set as 1.0, and all other values are expressed relative to this. Data are based on 3 independent experiments, bars represent SEs.

The effect of the fungus on plant performance under Pi stress was assessed by measurements of the efficiency of the photosynthetic electron transport (Fv/Fm) of photosystem II reaction center. A total of 48 h after transfer to $\text{Ca}_3(\text{PO}_4)_2$ -medium, the Fv/Fm value of the uncolonized seedlings was lower than that of the colonized seedlings. Following 96 h after transfer to $\text{Ca}_3(\text{PO}_4)_2$ -medium, this was reversed (Figure 4). This indicates that the plant initially benefits from the presence of the fungus, whereas, at the end of the experiments, this is no longer the case. The fungus tries to escape from the medium with insoluble Pi and prefers to grow on the host plant, despite the fact that it can solubilize $\text{Ca}_3(\text{PO}_4)_2$.

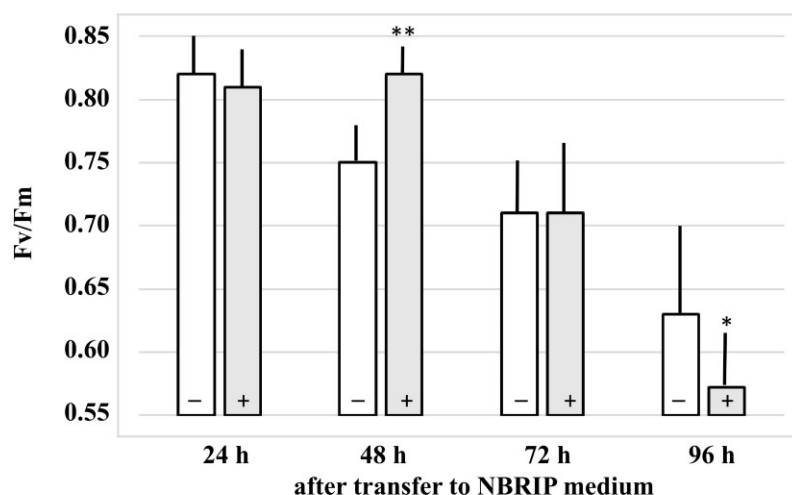


Figure 4. Maximum quantum yield of the photosystem II (Fv/Fm) after the transfer of *Arabidopsis* seedlings to NBRIP medium. At the time point of transfer to the NBRIP medium, the seedlings were either exposed to *Trichoderma* (+) or mock-treated (-). Data are based on 5 independent experiments, bars represent SEs. * indicates significant difference of *Trichoderma*-treated vs. non-treated roots (* $p < 0.05$; ** $p < 0.005$).

3.2. *Trichoderma* Effects on the Pi Starvation Response in Roots

PHOSPHATE1 (PHO1) transfers Pi from root to shoot via Pi export into root xylem vessels. As expected, expression of this Pi starvation marker gene was upregulated in the roots after transfer of the seedlings to $\text{Ca}_3(\text{PO}_4)_2$ -containing medium (Figure 5). Interestingly, 48 h after the transfer, the *PHO1* mRNA level was higher in the roots of the colonized seedlings when compared to the uncolonized controls, whereas this was reversed 96 h after the transfer. A similar regulation was observed for the transcript levels of the high affinity Pi transporter *Pht1;1* and *Pht1;4* (Figure 5). This suggests that the fungus reduces the Pi starvation response during the early colonization phase, whereas the beneficial effect of the fungus is lost after 96 h. A possible explanation could be that the fungus initially provides Pi to the roots, either by direct transport from the fungal to the plant cell, or from the residual external soluble Pi. The mRNA level for *PHR1* increases only marginally under Pi stress and root colonization (Figure 5), even though the transcription factor is considered as a central regulator controlling *PHT1* expression and Pi homeostasis in *Arabidopsis* ([27] and refs. therein). In addition, the *WRKY6* mRNA level does not change significantly in response to the applied Pi stress or fungal root colonization (Figure 5). In conclusion, and consistent with the photosynthetic parameters (Figure 4), it appears that, during the first period after transfer to the NBRIP medium, the colonized roots suffer less under Pi starvation than the uncolonized controls, as evident from the lower expression levels of *PHO1*, *Pht1;1*, and *Pht1;4*.

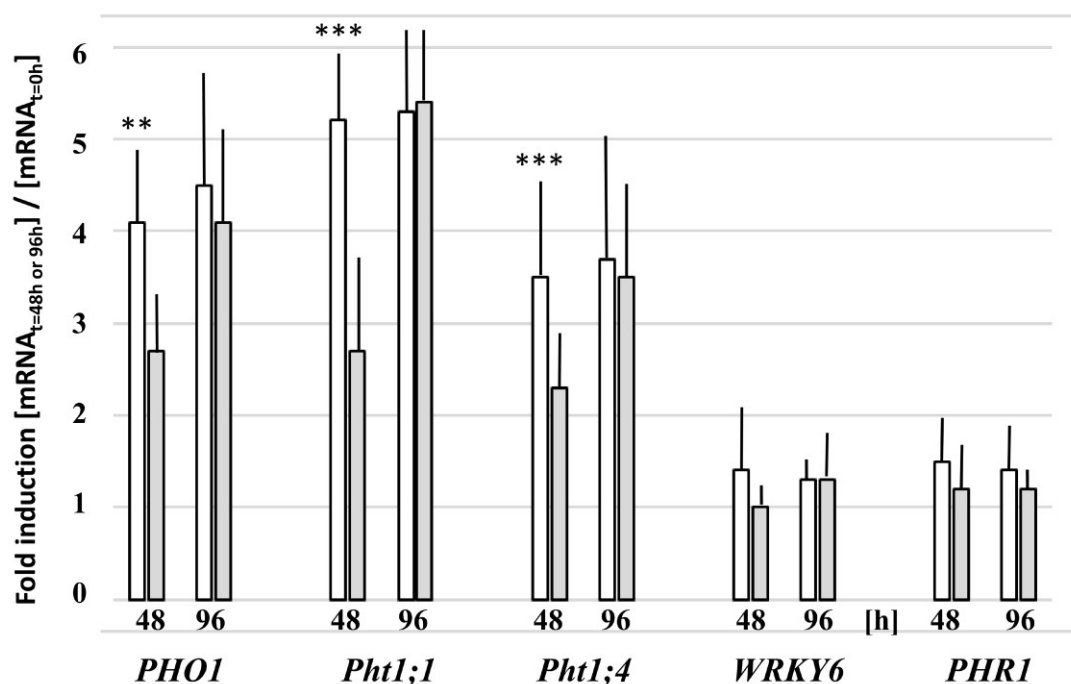


Figure 5. Relative mRNA levels for the Pi transporters *Pht1;1* and *Pht1;4*, as well as the Pi starvation regulators *PHO1*, *WRKY6*, and *PHR1* in the roots of *Arabidopsis* seedlings after transfer to NBRIP medium for 48 h or 96 h. Upon transfer to the NBRIP medium, the seedlings were either cocultured with *Trichoderma* (grey) or mock-treated (white). The mRNA levels are expressed relative to the levels in the roots at the time point of transfer to NBRIP medium ($t = 0$ h). Based on 3 independent experiments; bars represent SEs. * indicates significant difference of non-treated vs. *Trichoderma*-treated roots (** $p < 0.005$; *** $p < 0.001$).

3.3. Fungal Colonization Does Not Activate Defense Gene Expression

The colonization of the roots, as well as aerial parts of the seedlings, by *Trichoderma* under Pi stress might be associated with defense gene activation. We checked classical marker genes for the jasmonate-dependent (*PDF1.2*) and salicylic-acid-dependent (*PR1*) defense pathways, but none of the investigated genes were upregulated more than twofold in the presence of the fungus (Figure 6). This suggests that the roots did not respond to the colonization by the activation of its defense machinery. Furthermore, abiotic stress often induces abscisic acid accumulation. However, the transcript level for the zeaxanthin epoxidase (*ZEP*) that functions in the first step of the biosynthesis of ABA was also not significantly regulated in response to Pi stress or root colonization (Figure 6). We conclude that the higher stress level of the *Arabidopsis* seedlings that were exposed to the fungus is not caused by more investment of the plant into defense against the aggressive fungal growth.

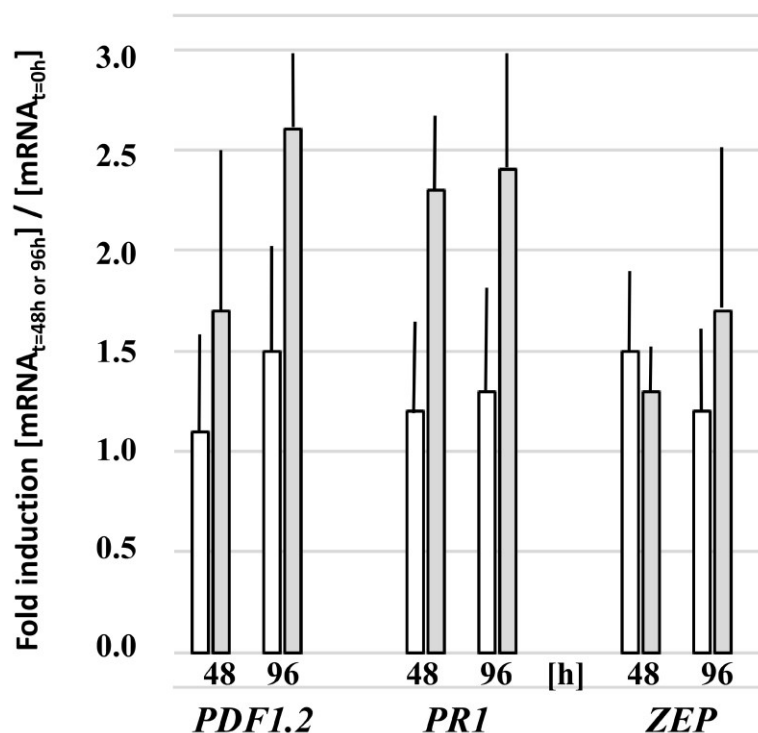


Figure 6. Relative mRNA levels for the defense-related proteins PDF1.2, PR1, and ZEP in the roots of *Arabidopsis* seedlings after transfer to NBRIP medium for 48 h or 96 h. Upon transfer to the NBRIP medium, the seedlings were either cocultured with *Trichoderma* (grey) or mock-treated (white). The mRNA levels are expressed relative to the levels in the roots at the time point of transfer to NBRIP medium ($t = 0$ h). Based on 3 independent experiments; bars represent SEs. No significant differences between the values of *Trichoderma*-treated vs. non-treated roots.

3.4. Root Colonization Alters Expression of *SUC1*, *SWEET2*, -11 and -12 in the Roots

Roots secrete a significant portion of sugars into the rhizosphere and deliver it to root-associated microbes. The increase in root colonization may influence the sugar distribution within the plant body, subsequently affecting plant survival. The sucrose transporter genes *SUC1* and *SUC2* are expressed in roots and their expression does not respond to Pi starvation in our experiment (Figure 7, Supplementary Figure S2). However, at 48 and 96 h of Pi stress, we observed a greater than fivefold increase in the *SUC1* transcript level in the colonized roots, while the *SUC2* transcript level did not respond to the fungus (Figure 7, Supplementary Figure S2). The monosaccharide transporter genes *STP1*, *STP13*, *ERD6*, and *ERD6-like6* are also expressed in roots, but they did not respond to the Pi stress or root colonization (Supplementary Figure S2). Among the *SWEET* sugar transporters, the *SWEET2* transcript level increased more than eight times in colonized roots (Figure 7), while there was no upregulation in the uncolonized controls. Furthermore, the *SWEET11* transcript level decreased more than tenfold, and that of *SWEET12* about sixfold 48 and 96 h after exposure to the fungus, but not in the uncolonized controls. *SWEET3* can be used as a control, since it is expressed in roots but neither responds to the fungus, nor to the Pi stress (Figure 7).

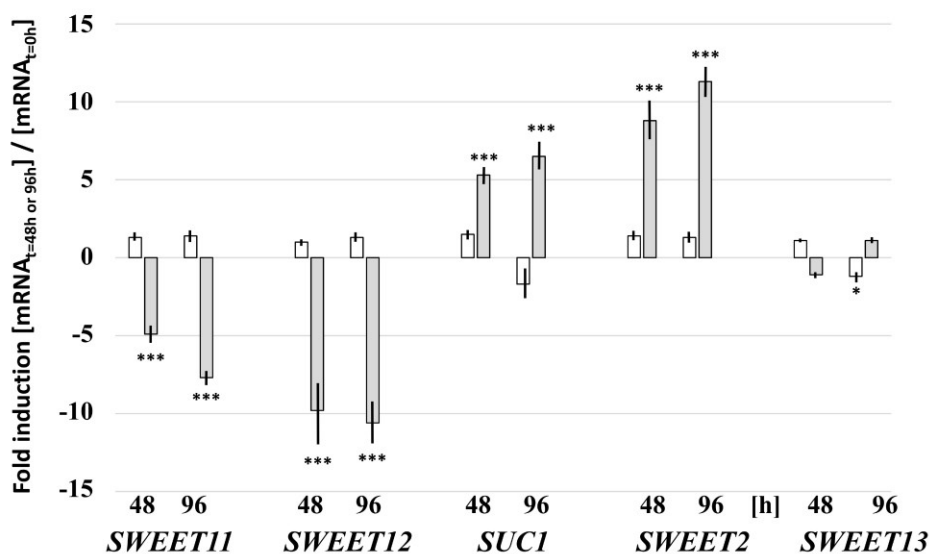


Figure 7. Relative mRNA levels for sugar transporter genes in the roots of *Arabidopsis* seedlings after transfer to NBRIP medium for 48 h or 96 h. Upon transfer to the NBRIP medium, the seedlings were either cocultured with *Trichoderma* (grey) or mock-treated (white). The mRNA levels are expressed relative to the levels in the roots at the time point of transfer to NBRIP medium ($t = 0$ h). Based on 3 independent experiments; bars represent SEs. * indicates significant difference of *Trichoderma*-treated vs. non-treated roots (* $p < 0.05$; *** $p < 0.001$).

Interestingly, the investigated *SUC*, *STP*, *ERD6*, and *ERD6-like6* transporter genes are also expressed in leaves, though to different extents than in roots, but we did not observe any significant response to the Pi stress or colonization (data not shown). Moreover, *SWEET11* and *-12* are expressed in leaves, although at much lower levels than in roots, and no regulation could be observed either (data not shown). The *SWEET2* transcript levels in the leaves are too low for meaningful interpretations.

These results show that *SUC1*, *SWEET2*, *-11*, and *-12* are specific targets of the fungus in roots under stress conditions.

4. Discussion

We established an artificial interaction system between *Arabidopsis* seedlings and a *Trichoderma* strain, which forces the fungus to escape from the growth medium and to colonize the roots, stems, and shoots of the seedlings. Without soluble Pi in the medium, the performance of the *Arabidopsis* seedlings is impaired and they ultimately die, which probably promotes the fast propagation of the fungus in the entire weakened host. The fungus can solubilize $\text{Ca}_3(\text{PO}_4)_2$ and slowly grows on the medium, but prefers to escape to the plant.

One reason could be that it is easier for the fungus to withdraw Pi from the plant than solubilizing it from the medium. However, this appears to be unlikely, because we do not observe a stronger Pi starvation response of the plants when they are colonized by the fungus. In particular, during the first 2 days after cocultivation, the starvation response was even weaker, suggesting that the struggle for Pi is not the main reason for the colonization of the host.

Pi starvation triggers the colonization of the plant and propagation of the mycelium to the aerial parts, presumably because it is less energy-consuming for the fungus to grow on the plant than on the medium, and because the plant is weakened and does not activate processes to restrict fungal colonization. Without Pi stress, the colonization is restricted to

the roots. It would be interesting to test whether other stresses will lead to similar strategies of the fungus.

However, the stronger colonization of the entire plant may force it to restrain the supply of reduced carbon to the fungus (cf. below). Therefore, our artificial system might mimic naturally occurring stress situations, in which beneficial plant/fungi symbiotic interactions in which only the roots are colonized by the microbes shift to more aggressive interactions which benefit the fungi. Since we did not observe a strong defense response of the weakened plant against fungal propagation, the interaction has more saprophytic than pathogenic features. Towards the end of the experiment, the plant dies and might provide material to the fungus which is used for their growth, similar or identical to saprophytic interactions. Several studies describe similar changes in fungal lifestyles. The establishment of a symbiotic interaction between *Arabidopsis* and *Colletotrichum tofieldiae*, which transfers Pi to the host and improves its growth under Pi limitation conditions, depends on the Pi availability, and Karandashov et al. [28] showed that the Pi stress causes a more saprophytic interaction. Grelet et al. [29] found that different *Mycena* species operate along a saprophytic–symbiotic continuum in association with *Ericaceae*. Intermediate interaction forms between endophytic and saprophytic lifestyles have also been proposed for wood-decaying fungi with different host species [30–32]; however, it is not clear how exogenous factors affect the interactions. An example for the adaptation to a symbiotic lifestyle provides *Archaeorhizomyces* [33,34], which colonize the roots in summer and are mainly absent during the colder seasons. Schadt et al. [33] proposed that *Archaeorhizomyces* might adjust their symbiotic lifestyle dependent on root-derived C compounds. Hacquard et al. [35] found genomic signatures in the transcriptomes of the beneficial root endophyte *Colletotrichum tofieldiae* and its pathogenic relative *C. incanum*, which are associated with the transition from pathogenic to beneficial lifestyles, and this included a narrowed repertoire of secreted effector proteins. Since we did not observe a strong defense response against the propagating fungal hyphae, nor a struggle for the limiting Pi source under our experimental conditions, access to sugar might be the main reason for the intense colonization. Like ectomycorrhiza fungi, endophytes mainly colonize the apoplastic space within the root and live on the root surface. Therefore, most of the sugar required for the hyphal growth should be taken up from the plant apoplast.

Trichoderma Manipulates Sugar Transport in Roots

The unloading of sucrose from the phloem in the roots occurs through a combination of symplastic and apoplastic pathways [36]. Cells in the root tip are connected to the phloem by plasmodesmata and form a symplastic domain [37,38]. In more mature areas of the root, cellular connections to the phloem are more limited, and transmembrane transport may be more important [39].

Apoplastic sugar unloading of the phloem in the roots is mainly mediated by *SWEET11* and *-12* in *Arabidopsis* roots ([18,40] and refs. therein). The higher demand for sugar due to the propagation of the hyphae results in the stimulation of photo-assimilate translocation from source to sink. In order to restrict sugar loss from the apoplast after unloading of the phloem, the plant downregulates *SWEET11* and *-12* (Figure 8). The involvement of SWEET transporters in beneficial and pathogenic plant/microbe interactions in roots is well-documented. Several *SWEET* genes in *Brasica* crops were significantly upregulated upon *P. brassicae* infection, the causal agent of clubroot [41]. Clubroot disease stimulates early steps of phloem differentiation and recruits SWEETs within developing galls [42]. Furthermore, MtSWEET11 is a nodule-specific sucrose transporter in *Medicago truncatula* [17,43,44].

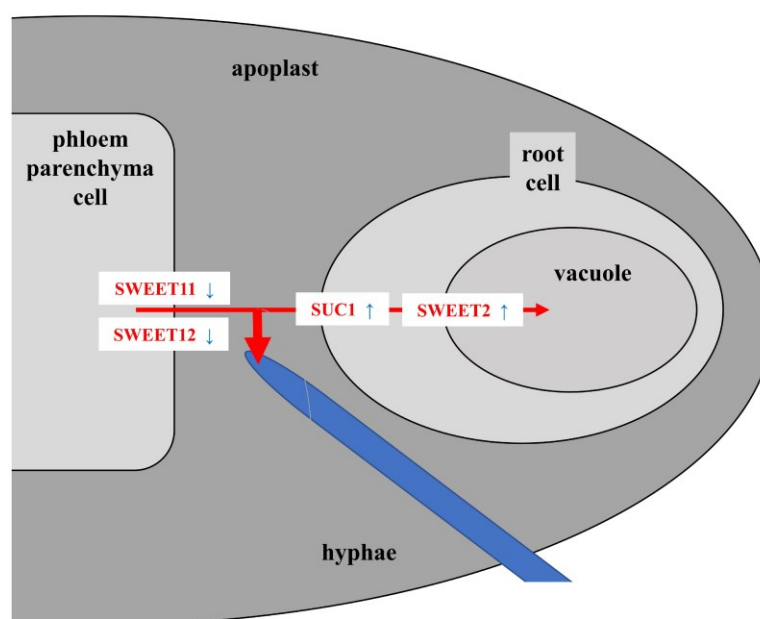


Figure 8. A model describing the regulation of sugar transporter genes in stress-exposed *Arabidopsis* roots in response to *Trichoderma* colonization. Upon increasing stress, the initial beneficial symbiotic interaction of *Trichoderma* with *Arabidopsis* roots shifts to an interaction with a saprophytic lifestyle of the fungus and a higher demand for sugar from the host. The endophytic fungus takes the sucrose mostly from the root apoplast, or from the rhizosphere (not shown) after secretion of the roots. The host responds to it by downregulating *SWEET11* and *-12*, which results in less unloading of sucrose from the phloem into the apoplastic space, and thus restriction of hyphal growth due to sugar shortage. Restricted sucrose availability in the apoplast stimulates uptake into the mesophyll root cells and upregulation of *SUC1* expression to promote sucrose uptake from the apoplast into the mesophyll root cells. Furthermore, the shortage of sucrose in the root cells stimulates *SWEET2* expression. *SWEET2* sequesters sucrose in the vacuole of the root cells, to further reduce sugar loss to the microbe.

SUC1 from *Arabidopsis* was one of the first H⁺-coupled sucrose transporters identified in plants [45,46], and, together with *SUC2*, is the most important sugar uptake carrier from the apoplast into the root cells [47,48]. Consistent with this, in *Arabidopsis* seedlings, *SUC1* expression is found in the elongation zone of the root and less in the root cap or zone of cell division, and *SUC1* expression in roots is induced by exogenous sucrose [48]. The most likely function for plasma-membrane-localized *SUC1* [48] is in the uptake of sucrose released into the apoplast by *SWEET* sucrose efflux transporters as part of the phloem unloading mechanism [2]. *SUC1* expression is upregulated by *Trichoderma*, but not by Pi stress, suggesting that the roots compete with the fungus for the apoplastic sucrose.

Removal of the sugar from the apoplast by stimulating *SUC1*-mediated uptake into the root cells restricts fungal growth (Figure 8). Interestingly, the response to the fungus is mainly observed for *SUC1*, but not for *SUC2* (Figure 7 and Supplementary Figure S2). Recently, Lasin et al. [49] demonstrated that *SUC1* introns act as strong enhancers of expression. The authors showed that a *SUC1* whole-gene *GUS* construct expressing a nonfunctional *SUC1* mutant, that is transport inactive, is defective in sucrose-induced *SUC1* expression when expressed in an *suc1* knock-out mutant. The results indicate that sucrose uptake via *SUC1* is required for sucrose-induced *SUC1* expression, and that the site for sucrose detection is intracellular [49]. Therefore, it is likely that the root cell recognizes

sucrose shortage due to the propagating hyphae in its apoplast, and responds to it by stimulating the uptake and upregulation of *SUC1* (Figure 8).

Besides *SUC1*, *SWEET2* is strongly upregulated in the stress-exposed colonized roots. *SWEET2* is located in the tonoplast of the mesophyll and epidermal root cells, and Chen et al. [19] proposed that the transporter modulates sugar secretion, possibly by reducing the availability of glucose sequestered in the vacuole, thereby limiting carbon loss to the rhizosphere. The reduced availability of sugar in the rhizosphere contributes to resistance to *Pythium*. Consistent with their interpretation, *SWEET2* might be involved in reducing the available sucrose by transporting it into the vacuole of the mesophyll cells (Figure 8). Several studies show that root infections by pathogenic microbes alter the expression of plant sugar transporters to restrict sugar loss to the microbes; for instance, *SWEET* genes are upregulated in pathogenic interactions with bacteria and fungi [50–53]. *SWEET11* is involved in disease resistance against the obligate biotrophic protist *P. brassicae*, the causal agent of clubroot [41]. Chen et al. [19] showed that the root-expressed vacuolar *SWEET2* regulates sugar secretion, specifically from epidermal cells of the root apex, which influences growth of pathogenic microbes.

Vargas et al. [53] investigated *T. virens*-colonized roots and showed that sucrose exuded by plants also has a tremendous influence on the sucrose-dependent network in the fungal cells. The authors investigated fungal sucrose transporters and showed that they are also important for the symbiotic association. This study clearly highlights the necessity for further investigations on the role of sucrose in establishing and maintaining symbiotic plant/fungus interactions.

In summary, it appears 4 out of the 56 sugar transporters in *Arabidopsis* play an important role in the regulatory circuit. The proposed model (Figure 8) can now be tested with other endophytes and host/plant combinations, different stress conditions, and genetic tools manipulating the sugar transporter genes discussed in our model.

Supplementary Materials: The following are available online at <https://www.mdpi.com/article/10.3390/microorganisms9061246/s1>, Figure S1: Acid phosphatase activity; Figure S2: *SUC2*, *STP1*, *STP13*, *ERD6* and *ERD6-like6* in the roots of *Arabidopsis* seedlings; Table S1: Primer pairs.

Author Contributions: Conceptualization, R.O., K.N.N. and R.U.S.; methodology, H.R. and Y.-H.T.; software, H.R. and Y.-H.T.; validation, H.R., Y.-H.T. and R.O.; formal analysis, H.R.; investigation, H.R.; resources, K.N.N., R.U.S., data curation, H.R.; writing—original draft preparation, H.R. and Y.-H.T.; writing—review and editing, R.O.; visualization and supervision, R.O.; project administration, Y.-H.T. and R.O.; funding acquisition, R.O. All authors have read and agreed to the published version of the manuscript.

Funding: The work was supported by the CRC1127 (Project ID: 239748522).

Institutional Review Board Statement: Not applicable.

Informed Consent Statement: Not applicable.

Data Availability Statement: Not applicable.

Acknowledgments: We would like to thank Claudia Röppischer and Sarah Mußbach for excellent technical assistance.

Conflicts of Interest: The authors declare no conflict of interest.

References

1. Sun, Y.; Wang, M.; Mur, L.A.J.; Shen, Q.; Guo, S. The cross-kingdom roles of mineral nutrient transporters in plant-microbe relations. *Physiol. Plant.* **2021**, *171*, 771–784. [CrossRef] [PubMed]
2. Durand, M.; Mainson, D.; Porcheron, B.; Maurousset, L.; Lemoine, R.; Pourtau, N. Carbon source–sink relationship in *Arabidopsis thaliana*: The role of sucrose transporters. *Planta* **2018**, *247*, 587–611. [CrossRef] [PubMed]
3. Kariman, K.; Barker, S.J.; Tibbett, M. Structural plasticity in root-fungal symbioses: Diverse interactions lead to improved plant fitness. *PeerJ* **2018**, *6*, e6030. [CrossRef]
4. Mandyam, K.G.; Jumpponen, A. Mutualism-parasitism paradigm synthesized from results of root-endophyte models. *Front. Microbiol.* **2015**, *5*, 776. [CrossRef] [PubMed]

5. Shin, H.; Shin, H.S.; Dewbre, G.R.; Harrison, M.J. Phosphate transport in Arabidopsis: Pht1;1 and Pht1;4 play a major role in phosphate acquisition from both low- and high-phosphate environments. *Plant J.* **2004**, *39*, 629–642. [[CrossRef](#)]
6. Gu, M.; Chen, A.; Sun, S.; Xu, G. Complex Regulation of Plant Phosphate Transporters and the Gap between Molecular Mechanisms and Practical Application: What Is Missing? *Mol. Plant* **2016**, *9*, 396–416. [[CrossRef](#)] [[PubMed](#)]
7. Hamburger, D.; Rezzonico, E.; Petétot, J.M.-C.; Somerville, C.; Poirier, Y. Identification and Characterization of the Arabidopsis PHO1 Gene Involved in Phosphate Loading to the Xylem. *Plant Cell* **2002**, *14*, 889–902. [[CrossRef](#)] [[PubMed](#)]
8. Chen, Y.-F.; Li, L.-Q.; Xu, Q.; Kong, Y.-H.; Wang, H.; Wu, W.-H. The WRKY6 Transcription Factor Modulates PHOSPHATE1 Expression in Response to Low Pi Stress in Arabidopsis. *Plant Cell* **2009**, *21*, 3554–3566. [[CrossRef](#)] [[PubMed](#)]
9. Rubio, V.; Linhares, F.; Solano, R.; Martín, A.C.; Iglesias, J.; Leyva, A.; Paz-Ares, J. A conserved MYB transcription factor involved in phosphate starvation signaling both in vascular plants and in unicellular algae. *Genes Dev.* **2001**, *15*, 2122–2133. [[CrossRef](#)]
10. Zhou, J.; Jiao, F.; Wu, Z.; Li, Y.; Wang, X.; He, X.; Zhong, W.; Wu, P. OsPHR2 Is Involved in Phosphate-Starvation Signaling and Excessive Phosphate Accumulation in Shoots of Plants. *Plant Physiol.* **2008**, *146*, 1673–1686. [[CrossRef](#)]
11. Bustos, R.; Castrillo, G.; Linhares, F.; Puga, M.I.; Rubio, V.; Pérez-Pérez, J.; Solano, R.; Leyva, A.; Paz-Ares, J. A Central Regulatory System Largely Controls Transcriptional Activation and Repression Responses to Phosphate Starvation in Arabidopsis. *PLoS Genet.* **2010**, *6*, e1001102. [[CrossRef](#)]
12. Guo, M.N.; Ruan, W.Y.; Li, C.Y.; Huang, F.L.; Zeng, M.; Liu, Y.Y.; Yu, X.M.; Ding, X.M.; Wu, Y.R.; Wu, Z.C.; et al. Integrative comparison of the role of the PHR1 subfamily in phosphate signaling and homeostasis in rice. *Plant Physiol.* **2015**, *168*, 1762–1776. [[CrossRef](#)]
13. Jain, A.; Nagarajan, V.K.; Raghobama, K.G. Transcriptional regulation of phosphate acquisition by higher plants. *Cell. Mol. Life Sci.* **2012**, *69*, 3207–3224. [[CrossRef](#)]
14. Castrillo, G.; Teixeira, P.J.; Paredes, S.H.; Law, T.F.; De Lorenzo, L.; Felcher, M.E.; Finkel, O.M.; Breakfield, N.W.; Mieczkowski, P.; Jones, P.M.C.D.; et al. Root microbiota drive direct integration of phosphate stress and immunity. *Nature* **2017**, *543*, 513–518. [[CrossRef](#)]
15. Hermans, C.; Hammond, J.P.; White, P.J.; Verbruggen, N. How do plants respond to nutrient shortage by biomass allocation? *Trends Plant Sci.* **2006**, *11*, 610–617. [[CrossRef](#)]
16. Hennion, N.; Durand, M.; Vriet, C.; Doidy, J.; Maurousset, L.; Lemoine, R.; Pourtau, N. Sugars en route to the roots. Transport, metabolism and storage within plant roots and towards microorganisms of the rhizosphere. *Physiol. Plant.* **2019**, *165*, 44–57. [[CrossRef](#)]
17. Eom, J.-S.; Chen, L.-Q.; Sosso, D.; Julius, B.T.; Lin, I.; Qu, X.-Q.; Braun, D.M.; Frommer, W.B. SWEETs, transporters for intracellular and intercellular sugar translocation. *Curr. Opin. Plant Biol.* **2015**, *25*, 53–62. [[CrossRef](#)]
18. Milne, R.J.; Perroux, J.M.; Rae, A.L.; Reinders, A.; Ward, J.M.; Offler, C.E.; Patrick, J.W.; Grof, C.P. Sucrose Transporter Localization and Function in Phloem Unloading in Developing Stems. *Plant Physiol.* **2017**, *173*, 1330–1341. [[CrossRef](#)]
19. Cheng, X.; Wen, J.; Tadege, M.; Ratet, P.; Mysore, K.S. Reverse Genetics in *Medicago truncatula* Using Tnt1 Insertion Mutants. *Methods Mol. Biol.* **2011**, *678*, 179–190. [[CrossRef](#)]
20. Tseng, Y.-H.; Rouina, H.; Groten, K.; Rajani, P.; Furch, A.C.U.; Reichelt, M.; Baldwin, I.T.; Nataraja, K.N.; Shaanker, R.U.; Oelmüller, R. An Endophytic Trichoderma Strain Promotes Growth of Its Hosts and Defends Against Pathogen Attack. *Front. Plant Sci.* **2020**, *11*, 573670. [[CrossRef](#)]
21. Murashige, T.; Skoog, F. A Revised Medium for Rapid Growth and Bio Assays with Tobacco Tissue Cultures. *Physiol. Plant.* **1962**, *15*, 473–497. [[CrossRef](#)]
22. Peskan-Berghofer, T.; Shahollari, B.; Giong, P.H.; Hehl, S.; Markert, C.; Blanke, V.; Kost, G.; Varma, A.; Oelmüller, R. Association of *Piriformospora indica* with *Arabidopsis thaliana* roots represents a novel system to study beneficial plant-microbe interactions and involves early plant protein modifications in the endoplasmic reticulum and at the plasma membrane. *Physiol. Plant.* **2004**, *122*, 465–477. [[CrossRef](#)]
23. Wagner, R.; Dietzel, L.; Braeutigam, K.; Fischer, W.; Pfannschmidt, T. The long-term response to fluctuating light quality is an important and distinct light acclimation mechanism that supports survival of *Arabidopsis thaliana* under low light conditions. *Planta* **2008**, *228*, 573–587. [[CrossRef](#)]
24. Maxwell, K.; Johnson, G.N. Chlorophyll fluorescence—A practical guide. *J. Exp. Bot.* **2000**, *51*, 659–668. [[CrossRef](#)]
25. Tabatabai, M.; Bremner, J. Use of *p*-nitrophenyl phosphate for assay of soil phosphatase activity. *Soil Biol. Biochem.* **1969**, *1*, 301–307. [[CrossRef](#)]
26. Murphy, J.; Riley, J. A modified single solution method for the determination of phosphate in natural waters. *Anal. Chim. Acta* **1962**, *27*, 31–36. [[CrossRef](#)]
27. Ueda, Y.; Sakuraba, Y.; Yanagisawa, S. Environmental Control of Phosphorus Acquisition: A Piece of the Molecular Framework Underlying Nutritional Homeostasis. *Plant Cell Physiol.* **2021**. online ahead of print. [[CrossRef](#)]
28. Karandashov, V.; Nagy, R.; Wegmuller, S.; Amrhein, N.; Bucher, M. Evolutionary conservation of a phosphate transporter in the arbuscular mycorrhizal symbiosis. *Proc. Natl. Acad. Sci. USA* **2004**, *101*, 6285–6290. [[CrossRef](#)] [[PubMed](#)]
29. Grelet, G.-A.; Ba, R.; Goeke, D.F.; Houliston, G.J.; Taylor, A.F.S.; Durall, D.M. A plant growth-promoting symbiosis between *Mycena galopus* and *Vaccinium corymbosum* seedlings. *Mycorrhiza* **2017**, *27*, 831–839. [[CrossRef](#)] [[PubMed](#)]
30. Smith, G.R.; Finlay, R.D.; Stenlid, J.; Vasaitis, R.; Menkis, A. Growing evidence for facultative biotrophy in saprotrophic fungi: Data from microcosm tests with 201 species of wood-decay basidiomycetes. *New Phytol.* **2017**, *215*, 747–755. [[CrossRef](#)] [[PubMed](#)]

31. Selosse, M.-A.; Dubois, M.-P.; Alvarez, N. Do Sebaciales commonly associate with plant roots as endophytes? *Mycol. Res.* **2009**, *113*, 1062–1069. [\[CrossRef\]](#)
32. Baldrian, P.; Kohout, P. Interactions of saprotrophic fungi with tree roots: Can we observe the emergence of novel ectomycorrhizal fungi? *New Phytol.* **2017**, *215*, 511–513. [\[CrossRef\]](#)
33. Schadt, C.; Martin, A.P.; Lipson, D.A.; Schmidt, S.K. Seasonal Dynamics of Previously Unknown Fungal Lineages in Tundra Soils. *Science* **2003**, *301*, 1359–1361. [\[CrossRef\]](#)
34. Rosling, A.; Cox, F.; Cruz-Martinez, K.; Ihrmark, K.; Grelet, G.-A.; Lindahl, B.D.; Menkis, A.; James, T.Y. Archaeorhizomycetes: Unearthing an Ancient Class of Ubiquitous Soil Fungi. *Science* **2011**, *333*, 876–879. [\[CrossRef\]](#)
35. Hacquard, S.; Kracher, B.; Hiruma, K.; Münch, P.C.; Garrido-Oter, R.; Thon, M.R.; Weimann, A.; Damm, U.; Dallery, J.F.; Hainaut, M.; et al. Survival trade-offs in plant roots during colonization by closely related beneficial and pathogenic fungi. *Nat. Commun.* **2016**, *7*, 11362. [\[CrossRef\]](#)
36. Braun, D.M.; Wang, L.; Ruan, Y.-L. Understanding and manipulating sucrose phloem loading, unloading, metabolism, and signalling to enhance crop yield and food security. *J. Exp. Bot.* **2014**, *65*, 1713–1735. [\[CrossRef\]](#)
37. Stadler, R.; Lauterbach, C.; Sauer, N. Cell-to-Cell Movement of Green Fluorescent Protein Reveals Post-Phloem Transport in the Outer Integument and Identifies Symplastic Domains in Arabidopsis Seeds and Embryos. *Plant Physiol.* **2005**, *139*, 701–712. [\[CrossRef\]](#)
38. Tian, H.; Baxter, I.R.; Lahner, B.; Reinders, A.; Salt, D.E.; Ward, J.M. Arabidopsis NPCC6/NaKR1 Is a Phloem Mobile Metal Binding Protein Necessary for Phloem Function and Root Meristem Maintenance. *Plant Cell* **2010**, *22*, 3963–3979. [\[CrossRef\]](#)
39. Ross-Elliott, T.J.; Jensen, K.H.; Haaning, K.S.; Wager, B.M.; Knoblauch, J.; Howell, A.H.; Mullendore, D.L.; Monteith, A.G.; Paultre, D.; Yan, D.; et al. Phloem unloading in Arabidopsis roots is convective and regulated by the phloem-pole pericycle. *eLife* **2017**, *6*, e24125. [\[CrossRef\]](#)
40. Durand, M.; Porcheron, B.; Hennion, N.; Maurousset, L.; Lemoine, R.; Pourtau, N. Water Deficit Enhances C Export to the Roots in *Arabidopsis thaliana* Plants with Contribution of Sucrose Transporters in Both Shoot and Roots. *Plant Physiol.* **2016**, *170*, 1460–1479. [\[CrossRef\]](#)
41. Li, H.; Li, X.; Xuan, Y.; Jiang, J.; Wei, Y.; Piao, Z. Genome Wide Identification and Expression Profiling of SWEET Genes Family Reveals Its Role During *Plasmiodiophora brassicae*-Induced Formation of Clubroot in *Brassica rapa*. *Front. Plant Sci.* **2018**, *9*, 207. [\[CrossRef\]](#) [\[PubMed\]](#)
42. Walerowski, P.; Gündel, A.; Yahaya, N.; Truman, W.; Sobczak, M.; Olszak, M.; Rolfe, S.; Borisjuk, L.; Malinowski, R. Clubroot Disease Stimulates Early Steps of Phloem Differentiation and Recruits SWEET Sucrose Transporters within Developing Galls. *Plant Cell* **2018**, *30*, 3058–3073. [\[CrossRef\]](#) [\[PubMed\]](#)
43. Kryvoruchko, I.S.; Sinharoy, S.; Torres-Jerez, I.; Sosso, D.; Pislariu, C.I.; Guan, D.; Murray, J.; Benedito, V.A.; Frommer, W.; Udvardi, M.K. MtSWEET11, a Nodule-Specific Sucrose Transporter of *Medicago truncatula*. *Plant Physiol.* **2016**, *171*, 554–565. [\[CrossRef\]](#) [\[PubMed\]](#)
44. Chen, L.-Q.; Hou, B.-H.; Lalonde, S.; Takanaga, H.; Hartung, M.L.; Qu, X.-Q.; Guo, W.-J.; Kim, J.-G.; Underwood, W.; Chaudhuri, B.; et al. Sugar transporters for intercellular exchange and nutrition of pathogens. *Nature* **2010**, *468*, 527–532. [\[CrossRef\]](#)
45. Riesmeier, J.; Willmitzer, L.; Frommer, W. Isolation and characterization of a sucrose carrier cDNA from spinach by functional expression in yeast. *EMBO J.* **1992**, *11*, 4705–4713. [\[CrossRef\]](#)
46. Sauer, N.; Stolz, J. SUC1 and SUC2: Two sucrose transporters from *Arabidopsis thaliana*; expression and characterization in baker's yeast and identification of the histidine-tagged protein. *Plant J.* **1994**, *6*, 67–77. [\[CrossRef\]](#)
47. Sivitz, A.B.; Reinders, A.; Johnson, M.E.; Krentz, A.D.; Grof, C.P.; Perroux, J.M.; Ward, J.M. Arabidopsis Sucrose Transporter AtSUC9. High-Affinity Transport Activity, Intragenic Control of Expression, and Early Flowering Mutant Phenotype. *Plant Physiol.* **2007**, *143*, 188–198. [\[CrossRef\]](#)
48. Sivitz, A.B.; Reinders, A.; Ward, J.M. Arabidopsis Sucrose Transporter AtSUC1 Is Important for Pollen Germination and Sucrose-Induced Anthocyanin Accumulation. *Plant Physiol.* **2008**, *147*, 92–100. [\[CrossRef\]](#)
49. Lasin, P.; Weise, A.; Reinders, A.; Ward, J.M. Arabidopsis Sucrose Transporter AtSUC1 introns act as strong enhancers of expression. *Plant Cell Physiol.* **2020**, *61*, 1054–1063. [\[CrossRef\]](#)
50. Desrut, A.; Moumen, B.; Thibault, F.; Le Hir, R.; Coutos-Thévenot, P.; Vriet, C. Beneficial rhizobacteria *Pseudomonas simiae* WCS417 induce major transcriptional changes in plant sugar transport. *J. Exp. Bot.* **2020**, *71*, 7301–7315. [\[CrossRef\]](#)
51. Ferrari, S.; Galletti, R.; Denoux, C.; De Lorenzo, G.; Ausubel, F.M.; Dewdney, J. Resistance to *Botrytis cinerea* Induced in Arabidopsis by Elicitors Is Independent of Salicylic Acid, Ethylene, or Jasmonate Signaling but Requires PHYTOALEXIN DEFICIENT3. *Plant Physiol.* **2007**, *144*, 367–379. [\[CrossRef\]](#)
52. Antony, G.; Zhou, J.; Huang, S.; Li, T.; Liu, B.; White, F.; Yang, B. Rice xa13 Recessive Resistance to Bacterial Blight Is Defeated by Induction of the Disease Susceptibility Gene Os-11N3. *Plant Cell* **2018**, *22*, 3864–3876. [\[CrossRef\]](#)
53. Vargas, W.A.; Crutcher, F.K.; Kenerley, C.M. Functional characterization of a plant-like sucrose transporter from the beneficial fungus *Trichoderma virens*. Regulation of the symbiotic association with plants by sucrose metabolism inside the fungal cells. *New Phytol.* **2010**, *189*, 777–789. [\[CrossRef\]](#)

Table S1: Primer pairs

The primer pairs used for the study.

Gene	forward	reverse
<i>PHO1</i>	AGACAACCGGGTGTACTTCTTGG	GTCCCACCATCTCCTTACACATTG
<i>WRKY6</i>	GTTGTTTCCTTCGCCGTCGTGG	ATGGACAGAGGATGGTCTGGTC
<i>Ph1;1</i>	CCTTTGGGTTCTATATGCG	TAACTCAGCCTCACCAGAG
<i>Ph1;4</i>	TGTGCCGGCCGAAATCT	TTGCTCCTAATTTTCTGATGCT
<i>PHR1</i>	AAACCAACCCGGCGATTCA	CAGCCCATTCATGCCAATCACTT
<i>PDF1.2</i>	CGCACCGGCAATGGTGG	ATCCATGTTTGGCTCCTTCG
<i>PR1</i>	GTAGGTGCTCTTGTCTTCCC	CACATAATCCCACGAGGATC
<i>ZEP</i>	GATGCAGCCAAATATGGGTCAAGG	GCCATTGCATGGATAATAGCGACTC
<i>SUC1</i>	GACCTTTCGACGCCTTGTTTC	AATACTCCACTAATCGCCGCTG
<i>SUC2</i>	GACCTTTCGACGCCTTGTTTC	AATACTCCACTAATCGCCGCTG
<i>STP1</i>	TGGAGGATGGTGAGTATGG	TGGTACTGTTCTTGCCCATCT
<i>STP13</i>	TATGGGACCGCCAAGATTA	AAGCTCCGACCGTTAGAAGAA
<i>ERD6</i>	ATAATGGCTGAGATATTTCCG	ATAAATACGATCGAACTGGC
<i>ERD6-like6</i>	GTGGAGGAACTTCACTCTGTA	GTTCTTCAAGAGTTTTGCCTT
<i>SWEET2</i>	CACGGTGGTACTTTGTCGGG	AACGGCATAAACTCAACGTCT
<i>SWEET3</i>	GAGTCGGCATCCTTCTCGAA	ACCAAGGCTGAGATTGCTGTC
<i>SWEET11</i>	GCCAATCTCAGTGGTTCGTC	GAAGAGGACTGCTTGCCATGT
<i>SWEET12</i>	CTCACATCTCCTGAACCAGTAGC	TGCAGCACTGTTCTAACTCCC
<i>UBIQUITIN5</i>	GACGCTTCATCTCGTCC	GTAAACGTAGGTGAGTCCA
<i>ACTIN2</i>	TCCAAGCTGTCTCTCCTTG	GAGGGCTGGAACAAGACTTC
<i>tef1</i>	TCAAGTCCGTTGAGATGCAC	CGTTCTTGACGTTGAAACCA

Figure S1: Acid phosphatase activity

Acid phosphatase activity (AcP) of *Trichoderma* spp in comparison to three control bacterial strains (top). Spectrophotometric determination of available phosphate concentration by *Trichoderma* spp in comparison to three control bacterial strains (bottom). Based on 3 independent experiments; bars represent SEs.

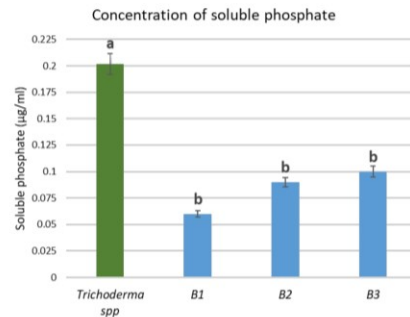
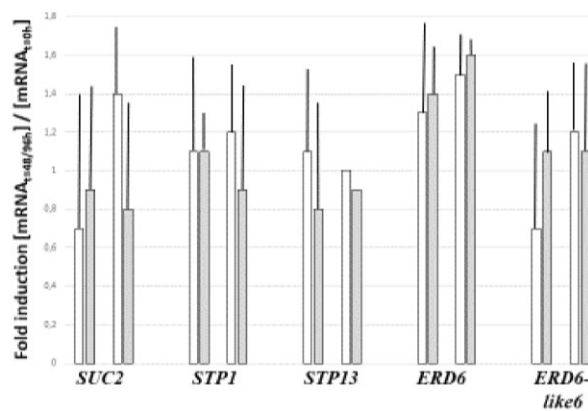


Figure S2: *SUC2*, *STP1*, *STP13*, *ERD6* and *ERD6-like6* in the roots of *Arabidopsis* seedlings

Relative mRNA levels for sugar transporter genes *SUC2*, *STP1*, *STP13*, *ERD6* and *ERD6-like6* in the roots of *Arabidopsis* seedlings after transfer to NBRIP medium for 48 h or 96 h. Upon transfer to the NBRIP medium, the seedlings were either co-cultured with *Trichoderma* (grey) or mock-treated (white). The mRNA levels are expressed relative to the levels in the roots at the time point of transfer to NBRIP medium (t = 0 h). Based on 3 independent experiments; bars represent SEs.



4.3 Manuscript 3

Comparative Secretome Analyses of *Trichoderma/Arabidopsis* Co-Cultures Identify Proteins for Salt Stress, Plant Growth Promotion, and Root Colonization

Hamid Rouina, Yu-Heng Tseng, Karaba N. Nataraja, Ramanan Uma Shaanker, Thomas Krüger, Olaf Kniemeyer, Axel Brakhage, Ralf Oelmüller

Published in *Frontiers in Ecology and Evolution* (2021)
Front. Ecol. Evol. 9:808430. doi: 10.3389/fevo.2021.808430



Comparative Secretome Analyses of *Trichoderma*/Arabidopsis Co-cultures Identify Proteins for Salt Stress, Plant Growth Promotion, and Root Colonization

Hamid Rouina¹, Yu-Heng Tseng¹, Karaba N. Nataraja², Ramanan Uma Shaanker³, Thomas Krüger⁴, Olaf Kniemeyer⁴, Axel Brakhage^{4,5} and Ralf Oelmüller^{1,2*}

¹ Department of Plant Physiology, Matthias Schleiden Institute of Genetics, Bioinformatics and Molecular Botany, Friedrich Schiller University Jena, Jena, Germany, ² School of Ecology and Conservation, University of Agricultural Sciences, Gandhi Krishi Vigyana Kendra (GKVK), Bengaluru, India, ³ Department of Crop Physiology, University of Agricultural Sciences, Gandhi Krishi Vigyana Kendra (GKVK), Bengaluru, India, ⁴ Molecular and Applied Microbiology, Leibniz Institute for Natural Product Research and Infection Biology - Hans Knöll Institute (HKI), Jena, Germany, ⁵ Institute of Microbiology, Friedrich Schiller University Jena, Jena, Germany

OPEN ACCESS

Edited by:

Stephan Polmann,
National Institute of Agricultural
and Food Research and Technology,
Spain

Reviewed by:

Paulina Guzmán-Guzmán,
Universidad Michoacana de San
Nicolás de Hidalgo, Mexico
Joy Michal Johnson,
Kerala Agricultural University, India

*Correspondence:

Ralf Oelmüller
b7oera@uni-jena.de

Specialty section:

This article was submitted to
Coevolution,
a section of the journal
Frontiers in Ecology and Evolution

Received: 03 November 2021

Accepted: 26 November 2021

Published: 04 January 2022

Citation:

Rouina H, Tseng Y-H,
Nataraja KN, Uma Shaanker R,
Krüger T, Kniemeyer O, Brakhage A
and Oelmüller R (2022) Comparative
Secretome Analyses
of *Trichoderma*/Arabidopsis
Co-cultures Identify Proteins for Salt
Stress, Plant Growth Promotion,
and Root Colonization.
Front. Ecol. Evol. 9:808430.
doi: 10.3389/fevo.2021.808430

Numerous *Trichoderma* strains are beneficial for plants, promote their growth, and confer stress tolerance. A recently described novel *Trichoderma* strain strongly promotes the growth of *Arabidopsis thaliana* seedlings on media with 50 mM NaCl, while 150 mM NaCl strongly stimulated root colonization and induced salt-stress tolerance in the host without growth promotion. To understand the dynamics of plant-fungus interaction, we examined the secretome from both sides and revealed a substantial change under different salt regimes, and during co-cultivation. Stress-related proteins, such as a fungal cysteine-rich Kp4 domain-containing protein which inhibits plant cell growth, fungal WSC- and CFEM-domain-containing proteins, the plant calreticulin, and cell-wall modifying enzymes, disappear when the two symbionts are co-cultured under high salt concentrations. In contrast, the number of lytic polysaccharide monoxygenases increases, which indicates that the fungus degrades more plant lignocellulose under salt stress and its lifestyle becomes more saprophytic. Several plant proteins involved in plant and fungal cell wall modifications and root colonization are only found in the co-cultures under salt stress, while the number of plant antioxidant proteins decreased. We identified symbiosis- and salt concentration-specific proteins for both partners. The Arabidopsis PYK10 and a fungal prenylcysteine lyase are only found in the co-culture which promoted plant growth. The comparative analysis of the secretomes supports antioxidant enzyme assays and suggests that both partners profit from the interaction under salt stress but have to invest more in balancing the symbiosis. We discuss the role of the identified stage- and symbiosis-specific fungal and plant proteins for salt stress, and conditions promoting root colonization and plant growth.

Keywords: *Trichoderma*, secretome, salt stress, endophyte, symbiosis, root colonization, lytic polysaccharide monoxygenases, PYK10

INTRODUCTION

Symbiotic *Trichoderma* species colonize host plants, often promote their growth and confer tolerance to various (a)biotic stresses (Shoresh et al., 2010; Contreras-Cornejo et al., 2011, 2021; Brotman et al., 2012; Mukherjee et al., 2012; Mangiest, 2020; Tseng et al., 2020), which make them attractive for agricultural applications. We recently described a novel salt-tolerant *Trichoderma* strain isolated from a stress-exposed *Leucas aspera* (Wild.) tree which is closely related to *T. confertum* (Tseng et al., 2020). The fungus also colonized the roots of *Arabidopsis thaliana* and *Nicotiana attenuata*, and the interaction of the *Trichoderma* spp. strain with *Arabidopsis* seedlings was strongly dependent on the salt concentration in the medium. The fungus promoted the growth of the host plants in soil and media with 50 mM NaCl, while no growth stimulation was observed without salt or concentrations >100 mM. Colonized plants were better protected against pathogen attacks and tolerated higher salt concentrations (Tseng et al., 2020).

The secretomes of beneficial fungi in association with host plants contain stress-, symbiosis-, and defense-specific proteins which orchestrate the diverse responses (Hermosa et al., 2013; Lamdan et al., 2015; Morán-Diez et al., 2015; Druzhinina et al., 2018; Nogueira-Lopez et al., 2018). Likewise, colonized roots respond to stress such as salt, e.g., by activating abscisic acid (ABA)-dependent responses (Kaushal, 2020; van Zelm et al., 2020) and have to balance them with appropriate responses which control root colonization. Overcolonization or aggressive behavior of the microbes activates defense-related responses such as the hormones jasmonic acid or salicylic acid, depending on the mode of interaction between the two partners (Mengistu, 2020). The fungi counteract the plant's defense by secretion of e.g., carbohydrate-binding enzymes for cell wall degradation, proteases, and mainly uncharacterized small cysteine-rich proteins. They weaken the plant and generate degradation products of plant polymers for the fungal primary metabolism. Secreted plant proteins, which are involved in defense to restrict hyphal propagation in the host, are activated by damage/microbe-associated molecular patterns (D/MAMPs) (Hermosa et al., 2013), such as breakdown products of chitin or β -glucans of the *Trichoderma* cell wall. Likewise, fungal (chitinases, β -1,3-glucanases, and proteases) and plant (pectinases, cellulases, and xylanases) cell wall hydrolases generate DAMPs by the degradation of their own cell wall or that of the symbiont (Sharon et al., 1993; Seidl et al., 2006; Djonovic et al., 2007; Martinez et al., 2008; Hermosa et al., 2013; Lamdan et al., 2015; Alkoorenee et al., 2017; Sarrocco et al., 2017; Silva et al., 2019). In return, fungi secrete effector proteins which inhibit plant defense (Kubicek et al., 2011; Guzmán-Guzmán et al., 2017; Mendoza-Mendoza et al., 2018).

Apart from the battle for establishing conditions for a stable symbiosis, many *Trichoderma* strains stimulate the host's growth. They can produce or stimulate the production of plant growth hormones, in particular auxin or auxin-precursors, or promote the nutrient supply from the rhizosphere to the host, or induce alterations in the root architecture which allows better access of the host to nutrients in the soil (Contreras-Cornejo et al., 2009;

Hermosa et al., 2012; Samolski et al., 2012; Ruocco et al., 2015; Nieto-Jacobo et al., 2017).

Very little is known about how plant and fungal secreted proteins are involved in these processes. Therefore, we investigated which proteins are secreted by the two partners under the different salt conditions to identify which of them are specific for the beneficial phase (50 mM NaCl), and for the phase when both partners suffer under salt stress (150 mM NaCl). Our results demonstrate that less stress-related proteins are secreted under co-culture conditions whereas the investment in proteins involved in colonization increases.

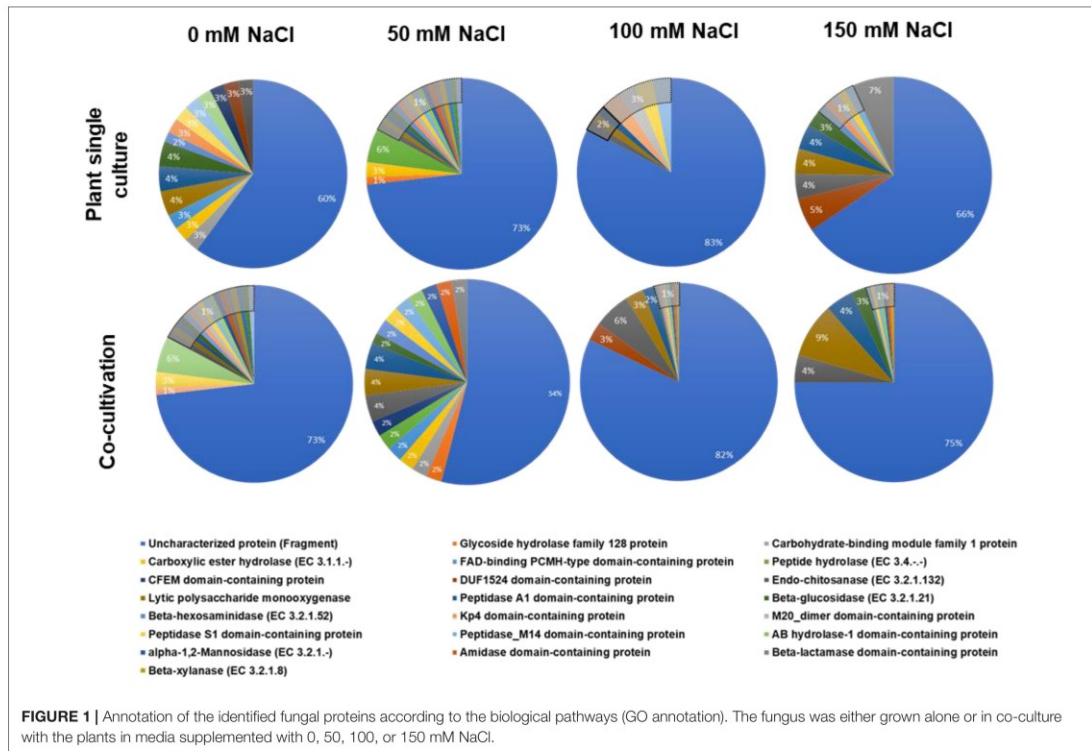
RESULTS AND DISCUSSION

Secretome Analysis of *Trichoderma* spp. and *Arabidopsis thaliana* Exposed to Different Salt Concentrations

Previously, we showed that co-cultivation of a *Trichoderma* strain with *Arabidopsis* seedlings resulted in growth promotion on media with 50 mM salt whereas, under higher salt concentrations, the fungus conferred salt tolerance to the host (Tseng et al., 2020). To identify plant and fungal proteins with specific functions in the interaction, we co-cultivated the symbionts, either alone or together, in a liquid plant nutrient medium (PNM) with 0, 50, 100, or 150 mM NaCl for 5 days. After centrifugation, the remaining culture media were filtered and proteins were isolated by solid-phase extraction followed by LC-MS/MS (liquid chromatography-tandem mass spectrometry) analysis (cf. section "Materials and Methods"). In total, 722 and 605 proteins from *Arabidopsis* and *Trichoderma* spp., respectively, were uniquely identified in all salt concentrations and three independent biological replicates. In the *Trichoderma* spp. cultures, 236, 114, 102, and 311 proteins were observed in at least 2 of 3 biological replicates in 0, 50, 100, and 150 mM NaCl, respectively, whereas 19, 107, 81, and 119 proteins were observed in the plant cultures. In the co-culture, 82, 135, 160, and 116 different plant proteins and 241, 248, 278, and 170 fungal proteins were observed, respectively, in each salt concentration. Just ten *Arabidopsis* and 49 *Trichoderma* spp. proteins were common to all salt concentrations and replicates (cf. data submission).

Classification of Secreted Fungal Proteins

The fungal proteins were classified according to their biological functions. The vast majority of them were uncharacterized (Figure 1). Furthermore, in many cases, a pathway is only represented by a single protein. Therefore, it is difficult to draw general conclusions from the pie diagrams shown in Figure 1 without a more detailed analysis of the individual proteins (cf. below). However, it is obvious that the percentage of proteins with known functions is almost twice as high in the exudate preparation from fungi grown in the co-culture with 50 mM NaCl compared to all other exudate preparations. More importantly, 9% of all identified fungal

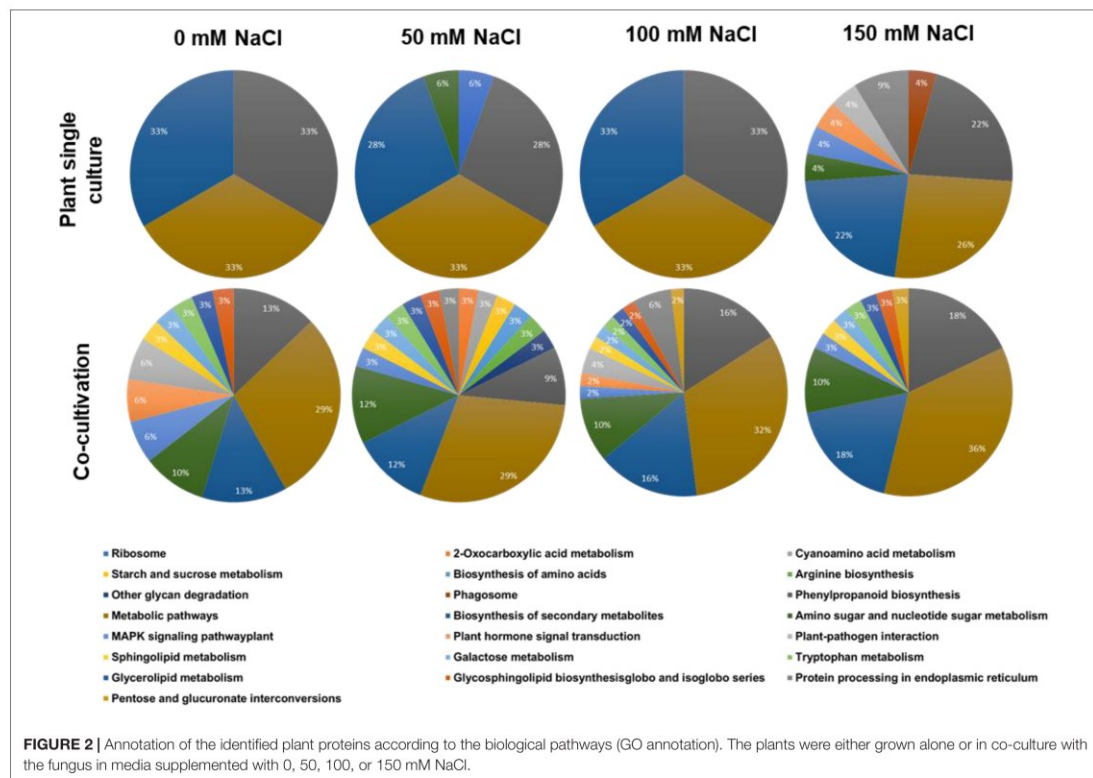


proteins in the exudate of the co-culture with 150 mM NaCl are lytic polysaccharide monooxygenases (Andlar et al., 2018; Forsberg et al., 2019; Almeida et al., 2021; Calderaro et al., 2021; Jagadeeswaran et al., 2021). These enzymes are major contributors to the recycling of carbon in nature, mainly by degradation of plant lignocellulose (Sagarika et al., 2021; Vuong and Master, 2021; Zerva et al., 2021). They catalyze the oxidative cleavage of glycosidic bonds in polysaccharides such as chitin and cellulose, hemicellulose or starch and their discovery has revolutionized our understanding of enzymatic biomass conversion (Manavalan et al., 2021; Wang et al., 2021). Lytic polysaccharide monooxygenases require oxygen and partners to donate electrons during catalytic action on the cellulose backbone which must be present in the cell wall and released into the apoplastic space (Rani Singhania et al., 2021). Due to their enormous potential for application in agricultural waste decomposition, the current research focusses on biochemical application. However, also a few studies showed that they are involved in plant/microbe interactions (reviewed in Jagadeeswaran et al., 2021). The diagram in **Figure 1** shows that lytic polysaccharide monooxygenases increase with increasing salt concentrations in the co-culture. This indicates that the fungus degrades more plant cell wall material under salt stress which might be an indication of a more aggressive behavior of the fungus under stress, associated with a shift toward a more saprophytic lifestyle.

Classification of the Secreted Plant Proteins

All identified plant proteins were classified according to their biological functions (**Figure 2**). Overall inspection of the generated pie diagrams for the plant proteins under the different salt conditions demonstrated that the diversity of the protein functions is much higher in the co-cultures with 0–100 mM salt compared to the diversity of the proteins from plants grown without the fungus (**Figure 2**). For instance, in media with 50 mM NaCl which favors growth promotion of the host, the identified proteins of plants growing alone belong to 4 categories, whereas those in the co-culture to 17 categories. In media with 150 mM NaCl, the complexity of the identified proteins of the plant growing without the fungus becomes more complex (cf. below), which is consistent with many observations that 150 mM salt induces massive salt stress responses. Overall, the result demonstrates that the fungus has a strong influence on the plant protein pattern, in particular in media with 0–100 mM salt.

Among all identified proteins, 193 plant and 199 fungal proteins were predicted to possess an N-terminal secretion sequence. After annotation according to the GO terms “molecular functions,” “biological processes,” and “cellular components,” the 20 most abundant proteins for each salt concentration were further analyzed. The number of proteins annotated as “Response to stress” in Arabidopsis cultures was



reduced when *Trichoderma* was present (Figure 3B). Only 4% of the secreted proteins in the co-culture without salt were annotated as “Response to stress” and none of them were present in the single cultures. In particular, the number of secreted plant proteins of the categories “Antioxidant activity,” “Peroxidase activity,” and “Oxidoreductase activity, acting on peroxide as acceptor” was highly reduced in the presence of *Trichoderma* spp. in media with 50, 100, or 150 mM NaCl (Figure 3C). This suggests that the fungus reduces oxidative stress to the host under salt stress. In contrast, proteins with predicted “Hydrolase activity” showed elevated abundances in the co-cultures with salt (Figure 3C).

Plant Secretome

We classified the secreted plant proteins into those which are only detectable in the presence of the fungus under low (i) or high (ii) salt concentrations, (iii) those which are detectable in the presence of the fungus under all salt conditions, and (iv) those which disappear in the presence of the fungus.

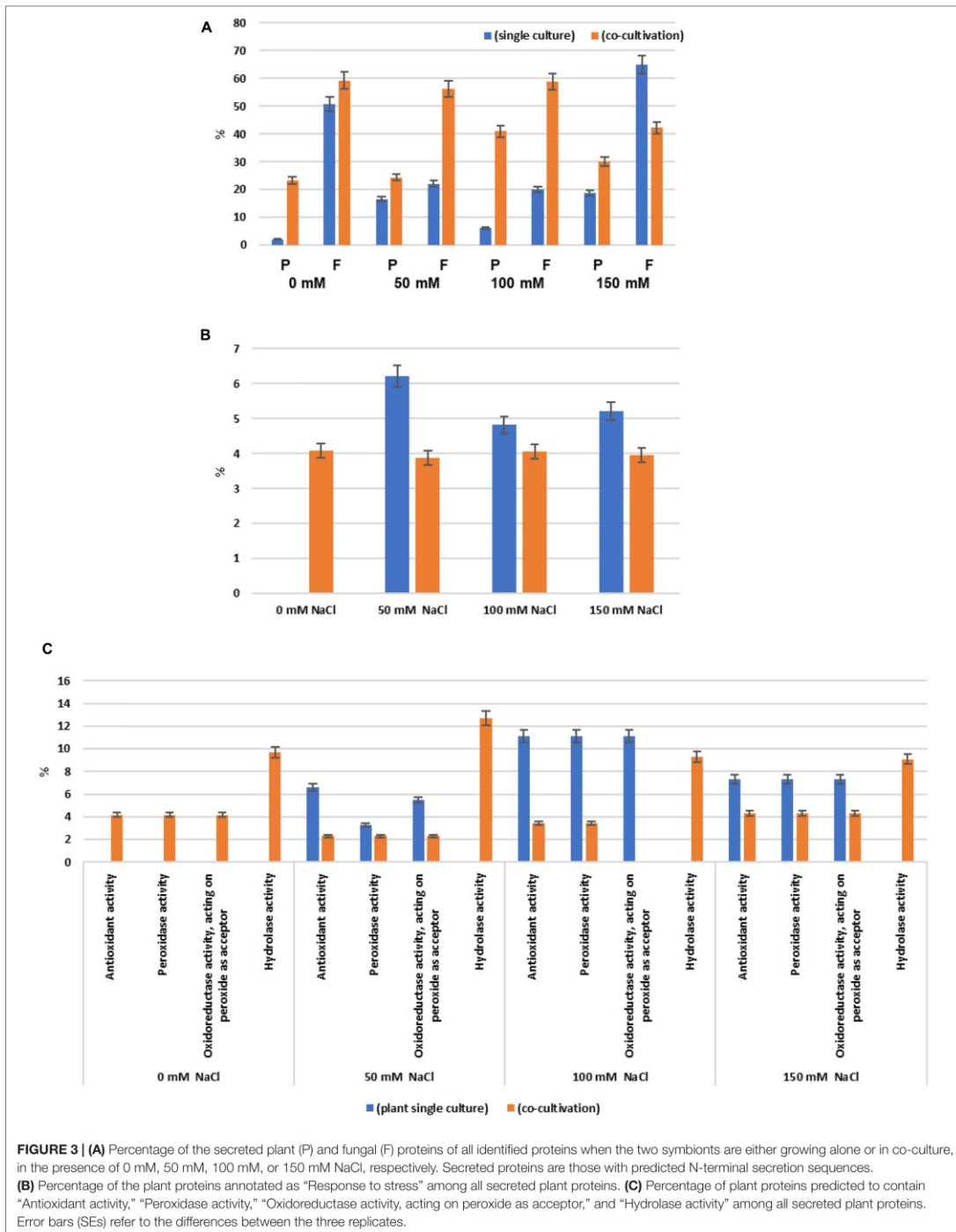
(i) Plant proteins which are only secreted in the presence of the fungus under 50 mM salt

Three plant proteins were only detected in co-cultures which stimulated plant growth (50 mM NaCl; Table 1; Tseng et al., 2020). PYK10 (Q9SR37) is the most

abundant β -glucosidase in *Brassicae* roots and a major constituent of endoplasmic reticulum (ER) bodies. Several studies showed that PYK10 is involved in the mutualistic interaction between *Arabidopsis* and the endophytic fungus *Piriformospora indica* (Thürich et al., 2018, and ref. therein). The protein is released from the ER bodies to the extracellular space after cell disruption. The detectability of this protein only in co-cultures with 50 mM NaCl suggests that it has a specific function under these conditions. Since one would expect more cell injury or disruption under higher salt conditions (cf. below), an uncontrolled accumulation of PYK10 in the exudate fraction under 50 mM salt conditions is unlikely. The two other plant proteins specific for this co-cultivation condition are the uncharacterized GDSL-motif-containing esterase Q9C7N5 and glycosyl hydroxylase P94078.

(ii) Plant proteins which are only secreted in co-cultures with high salt

Plant proteins that are specific for exudates with high salt are mainly involved in stress responses (Table 1). DEGRADATION OF PERIPLASMIC PROTEIN 8 (DEG8; Q9FMA9), RESPONSIVE TO DEHYDRATION 19 (P43296) and the lectins Q9LJR2 and Q9LK72 are related to salt and/or microbial stress (Bernier and Berna, 2001; Lyou et al., 2009). Q9LV60 is a stress-inducible



receptor-like kinase and the lipid recognition protein F4J7G5 is involved in sterol transport under stress (TAIR; arabidopsis.org). The mannose-binding lectin Q9ZVA4 has anti-fungal activities (Wu and Bao, 2013; Barre et al., 2019; Ghahremani et al., 2019), and the EPITHIOLSPECIFIER MODIFIER 1 Q9LJG3 participates in isothiocyanate production during glucosinolate hydrolysis (Burow et al., 2008; cf. Sato et al., 2019). Finally, the oligogalacturonidase oxidases Q9SA85/7 generate oligomers which function as DAMPs for the activation of the plant immune system (Benedetti et al., 2018). Besides proteins involved in salt stress responses, the appearance of defense-related proteins indicates that the fungus becomes more aggressive (cf. below) and the plant activates its defense machinery to restrict fungal growth. Consistent with this interpretation, we observe a strong increase in root colonization when the salt concentration increases to 150 mM (Tseng et al., 2020). Hyphae are not only found in roots but also around and in the stem tissue as well as on leaves (Figure 4).

- (iii) **Plant proteins from co-cultures under all salt conditions**
Plant proteins with known functions which were detected in the presence of the fungus under all salt conditions (Table 1) are α -galactosidase 3 (Q8VXZ7)

which hydrolyzes β -L-arabinofuranose in cell wall-localized arabinogalactan-proteins (Imaizumi et al., 2017), the β -xylosidase Q9FLG1 involved in systemic acquired resistance (Breitenbach et al., 2014), the cysteine proteinase RESPONSIVE TO DEHYDRATION 21(A) (P43297) which is involved in immunity under drought stress (Ormancey et al., 2019; Pogorelko et al., 2019; Liu et al., 2020) and the chitinase Q9M2U5 which participates in cell wall remodeling and degradation of *Trichoderma* hyphae (Kappel and Gruber, 2020). All these proteins have protective functions in plant/microbe interactions, with a focus on the cell wall, and accumulate independently of salt stress.

- (iv) **Plant proteins that disappear in the presence of the fungus**

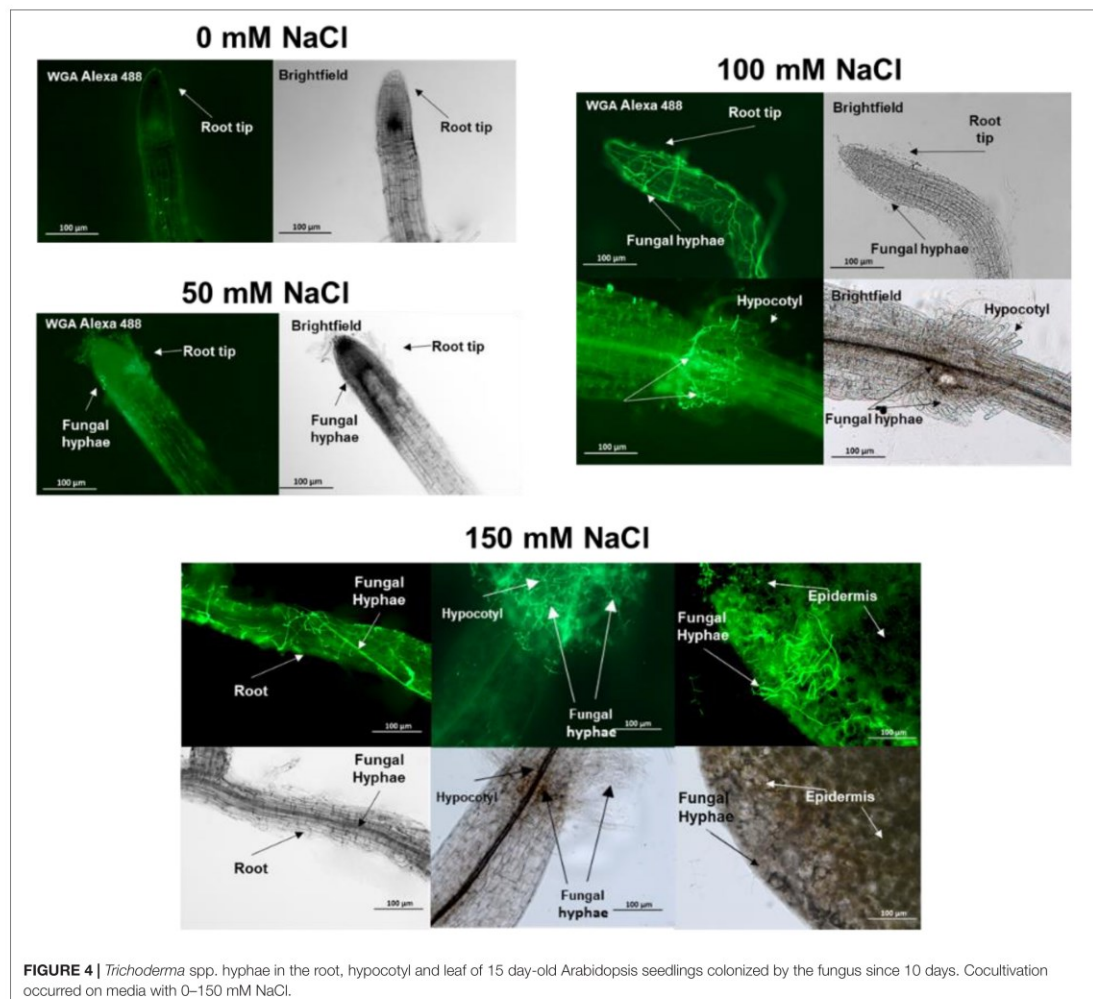
Proteins that are only found in the absence of the fungus are either not synthesized/released by the host, because they are not required under symbiotic conditions, or they are degraded by fungal enzymes, e.g., for weakening the plant to allow better colonization (Table 2). The lipid-transfer proteins (LTPs, Q9FJ65, Q9LV65) respond to drought and salt stress (Yeats and Rose, 2008; Goldack et al., 2014). Q9FJ65 increases the glutathione content and enhances pathogen resistance (McLaughlin et al., 2015). DIR-1 like (Q9LV65) has an overlapping function with DIR1 involved in systemic acquired resistance (Champigny et al., 2013). The absence of this protein in the co-culture suggests that the fungus restricts systemic signaling under salt stress. The β -glucosidase 1 Q9SCW1 and pectin methylesterase inhibitor O49297 are involved in cell wall remodeling (Moneo-Sánchez et al., 2019). The disappearance of these two enzymes in the co-culture indicates that the fungus reduces the pressure on the plant to adapt the cell wall to salt stress. Calreticulin (O04151) accumulation indicates ER stress, which appears to be reduced in the co-culture as well. β -glucosides and lipid-transfer proteins are involved in membrane stabilization under biotic (Q9LLR6) and abiotic stress (Q9LLR6, Q9LLR7 Q9FF10) (cf. TAIR)¹. PELPK1 (Q9LXB8) might be an important target of fungal signals to restrict root growth under salt stress (Rashid and Deyholos, 2011; Guo et al., 2013). In summary, the functional analysis of the proteins which disappear in the co-culture under salt stress, is in line with the overall analysis that the fungus reduces salt stress for the plant (e.g., results in Figure 1). On the other hand, in spite of the strong increase in root colonization in media with 150 mM NaCl (Figure 3), stress-related proteins which are found in uncolonized roots disappear in the presence of the fungus (Table 1). A detailed analysis of the identified proteins might help to understand how the balance between beneficial features in the symbiotic interaction and restriction of fungal growth is achieved.

The comparative analysis identified secreted plant proteins that are specific for the described conditions. While some of them

TABLE 1 | Secreted plant proteins in the presence of the fungus under the different salt concentrations.

Accession	0 mM NaCl	50 mM NaCl	100 mM NaCl	150 mM NaCl
Q8VXZ7	X	X	X	X
Q7XA63	X	X	X	X
Q94AG1	X	X	X	X
Q9FLG1	X	X	X	X
P43297	X	X	X	X
Q9SK10	X	X	X	X
Q8RYE7	X	X	X	X
O24603	X	X	X	X
Q9M2U5	X	X	X	X
Q1H5B3	X	X	X	X
Q84WT8		X	X	X
P94014		X	X	X
Q9LXQ2	X		X	X
A8MQX6	X	X	X	
Q9ZVA4			X	X
Q9LJG3			X	X
Q9SKL6	X		X	
Q9SUX0	X		X	
P19171		X		X
Q9ZVA2		X	X	
Q9C7N5		X		
P94078		X		
Q9SR37		X		
Q9SA87			X	
Q9SA85			X	
P43296			X	
Q9LV60				X
Q9FMA9				X
F4J7G5				X
Q9LJF2				X
Q9LK72				X

¹arabidopsis.org



are well characterized (e.g., PYK10), barely anything is known for others. Their appearance in the plant secretome under the specific conditions and the context of other proteins should be investigated in the future in more detail.

Fungal Secretome Fungal Proteins in the Co-culture

Without salt in the co-cultivation medium, only three fungal enzymes with known functions were found: the glucosaminidase A0A2T4AMN0 removes glucosamine from chitosans, the monooxygenase A0A2T3ZSA1 and the glucosidase A0A2T4A915 are involved in polysaccharide catabolism. The absence of these proteins in salt-containing media suggests specific functions of these enzymes in cell wall degradation.

In media with 50 mM salt, the number of secreted fungal enzymes involved in catabolism is higher: we found the β -xylanase A0A2T4A4K2 and β -1,3-glucanase A0A2T4ADC1 involved in polysaccharide catabolism, the peptidases A0A2T3ZS57, A0A2T4A515, and A0A2T4AAN8 and three uncharacterized proteins (A0A1P8ATL2, A0A2T4A7S8, A0A2T4A7H4). The catabolic enzymes might be important for the generation of metabolites required for the stimulation of the growth of the host. A prenylcysteine lyase (A0A2T4AFC0) generates cysteine, H_2O_2 , and an isoprenoid aldehyde. The H_2O_2 generated by this enzyme might participate in promoting lateral root and root hair development and thus root growth of the host. Furthermore, the release of a farnesyl or geranyl-geranyl residue from the cysteine of a lipoprotein suggests that the fungus might interfere with the isoprenoid metabolism of the plant.

Trichoderma-Secreted Proteins That Disappear in the Co-culture Under Salt Stress

The fungus secretes 11 proteins in a medium with 150 mM salt which disappear in the co-culture (Table 3). A0A2T4AS91 is a cysteine-rich Kp4 domain-containing protein, which inhibits cell growth and division by blocking calcium uptake and signaling (Gu et al., 1995; Gage et al., 2002) and responds to environmental stress (Skamnioti et al., 2008; Brown, 2011; Zapparata et al., 2021). Two CFEM domain-containing proteins (A0A2T4ATW6 and A0A2T4APB9) with predicted GPI anchors (Kulkarni et al., 2003; Zhang et al., 2015; Tan et al., 2017) are proposed to function in surface sensing and stress-tolerance (Sabnam and Barman, 2017; Zhu et al., 2017), heme-iron acquisition (Nasser et al., 2016), cell wall stability and biofilm formation (Vaknin et al., 2014). Recent studies also showed the involvement of the CFEM motif in redox regulation in rice blast (Kou et al., 2017). Furthermore, the cell wall stress-responsive (WSC) domain in A0A2T4AAU9 function as a sensor of multiple stresses at the surface of the plasma membrane (Tong et al., 2016, 2019; Oide et al., 2019) and might be involved in β -glucan remodeling in the fungal cell wall (Wawra et al., 2019). The disappearance of these proteins in the presence of the host indicates that the fungus suffers less under salt stress in the symbiosis which might be the driving force for the intensified root colonization.

Malondialdehyde Levels and Antioxidant Enzyme Activities

The malondialdehyde (MDA) level is an indicator of oxidative stress. In the absence of salt in the culture medium, the MDA level was identical in seedlings with and without *Trichoderma*. With increasing salt concentrations, the MDA level increased and was always lower in the presence of the fungus. The fungal inhibition in media with up to 100 mM NaCl was <10%, whereas 21% reduction was observed with 150 mM NaCl (Figure 5). Furthermore, the activities of the antioxidant enzymes superoxide dismutase (SOD), catalase (CAT) and glutathione reductase (GR) increased with increasing salt concentrations in the medium, and the activity levels were always lower in the presence of the fungus (Figure 5). These results are consistent

TABLE 2 | Plant proteins with predicted N-terminal secretion sequences in media with/without salt in the absence of the fungus.

Accession	0 mM NaCl	50 mM NaCl	100 mM NaCl	150 mM NaCl
Q9FJ65		x		
O49297		X		x
Q9LV65		x		x
Q9SCW1			X	x
Q9M9M3				x
Q9MAS9				X
F4HT37				x
O04151				x
O65351				x
Q9FF10				x
Q9LLR6				x
Q9LLR7				x
Q9LXB8				x

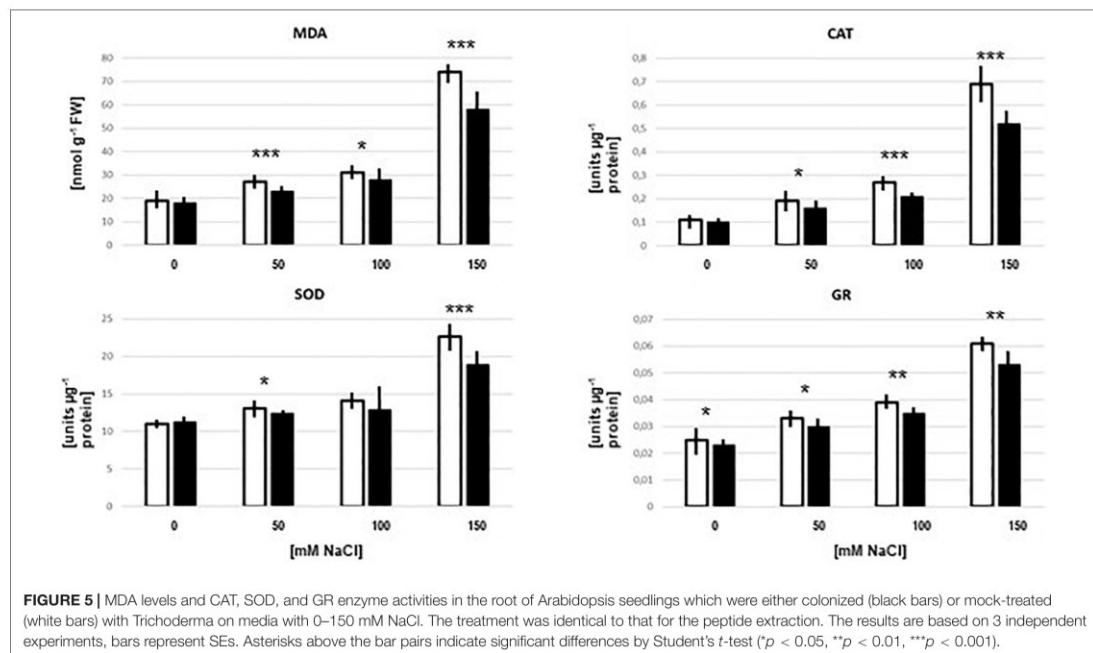
TABLE 3 | Fungal proteins secreted under specific salt conditions in the co-culture.

Accession	0 mM NaCl	50 mM NaCl	100 mM NaCl	150 mM NaCl
A0A1P8ATL2		x		
A0A2T3ZS57		x		
A0A2T4A4K2		x		
A0A2T4A515		x		
A0A2T4AF0C		x		
A0A2T4ADC1		x		
A0A2T4AAN8		x		
A0A2T4A7S8		x		
A0A2T4A7H4		x		
A0A2T4AKF9	x	x		
A0A2T4A4Q9	x	x		
A0A2T4APW4	x	x	x	
A0A2T4AKE5	x	x	x	
A0A2T4A4Q7	x	x	x	
A0A2T4ASK4	x	x	x	
A0A2T4AQ23	x	x	x	X
A0A2T4AA29		x	x	
A0A2T4A915		x	x	
A0A2T4ACR7		x	x	
A0A2T4ACB9		x	x	
A0A2T4ACC9		x	x	X
A0A2T3ZYE2		x	x	X
A0A2T3ZY02		x	x	X
A0A2TZV17	x			
A0A2T3ZSA1	x			
A0A2T4A915	x			
A0A2T4AI25	x			
A0A2T4AMN0	x			
A0A2T4AQC4	x			
A0A2T4A8A3	x		x	
A0A2T4A5D1			x	
A0A2T4AM78			x	
A0A2T4AU78			x	
A0A2T4ASE2			x	

with the interpretation of the proteomic data that the fungus reduces salt stress for the plants, despite the massive increase in root colonization in 150 mM NaCl. Apparently, interaction is still better than living alone. Furthermore, without salt in the medium, the roots do not profit from the presence of the fungus. Consistent with the microscopic data (Figure 4), and the observation that without salt, no growth-promoting effect of the fungus on Arabidopsis seedlings can be detected (Tseng et al., 2020), it appears that there is barely any interaction between the two partners without salt. The sharp difference in the symbiotic interaction between 0 mM and 50 mM NaCl needs to be investigated in more detail.

CONCLUSION

The plant and fungal secretome patterns differ substantially under different salt conditions and when the two organisms are co-cultured. Overall, the identified proteins support the



idea that the symbiotic interaction between the two organisms has an advantage for both partners under salt stress. The number of plant enzymes involved in oxidative stress is lower (Figure 3) and fungal proteins with known functions in stress sensing are reduced in co-cultures with 150 mM NaCl. The high salt concentration promotes root colonization by the fungus and the higher demand for nutrients by the microbe is visible by the appearance of fungal catabolic enzymes. Not surprisingly, the root counteracts the increased root colonization by releasing proteins with antifungal activities. However, comparison of the number of apoplastic plant proteins in co-cultures with high salt (ii) with fungal proteins which attack the plant cell wall (Figure 1 and Table 3) indicates that the plant apoplastic defense machinery is probably too weak to restrict fungal propagation in the host under salt stress. It would be interesting to see how the protein composition within the plant cell responds to the hyphal propagation and whether the host accumulates proteins which restrict fungal entry into the host cell or reduce loss of nutrients to the microbe.

Only a few proteins are exclusively found under co-cultivation conditions which resulted in the promotion of plant growth. Among them is the well-characterized plant PYK10. Since this abundant root protein is not detectable in exudate preparation from co-cultures with no or higher NaCl concentrations, nor in the plant cultures without the fungus, it is tempting to speculate that PYK10 is involved in beneficial features of the symbiosis resulting in plant growth promotion. Moreover, the appearance of this protein in this specific exudate fraction

suggests the existence of a secretion mechanism that operates under the growth-stimulating conditions. Among the fungal proteins which are specific for co-cultures with 50 mM NaCl, the H₂O₂-generating prenylcysteine lyase has the potential to promote root growth.

Besides the general reduction of plant enzymes with antioxidant activities in co-cultures with 150 mM salt, also proteins with other functions confirm that symbiotic roots are less stressed. Examples are calreticulin for ER stress, cell wall remodeling and membrane-stabilizing enzymes, but also PELPK1 involved in root growth inhibition. The majority of fungal proteins which disappear in the co-culture with 150 mM salt stabilize the plasma membrane or senses stress.

Numerous studies investigated the *Trichoderma* secretome in symbiotic interactions with hosts (e.g., Gómez-Mendoza et al., 2014; Lamdan et al., 2015; González-López et al., 2021; Zhao et al., 2021). Besides similarities in the protein patterns and their interpretation (cf. Lamdan et al., 2015; Nogueira-Lopez et al., 2018) several *Trichoderma* proteins proposed to be involved in root colonization are not found in our study, such as the secreted cysteine-rich proteins swollenins, hydrophobins, and SM1 or SM2 (Viterbo and Chet, 2006; Brotman et al., 2008; Crutcher et al., 2015; Guzmán-Guzmán et al., 2017). We provide a list of proteins that are secreted under specific salt conditions. Since these conditions also influence the symbiotic interaction, the role of these proteins should be investigated in more detail. Finally, the role of the lytic polysaccharide monoxygenases for symbiotic plant/fungus interactions requires more attention.

MATERIALS AND METHODS

Cultivation of the Symbionts Alone and in Co-culture

Growth Conditions of Plants and Fungus

Arabidopsis thaliana (ecotype Columbia-0) seeds were surface-sterilized with a solution containing sterile distilled water (dH₂O), sodium lauroyl sarcosinate, and DanKlorix (GP GABA GmbH Hamburg, Germany; 64%, 4%, 32%; v/v) for 8 min under constant shaking, followed by six rinses with dH₂O. Surface-sterile seeds were sown on MS media supplemented with 0.3% gelrite (Murashige and Skoog, 1962). After cold treatment at 4°C for 48 h, plates were incubated for 10 days at 22°C under continuous illumination (100 μmol m⁻² s⁻¹). The *Trichoderma* strain was propagated on KM medium (pH 6.5) for a week at 25°C in the dark (Tseng et al., 2020).

Co-cultivation of *A. thaliana* and *Trichoderma* strain was performed under *in vitro* culture conditions. Ten-day-old *A. thaliana* seedlings of equal sizes were directly transferred from MS medium to the plant nutrient medium (PNM) medium. The fungus was grown on PNM plates. The co-cultivation of *Arabidopsis* plants and *Trichoderma* strain were performed on PNM medium with the salt concentrations mentioned in the text. A 5 mm plug of the *Trichoderma* strain was placed at the center of co-cultivation's plate, as control only a plaque of the medium without hyphae was transferred. Microscopic analyses occurred after 5 day-incubation at 22°C under continuous illumination (100 μmol m⁻² s⁻¹) (Peškan-Berghöfer et al., 2004; Tseng et al., 2020). For the secretome analysis, the co-cultivation (or growth of the partners alone) was performed in liquid PNM with 0, 50, 100, or 150 mM NaCl for 5 days. After centrifugation, the remaining culture media were filtered and proteins were isolated by solid-phase extraction followed by LC-MS/MS (liquid chromatography-tandem mass spectrometry) analysis.

In-Solution Digest

The culture supernatant was filtered through 3 kDa MWCO spin filters (VWR) at 16,000 × g for 10 min. The protein retentate was resolubilized in 25 μl 100 mM TEAB and the solution was mixed with 25 μl 2,2,2-trifluoroethanol. Reduction and alkylation of cysteine thiols were performed by the addition of each 1 μL of 500 mM TCEP (tris(2-carboxyethyl) phosphine) and 625 mM 2-chloroacetamide incubated at 70°C for 30 min. The proteins were further cleaned up using C4 spin columns (Thermo Fisher Scientific): Acetonitrile (ACN) for reconstitution, 0.1% trifluoroacetic acid (TFA) for equilibration, loading, and washing, 0.1% TFA in 80:20 ACN/H₂O (v/v) for elution. Proteins were dried in a vacuum evaporator (Eppendorf), resolubilized in 50 μl of 100 mM TEAB, and digested overnight (18 h) with a Trypsin + LysC mixture (Promega) at a protein to protease ratio of 25:1. Samples were vacuum-evaporated, resolubilized in 25 μL of 0.05% TFA in H₂O/ACN 98/2 (v/v), and filtered through Ultrafree-MC 0.2 μm PTFE membrane spin filters (Merck-Millipore) at 14 000 × g for 15 min. The filtrate was transferred to HPLC vials and injected into the LC-MS/MS instrument. Each sample was measured in triplicate (3 analytical replicates of 3

biological replicates of 16 different conditions equals 144 LC-MS/MS runs).

Liquid Chromatography-Tandem Mass Spectrometry Analysis

LC-MS/MS analysis was performed on an Ultimate 3,000 nano RSLC system connected to a QExactive Plus mass spectrometer (both Thermo Fisher Scientific, Waltham, MA, United States). Peptide trapping for 5 min on an Acclaim Pep Map 100 column (2 cm × 75 μm, 3 μm) at 5 μL/min was followed by separation on an analytical Acclaim Pep Map RSLC nano column (50 cm × 75 μm, 2 μm). Mobile phase gradient elution of eluent A (0.1% (v/v) formic acid in water) mixed with eluent B (0.1% (v/v) formic acid in 90/10 acetonitrile/water) was performed as follows: 0 min at 4% B, 4 min at 5% B, 6 min at 6% B, 14 min at 10% B, 20 min at 14% B, 35 min at 20% B, 42 min at 26% B, 46 min at 32% B, 52 min at 42% B, 55 min at 50% B, 58 min at 65% B, 60–64.9 min at 96% B, 65–90 min at 4% B.

Positively charged ions were generated at a spray voltage of 2.2 kV using a stainless steel emitter attached to the Nanospray Flex Ion Source (Thermo Fisher Scientific). The quadrupole/orbitrap instrument was operated in Full MS/data-dependent MS2 (Top10) mode. Precursor ions were monitored at m/z 300–1,500 at a resolution of 70,000 FWHM (full width at half maximum) using a maximum injection time (IT_{max}) of 120 ms and an AGC (automatic gain control) target of 1 · 10⁶. Precursor ions with a charge state of z = 2–5 were filtered at an isolation width of m/z 1.6 amu for further HCD fragmentation at 30% normalized collision energy (NCE). MS2 ions were scanned at 17,500 FWHM (IT_{max} = 120 ms, AGC = 2 · 10⁵) using a fixed first mass of m/z 120 amu. Dynamic exclusion of precursor ions was set to 30 s and the underfill ratio was set to 1.0%. The LC-MS/MS instrument was controlled by Chromeleon 6.8, QExactive Tune 2.8 and Xcalibur 4.0 software.

Protein Database Search

Tandem mass spectra were searched against the UniProt databases of *A. thaliana* and *T. harzianum* by using Proteome Discoverer (PD) 2.2 (Thermo) and the algorithms of Mascot 2.4.1 (Matrix Science, United Kingdom), Sequest HT (version of PD2.2) and MS Amanda 2.0. Two missed cleavages were allowed for the tryptic digestion. The precursor mass tolerance was set to 10 ppm and the fragment mass tolerance was set to 0.02 Da. Modifications were defined as dynamic Met oxidation and protein N-term acetylation as well as static Cys carbamidomethylation. A strict false discovery rate (FDR) < 1% (peptide and protein level) was required for positive protein hits. If only 1 peptide per protein has been identified the hit was accepted if the Mascot score was > 30 or the MS Amanda score was > 300 or the Sequest score was > 4. The Percolator node of PD2.2 and a reverse decoy database was used for q-value validation of spectral matches. Only rank 1 proteins and peptides of the top-scored proteins were counted. Label-free protein quantification was based on the Minora algorithm of PD2.2 using a signal-to-noise ratio > 5. Imputation of missing qn values was applied by setting the abundance to 75% of the lowest abundance identified for each sample. Significantly

different abundances were based on a fold change >4, a ratio-adjusted significance level <0.05, which is the *p*-value calculated by the 2s *t*-test divided by the log2 ratio, and the proteins needed to be identified at least in 2 of 3 biological replicates of the sample group with the highest abundance.

Databank Analyses

All identified proteins were examined for an N-terminal secretion sequence, using the TargetP 1.1,² SignalP 4.1,³ and Predotar 1.3⁴ software (Tan et al., 2017; Emanuelsson et al., 2007). The secreted protein candidates were classified according to their Gene ontology (GO) terms using ShinyGO (Ashburner et al., 2000; Gene Ontology Consortium, 2015), or the classification occurred according to their functional description on UniProt Database.

Root Colonization Analyzed by Microscopy

The entire Arabidopsis roots, root tips, hypocotyls and leaves were imaged using an AXIO Imager.M2 (Zeiss Microscopy GmbH, Jena, Germany) equipped with a 10x objective (N-Achroplan 10x/0.3). The bright field and fluorescence images (EX 545/25 and EM 605/70) were recorded with a color camera (AXIOCAM 503 color Zeiss, Jena, Germany) by use of an EGFP (EM 525/50 nm) and DsRED filter (EM 605/70 nm). Digital images were processed with the ZEN software (Zeiss, Jena, Germany), treated with Adobe R Photoshop to optimize brightness, contrast, and coloring and to overlay the photomicrographs to confirm fluorescence information.

² <http://www.cbs.dtu.dk/services/TargetP/>

³ <http://www.cbs.dtu.dk/services/SignalP/>

⁴ <https://urgi.versailles.inra.fr/Tools/Predotar>

REFERENCES

- Alkoorenee, J. T., Aledan, T. R., Ali, A. K., Lu, G., Zhang, X., Wu, J., et al. (2017). Detecting the hormonal pathways in oilseed rape behind induced systemic resistance by trichoderma harzianum TH12 to *Sclerotinia sclerotiorum*. *PLoS One* 12:e0168850. doi: 10.1371/journal.pone.0168850
- Almeida, D. A., Horta, M. A. C., Ferreira Filho, J. A., Murad, N. F., and de Souza, A. P. (2021). The synergistic actions of hydrolytic genes reveal the mechanism of *Trichoderma harzianum* for cellulose degradation. *J. Biotechnol.* 334, 1–10. doi: 10.1016/j.jbiotec.2021.05.001
- Andlar, M., Rezić, T., Mardetko, N., Kracher, D., Ludwig, R., and Šantek, B. (2018). Lignocellulose degradation: an overview of fungi and fungal enzymes involved in lignocellulose degradation. *Eng. Life Sci.* 18, 768–778. doi: 10.1002/elsc.201800039
- Ashburner, M., Ball, C. A., Blake, J. A., Botstein, D., Butler, H., Cherry, J. M., et al. (2000). Gene ontology: tool for the unification of biology. the gene ontology consortium. *Nat. Genet.* 25, 25–29. doi: 10.1038/75556
- Barre, A., Simplicien, M., Benoist, H., Van Damme, E. J. M., and Rougé, P. (2019). Mannose-specific lectins from marine algae: diverse structural scaffolds associated to common virucidal and anti-cancer properties. *Mar. Drugs* 17:440. doi: 10.3390/md17080440
- Benedetti, M., Verrascina, I., Pontiggia, D., Locci, F., Mattei, B., De Lorenzo, G., et al. (2018). Four Arabidopsis berberine bridge enzyme-like proteins are specific oxidases that inactivate the elicitor-active oligogalacturonides. *Plant J.* 94, 260–273. doi: 10.1111/tpj.13852
- Bernier, F., and Berna, A. (2001). Germins and germin-like proteins: plant do-all proteins. But what do they do exactly? *Plant Physiol. Biochem.* 39, 545–554. doi: 10.1016/s0981-9428(01)01285-2
- Breitenbach, H. H., Wenig, M., Wittek, F., Jordá L., Maldonado-Alconada, A. M., Sarioglu, H., et al. (2014). Contrasting roles of the apoplastic aspartyl protease apoplastic, enhanced disease susceptibility1-dependent1 and legume lectin-like Protein1 in arabidopsis systemic acquired resistance. *Plant Physiol.* 165, 791–809. doi: 10.1104/pp.114.239665
- Brotman, Y., Briff, E., Viterbo, A., and Chet, I. (2008). Role of swollenin, an expansin-like protein from trichoderma, in plant root colonization. *Plant Physiol.* 147, 779–789. doi: 10.1104/pp.108.116293
- Brotman, Y., Liseč, J., Méret, M., Chet, I., Willmitzer, L., and Viterbo, A. (2012). Transcript and metabolite analysis of the Trichoderma-induced systemic resistance response to *Pseudomonas syringae* in *Arabidopsis thaliana*. *Microbiology* 158, 139–146. doi: 10.1099/mic.0.052621-0
- Brown, D. W. (2011). The KP4 killer protein gene family. *Curr. Genet.* 57, 1–62. doi: 10.1007/s00294-010-0326-y
- Burow, M., Zhang, Z.-Y., Ober, J. A., Lambrix, V. M., Wittstock, U., Gershenzon, J., et al. (2008). ESP and ESM1 mediate indol-3-acetonitrile production from indol-3-ylmethyl glucosinolate in Arabidopsis. *Phytochemistry* 69, 663–671. doi: 10.1016/j.phytochem.2007.08.027
- Calderaro, F., Bevers, L. E., and van den Berg, M. A. (2021). Oxidative power: tools for assessing LPMO activity on cellulose. *Biomolecules* 11:1098. doi: 10.3390/biom11081098
- Champigny, M. J., Isaacs, M., Carella, P., Faubert, J., Fobert, P. R., and Cameron, R. K. (2013). Long distance movement of DIR1 and investigation of the role of

Malondialdehyde Levels and Antioxidant Enzyme Activities

The assays for malondialdehyde levels and antioxidant enzyme activities were described in detail in Tsai et al. (2020). About 50 seedlings were collected from the co-cultivation (or growth of the plant partner alone) after 5 days from liquid PNM with 0, 50, 100, or 150 mM NaCl, as outlined above. Data are based on 3 repetitions, bars represent SEs.

DATA AVAILABILITY STATEMENT

The mass spectrometry proteomics data have been deposited to the ProteomeXchange Consortium via the PRIDE (Perez-Riverol et al., 2019) partner repository with the dataset identifier PXD028957.

AUTHOR CONTRIBUTIONS

HR and Y-HT designed and performed the experiments. TK, OK, and AB performed the LC-MS/MS analysis. KN, RU, and RO supervised and coordinated the experiments. All authors contributed to the article and approved the submitted version.

FUNDING

This work was supported by the DFG (Deutsche Forschungsgemeinschaft) within the scope of CRC1127 ChemBioSys (project number 239748522, projects A3 and B2) and CRC/TR 124 FungiNet (project number 210879364, project Z2).

- DIR1-like during systemic acquired resistance in Arabidopsis. *Front. Plant Sci.* 4:230. doi: 10.3389/fpls.2013.00230
- Contreras-Cornejo, H. A., Macías-Rodríguez, L., Beltrán-Peña, E., Herrera-Estrella, A., and López-Bucio, J. (2011). Trichoderma-induced plant immunity likely involves both hormonal- and camalexin-dependent mechanisms in *Arabidopsis thaliana* and confers resistance against necrotrophic fungi *Botrytis cinerea*. *Plant Signal. Behav.* 6, 1554–1563. doi: 10.4161/psb.6.10.17443
- Contreras-Cornejo, H. A., Macías-Rodríguez, L., Cortés-Penagos, C., and López-Bucio, J. (2009). Trichoderma virens, a plant beneficial fungus, enhances biomass production and promotes lateral root growth through an auxin-dependent mechanism in Arabidopsis. *Plant Physiol.* 149, 1579–1592. doi: 10.1104/pp.108.130369
- Contreras-Cornejo, H. A., Macías-Rodríguez, L., Real-Santillán, R. O., López-Carmona, D., García-Gómez, G., Galicia-Gallardo, A. P., et al. (2021). In a belowground multitrophic interaction, *Trichoderma harzianum* induces maize root herbivore tolerance against *Phyllophaga vetula*. *Pest Manag. Sci.* 77, 3952–3963. doi: 10.1002/ps.6415
- Crutcher, F. F., Moran-Diez, M. E., Ding, S., Liu, J., Horwitz, B. A., Mukherjee, P. K., et al. (2015). A paralog of the proteinaceous elicitor SM1 is involved in colonization of maize roots by *Trichoderma virens*. *Fungal Biol.* 119, 476–486. doi: 10.1016/j.funbio.2015.01.004
- Djonovic, S., Vargas, W. A., Kolomiets, M. V., Horndeski, M., Wiest, A., and Kenerley, C. M. (2007). A proteinaceous elicitor Sm1 from the beneficial fungus *Trichoderma virens* is required for induced systemic resistance in maize. *Plant Physiol.* 145, 875–889. doi: 10.1104/pp.107.103689
- Druzhinina, I. S., Chenthamara, K., Zhang, J., Atanasova, L., Yang, D., Miao, Y., et al. (2018). Massive lateral transfer of genes encoding plant cell wall-degrading enzymes to the mycoparasitic fungus *Trichoderma* from its plant-associated hosts. *PLoS Genet.* 14:e1007322. doi: 10.1371/journal.pgen.1007322
- Emanuelsson, O., Brunak, S., Heijne, G., and von Nielsen, H. (2007). Locating proteins in the cell using TargetP, SignalP and related tools. *Nat. Protoc.* 2, 953–971. doi: 10.1038/nprot.2007.131
- Forsberg, Z., Sorlie, M., Petrović, D., Courtade, G., Achmann, F. L., Vaaje-Kolstad, G., et al. (2019). Polysaccharide degradation by lytic polysaccharide monoxygenases. *Curr. Opin. Struct. Biol.* 59, 54–64.
- Gage, M. J., Bruenn, J., Fischer, M., Sanders, D., and Smith, T. J. (2002). KP4 fungal toxin inhibits growth in *Ustilago maydis* by blocking calcium uptake. *Mol. Microbiol.* 41, 775–785. doi: 10.1046/j.1365-2958.2001.02554.x
- Gene Ontology Consortium (2015). Going forward. *Nucleic Acids Res.* 43, D1049–D1056.
- Ghahremani, M., Tran, H., Biglou, S. G., O’Gallagher, B., She, Y. M., and Plaxton, W. C. (2019). A glycoform of the secreted purple acid phosphatase AtPAP26 co-purifies with a mannose-binding lectin (AtGAL1) upregulated by phosphate-starved Arabidopsis. *Plant Cell Environ.* 42, 1139–1157. doi: 10.1111/pce.13432
- Gollack, D., Li, C., Mohan, H., and Probst, N. (2014). Tolerance to drought and salt stress in plants: unraveling the signaling networks. *Front. Plant Sci.* 5:151. doi: 10.3389/fpls.2014.00151
- Gómez-Mendoza, D. P., Junqueira, M., do Vale, L. H., Domont, G. B., Ferreira Filho, E. X., Sousa, M. V., et al. (2014). Secretomic survey of *Trichoderma harzianum* grown on plant biomass substrates. *J. Proteome Res.* 13, 1810–1822. doi: 10.1021/pr400971e
- González-López, M. D. C., Jijón-Moreno, S., Daut-Castro, M., Ovando-Vázquez, C., Ziv, T., Horwitz, B. A., et al. (2021). Secretome analysis of Arabidopsis-Trichoderma atroviride interaction unveils new roles for the plant glutamate:glyoxylate aminotransferase GGAT1 in plant growth induced by the fungus and resistance against *Botrytis cinerea*. *Int. J. Mol. Sci.* 22:6804. doi: 10.3390/ijms22136804
- Gu, F., Khimani, A., Rane, S. G., Flurkey, W. H., Bozarth, R. F., and Smith, T. J. (1995). Structure and function of a virally encoded fungal toxin from *Ustilago maydis*: a fungal and mammalian Ca²⁺ channel inhibitor. *Structure* 3, 805–814. doi: 10.1016/s0969-2126(01)00215-5
- Guo, L., Yang, H., Zhang, X., and Yang, S. (2013). Lipid transfer protein 3 as a target of MYB96 mediates freezing and drought stress in Arabidopsis. *J. Exp. Bot.* 64, 1755–1767. doi: 10.1093/jxb/ert040
- Guzmán-Guzmán, P., Alemán-Duarte, M. I., Delaye, L., Herrera-Estrella, A., and Olmedo-Monfil, V. (2017). Identification of effector-like proteins in *Trichoderma* spp. and role of a hydrophobin in the plant-fungus interaction and mycoparasitism. *BMC Genet.* 18:16. doi: 10.1186/s12863-017-0481-y
- Hermosa, R., Rubio, M. B., Cardoza, R. E., Nicolás, C., Monte, E., and Gutiérrez, S. (2013). The contribution of *Trichoderma* to balancing the costs of plant growth and defense. *Int. Microbiol.* 16, 69–80. doi: 10.2436/20.1501.01.181
- Hermosa, R., Viterbo, A., Chet, I., and Monte, E. (2012). Plant-beneficial effects of *Trichoderma* and of its genes. *Microbiology* 158, 17–25. doi: 10.1099/mic.0.052274-0
- Imaizumi, C., Tomatsu, H., Kitazawa, K., Yoshimi, Y., Shibano, S., Kikuchi, K., et al. (2017). Heterologous expression and characterization of an Arabidopsis β -1-arabinopyranosidase and α -D-galactosidases acting on β -1-arabinopyranosyl residues. *J. Exp. Bot.* 68, 4651–4661. doi: 10.1093/jxb/erx279
- Jagadeeswaran, G., Veale, L., and Mort, A. J. (2021). Do lytic polysaccharide monoxygenases aid in plant pathogenesis and herbivory? *Trends Plant Sci.* 26, 142–155. doi: 10.1016/j.tplants.2020.09.013
- Kappel, L., and Gruber, S. (2020). “Chitin and chitosan—important structural components in *Trichoderma* cell wall remodeling,” in *New and Future Developments in Microbial Biotechnology and Bioengineering. Recent Developments in Trichoderma Research*, eds V. K. Gupta, S. Zeilinger and H. B. Singh. (Amsterdam: Elsevier).
- Kaushal, M. (2020). Insights into microbially induced Salt Tolerance and Endurance Mechanisms (STEM) in plants. *Front. Microbiol.* 11:1518. doi: 10.3389/fmicb.2020.01518
- Kubicek, C. P., Herrera-Estrella, A., Seidl-Seiboth, V., Martínez, D. A., Druzhinina, I. S., and Thon, M. (2011). Comparative genome sequence analysis underscores mycoparasitism as the ancestral life style of *Trichoderma*. *Genome Biol.* 12:R40. doi: 10.1186/gb-2011-12-4-r40
- Kulkarni, R. D., Kelkar, H. S., and Dean, R. A. (2003). An eight-cysteine-containing CFEM domain unique to a group of fungal membrane proteins. *Trends Biochem. Sci.* 28, 118–121. doi: 10.1016/S0968-0004(03)00025-2
- Lamdan, N. L., Shalaby, S., Ziv, T., Kenerley, C. M., and Horwitz, B. A. (2015). Secretome of *Trichoderma* interacting with maize roots: role in induced systemic resistance. *Mol. Cell. Proteomics* 14, 1054–1063. doi: 10.1074/mcp.M114.046607
- Liu, Y., Wang, K., Cheng, Q., Kong, D., Zhang, X., Wang, Z., et al. (2020). Cysteine protease RD21A regulated by E3 ligase SINAT4 is required for drought-induced resistance to *Pseudomonas syringae* in Arabidopsis. *J. Exp. Bot.* 71, 5562–5576. doi: 10.1093/jxb/era255
- Lyou, S. H., Park, H. J., Jung, C., Sohn, H. B., Lee, G., Kim, C. H., et al. (2009). The Arabidopsis AtLEC gene encoding a lectin-like protein is up-regulated by multiple stimuli including developmental signal, wounding, jasmonate, ethylene, and chitin elicitor. *Mol. Cells* 27, 75–81. doi: 10.1007/s10059-009-0007-1
- Manavalan, T., Stepanov, A. A., Hegnar, O. A., and Eijnsink, V. G. H. (2021). Sugar oxidoreductases and LPMOs - two sides of the same polysaccharide degradation story? *Carbohydr. Res.* 505:108350. doi: 10.1016/j.carres.2021.108350
- Mangiest, A. A. (2020). Endophytes: colonization, behaviour, and their role in defense mechanism. *Int. J. Microbiol.* 3:6927219. doi: 10.1155/2020/6927219
- Martinez, D., Berka, R. M., Henrissat, B., Saloheimo, M., Arvas, M., Baker, S. E., et al. (2008). Genome sequencing and analysis of the biomass-degrading fungus *Trichoderma reesei* (syn. *Hypocrea jecorina*). *Nat. Biotechnol.* 26, 553–602008. doi: 10.1038/nbt1403
- McLaughlin, J. E., Bin-Umer, M. A., Widiez, T., Finn, D., McCormick, S., and Tumer, N. E. (2015). A lipid transfer protein increases the glutathione content and enhances Arabidopsis resistance to a Trichothecene Mycotoxin. *PLoS One* 10:e0130204. doi: 10.1371/journal.pone.0130204
- Mendoza-Mendoza, A., Zaid, R., Lawry, R., Hermosa, R., Monte, E., Horwitz, B. A., et al. (2018). Molecular dialogues between *Trichoderma* and roots: role of the fungal secretome. *Fungal Biol. Rev.* 32, 62–85. doi: 10.1016/j.fbr.2017.12.001
- Mengistu, A. A. (2020). Endophytes: colonization, behaviour, and their role in defense mechanism. *Int. J. Microbiol.* 2020:6927219.
- Moneo-Sánchez, M., Alonso-Chico, A., Knox, J. P., Dopico, B., Labrador, E., and Martín, I. (2019). β -(1,4)-Galactan remodelling in Arabidopsis cell walls affects the xyloglucan structure during elongation. *Planta* 249, 351–362. doi: 10.1007/s00425-018-3008-5
- Morán-Diez, M. E., Trushina, N., Lamdan, N. L., Rosenfelder, L., Mukherjee, P. K., Kenerley, C. M., et al. (2015). Host-specific transcriptomic pattern of

- Trichoderma virens* during interaction with maize or tomato roots. *BMC Genomics* 16:8. doi: 10.1186/s12864-014-1208-3
- Mukherjee, P. K., Horwitz, B. A., and Kenerley, C. M. (2012). Secondary metabolism in *Trichoderma* - a genomic perspective. *Microbiology* 158, 35–45. doi: 10.1099/mic.0.053629-0
- Murashige, T., and Skoog, F. (1962). A revised medium for rapid growth and bio assays with tobacco tissue cultures. *Physiol. Plant.* 15, 473–497. doi: 10.1111/j.1399-3054.1962.tb08052.x
- Nasser, L., Weissman, Z., Pinsky, M., Amartely, H., Dvir, H., and Kornitzer, D. (2016). Structural basis of haem-iron acquisition by fungal pathogens. *Nat. Microbiol.* 1:16156. doi: 10.1038/nmicrobiol.2016.156
- Nieto-Jacobo, M. F., Steyaert, J. M., Salazar-Badillo, F. B., Nguyen, D. V., Rostás, M., Braithwaite, M., et al. (2017). Environmental growth conditions of *trichoderma* spp. affects indole acetic acid derivatives, volatile organic compounds, and plant growth promotion. *Front. Plant Sci.* 8:102. doi: 10.3389/fpls.2017.00102
- Nogueira-Lopez, G., Greenwood, D. R., Middleditch, M., Winefield, C., Eaton, C., Steyaert, J. M., et al. (2018). The apoplastic secretome of *Trichoderma virens* during interaction with maize roots shows an inhibition of plant defence and scavenging oxidative stress secreted proteins. *Front. Plant Sci.* 9:409. doi: 10.3389/fpls.2018.00409
- Oide, S., Tanaka, Y., Watanabe, A., and Inui, M. (2019). Carbohydrate-binding property of a cell wall integrity and stress response component (WSC) domain of an alcohol oxidase from the rice blast pathogen *Piricularia oryzae*. *Enzyme Microb. Technol.* 125, 13–20. doi: 10.1016/j.enzmictec.2019.02.009
- Ormaney, M., Thuleau, P., van der Hoorn, R. A. L., Grat, S., Testard, A., Kamal, K. Y., et al. (2019). Sphingolipid-induced cell death in *Arabidopsis* is negatively regulated by the papain-like cysteine protease RD21. *Plant Sci.* 280, 12–17. doi: 10.1016/j.plantsci.2018.10.028
- Perez-Riverol, Y., Csordas, A., Bai, J., Bernal-Llinares, M., Hewapathirana, S., Kundu, D. J., et al. (2019). The PRIDE database and related tools and resources in 2019: improving support for quantification data. *Nucleic Acids Res.* 47, D442–D450. doi: 10.1093/nar/gky1106
- Peškan-Berghöfer, T., Shahollari, B., Giong, P. H., Hehl, S., Markert, C., Blanke, V., et al. (2004). Association of *Piriformospora indica* with *Arabidopsis thaliana* roots represents a novel system to study beneficial plant–microbe interactions and involves early plant protein modifications in the endoplasmic reticulum and at the plasma membrane. *Physiol. Plant.* 122, 465–477.
- Pogorelko, G. V., Juvalé, P. S., Rutter, W. B., Hütten, M., Maier, T. R., Hewezi, T., et al. (2019). Re-targeting of a plant defense protease by a cyst nematode effector. *Plant J.* 98, 1000–1014. doi: 10.1111/tpj.14295
- Rani Singhania, R., Dixit, P., Kumar Patel, A., Shekher Giri, B., Kuo, C. H., Chen, C. W., et al. (2021). Role and significance of lytic polysaccharide monoxygenases (LPMOs) in lignocellulose deconstruction. *Bioresour. Technol.* 335:125261. doi: 10.1016/j.biortech.2021.125261
- Rashid, A., and Deyholos, M. K. (2011). PELPK1 (At5g09530) contains a unique pentapeptide repeat and is a positive regulator of germination in *Arabidopsis thaliana*. *Plant Cell Rep.* 9, 1735–1745. doi: 10.1007/s00299-011-1081-3
- Ruocco, M., Lanzuise, S., Lombardi, N., Woo, S. L., Vinale, F., Marra, R., et al. (2015). Multiple roles and effects of a novel *Trichoderma* Hydrophobin. *Mol. Plant Microb. Interact.* 28, 167–179. doi: 10.1094/MPMI-07-14-0194-R
- Sabnam, N., and Barman, R. (2017). WISH, a novel CFEM GPCR is indispensable for surface sensing, asexual and pathogenic differentiation in rice blast fungus. *Fungal Genet. Biol.* 105, 37–51. doi: 10.1016/j.fgb.2017.05.006
- Sagarika, M. S., Parameswaran, C., Senapati, A., Barala, J., Mitra, D., Prabhukarthikeyan, S. R., et al. (2021). Lytic polysaccharide monoxygenases (LPMOs) producing microbes: a novel approach for rapid recycling of agricultural wastes. *Sci. Total Environ.* 806:150451. doi: 10.1016/j.scitotenv.2021.150451
- Samolski, I., Rincón, A. M., Pinzón, L. M., Viterbo, A., and Monte, E. (2012). The *qid74* gene from *Trichoderma harzianum* has a role in root architecture and plant biofertilization. *Microbiology* 158, 129–138. doi: 10.1099/mic.0.053140-0
- Sarrocchio, S., Matarese, F., Baroncelli, R., Vannacci, G., Seidl-Seiboth, V., Kubicek, C. P., et al. (2017). The constitutive endopolylacturonase TvPG2 regulates the induction of plant systemic resistance by *Trichoderma virens*. *Phytopathology* 107, 537–544. doi: 10.1094/PHYTO-03-16-0139-R
- Sato, Y., Tezuka, A., Kashima, M., Shimizu-Inatsugi, R., Yamazaki, M., et al. (2019). Transcriptional variation in glucosinolate biosynthetic genes and inducible responses to aphid herbivory on field-grown *Arabidopsis thaliana*. *Front. Sci.* 10:787. doi: 10.3389/fgene.2019.00787
- Seidl, V., Marchetti, M., Schandl, R., Allmaier, G., and Kubicek, C. P. (2006). Epl1, the major secreted protein of *Hypocrea atroviridis* on glucose, is a member of a strongly conserved protein family comprising plant defense response elicitors. *FEBS J.* 273, 4346–4359. doi: 10.1111/j.1742-4658.2006.05435.x
- Sharon, A., Fuchs, Y., and Anderson, J. D. (1993). The elicitation of ethylene biosynthesis by a *Trichoderma* xylanase is not related to the cell wall degradation activity of the enzyme. *Plant Physiol.* 102, 1325–1329. doi: 10.1104/pp.102.4.1325
- Shoresh, M., Harman, G. E., and Mastouri, F. (2010). Induced systemic resistance and plant responses to fungal biocontrol agents. *Annu. Rev. Phytopathol.* 48, 21–43. doi: 10.1146/annurev-phyto-073009-114450
- Silva, R. N., Monteiro, V. N., Steindorff, A. S., Gomes, E. V., Noronha, E. F., and Ulhoa, C. J. (2019). *Trichoderma/pathogen/plant* interaction in pre-harvest food security. *Fungal Biol.* 123, 565–583. doi: 10.1016/j.funbio.2019.06.010
- Skamnioti, P., Furlong, R. F., and Gurr, S. J. (2008). The fate of gene duplicates in the genomes of fungal pathogens. *Commun. Integr. Biol.* 1, 196–198. doi: 10.4161/cib.1.2.7144
- Small, I., Peeters, N., Legeai, F., and Lurin, C. (2004). Predotar: a tool for rapidly screening proteomes for N-terminal targeting sequences. *Proteomics* 4, 1581–1590. doi: 10.1002/pmic.200300776
- Tan, Y. H., Ramanujam, R., and Naqvi, N. (2017). Structure-function analyses of the Pth11 receptor reveal an important role for CFEM motif and redox regulation in rice blast. *New Phytol.* 214, 330–342. doi: 10.1111/nph.14347
- Thürich, J., Meichsner, D., Furch, A. C. U., Pfalz, J., Krüger, T., Kniemeyer, O., et al. (2018). *Arabidopsis thaliana* responds to colonisation of *Piriformospora indica* by secretion of symbiosis-specific proteins. *PLoS One* 13:e0209658. doi: 10.1371/journal.pone.0209658
- Tong, S. M., Chen, Y., Zhu, J., Ying, S. H., and Feng, M. G. (2016). Subcellular localization of five singular WSC domain-containing proteins and their roles in *Beauveria bassiana* responses to stress cues and metal ions. *Environ. Microbiol. Rep.* 8, 295–304. doi: 10.1111/1758-2229.12380
- Tong, S.-M., Wang, D. Y., Gao, B. J., Ying, S. H., and Feng, M. G. (2019). The DUF1996 and WSC domain-containing protein Wsc11 acts as a novel sensor of multiple stress cues in *Beauveria bassiana*. *Cell Microbiol.* 21:e13100. doi: 10.1111/cmi.13100
- Tsai, H.-J., Shao, K.-H., Chan, M. C., Cheng, C.-P., Yeh, K.-W., Oelmüller, R., et al. (2020). *Piriformospora indica* symbiosis improves water stress tolerance of rice through regulating stomata behavior and ROS scavenging systems. *Plant Signal. Behav.* 15:1722447. doi: 10.1080/15592324.2020.1722447
- Tseng, Y. H., Rouina, H., Groten, K., Rajani, P., Furch, A. C. U., Reichelt, M., et al. (2020). An endophytic *trichoderma* strain promotes growth of its hosts and defends against pathogen attack. *Front. Plant Sci.* 11:573670. doi: 10.3389/fpls.2020.573670
- Vaknin, Y., Shadkhan, Y., Levinsky, E., Morozov, M., Romano, J., and Oshero, N. (2014). The three *Aspergillus fumigatus* CFEM-domain GPI-anchored proteins (CfmA-C) affect cell-wall stability but do not play a role in fungal virulence. *Fungal Genet. Biol.* 63, 55–64. doi: 10.1016/j.fgb.2013.12.005
- van Zelm, E., Zhang, Y., and Testerink, C. (2020). Salt tolerance mechanisms of plants. *Annu. Rev. Plant Biol.* 71, 403–433.
- Viterbo, I., and Chet, T. (2006). Hyd1, a new hydrophobin gene from the biocontrol agent *Trichoderma asperellum*, is involved in plant root colonization. *Mol. Plant Pathol.* 7, 249–258. doi: 10.1111/j.1364-3703.2006.00335.x
- Vuong, T. V., and Master, E. R. (2021). Enzymatic upgrading of heteroxylans for added-value chemicals and polymers. *Curr. Opin. Biotechnol.* 73, 51–60. doi: 10.1016/j.copbio.2021.07.001
- Wang, D., Li, Y., Zheng, Y., and Hsieh, Y. S. Y. (2021). Recent advances in screening methods for the functional investigation of lytic polysaccharide monoxygenases. *Front. Chem.* 9:653754. doi: 10.3389/fchem.2021.653754
- Wawra, S., Fesel, P., Widmer, H., Neumann, U., Lahrmann, U., Becker, S., et al. (2019). FGB1 and WSC3 are in planta-induced β -glucan-binding fungal lectins with different functions. *New Phytol.* 222, 1493–1506. doi: 10.1111/nph.15711
- Wu, L., and Bao, J. K. (2013). Anti-tumor and anti-viral activities of *Galanthus nivalis* agglutinin (GNA)-related lectins. *Glycoconj. J.* 30, 269–279. doi: 10.1007/s10719-012-9440-z

- Yeats, T. H., and Rose, J. K. C. (2008). The biochemistry and biology of extracellular plant lipid-transfer proteins (LTPs). *Protein Sci.* 17, 191–198. doi: 10.1110/ps.073300108
- Zapparata, A., Baroncelli, R., Brandström Durling, M., Kubicek, C. P., Karlsson, M., Vannacci, G., et al. (2021). Fungal cross-talk: an integrated approach to study distance communication. *Fungal Genet. Biol.* 148:103518. doi: 10.1016/j.fgb.2021.103518
- Zerva, A., Pentari, C., Ferousi, C., Nikolaiivits, E., Karnaouri, A., and Topakas, E. (2021). Recent advances on key enzymatic activities for the utilisation of lignocellulosic biomass. *Bioresour. Technol.* 28:126058. doi: 10.1016/j.biortech.2021.126058
- Zhang, Z.-N., Wu, Q.-Y., Zhang, G.-Z., Zhu, Y.-Y., Murphy, R. W., Liu, Z., et al. (2015). Systematic analyses reveal uniqueness and origin of the CFEM domain in fungi. *Sci. Rep.* 5:3032. doi: 10.1038/srep13032
- Zhao, Z., Cai, F., Gao, R., Ding, M., Jiang, S., Chen, P., et al. (2021). At least three families of hyphosphere small secreted cysteine-rich proteins can optimize surface properties to a moderately hydrophilic state suitable for fungal attachment. *Environ. Microbiol.* 23, 5750–5768. doi: 10.1111/1462-2920.15413
- Zhu, W., Wie, W., Wu, Y., Zhou, Y., Peng, F., Zhang, S., et al. (2017). BcCFEM1, a CFEM domain-containing protein with putative gpi-anchored site, is involved in pathogenicity, conidial production, and stress tolerance in *Botrytis cinerea*. *Front Microbiol.* 8:1807. doi: 10.3389/fmicb.2017.01807
- Conflict of Interest:** The authors declare that the research was conducted in the absence of any commercial or financial relationships that could be construed as a potential conflict of interest.
- Publisher's Note:** All claims expressed in this article are solely those of the authors and do not necessarily represent those of their affiliated organizations, or those of the publisher, the editors and the reviewers. Any product that may be evaluated in this article, or claim that may be made by its manufacturer, is not guaranteed or endorsed by the publisher.

Copyright © 2022 Rouina, Tseng, Nataraja, Uma Shaanker, Krüger, Knimeyer, Brakhage and Oelmüller. This is an open-access article distributed under the terms of the Creative Commons Attribution License (CC BY). The use, distribution or reproduction in other forums is permitted, provided the original author(s) and the copyright owner(s) are credited and that the original publication in this journal is cited, in accordance with accepted academic practice. No use, distribution or reproduction is permitted which does not comply with these terms.

4.4 Manuscript 4

Tris(methylthio)methane Produced by *Mortierella hyalina* Affects Sulfur Homeostasis in *Arabidopsis*

Yu-Heng Tseng, Stefan Bartram, Sandra S. Scholz, Michael Reichelt, Anja K. Meents, Anatoli Ludwig, Axel Mithöfer, Ralf Oelmüller

Submitted to Scientific Reports (2021)

Preprint: Authorea. July 06, 2021. doi: 10.22541/au.162428733.37123941/v2

Your submissions

Track your submissions

Tris(methylthio)methane Produced by *Mortierella hyalina* Affects Sulfur Homeostasis in *Arabidopsis*

Corresponding Author: Ralf Oelmüller

Scientific Reports

7fad67ae-d130-48f4-a679-ad6d2016f2a2 | v.2.1

1 Reviewer report received 24 Apr 22

If you have submitted any articles to us via any other submissions system, e.g. Editorial Manager or eJournalPress, please log in to, or use notification emails from that system for article tracking information. Still have a question? [Contact us](#)

© 2022 Springer Nature.
[About Springer Nature](#)

[Springer Nature](#)
[Help and support](#)

[Privacy Settings](#)

Tris(methylthio)methane Produced by *Mortierella hyalina* Affects Sulfur Homeostasis in *Arabidopsis*

Y-H. Tseng¹, S. Bartram², M. Reichelt², S. S. Scholz¹, A. K. Meents^{1,3}, A. Ludwig¹, A. Mithöfer³, R. Oelmüller^{1*}

¹ Department of Plant Physiology, Matthias Schleiden Institute of Genetics, Bioinformatics and Molecular Botany, Friedrich-Schiller-University Jena, Jena, 07743, Germany

² Department of Natural Product Biosynthesis, Max Planck Institute for Chemical Ecology, Jena, 07745, Germany

³ Research Group Plant Defense Physiology, Max Planck Institute for Chemical Ecology, Jena, 07745, Germany

*corresponding author: ralf.oelmueller@uni-jena.de

Abstract

Microbial volatiles are important factors in symbiotic interactions with plants. *Mortierella hyalina* is a beneficial root-colonizing fungus with a garlic-like smell, and promotes growth of *Arabidopsis* seedlings. GC-MS analysis of the *M. hyalina* headspace and NMR analysis of the extracted essential oil identified the sulfur-containing volatile tris(methylthio)methane (TMTM) as the major compound. Incorporation of the sulfur from the fungal volatile into plant metabolism was shown by ³⁴S labeling experiments. Under sulfur deficiency, TMTM downregulated sulfur deficiency-responsive genes, prevented glucosinolate (GSL) and glutathione (GSH) diminishment, and sustained plant growth. However, excess TMTM led to accumulation of GSH and GSL and reduced plant growth. Since TMTM is not directly incorporated into cysteine, we propose that the volatile from *M. hyalina* influences the plant sulfur metabolism by interfering with the GSH metabolism, and alleviates sulfur imbalances under sulfur stress.

Introduction

Sulfur is an indispensable macronutrient required for proper plant growth, development and physiology. It is first incorporated into cysteine, and further into methionine, or glutathione (GSH), vitamins and cofactors, such as thiamine and biotin, to carry out important biochemical processes. Notable examples are the iron-sulfur (Fe-S) clusters which are required for electron transport in photosynthesis, reduction and assimilation of sulfur and nitrogen ¹. In *Brassicales*, assimilation of sulfur contributes to the biosynthesis of glucosinolates (GSL), which are essential defense molecules against herbivores and pathogens ^{2,3}. Although being classified as secondary metabolites, GSLs can hold up to 30% of total sulfur content in the plant body and serves as sulfur reservoir ^{4,5}.

In natural environments, microorganisms play an important role in providing sulfate (SO₄²⁻), the primary sulfur source accessible, to roots for the biosynthesis of sulfur-containing compounds in plants. As early as in 1877, scientists already knew that elemental sulfur (S⁰) can be oxidized to sulfate, and microbes were thought to be an essential part of it ⁶. It was few decades later that scientists isolated the S-oxidizing bacteria *Thiobacillus denitrificans* and *T. thioparus*, and showed that they produce sulfate from S⁰ ⁶⁻⁸. It is now known that microorganisms possess sulfatases to mineralize organic sulfur, thereby releasing sulfate into the rhizosphere ^{9,10}. Furthermore, fungi were shown to mobilize sulfate-esters and activate arylsulfatase activity under sulfur-limiting conditions ¹¹⁻¹⁴. Fungal symbionts are also crucial in supporting plants with sulfur. Mycorrhizal fungi are notable example for the promotion of sulfur uptake, as shown in maize, clover and tomato ^{15,16}. The expression of sulfate transporters in plants can also be influenced by mycorrhizal fungi, resulting in improved sulfur status in host plants under sulfur deficient condition ¹⁷.

Volatile organic compounds (VOCs) from microorganisms present another possible route to provide sulfur to plants. Dimethyl disulfide (DMDS) is produced by the bacteria *Serratia odorifera* and *Bacillus spp.* B55. Under sulfur deficiency, DMDS can sustain plant growth and increase root branching¹⁸. Labeling experiment demonstrated that the S-containing volatile is taken up by the plants^{18,19}. Compared to bacteria, much less is known about sulfur-containing volatiles produced by fungi²⁰. Besides DMDS, mercaptoacetone, 3-methylsulfanylpropan-1-ol, benzothiazole, 2-acetylthiazole, 3,5-dimethyl-1,2,4-trithiolane, 5-(1-propynyl)-thiophen-2-carbaldehyde and sulfur dioxide (SO₂) were identified from various fungi²⁰. Not much is known about the mechanisms of their incorporation into the plant metabolism, but SO₂ can cross cell membranes directly from the surrounding air and influence sulfur distribution within leaf tissue²¹⁻²³.

Incorporation of sulfur is a multi-step process. In soil, it starts primarily with the assimilation of sulfate by sulfate transporters (SULTRs) in the root cells. SULTR1;1 and SULTR1;2 act as the primary sulfate transporters. SULTR2;1 is located in the xylem and pericycle and responsible for root-shoot sulfur transport²⁴⁻²⁸. Once the sulfate is in root tissue, it is incorporated alongside with ATP into adenosine-5'-phosphosulfate (APS) via the enzyme ATP sulfurylase (ATPS). APS serves as the branching point between primary and secondary metabolism. Through APS reductase, APS is transformed into sulfite (SO₃²⁻), and subsequently reduced to sulfide (S²⁻) by sulfite reductase. With O-acetyl-serine(thiol)lyase (OASTL), sulfide is further incorporated into O-acetylserine (OAS) to form the amino acid cysteine for primary metabolism²⁹. On the other hand, APS goes into secondary metabolism through APS kinase, which catalyzes the formation of 3'-phosphoadenosine-5'-phosphosulfate (PAPS). PAPS serves as the molecule required for the last step of glucosinolate biosynthesis³⁰.

Sulfur assimilation and dynamics are highly regulated under sulfur deficiency. In *Arabidopsis*, *SULFUR LIMITATION1 (SLIMI)* is a central regulator of sulfur deficiency. The transcription factor of the EIL family induces the expression of genes for sulfur uptake transporters. Furthermore, genes for GSL catabolism are stimulated while those for GSL biosynthesis are repressed, thereby releasing sulfur from the GSL storage for proper plant growth³¹. Correspondingly, mutants defect in *SLIMI* cannot respond to sulfur deficiency, and show reduced root growth³¹. Finally, *SULFUR DEFICIENT INDUCED (SDI) 1* and *SDI2* are often used as marker genes to monitor sulfur deficiency³². *SDI1* is localized in the nucleus, and can repress GSL biosynthesis by interacting with MYB28, a major transcription factor for aliphatic GSL biosynthesis³²⁻³⁴. All these components fine tune the sulfur status in the plant body to optimize plant competence in response to sulfur limitation.

Mortierella hyalina belongs to the phylum *Mucoromycota*. It possesses a distinctive garlic-like smell in synthetic culture. In the co-cultivation experiments with *Arabidopsis thaliana* seedlings, *M. hyalina* promoted plant growth³⁵. Similar results were obtained for three other *Mortierella* strains with garlic-like smells, while the growth responses were less for two strains which did not smell (Figure S1). In this study, we address the question whether the volatile from *M. hyalina* interferes with the plant metabolism and might be involved in the regulation of sulfur stress. The headspace of *M. hyalina* was analyzed by GC-MS to identify those VOCs which are potentially involved in plant nutrition. By NMR, a sulfur-containing volatile, tris(methylthio)methane (TMTM; CAS Number 5418-86-0), was identified as the major chemical in the fungal headspace. Incorporation of the sulfur from the fungal volatile into plant metabolism was shown with stable sulfur isotope labeling experiments. Under sulfur deficiency, TMTM restored plant growth, reduced the consumption of sulfur-containing metabolites, and reduced the response of seedlings to sulfur deficiency. We propose that TMTM maintains sulfur homeostasis in the plant under sulfur limitation condition. Finally, biochemical analyses examining cysteine biosynthesis did not show direct incorporation of TMTM into O-acetylserine (OAS), suggesting that additional biochemical steps are involved before the sulfur from TMTM is incorporated into cysteine, or non-canonical incorporation mechanisms different from sulfate assimilation are involved.

Materials and Methods

Growth medium and conditions for seedlings and fungi

Seeds of wild-type *A. thaliana* (ecotype Columbia-0), and *slim1*³¹ mutant were surface-sterilized for 8 mins in sterilization solution containing lauryl sarcosine (1%) and Clorix cleaner (23%). Surface-sterilized seeds were washed with sterilized water 8 times and placed on Petri dishes with MS medium supplemented with 0.3% gelrite³⁶. The MS medium contains 1.5 mM MgSO₄. After cold treatment at 4 °C for 48 - 72 hours, plates were incubated at 22 °C under long day conditions (16 hours light/ 8 hours dark; 80 μmol m⁻² s⁻¹). Wild-type *A. thaliana* (ecotype Columbia-0) was curated in the lab. The *slim1* mutant was kindly provided by Prof. Dr. Stanislav Kopriva.

Sulfur deficiency assays were performed with MGRL medium³⁷. 1 L of MGRL medium contains 1.75 mM NaH₂PO₄, 1.75 mM Na₂HPO₄, 2 mM Ca(NO₃)₂, 1.5 mM MgSO₄, 3 mM KNO₃, 67 μM Na₂EDTA, 30 μM H₃BO₃, 10.3 μM MnSO₄, 8.6 μM FeSO₄, 1 μM ZnSO₄, 1.0 μM CuSO₄, 130 nM CoCl₂, 24 nM (NH₄)₆Mo₇O₂₄, 1% sucrose, 0.3% Gelrite, pH 5.6. For MGRL medium with reduced sulfate, MgSO₄ was replaced by MgCl₂. The total sulfate concentration in high (HS) and low (LS) sulfate MGRL medium is 1520.9 μM and 20.9 μM, respectively.

Mortierella strains (*M. hyalina*, FSU-509; *M. alpina*, SF002698; *M. turficola*, SF009851; *M. vinacea*, SF002701; *M. longicollis*, SF009830) were obtained from Jena Microbial Resource Center (Jena, Germany). They were grown on Potato-Dextrose-Agar (PDA), pH 6.5, and at 23 °C in the dark³⁸ for fresh subcultures and desiccator assays.

For the sulfur labeling assays, *M. hyalina* was grown on KM medium modified from³⁹: 1 L of the medium contains 7.06 mM NaNO₃, 6.98 mM KCl, 11.17 mM KH₂PO₄, 177.9 μM H₃BO₃, 6.4 μM CuCl₂, 76.5 μM ZnCl₂, 7.28 μM CoCl₂, 0.89 μM (NH₄)₆Mo₇O₂₄, 29.6 μM MnCl₂, 20 μM Na₂EDTA, 20 μM FeCl₂, 2% glucose, 0.2% peptone/trypton, 0.1% yeast extract, 0.1% casein hydrolysate, 1% agar. Finally, 2.11 mM ammonium sulfate ((NH₄)₂³²SO₄ or (NH₄)₂³⁴SO₄) was added to make the unlabeled (³²S)/ labeled (³⁴S) medium, respectively.

Tris(methylthio)methane and ³⁴S ammonium sulfate were purchased from Sigma-Aldrich (Germany).

Desiccator assay and sulfur labeling experiment

Twenty-one 10-d old *Arabidopsis* seedlings germinated on MS were transferred to a Petri dish with sucrose-free MS medium (14.5 cm in diameter). In a 2.5 L desiccator, a 7-d old fungal culture grown on PDA was placed at the bottom. A plastic inlay with holes was inserted in the middle of the desiccator, and the big Petri-dish with seedlings was placed on top of it. To ensure sterility of the experiment, the seam of the desiccator was wrapped with 3M Micropore tape (Figure S2). Fungus and seedlings were incubated at 22 °C under long day conditions (16 hours light/ 8 hours dark; 80 μmol m⁻² s⁻¹) for 14 days. Number of inflorescence (flower stalk) and shoot fresh weight were measured.

The same procedure was followed for sulfur labeling experiments, in which a 7-d old *M. hyalina* culture grown on labeled/unlabeled KM medium and 16 10-d old *Arabidopsis* seedlings were used. Root and shoot tissues were collected after 14 days for analysis.

Sulfur deficiency assay with MGRL agar medium

After germinating on MS medium for 5 days, seedlings were rinsed gently with sterilize water and transferred to MGRL agar medium with high (1520.9 μM) or low (20.9 μM) sulfate concentrations and grown for 7 days.

To measure the influence of TMTM on seedling's fresh and dry weights, a 3-compartments Petri dish (92 mm in diameter, Sarstedt, Germany) was used. Two compartments were filled with MGRL agar medium, both containing either high or low sulfate concentrations. A sheet of sterilized paper was put in the third empty compartment, to which 10 μL sterilized water and a 10 μL mixture with 0, 10, 100 or 1000 μg TMTM dissolved in dichloromethane was applied.

For monitoring root growth, 5 days-old seedlings were transferred onto high or low sulfate MGRL agar medium on a square plate (100 x 100 x 20 mm; Sarstedt, Germany). A sheet of sterilized paper was put on to the bottom of the plate, and TMTM was applied onto it as described above. Plates

were incubated vertically. Root length was measured directly after transfer and after 7 days of treatment.

RNA isolation, and primers and qPCR

RNA was extracted with TRIzo Reagent (Invitrogen, Germany) following the guideline provided by the manufacturer. Traces of DNA in the RNA samples were digested with TURBO Dnase (Thermo Fisher Scientific, Germany), and cDNA synthesis was performed with Omniscript RT Kit (Qiagen, Germany), following manufacturer's instructions.

Each 20 μ L qPCR reaction contained 2 μ L of 10 x DreamTaq Buffer (Thermo Fisher Scientific, Germany), 0.2 mM dNTP, 0.5 μ M forward/reverse primer, 40 ng cDNA, 1 μ L 20 x Evagreen (Biotum, Germany) and 1.5 U of DreamTaq DNA Polymerase (Thermo Fisher Scientific, Germany). Real-time PCR reaction was conducted with CFX Connect Real-Time PCR Detection System (Bio-Rad, Germany). The initial denaturation step was set at 95 °C for 3 min, followed by 40 cycles of denaturation at 95 °C for 10 s, annealing at 60 °C for 50 s, and extension at 72 °C for 1 min. Melt curve analysis was performed by incubating at 95 °C for 10 s, 65 °C 5s, and increase to 95 °C at 0.5 °C/5 s increment. Melt curve analysis showed a single peak for all genes analyzed. Values were normalized to the housekeeping gene *RPS18B* (AT1G34030) for gene expression analysis. Gene-specific primer pairs used in this study and the gene accession numbers are listed in Table S1.

GC-MS analysis of *M. hyalina* headspace

Headspace volatiles of a slant culture of *M. hyalina* grown on potato dextrose agar (PDA) in a glass tube with stopper were collected 14 days after inoculation with a solid phase micro extraction (SPME) fiber (Aldrich, red fiber, 100 μ m PDMS) over 2 hours. As a control, the headspace of the medium alone (PDA) was collected.

SPME fibers were desorbed in the injection port of a GC at 220 °C in splitless mode and a helium flow of 1 mL/min through the chromatographic column connected. The volatiles were separated chromatographically on a ZB-5 ms column (30 m x 0.25 mm x 0.25 μ m, Phenomenex) with an GC-oven temperature program starting at 45 °C for 2 min, then heating up to 220 °C with a rate of 10°C/min, followed by a heating rate of 30°C/min to 280°C, and was maintained for 1.83 min. The column was connected to a time-of-flight mass spectrometer (GCT, Micromass) via a transfer line (280 °C). Ion source temperature was set to 250 °C and ionization energy was 70 eV. For high resolution MS (HR-MS), heptacosane was continuously streaming into the source and the calibrated HR-MS profile was locked at m/z 218.9856.

A mixture of *n*-alkanes C₈ - C₂₀ in *n*-hexane (Aldrich) was measured before and after a sample sequence under the same conditions except for the injector split ratio (1:50). Retention times of the *n*-alkanes were used to calculate the retention index (RI) for each peak in the GC-MS chromatogram according to the method of ⁵².

Compounds were identified based on their mass spectra (MS) in combination with their individual RIs in comparison to MS and RI database ⁴⁰ using MassFinder software ⁴¹ in combination with NIST MS Search. Authentic reference compounds were used additionally for identification. For relative quantification, identified peaks of the GC-MS total ion chromatogram (TIC) were integrated.

Identification of the S-containing volatile from *M. hyalina*

To identify the main S-containing volatile produced by *M. hyalina*, the compound needed to be enriched for further analysis. For that, *M. hyalina* was cultured in liquid PDA media for two weeks at 23 °C in the dark without shaking. The fungus mats produced on the surface of the media were collected (total FW \approx 180 g), rinsed twice with tap water and cut into pieces. The fungus material was subjected to hydro-distillation to obtain the essential oil which was further analyzed by NMR and GC-MS.

GSL analysis by HPLC-UV

Fresh seedlings (20 to 100 mg) were harvested, weighed and freeze-dried until constant weight and ground to fine powder. GSLs were extracted with 1 mL of 80% methanol solution containing 0.05 mM of Sinalbin as internal standard. After centrifugation, 700 μ L of extract was loaded onto DEAE Sephadex A 25 columns and treated with arylsulfatase for desulfation (Sigma-Aldrich). The eluted desulfo-GSLs were separated using high performance liquid chromatography (Agilent 1100 HPLC system, Agilent Technologies) on a reversed phase column (Nucleodur Sphinx RP, 250 x 4.6 mm, 5 μ m, Macherey-Nagel, Düren, Germany) with a water (A) - acetonitrile (B) gradient: 0 - 1.0 min, 1.5% B; 1.0 - 6.0 min, 1.5-5% B; 6.0 - 8.0 min, 5 - 7% B; 8.0 - 18.0 min, 7 - 21% B; 18.0 - 23.0 min, 21 - 29% B; 23.0 - 23.1 min, 29 - 100% B; 23.1 - 24.0 min 100% B and 24.1 - 28.0 min 1.5% B; flow 1.0 mL min⁻¹. Detection was performed with a photodiode array detector and peaks were integrated at 229 nm. Desulfated GSLs were identified by comparison of their retention time and UV spectra to those of purified standards previously extracted from *A. thaliana*⁴². We used the following molar response factors for quantification of individual GSL relative to the internal standard Sinalbin: 2.0 for aliphatic GSLs and 0.5 for indolic GSLs⁴³.

Relative quantification of GSH by LC-MS/MS

Relative quantification of GSH was achieved on an Agilent 1200 series HPLC system (Agilent Technologies) coupled to a tandem mass spectrometer API 3200 (Applied Biosystems, Darmstadt, Germany) via electrospray ionization (ESI) in positive ionization mode. An aliquot of the raw extract from GSL analysis (see above) was injected. A Zorbax Eclipse XDB-C18 column (Agilent Technologies) was used for separation. 0.05% formic acid and acetonitrile were used as solvent A and B, respectively, at a flow rate of 1.1 mL/min with the following profile: 0 - 0.5 min, 3 - 15% B; 0.5 - 2.5 min, 15% - 85% B; 2.5 - 2.6 min, 85 - 100% B; 2.6 - 3.5 min, 100% B, 3.5 - 3.6 min, 100% B - 3% B and 3.6 - 6.0 min 3% B. The MS parameters were optimized as follows: ion spray voltage, 5500 V; turbo gas temperature, 650°C; collision gas, 3 psi; curtain gas, 35 psi; ion source gas 1, 60 psi; ion source gas 2, 60 psi. MRM for the parent ion - product ion was set as follows: m/z 308.1 - 179.1 (CE, 17 V; DP, 46 V) for GSH. Relative quantification was accomplished and expressed in relative peak area units of the LC-MS/MS signal per mg fresh weight.

Determination of incorporation of ³⁴S into plant GSH and GSLs by LC-ESI-Q-ToF-MS

To determine the ³⁴S incorporation into plant metabolites, ultra-high-performance liquid chromatography–electrospray ionization–high resolution mass spectrometry (UHPLC–ESI–HRMS) was performed with a Dionex Ultimate 3000 series UHPLC (Thermo Scientific, Germany) and a Bruker timsToF mass spectrometer (Bruker Daltonics, Bremen, Germany). UHPLC was done by applying a Zorbax Eclipse XDB-C18 column (100 mm × 2.1 mm, 1.8 μ m, Agilent Technologies, Waldbronn, Germany) with a solvent system of 0.1% formic acid (A) and acetonitrile (B) at flow rate of 0.3 mL/min. The elution profile was as follows: 0 to 0.5 min, 5% B; 0.5 to 11.0 min, 5-60% B in A; 11.0 to 11.1 min, 60-100% B, 11.1 to 12.0 min, 100% B and 12.1 to 15.0 min 5% B. For the coupling of LC to MS, electrospray ionization (ESI) in positive and negative ionization mode, for GSH and GSL, respectively, was used. The mass spectrometer was set with the parameters: capillary voltage 4.5/3.5 KV, end plate offset of 500 V, nebulizer pressure 2.8 bar, nitrogen at 280 °C at flow rate of 8 L/min as drying gas. Acquisition was conducted at 12 Hz with a mass range from m/z 50 to 1500. At the beginning of each chromatographic analysis, 10 μ L of a sodium formate-isopropanol solution (10 mM solution of NaOH in 50/50 (v/v%) isopropanol- water containing 0.2% formic acid) was injected into the dead volume for recalibration of the mass spectrometer with the expected cluster ion m/z values. Peak areas were integrated from extracted ion chromatogram traces of the monoisotopic molecular ion peak ([M+H]⁺, [M-H]⁻) and of the isotopologues that could be detected with an isolation width of m/z +/- 0.002. Details of m/z values of isotopologues are listed in Table S2. First we calculated the percentage of single isotopologues (% isotopologue) as a proportion of the sum of all isotopologues for each single compound (i.e. % of the monoisotopic molecular ion peak = peak area of the monoisotopic molecular ion peak * 100% / (peak area of the monoisotopic molecular ion peak + (peak area of “isotopologue+1”) + (peak area of “isotopologue+2”) + (peak area of

“isotopologue+3”) + (peak area of “isotopologue+4”). In order to determine the incorporation of ^{34}S , the $^{34}\text{S}/^{32}\text{S}$ ratio was calculated ($^{34}\text{S}/^{32}\text{S}$ ratio = % “isotopologue + 2”/ % of the monoisotopic molecular ion peak).

Determination of incorporation of ^{34}S into plant amino acids by GC-Orbitrap-HR-MS analysis

L-Methionine and L-Cysteine standards were obtained from Sigma-Aldrich (Taufkirchen, Germany). Stock standard solutions of each individual amino acid were prepared in a methanol/ NH_4OH (8M) (1:1, v:v) buffer and stored at -20°C . Methyl chloroformate and pyridine were obtained from Sigma-Aldrich, chloroform and HCl from Carl Roth GmbH (Karlsruhe, Germany).

Total protein hydrolysis, amino acid extraction and derivatization followed a protocol by ⁴⁴ with some modifications. In short: 15 to 35 mg plant material (fresh weight) suspended in 1 mL HCl (10 mM) were homogenized with a TissueLyser II (Quiagen GmbH, Hilden, Germany) using tungsten carbide balls (2 x 3min at 25 Hz). After vortexing for 30 min at 37°C and centrifugation at 20,000 g, the supernatant was added to a strong cation exchange solid phase extraction cartridge (HyperSep SCX, bed weight: 50 mg, volume 1 mL (60108-420; Thermo Fisher Scientific, Darmstadt, Germany)), pre-activated with 1 mL 0.01 M HCl and 1 mL ultrapure water (3 x). After washing with methanol/water (80/20, v/v), the cartridge was eluted with 500 μL of freshly prepared methanol/ NH_4OH (8M) (1:1, v:v) buffer.

A sample of 400 μL was evaporated to dryness in a gentle nitrogen stream and re-suspended in 50 μL of the elution buffer. 10 μL of pyridine were added and vortexed for 10 s followed by adding 10 μL of methyl chloroformate and mixed for 10 min. The derivatization products were extracted by adding 50 μL chloroform and 50 μL sodium bicarbonate solution (50 mM), followed by vortexing for 2 min. After phase separation the lower organic phase was transferred to a new glass vial insert and dried for 30 min with anhydrous sodium sulfate. The dried solution was transferred to a micro insert (100 μL) and stored at -80°C for further GC-MS analysis.

Gas chromatography-Orbitrap-high resolution-mass spectrometry analyses were carried out on a Trace 1310 series GC with split/splitless injector coupled to a Q Exactive GC Orbitrap mass spectrometer (Thermo Fisher Scientific, Bremen, Germany). Separations were obtained with a fused silica capillary column (ZB SemiVolatiles, 30 mm \times 25 μm , 0.25 μm + 10m guard column, Zebron, Phenomenex, Aschaffenburg, Germany) using Helium at a flow rate of 1 $\text{mL}\cdot\text{min}^{-1}$. The injection volume was 4 μL and the injector was operated in splitless with surge mode (25 kPa for 1 min followed by a split flow of 20 $\text{mL}\cdot\text{min}^{-1}$) at 240°C . Programmed GC oven temperature started at 70°C for 3 min, raised at $25^\circ\text{C}\cdot\text{min}^{-1}$ to 280°C , and held for 5 min with 16.4 min total GC run time. The transfer line temperature was set to 250°C and the ion source was operated in positive EI mode at 300°C and 70 eV ionization energy. Resolution of the Orbitrap was set to 120000 at 200 Da and the acquisition started at 6.5 min with a mass range from 34 to 300 amu.

Data acquisition and evaluation was performed using Xcalibur (Thermo Fisher Scientific).

OASTL activity assay monitoring cysteine biosynthesis

200 mg *Arabidopsis* wild-type *Col-0* leaves were homogenized in liquid nitrogen. 0.5 mL extraction buffer (50 mM HEPES-KOH, pH 7.5; 10 mM KCl; 1 mM EDTA; 1 mM EGTA; 30 mM DTT; 0.5 mM PMSF and 10% (v/v) glycerol) was added and mixed at 4°C for 10 min with frequent shaking. After centrifugation at 16,000 g for 10 min, supernatant was collected. Protein concentration was measured with ROTIQuant (Carl-Roth, Germany) following manufacturer's instruction.

The OASTL activity assay was carried out in a volume of 0.1 mL containing 10 mg protein extract, 100 mM HEPES-KOH pH 7.5; 5 mM DTT; 10 mM OAS and 10 mM Na_2S or 4 mM TMTM. The reaction was initiated by the addition of OAS, and was incubated for 10 min at 25°C . Termination of the reaction was done by adding 50 μL of 20% (w/v) trichloroacetic acid followed by centrifugation at 12500 g.

100 μ L of the supernatant was transferred to a new tube and incubated in 200 μ L of 134 mM Tris-HCl, pH 8.0 and 1 mM DTT at room temperature for 30 min. The reduced sample was mixed with 200 μ L acetic acid and 200 μ L ninhydrin reagent (250 mg ninhydrin dissolved in 6 mL acetic acid and 4 mL concentrated HCl). The tube was incubated at 90 °C for 10 min, then cooled rapidly on ice for 2 min. The sample was diluted with 95% ethanol and measured at 560 nm to quantify the synthesized cysteine.

Measurement of root length

Plates were scanned with an Epson scanner (Perfection V600 Photo, Epson, Germany). Files were imported into ImageJ⁴⁵. Root length was measured by SmartRoot plug-in with semi-automated root tracing method⁴⁶.

Statistical tests

Statistical tests were performed using R studio version 1.1.463 with R version 3.4.4. Figures were plotted using Python 3.7.4 and arranged with LibreOffice Draw 5.1.6.2.

All the experiments were performed in accordance with relevant guidelines and regulations.

Results

M. hyalina produces the sulfur-containing volatile tris(methylthio)methane (TMTM)

To identify the volatiles from *M. hyalina* which are responsible for the garlic-like smell, the GC-MS chromatograms of SPME volatile collections of the headspace of slant cultures of *M. hyalina* were compared with the collections from the headspace of the growth medium. Three major constituents could be identified (Figure 1) of which the HR-MS of the molecular ions M^+ and $[M+2]^+$ (for the ³⁴S isotopologue) revealed the molecular formulas $C_3H_8S_2$ (m/z measured 108.0062, 110.0020 calc. 108.0062, 110.0020; RI 894; 2% rel.), $C_3H_8S_3$ (m/z measured 137.9626, 139.9585 calc. 137.9626, 139.9584; RI 1197; 2% rel.), and $C_4H_{10}S_3$ (m/z measured 153.9942, 155.9910 calc. 153.9939, 155.9897, RI 1217; 96% rel.). $C_3H_8S_2$ and $C_3H_8S_3$ could be identified as bis(methylthio)methane (RI_{lit.} 889) and dimethyl trithiocarbonate (RI_{lit.} 1196), respectively by comparison of their mass spectra and RI with the datasets of the NIST library and additionally with mass spectra and RI of authentic samples recorded under the same conditions.

For $C_4H_{10}S_3$, the major compound of the headspace of *M. hyalina*, library searches in NIST and Wiley mass spectra databases revealed no hit in combination with the RI. Therefore *M. hyalina* was extracted by hydro distillation. The obtained essential oil consisted mainly of three compounds (by GC-MS): Octenol-3-ol (22.4%) 3-octenone (21.7%) and $C_4H_{10}S_3$ (27.3%). NMR analysis of the mixture could reduce the structure motive of $C_4H_{10}S_3$ to $(CH_3-X)_n-CH$ (X = S, O, etc.) which in combination with the empirical formula $C_4H_{10}S_3$ from HR-MS led to the structure of tris(thiomethyl)methane. Comparison with an authentic sample of tris(methylthio)methane (Aldrich) showed to be identical with respect to NMR and mass spectra, and RI (Figure 1 and Table 1).

Sulfur atoms from TMTM are incorporated into plant metabolites

To test whether sulfur from TMTM is incorporated into plant material, we grew *M. hyalina* on modified KM medium with addition of ³²S- or ³⁴S-ammonium sulfate, and co-cultivated them together with *Arabidopsis* seedlings in the same desiccator, but without direct physical contact. After 14 days, shoot and root tissues were collected, and the ³⁴S/³²S ratio of GSLs and GSH was analyzed with LC-MS. For the shoots, a significant increase of the ³⁴S/³²S ratios for the GSLs was detected (8.8%→12.8% for 4MOI3M; 8.4% → 12.6% for I3M; 14% → 16.6% for 8MSOO; 13.7% → 16.7% for 4MSOB; Figure 2; Figure S3 and S4). The ratio was also higher for the GSH in the shoots (4.4% → 6.3%). With the exception of 8MSOO, for which we also observed a significant increase in the roots (11.3% → 15.4%), the increases for the other compounds were much less (4.1% → 4.3%; Figure 2A and 2B; Figure S3 and S4).

As a proxy for the sulfur incorporation into *Arabidopsis* protein, we chose the sulfur containing amino acids cysteine and methionine from the total hydrolysate of *Arabidopsis* plant material. After derivatization, the relative amount of ^{34}S was monitored by evaluating $[\text{M}+2]^+$ to $[\text{M}]^+$ ratio of sulfur containing ions using GC-high resolution mass spectrometry.

Due to the fact that the molecular ions and their M+2 isotopomers are not detectable (cysteine) or at a very low abundance (methionine), we chose the following sulfur containing fragments for the evaluation of relative ^{34}S abundance: For cysteine $[\text{C}_4\text{H}_5\text{O}_2^{32}\text{S}]^+$ m/z: 117.0005 vs. $[\text{C}_4\text{H}_5\text{O}_2^{34}\text{S}]^+$ m/z: 118.9963; $[\text{C}_4\text{H}_6\text{O}_2\text{N}^{32}\text{S}]^+$ m/z: 132.0114 vs. $[\text{C}_4\text{H}_6\text{O}_2\text{N}^{34}\text{S}]^+$ m/z: 134.0072; $[\text{C}_6\text{H}_{10}\text{O}_4\text{N}^{32}\text{S}]^+$ m/z: 192.0325 vs. $[\text{C}_6\text{H}_{10}\text{O}_4\text{N}^{34}\text{S}]^+$ m/z: 194.0283 and for methionine $[\text{C}_2\text{H}_5^{32}\text{S}]^+$ m/z: 61.0106 vs. $[\text{C}_2\text{H}_5^{34}\text{S}]^+$ m/z: 63.0064; $[\text{C}_6\text{H}_{12}\text{O}_2\text{N}^{32}\text{S}]^+$ m/z: 162.0583 vs. $[\text{C}_6\text{H}_{12}\text{O}_2\text{N}^{34}\text{S}]^+$ m/z: 164.0541; $[\text{C}_7\text{H}_{11}\text{O}_3\text{N}^{32}\text{S}]^+$ m/z: 189.0454 vs. $[\text{C}_7\text{H}_{11}\text{O}_3\text{N}^{34}\text{S}]^+$ m/z: 191.0412, respectively (Figure S5 and S6). The $^{34}\text{S}/^{32}\text{S}$ ratio given in percent of the respective ^{34}S isotopomeric fragment was extracted from each GC-MS run by averaging over three MS scans at the respective retention time (9.76 min, cysteine derivative, 9.30 min, methionine derivative) in each run.

From three biological replicates, the mean $^{34}\text{S}/^{32}\text{S}$ ratios for the individual amino acids in plants under treatment with a substrate containing ^{34}S at natural abundance vs. the ^{34}S enriched substrate were 3.31% (SE \pm 0.22) vs. 8.88% (SE \pm 0.75) for cysteine ($p < 0.001$) and 3.84% (SE \pm 0.38) vs. 6.19% (SE \pm 0.33) for methionine ($p < 0.001$), respectively (Figure 2C).

In conclusion, sulfur from *M. hyalina* headspace is incorporated into the plant amino acids, GSLs and GSH.

TMTM influences plant growth under sulfur deficiency

Since TMTM contains sulfur, we tested the effect of the volatile on *Arabidopsis* plants. Five days-old seedlings were transferred to MGRM agar medium with either high sulfate (HS) or low sulfate (LS) and applied with 0, 10, 100 or 1000 μg TMTM. After 7 days, the fresh and dry weights of the total seedlings, the shoots and the roots were analyzed. Figure 3 shows the effects of TMTM on the weights of seedlings grown under LS in comparison to seedlings grown sufficient sulfur in the medium (HS). In all instances, TMTM had the strongest growth promoting effect for seedlings grown on LS supplemented with 10 or 100 μg TMTM (Figure 3). The high dose of 1000 μg TMTM reduced plant growth. In summary, low doses of TMTM (10 - 100 μg) had positive effects on plant fresh and dry weights under sulfur deficiency, while the higher dose (1000 μg) had a negative effect.

We also tested whether TMTM promoted growth of seedlings which were grown on medium with sufficient sulfur (cf. Methods and Materials). Different doses of pure TMTM were applied to 10-days old seedlings grown on HS medium in desiccator for 1 or 2 weeks. Although the same trend was visible, the growth promoting effect of the volatile was not significant (data not shown).

TMTM maintains root growth under sulfur deficiency

To examine whether TMTM affects the root growth under sulfur deficiency, 5-days old seedlings of wild-type (*Col-0*) and *slim1*, a mutant which fails to respond to sulfur deficiency³¹, were transferred to LS medium and grown vertically for additional 7 days. Figure 4 shows the increase in the root lengths after 7 days. Compared to LS condition without TMTM, the root lengths of both wild-type (WT) and *slim1* seedlings were significantly higher when they were exposed to 100 μg TMTM (\approx 9% and 7% increase for WT and *slim1*, respectively; Figure 4A and 4B) and reached the level of seedlings which were grown on HS medium without the volatile. In accordance with the fresh and dry weight data, addition of 1000 μg TMTM reduced the root growth rate in WT for about 10% (Figure 4A). Interestingly, the reduction in root growth was not affected in *slim1* (\approx 1% reduction compared to LS without TMTM; Figure 4B). The differences might be due to an effect of TMTM on the sulfur homeostasis.

TMTM reduces sulfur deficiency responses

To test whether TMTM serves as sulfur source and affects the sulfur homeostasis of *Arabidopsis* seedlings, we tested the effect of the volatile on the expression of sulfur-responsive genes

and the sulfur metabolite dynamics. Under sulfur limitation conditions, expression of sulfur transporters *SULTR1;1*, *SULTR1;2* and *SULTR2;1* was upregulated. Two days after exposure to the volatile, we observed a gradual decrease of their transcript levels and the effect increased with increasing TMTM amounts. Furthermore, the expression of the GSL repressor genes *SDII* and *SDI2* was significantly down-regulated by TMTM, again in a dosage-dependent manner (Figure 5A). We further examined the expression of genes involved in the GSL and GSH metabolisms (i.e., *BRANCHED-CHAIN AMINOTRANSFERASE4*, *BCAT4*; *SULFOTRANSFERASE*, *SOTs*; *GLUTAMATE-CYSTEINE LIGASE*, *GSH1*; *GLUTATHIONE SYNTHETASE*, *GSH2*; two *CYTOCHROME P450*, *CYP79B2* and *CYP79F2*). With 10 and 100 µg TMTM, their expression levels were similar to those in seedlings grown on HS medium, and with 1000 µg TMTM, their expression levels increased slightly.

Seven days after volatile application, *SDII* was significantly up-regulated with 10 µg TMTM, while with 100 or 1000 µg TMTM, both *SDII* and *SDI2* remained down-regulated compared to LS without TMTM (Figure 5B). The expression levels of the GSL metabolism genes *CYP79B2* and *SOTs* increased to the levels in seedlings grown on LS without TMTM, and with 1000 µg TMTM, they showed the highest expression.

In conclusion, after the application of 100 µg TMTM to LS-exposed seedlings, expression of the examined genes is similar to that of the seedlings grown on HS medium, and this is observed from the second to the 7th day. We propose that low doses of TMTM (10 and 100 µg) diminish sulfur stress by adjusting the expression of the analyzed genes to the expression levels found under HS conditions. Upregulation of *SDII* and *SDI2* in LS-grown seedlings exposed to 10 µg TMTM for 7 days indicates that this dose is too low to repress the sulfur-deficiency response after longer time periods.

TMTM maintained GSH and GSL levels under sulfur deficiency

Cysteine is the first metabolite synthesized during sulfur assimilation, while GSH and GSLs contain large portions of the total sulfur pool. Under sulfur deficiency, these metabolites are broken down, and the sulfur is recycled for primary growth^{4,47}. We measured the GSH and GSLs level to investigate whether TMTM influences the plant sulfur homeostasis at this level.

Two, four and seven days after application of 1000 µg TMTM, the GSH level was significantly increased compared to the untreated control. Even 100 µg TMTM stimulated the GSH level, which was similar to that found in seedlings grown on HS (Figure 6A).

A similar pattern was observed for the total GSL levels. After 2 days, the GSLs slightly increased with increasing TMTM concentrations (Figure 6B). The effect broadened after 4 days. On LS without TMTM, total GSL level was significantly lowered compared to the rest of the treatments, indicating the breakdown of GSLs under sulfur limitation (Figure 6B). Similar to the results obtained for GSH, application of 100 µg TMTM maintained the total GSL level at the same level found in seedlings grown on HS medium without the volatile after 7 days (Figure 6B). We conclude that 100 µg TMTM established sulfur homeostasis in LS-grown seedlings which is comparable to the conditions in seedlings grown on HS. Furthermore, incorporation of TMTM can be observed in seedlings treated with 1000 µg TMTM, since they showed significantly higher amounts of GSH and GSLs than the unexposed controls.

OASTL does not incorporate sulfur from TMTM into cysteine

Sulfate is normally reduced to sulfide, which is as substrate for OASTLs to form cysteine. Cysteine is further converted to GSH, methionine or other sulfur-containing metabolites. TMTM is an organosulfide, containing 3 sulfide groups. We tested if plants can synthesize cysteine using TMTM as substrate. An OASTL activity assay was conducted by incubating total protein extract from wild-type *A. thaliana* (ecotype *Col-0*) leaves with OAS and either Na₂S or TMTM as substrate. Cysteine production was only observed when Na₂S was used as substrate (Figure 7). In another experimental setup, total protein extract, OAS, Na₂S and TMTM were incubated in the same reaction tube. Also under this condition, cysteine was produced, which indicates that OASTL activity was not

hindered by TMTM. We conclude that TMTM is not a direct substrate for sulfur incorporation into cysteine by OASTL under our experimental conditions (Figure 7).

Discussion

In this study, we identified a fungal volatile, TMTM, as the main component in the headspace of the beneficial fungus *M. hyalina*. Application of TMTM participated in maintaining the sulfur homeostasis in *Arabidopsis* seedlings under sulfur deficiency. At low concentrations (10 – 100 μg), TMTM compensated sulfur-limitation responses of the seedlings: the volatile restored growth and root development which were inhibited under sulfur-limiting conditions, restricted the upregulation of sulfur deficiency marker genes (*SULTRs*, *SDII* and *SDI2*), or the breakdown of GSL and the accumulation of GSH. On medium with HS, these TMTM effects were not detectable. TMTM shifted the measured parameters in LS plants to those found in seedlings grown on HS medium without TMTM application. Higher concentration induced toxic or inhibitory effects, altered the sulfur homeostasis, and restricted plant growth. However, TMTM was not directly incorporated into cysteine by OASTLs, and is not inhibiting their function. This suggests that cysteine might not be a direct product of TMTM incorporation, or TMTM must be processed before its sulfur atoms can be incorporated into cysteine.

Plants reduce the CO_2 concentration in closed systems which has to be considered in experimental designs with volatiles^{48,49}. In preliminary experiments, we co-cultivated *Arabidopsis* seedlings with 5 different *Mortierella* strains with comparable growth rates and metabolite features. Since the three fungi with distinctive garlic-like smells (*M. hyalina*, *M. alpina*, *M. turficolalis*) induced a stronger growth promotion compared to two non-smelling strains (*M. vinacea*, *M. longicollis*; Figure S1), we hypothesized that the sulfur-containing volatiles from the fungi might be involved in the growth regulation (Figure 2). The major volatile in the headspace of one of these fungi, *M. hyalina*, was TMTM, and its abundance prompted us to investigate it in this study. The stronger growth of seedlings which are growing in the presence of the fungus compared to those treated with TMTM demonstrates that the investigated volatile is not the only factor involved in the growth promoting effect. Nevertheless, the stabilizing effect of TMTM on the sulfur homeostasis allows better plant performance under sulfur stress.

Plants respond to sulfur limitation in various ways. The first response is up-regulation of sulfate transporters (*SULTRs*) to increase sulfate uptake from root^{24–28}. On the other hand, genes for GSL biosynthesis (e.g., *BCAT4*, *CYP79B2* and *CYP79F2*) are down-regulated, while those repressing GSL biosynthesis (*SDII* and *SDI2*) are up-regulated. These responses help plants to remobilize sulfur to sustain growth^{50–52}. Among the inspected genes, the sulfur starvation genes *SULTR1;1*, *SULTR1;2*, *SULTR2;1* and both *SDII* and *SDI2* were down-regulated in a TMTM dose-dependent manner in plants which suffer from sulfur limitation (Figure 5A and 5B). Since the sulfur in TMTM can be incorporated into the plant material, the expression of the above-mentioned genes and those involved in GSL and GSH metabolism is similar to seedlings grown under HS condition without TMTM. Moreover, excessive TMTM results in the upregulation of these genes, indicating that these plants are actively moving excess sulfur to secondary metabolites. This is in accordance with a recent study by⁴⁷, showing a retrograde sulfur flow from glucosinolates to cysteine in *Arabidopsis*. Interestingly, the mRNA levels for GSL and GSH metabolism genes was higher in seedlings after 2 days on LS medium without TMTM compared to seedlings grown on HS medium. This might be caused by higher sulfate influx from the medium due to up-regulation of *SULTRs*. The plants actively metabolize the assimilated sulfate into various metabolites and utilize this as a store to sustain growth under sulfur limitations.

The effect is also observed at the metabolic level. Under sulfur limitation, the GSH and GSL levels decreased. However, 100 μg TMTM maintained the levels high under sulfur starvation conditions (Figure 6). Again, besides maintaining sulfur homeostasis, excess sulfur from the high TMTM dose is largely metabolized into secondary metabolites.

Imbalances in the sulfur pool have severe consequences for plant growth and yield^{53–55}. Under LS, biomass production and root growth were significantly reduced (Figure 3 and 4). This could be restored by the application of TMTM in low doses. We propose that TMTM maintains the sulfur homeostasis and allows root growth which is comparable to that under HS conditions (Figure 4). Furthermore, it appears that excess TMTM tilts the sulfur homeostasis and shifts the sulfur towards the secondary metabolite pool, resulting in reduced plant biomass production and root growth (Figure 3 and 4).

Growth regulation by TMTM *via* sulfur homeostasis is further supported by the response of WT and *slim1* seedlings to high TMTM dose. 1000 µg TMTM inhibited root growth in WT seedlings, but not in *slim1* (Figure 4). Apparently, lower doses of TMTM stimulated root growth in LS because the volatile influences the sulfur homeostasis. As a result, the root growth was comparable to seedling's growth on HS without the volatile. However, the high dose (1000 µg) of TMTM could provide too much sulfur to the LS-grown WT seedlings, which may result in the activation of stress responses and ultimately growth retardation. On the other hand, because *slim1* could not mobilize sulfur from its secondary metabolites³¹, these seedlings showed a higher tolerance to excess TMTM. The different response of the two genotypes to excess TMTM is consistent with the idea that TMTM-induced changes in the sulfur homeostasis influence root growth.

It is known that plants are able to assimilate gaseous sulfur compounds, such as SO₂ and H₂S^{21,56,57}. They are also able to assimilate other sulfur-containing organic volatiles produced by microbes. One example is dimethyl disulfide¹⁸. Nevertheless, how organosulfides are metabolized inside the plant remains unknown.

Diallyl disulfide (DADS), a volatile from garlic, is perhaps the best studied organosulfide, due to its anticancer ability^{58–61}. It increases GSH levels and regulates antioxidant enzyme activity, leading to reduced oxidative stress in animal models^{62–64}. In plants, DADS also affects sulfur metabolism genes^{65–67}. Metabolism of DADS and other organosulfides generates H₂S^{68–71}. Studies on how DADS and other organosulfides are metabolized suggest the involvement of GSH and cysteine^{69–71}. The reaction between DADS and GSH produces S-allyl GSH and a short-lived intermediate allyl perthio through α -carbon nucleophilic substitution. The allyl perthio reacts with a second GSH, resulting in the release of H₂S and S-allyl GSH disulfide⁷¹.

We found that 1000 µg TMTM increased both the GSH and GSL levels, and the GSH level responded faster to the volatile treatment (Figure 6A and 6B). A possible explanation could be that incorporation of sulfur from TMTM into the plant metabolism is connected to GSH. We tested if TMTM can be a direct substrate for OASTLs and found that this is not the case (Figure 7). Therefore, unlike sulfate assimilation, TMTM might first interfere with the GSH/GSSG system. This might lead to the cleavage of the C-S bonds and sulfur incorporation into plant. A detailed metabolome analysis of early sulfur-containing compounds after TMTM treatment might elucidate early steps in the role of this novel volatile.

Acknowledgement

We kindly thank Claudia Röppischer and Sarah Mußbach for technical assistance and Prof. Dr. Stanislav Kopriva for providing us the *slim1* mutant. Our special thanks go to Dr. Nico Ueberschaar (MS-Platform, FSU Jena) for support with the HR-MS measurements. This work was supported by the DFG (CRC1127).

References

1. Raven, J. A., Evans, M. C. W. & Korb, R. E. The role of trace metals in photosynthetic electron transport in O₂-evolving organisms. *Photosynth. Res.* **60**, 111–150 (1999).
2. Bakhtiari, M. & Rasman, S. Variation in below-to aboveground systemic induction of glucosinolates mediates plant fitness consequences under herbivore attack. *J. Chem. Ecol.* **46**, 317–329 (2020).

3. Ting, H.-M. *et al.* The role of a glucosinolate-derived nitrile in plant immune responses. *Front. Plant Sci.* **11**, (2020).
4. Falk, K. L., Tokuhisa, J. G. & Gershenzon, J. The effect of sulfur nutrition on plant glucosinolate content: Physiology and molecular mechanisms. *Plant Biol.* **9**, 573–581 (2007).
5. Aghajanzadeh, T., Hawkesford, M. J. & De Kok, L. J. The significance of glucosinolates for sulfur storage in Brassicaceae seedlings. *Front. Plant Sci.* **5**, 704 (2014).
6. Lipman, J. G., Mclean, H. C. & Lint, H. C. Sulfur oxidation in soils and its effect on the availability of mineral phosphates. *Soil Sci.* **2**, 499–538 (1916).
7. Beijerinck, M. W. Phenomenes de reduction produits par les microbes. *Arch. Néerlandaises Sci. Exactes Nat. (Section 2)* **9**, 131–157 (1904).
8. Waksman, S. A. & Joffe, J. S. Microorganisms concerned in the oxidation of sulfur in the soil: II. Thiobacillus thiooxidans, a new sulfur-oxidizing organism isolated from the soil. *J. Bacteriol.* **7**, 239–256 (1922).
9. Deng, S. P. & Tabatabai, M. A. Effect of tillage and residue management on enzyme activities in soils: III. Phosphatases and arylsulfatase. *Biol. Fertil. Soils* **24**, 141–146 (1997).
10. Kertesz, M. A. Riding the sulfur cycle--metabolism of sulfonates and sulfate esters in gram-negative bacteria. *FEMS Microbiol. Rev.* **24**, 135–175 (2000).
11. Fitzgerald, J. W. Sulfate ester formation and hydrolysis: a potentially important yet often ignored aspect of the sulfur cycle of aerobic soils. *Bacteriol. Rev.* **40**, 698–721 (1976).
12. Marzluf, G. A. Molecular genetics of sulfur assimilation in filamentous fungi and yeast. *Annu. Rev. Microbiol.* **51**, 73–96 (1997).
13. Omar, S. A. & Abd-Alla, M. H. Physiological aspects of fungi isolated from root nodules of faba bean (*Vicia faba* L.). *Microbiol. Res.* **154**, 339–347 (2000).
14. Baum, C. & Hryniewicz, K. Clonal and seasonal shifts in communities of saprotrophic microfungi and soil enzyme activities in the mycorrhizosphere of *Salix* spp. *J. Plant Nutr. Soil Sci.* **169**, 481–487 (2006).
15. Gray, L. E. & Gerdemann, J. W. Uptake of sulphur-35 by vesicular-arbuscular mycorrhizae. *Plant Soil* **39**, 687–689 (1973).
16. Cavagnaro, T. R. *et al.* Arbuscular mycorrhizas, microbial communities, nutrient availability, and soil aggregates in organic tomato production. *Plant Soil* **282**, 209–225 (2006).
17. Giovannetti, M., Tolosano, M., Volpe, V., Kopriva, S. & Bonfante, P. Identification and functional characterization of a sulfate transporter induced by both sulfur starvation and mycorrhiza formation in *Lotus japonicus*. *New Phytol.* **204**, 609–619 (2014).
18. Meldau, D. G. *et al.* Dimethyl disulfide produced by the naturally associated bacterium *Bacillus* sp B55 promotes *Nicotiana attenuata* growth by enhancing sulfur nutrition. *Plant Cell* **25**, 2731–2747 (2013).
19. Kai, M. *et al.* *Serratia odorifera*: analysis of volatile emission and biological impact of volatile compounds on *Arabidopsis thaliana*. *Appl. Microbiol. Biotechnol.* **88**, 965–976 (2010).

20. Dickschat, J. S. Fungal volatiles – a survey from edible mushrooms to moulds. *Nat. Prod. Rep.* **34**, 310–328 (2017).
21. Randewig, D. *et al.* Sulfite oxidase controls sulfur metabolism under SO₂ exposure in *Arabidopsis thaliana*. *Plant Cell Environ.* **35**, 100–115 (2012).
22. Pfanz, H., Martinoia, E., Lange, O.-L. & Heber, U. Mesophyll resistances to SO₂ fluxes into leaves. *Plant Physiol.* **85**, 922–927 (1987).
23. Rennenberg, H. & Polle, A. Metabolic consequences of atmospheric sulphur influx into plants. in *Plant Responses to the Gaseous Environment: Molecular, metabolic and physiological aspects* (eds. Alscher, R. G. & Wellburn, A. R.) 165–180 (Springer Netherlands, 1994). doi:10.1007/978-94-011-1294-9_9.
24. Takahashi, H., Kopriva, S., Giordano, M., Saito, K. & Hell, R. Sulfur assimilation in photosynthetic organisms: molecular functions and regulations of transporters and assimilatory enzymes. *Annu. Rev. Plant Biol.* **62**, 157–184 (2011).
25. Shibagaki, N. *et al.* Selenate-resistant mutants of *Arabidopsis thaliana* identify Sultr1;2, a sulfate transporter required for efficient transport of sulfate into roots. *Plant J.* **29**, 475–486 (2002).
26. Yoshimoto, N., Takahashi, H., Smith, F. W., Yamaya, T. & Saito, K. Two distinct high-affinity sulfate transporters with different inducibilities mediate uptake of sulfate in *Arabidopsis* roots. *Plant J.* **29**, 465–473 (2002).
27. Kataoka, T., Hayashi, N., Yamaya, T. & Takahashi, H. Root-to-shoot transport of sulfate in *Arabidopsis*. Evidence for the role of Sultr3;5 as a component of low-affinity sulfate transport system in the root vasculature. *Plant Physiol.* **136**, 4198–4204 (2004).
28. Takahashi, H. *et al.* Regulation of sulfur assimilation in higher plants: A sulfate transporter induced in sulfate-starved roots plays a central role in *Arabidopsis thaliana*. *Proc. Natl. Acad. Sci.* **94**, 11102–11107 (1997).
29. Mugford, S. G., Lee, B.-R., Koprivova, A., Matthewman, C. & Kopriva, S. Control of sulfur partitioning between primary and secondary metabolism: *Sulfur partitioning*. *Plant J.* **65**, 96–105 (2011).
30. Mugford, S. G. *et al.* Disruption of adenosine-5'-phosphosulfate kinase in *Arabidopsis* reduces levels of sulfated secondary metabolites. *Plant Cell* **21**, 910–927 (2009).
31. Maruyama-Nakashita, A., Nakamura, Y., Tohge, T., Saito, K. & Takahashi, H. *Arabidopsis* SLIM1 is a central transcriptional regulator of plant sulfur response and metabolism. *Plant Cell* **18**, 3235–3251 (2006).
32. Aarabi, F. *et al.* Sulfur deficiency-induced repressor proteins optimize glucosinolate biosynthesis in plants. *Sci. Adv.* **2**, e1601087 (2016).
33. Hirai, M. Y. *et al.* Omics-based identification of *Arabidopsis* Myb transcription factors regulating aliphatic glucosinolate biosynthesis. *Proc. Natl. Acad. Sci. U. S. A.* **104**, 6478–6483 (2007).

34. Gigolashvili, T., Yatusевич, R., Berger, B., Müller, C. & Flügge, U.-I. The R2R3-MYB transcription factor HAG1/MYB28 is a regulator of methionine-derived glucosinolate biosynthesis in *Arabidopsis thaliana*. *Plant J.* **51**, 247–261 (2007).
35. Johnson, J. M. *et al.* the beneficial root-colonizing fungus *Mortierella hyalina* promotes the aerial growth of *Arabidopsis* and activates calcium-dependent responses that restrict *Alternaria brassicae* –induced disease development in roots. *Mol. Plant. Microbe Interact.* **32**, 351–363 (2019).
36. Murashige, T. & Skoog, F. A revised medium for rapid growth and bio assays with tobacco tissue cultures. *Physiol. Plant.* **15**, 473–497 (1962).
37. Fujiwara, T., Hirai, M. Y., Chino, M., Komeda, Y. & Naito, S. Effects of sulfur nutrition on expression of the soybean seed storage protein genes in transgenic petunia. *Plant Physiol.* **99**, 263–268 (1992).
38. Bains, P. S. & Tewari, J. P. Purification, chemical characterization and host-specificity of the toxin produced by *Alternaria brassicae*. *Physiol. Mol. Plant Pathol.* **30**, 259–271 (1987).
39. Hill, T. & Käfer, E. Improved protocols for *Aspergillus* minimal medium: Trace element and minimal medium salt stock solutions. *Fungal Genet Newsl* **48**, 20–21 (2001).
40. National Institute of Standards and Technology. *NIST/EPA/NIH Mass Spectral & Retention Index Library*. (2014).
41. Hochmuth, D. *Massfinder v. 4.21*. (Hochmuth Scientific Consulting, 2010).
42. Brown, P. D., Tokuhisa, J. G., Reichelt, M. & Gershenzon, J. Variation of glucosinolate accumulation among different organs and developmental stages of *Arabidopsis thaliana*. *Phytochemistry* **62**, 471–481 (2003).
43. Burow, M., Müller, R., Gershenzon, J. & Wittstock, U. Altered glucosinolate hydrolysis in genetically engineered *Arabidopsis thaliana* and its influence on the larval development of *Spodoptera littoralis*. *J. Chem. Ecol.* **32**, 2333–2349 (2006).
44. Vancompernelle, B., Croes, K. & Angenon, G. Optimization of a gas chromatography-mass spectrometry method with methyl chloroformate derivatization for quantification of amino acids in plant tissue. *J. Chromatogr. B Analyt. Technol. Biomed. Life. Sci.* **1017–1018**, 241–249 (2016).
45. Schindelin, J. *et al.* Fiji: an open-source platform for biological-image analysis. *Nat. Methods* **9**, 676–682 (2012).
46. Lobet, G., Pagès, L. & Draye, X. A novel image-analysis toolbox enabling quantitative analysis of root system architecture. *Plant Physiol.* **157**, 29–39 (2011).
47. Sugiyama, R. *et al.* Retrograde sulfur flow from glucosinolates to cysteine in *Arabidopsis thaliana*. *Proc. Natl. Acad. Sci.* **118**, (2021).
48. Naznin, H. A., Kimura, M., Miyazawa, M. & Hyakumachi, M. Analysis of volatile organic compounds emitted by plant growth-promoting fungus *Phoma* sp. GS8-3 for growth promotion effects on tobacco. *Microbes Environ.* **28**, 42–49 (2013).

49. Piechulla, B., Lemfack, M. C. & Kai, M. Effects of discrete bioactive microbial volatiles on plants and fungi. *Plant Cell Environ.* **40**, 2042–2067 (2017).
50. Lewandowska, M. & Sirko, A. Recent advances in understanding plant response to sulfur-deficiency stress. *Acta Biochim. Pol.* **55**, 457–471 (2008).
51. Frerigmann, H. & Gigolashvili, T. Update on the role of R2R3-MYBs in the regulation of glucosinolates upon sulfur deficiency. *Front. Plant Sci.* **5**, (2014).
52. Borpatragohain, P., Rose, T. J. & King, G. J. Fire and brimstone: molecular interactions between sulfur and glucosinolate biosynthesis in model and crop Brassicaceae. *Front. Plant Sci.* **7**, (2016).
53. Zhao, F., Hawkesford, M. & McGrath, S. Sulphur assimilation and effects on yield and quality of wheat. *J. Cereal Sci.* **30**, 1–17 (1999).
54. Lunde, C. *et al.* Sulfur starvation in rice: the effect on photosynthesis, carbohydrate metabolism, and oxidative stress protective pathways. *Physiol. Plant.* **134**, 508–521 (2008).
55. Jobe, T. O., Zenzen, I., Rahimzadeh Karvansara, P. & Kopriva, S. Integration of sulfate assimilation with carbon and nitrogen metabolism in transition from C3 to C4 photosynthesis. *J. Exp. Bot.* **70**, 4211–4221 (2019).
56. Lee, H. K. *et al.* The relationship between SO₂ exposure and plant physiology: a mini review. *Hortic. Environ. Biotechnol.* **58**, 523–529 (2017).
57. Ausma, T. & De Kok, L. J. Atmospheric H₂S: impact on plant functioning. *Front. Plant Sci.* **10**, (2019).
58. Yi, L. & Su, Q. Molecular mechanisms for the anti-cancer effects of diallyl disulfide. *Food Chem. Toxicol. Int. J. Publ. Br. Ind. Biol. Res. Assoc.* **57**, 362–370 (2013).
59. Xiong, T. *et al.* Tristetraprolin: A novel target of diallyl disulfide that inhibits the progression of breast cancer. *Oncol. Lett.* **15**, 7817–7827 (2018).
60. Agassi, S. F. T., Yeh, T.-M., Chang, C.-D., Hsu, J.-L. & Shih, W.-L. Potentiation of differentiation and apoptosis in a human promyelocytic leukemia cell line by garlic essential oil and its organosulfur compounds. *Anticancer Res.* **40**, 6345–6354 (2020).
61. Li, Y., Wang, Z., Li, J. & Sang, X. Diallyl disulfide suppresses FOXM1-mediated proliferation and invasion in osteosarcoma by upregulating miR-134. *J. Cell. Biochem.* (2018) doi:10.1002/jcb.28003.
62. Demeule, M. *et al.* Diallyl disulfide, a chemopreventive agent in garlic, induces multidrug resistance-associated protein 2 expression. *Biochem. Biophys. Res. Commun.* **324**, 937–945 (2004).
63. Hassanein, E. H. M. *et al.* Diallyl disulfide ameliorates methotrexate-induced nephropathy in rats: Molecular studies and network pharmacology analysis. *J. Food Biochem.* e13765 (2021) doi:10.1111/jfbc.13765.
64. Wei, X. *et al.* Acute diallyl disulfide administration prevents and reverses lipopolysaccharide-induced depression-like behaviors in mice via regulating neuroinflammation and oxidonitrosative stress. *Inflammation* (2021) doi:10.1007/s10753-021-01423-0.

65. Cheng, F., Cheng, Z.-H. & Meng, H.-W. Transcriptomic insights into the allelopathic effects of the garlic allelochemical diallyl disulfide on tomato roots. *Sci. Rep.* **6**, 38902 (2016).
66. Cheng, F., Ali, M., Liu, C., Deng, R. & Cheng, Z. Garlic allelochemical diallyl disulfide alleviates autotoxicity in the root exudates caused by long-term continuous cropping of tomato. *J. Agric. Food Chem.* **68**, 11684–11693 (2020).
67. Yang, F. *et al.* Identification and Allelopathy of Green Garlic (*Allium sativum* L.) Volatiles on scavenging of cucumber (*Cucumis sativus* L.) reactive oxygen species. *Mol. Basel Switz.* **24**, (2019).
68. Kim, T. J., Lee, Y. J., Ahn, Y. J. & Lee, G.-J. Characterization of H₂S releasing properties of various H₂S donors utilizing microplate cover-based colorimetric assay. *Anal. Biochem.* **574**, 57–65 (2019).
69. Cai, Y.-R. & Hu, C.-H. Computational study of H₂S release in reactions of diallyl polysulfides with thiols. *J. Phys. Chem. B* **121**, 6359–6366 (2017).
70. Bolton, S. G., Cerda, M. M., Gilbert, A. K. & Pluth, M. D. Effects of sulfane sulfur content in benzyl polysulfides on thiol-triggered H₂S release and cell proliferation. *Free Radic. Biol. Med.* **131**, 393–398 (2019).
71. Liang, D., Wu, H., Wong, M. W. & Huang, D. Diallyl trisulfide is a fast H₂S donor, but diallyl disulfide is a slow one: the reaction pathways and intermediates of glutathione with polysulfides. *Org. Lett.* **17**, 4196–4199 (2015)., 1–17.

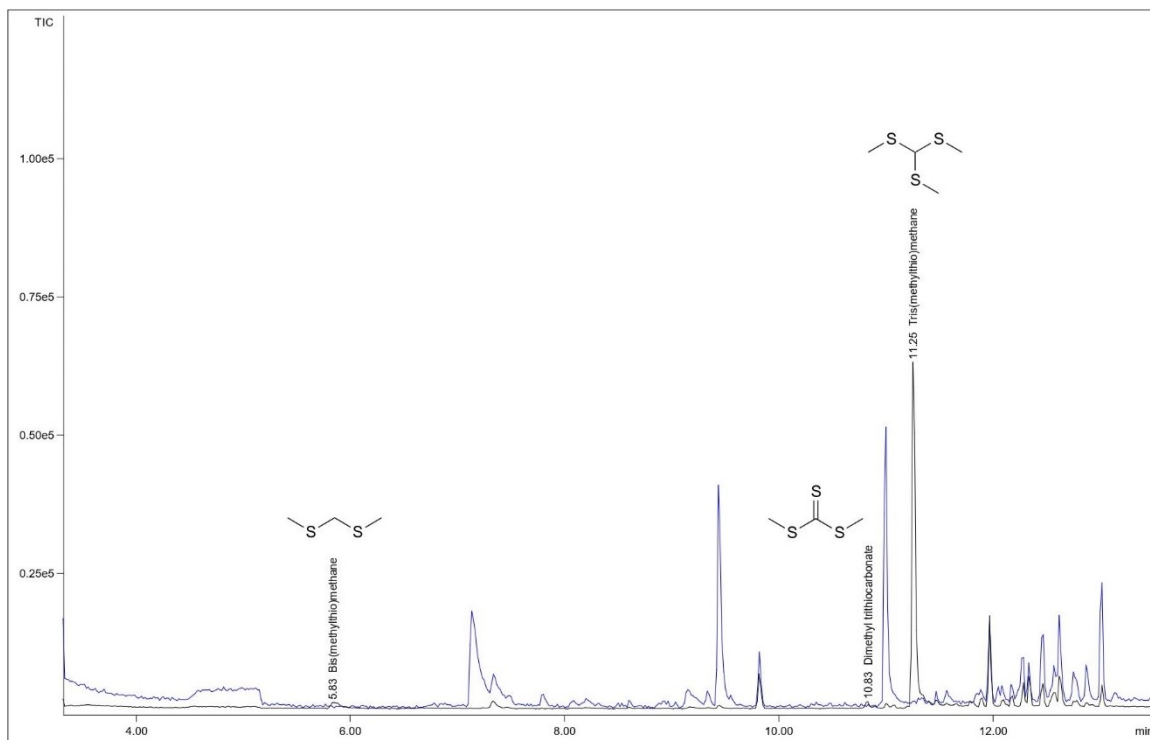


Figure 1. GC-MS chromatogram of the headspace of *M. hyalina* (black) and the growth medium alone (blue). Identified signals are not present in the headspace of the growth medium. The three strong signals in the chromatogram of the headspace of the growth medium could be identified by MS and RI as benzaldehyde (7.13 min) nonanal (9.44 min), and decanal (11.00 min).

Table 1. Mass spectra and retention indices in comparison with authentic samples.

RT	Compound	Formula by HR-MS	CAS #	Retention index	RI* (lit)	Rel %	Authentic reference
5.83	Bis(methylthio)methane	C ₃ H ₈ S ₂	[1618-26-4]	894	889	2%	y
10.83	Dimethyl trithiocarbonate	C ₃ H ₆ S ₃	[2314-48-9]	1197	1196	2%	y
11.25	Tris(methylthio)methane	C ₄ H ₁₀ S ₃	[5418-86-0]	1217	§)	98%	y

*) The RI given in the NIST MS database and by other authors as well as the mass spectrum of Tris(methylthio)methane published there and in the Wiley MS database are not correct. GC-MS of an authentic sample purchased from Aldrich revealed an RI of 1217 and a mass spectrum identical to the mass spectrum of the compound at the identical retention time from the headspace of *M. hyalina*.

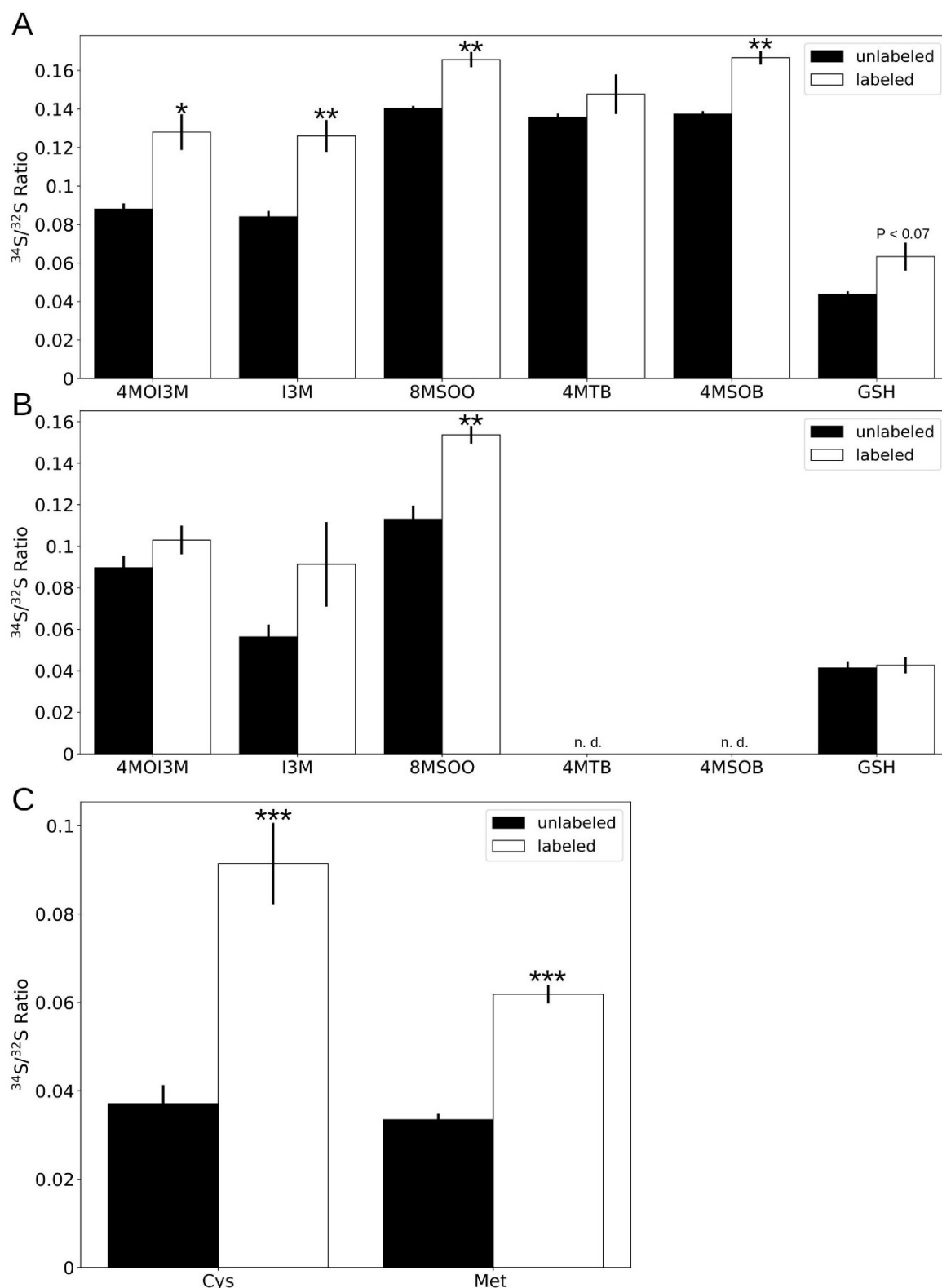


Figure 2. Sulfur atoms from fungal volatiles are incorporated into plant tissues. (A) and (B) $^{34}\text{S}/^{32}\text{S}$ ratios of glucosinolates and glutathione in shoot (A) and root (B) tissues. (C) $^{34}\text{S}/^{32}\text{S}$ ratios in cysteine (Cys) and methionine (Met) from *Arabidopsis* shoot. *M. hyalina* was grown on modified KM plates with the addition of ^{32}S -ammonium sulfate (unlabeled) or ^{34}S -ammonium sulfate (labeled), and co-cultivated with *Arabidopsis* seedlings in a desiccator. Error bars represent SEs from 3 biological replicates, each contains at least 3 technical replicates from 16 seedlings. Asterisks indicate significance level from Student's Ttest between unlabeled and labeled samples (* $P < 0.05$; ** $P < 0.01$; *** $P < 0.001$). n.d.: not detected.

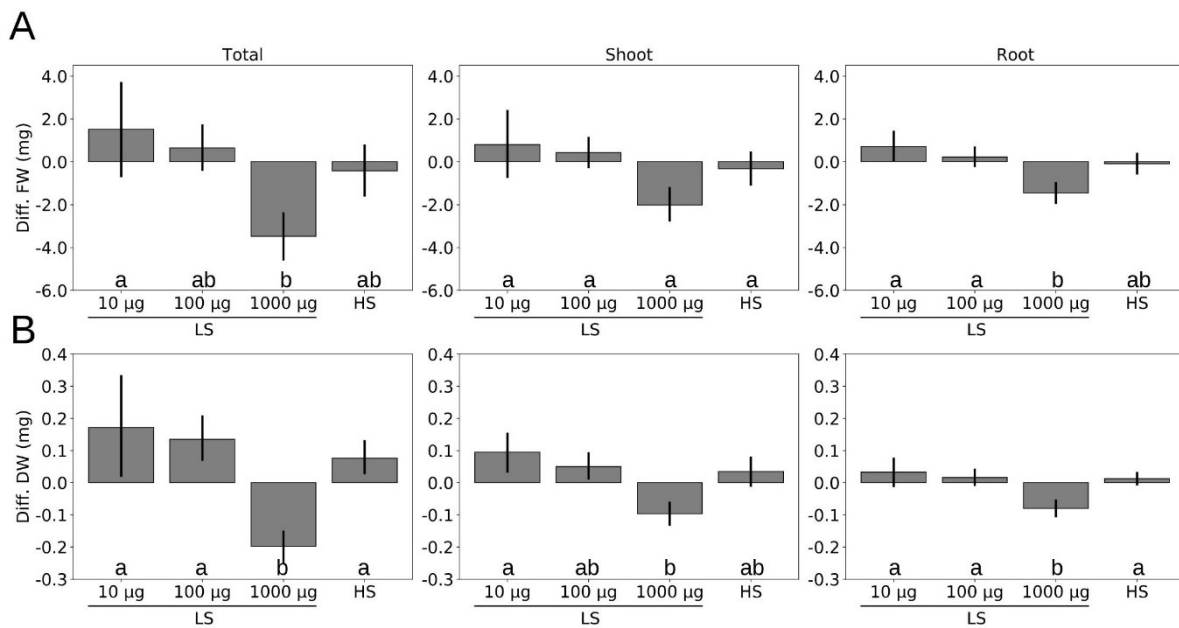


Figure 3. Fungal volatile influences *A. thaliana* growth under sulfur deficiency. (A) and (B) Differences in fresh weight (A) and in dry weight (B) of seedlings grown on high sulfate (HS) or on low sulfate (LS) MGRL medium with addition of TMTM (10, 100 and 1000 µg) to seedlings grown on LS without TMTM. Error bars represent SEs from at least 5 independent biological replicates, each with 8 seedlings. Statistical significance was determined by Duncan's multiple range test with p -value < 0.05 , and indicated with lower-case alphabets.

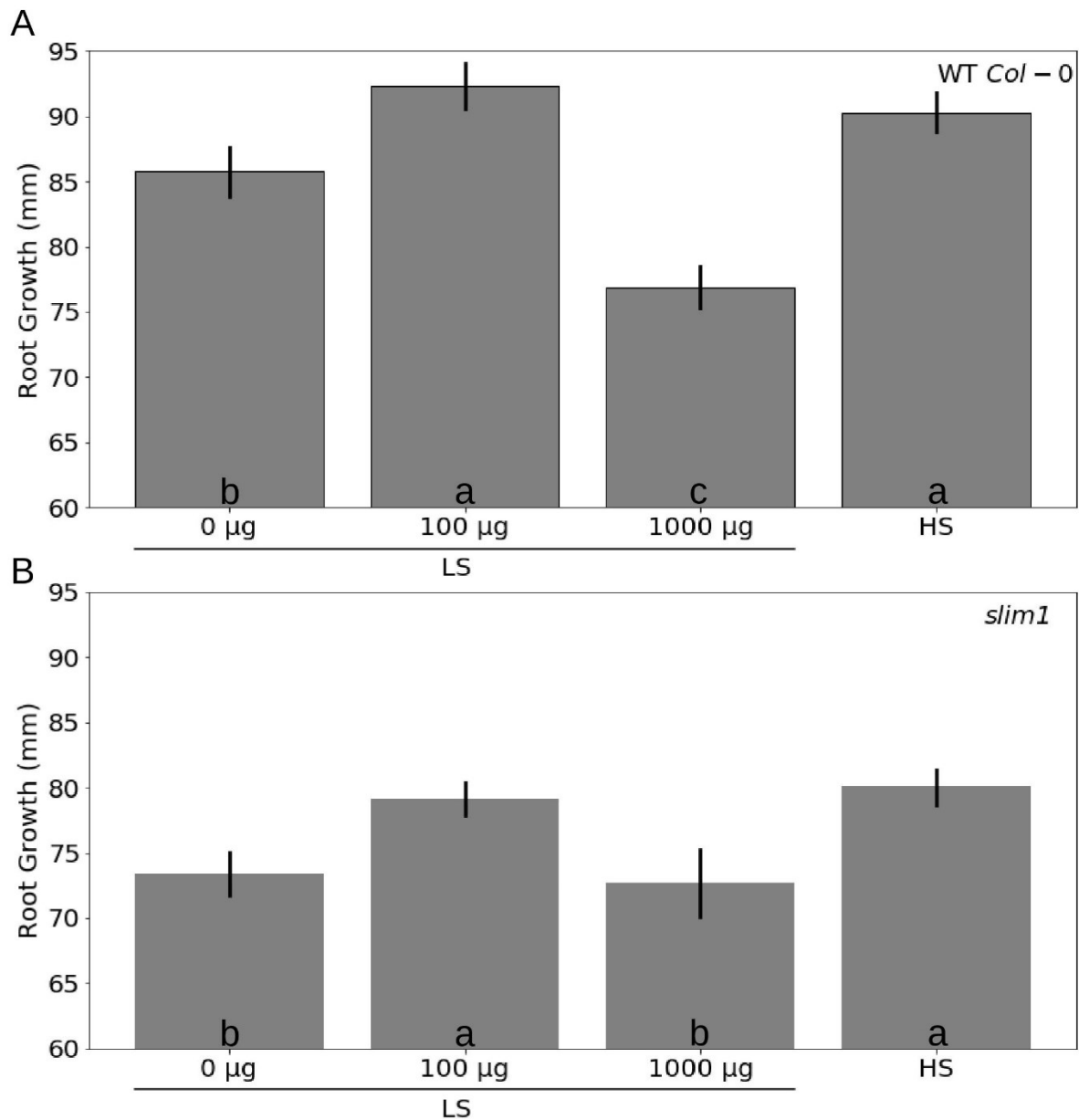
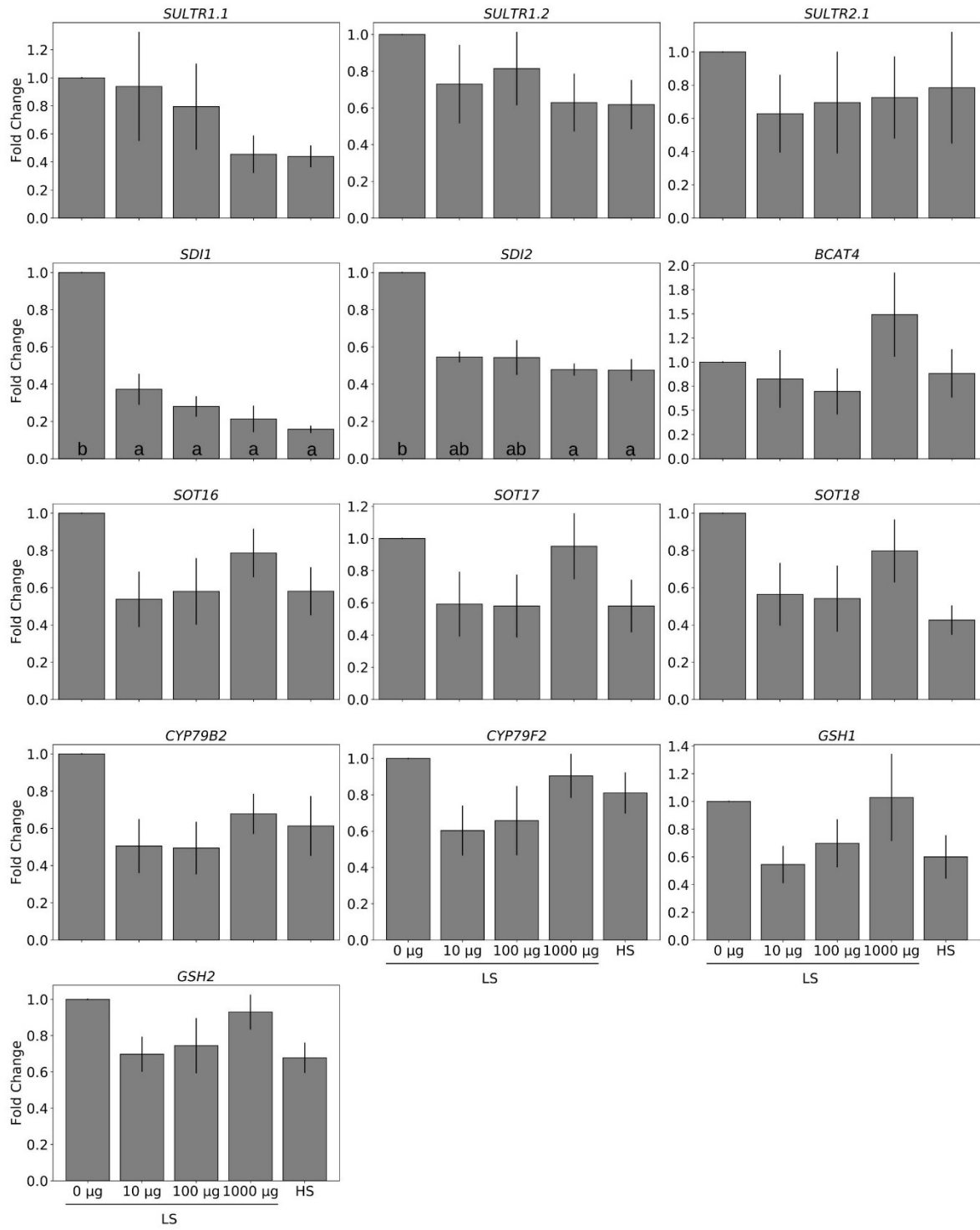


Figure 4. TMTM contributes positively to root growth. Wild-type (A) or *slim1* (B) seedlings' root growth on high sulfate medium (HS) or on low sulfate medium (LS) with addition of 0, 100 or 1000 µg TMTM was measured 7 days after application. Error bars represent SEs from at least 6 biological replicates for wildtype and 8 biological replicates for *slim1*. Statistical significance was determined by Duncan's multiple range test with p-value < 0.05, and indicated with lower-case letters.

A



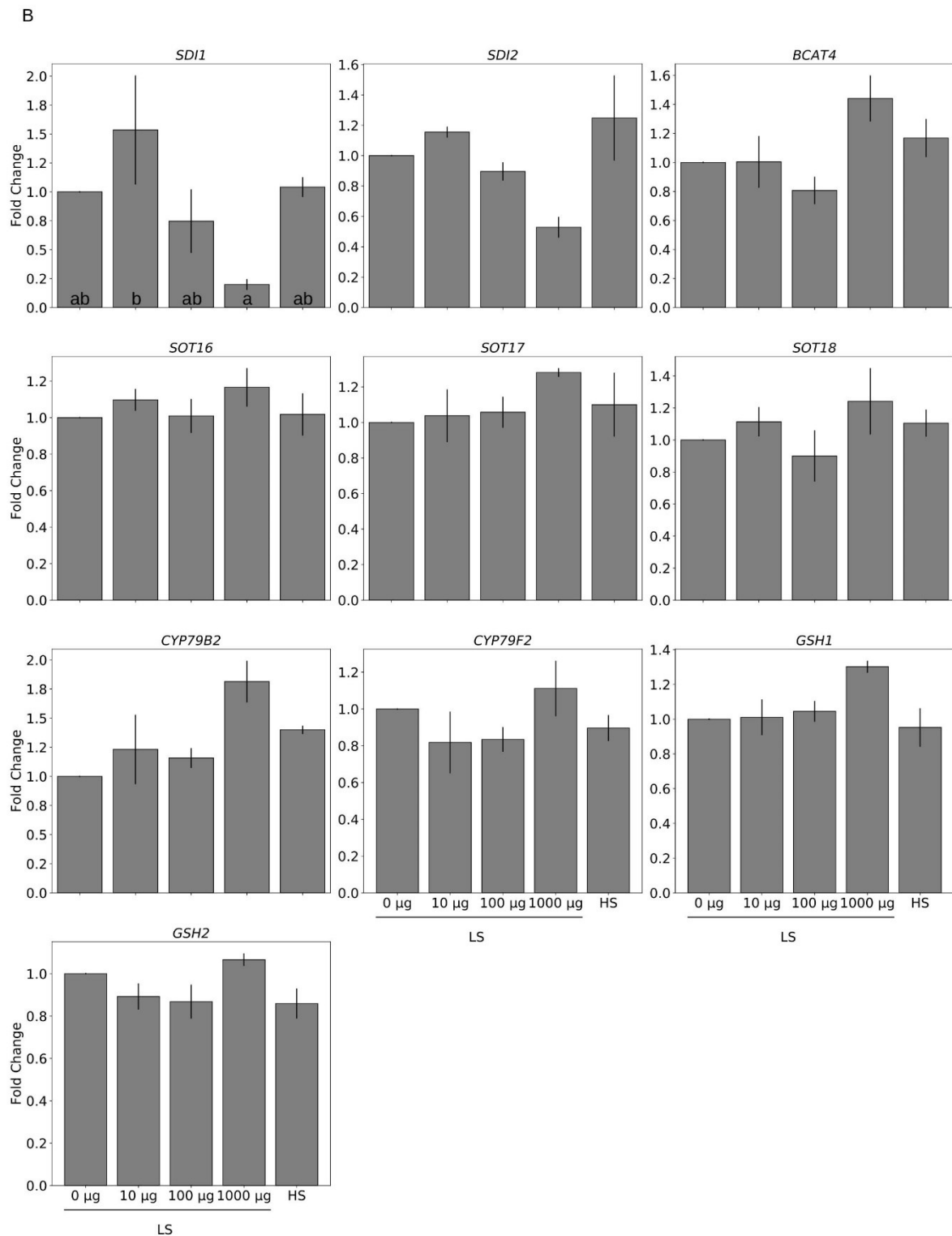


Figure 5. TMTM reduces plant response towards sulfur deficiency. Gene expression was analyzed 2 days (A) and 7 days (B) after TMTM application. Values were normalized to seedlings grown on low sulfate (LS) MGRL medium without TMTM (0 µg), and expressed as fold change. RNA for each treatment was extracted from total seedlings (combining root and shoot). Error bars represent SEs from 3 biological replicates, each with 8 seedlings. Statistical significance was conducted on dCq values, determined by Duncan's multiple range test with p-value < 0.05, and indicated with lower-case alphabets.

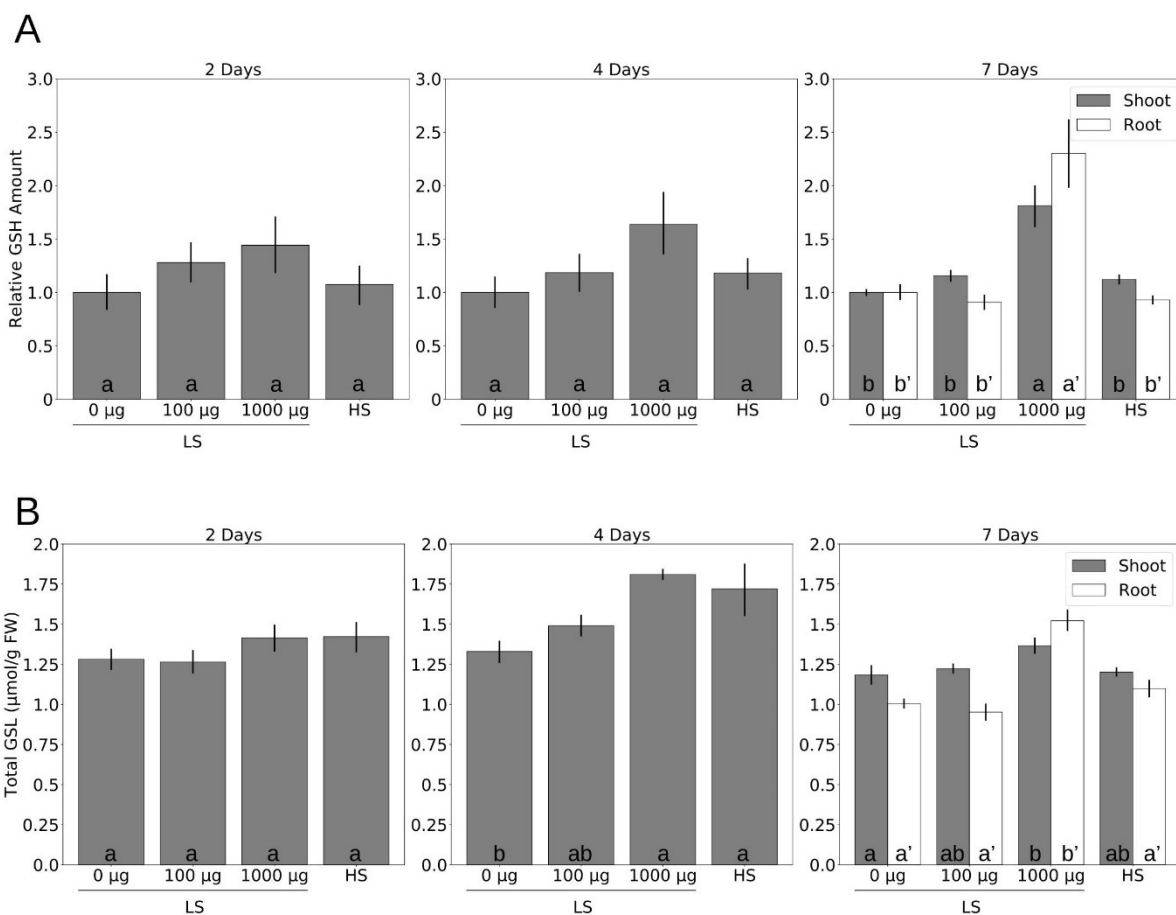


Figure 6. TMTM maintains sulfur-containing metabolites under sulfur deficiency. (A) Relative glutathione (GSH) level and (B) total glucosinolate (GSL) level in seedlings grown on low sulfate (LS) MGRL medium with addition of TMTM (0, 100 and 1000 µg) and seedlings grown on high sulfate (HS) MGRL medium 2, 4 and 7 days after treatment. Error bars represent SEs from at least 5 biological replicates, each with 8 seedlings. Statistical significance was determined by Duncan's multiple range test with p -value < 0.05 , and indicated with lower-case alphabets.

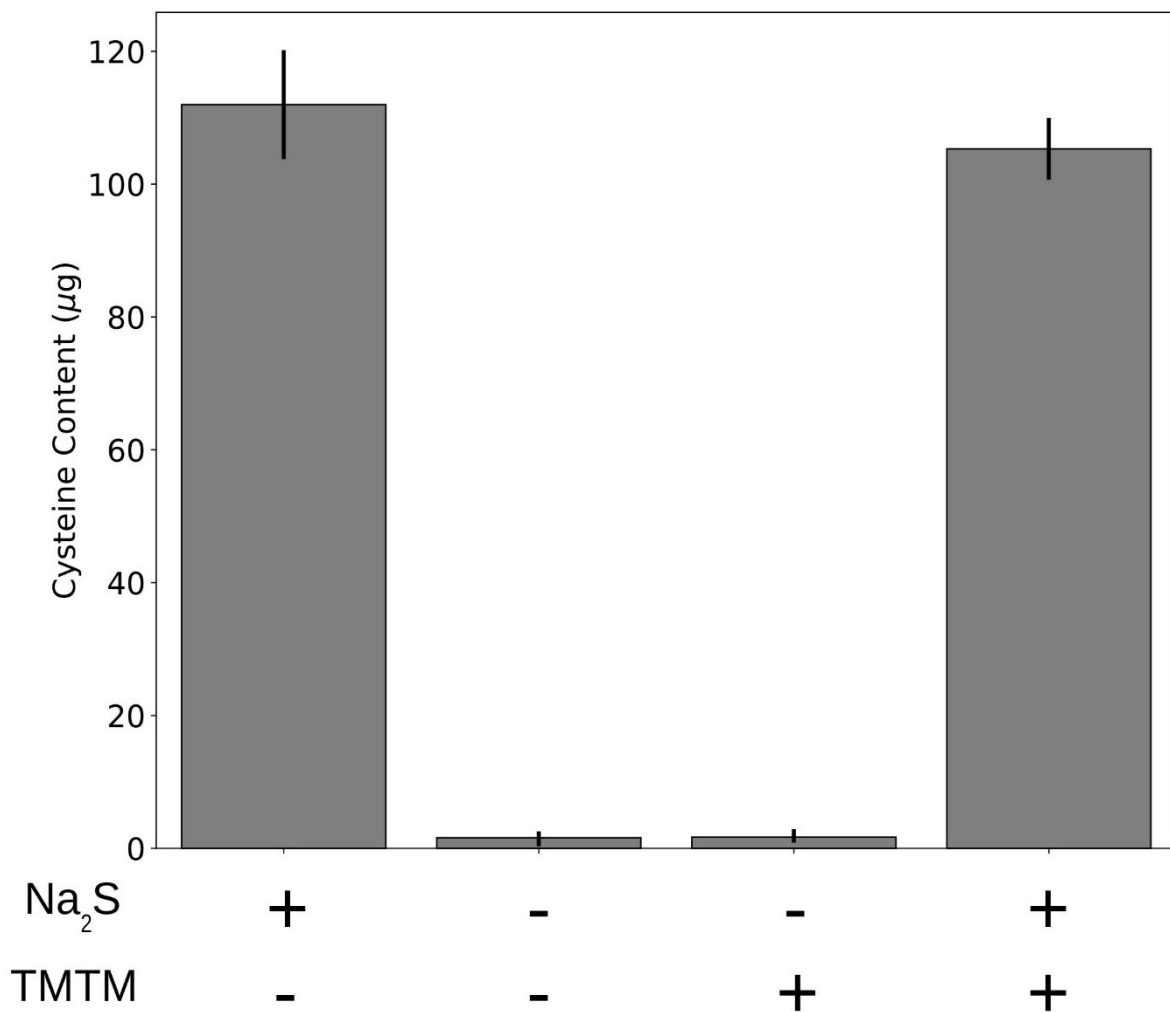


Figure 7. Incorporation of TMTM requires more than OASTLs. Cysteine biosynthesis was monitored in 4 parallel samples. In each sample, either Na₂S, water, TMTM or both NA2 S and TMTM was added as substrate for OASTLs. Error bars represent SEs from 3 independent measurement using total protein extract from 3 different biological replicates.

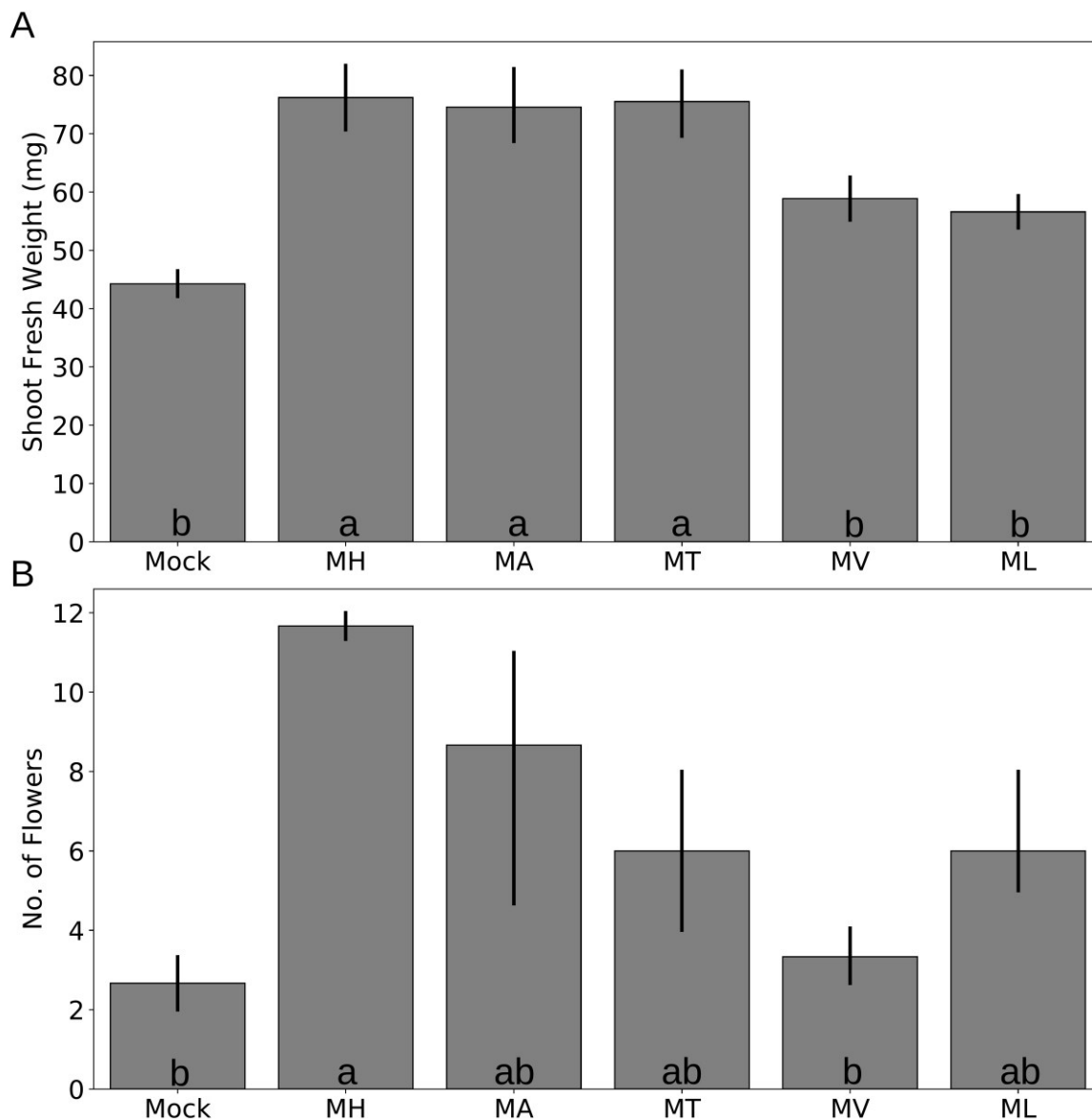
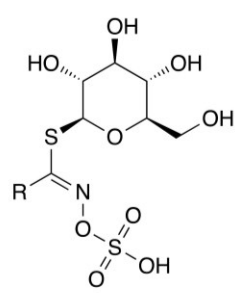


Figure S1. Fungal volatiles from *M. hyalina* promote *Arabidopsis* growth. Shown are (A) Shoot fresh weight and (B) number of flower buds. Mock, without fungus. MH, *Mortierella hyalina*. MA, *Mortierella alpina*. MT, *Mortierella turficola*. ML, *Mortierella longicollis*. MV, *Mortierella vinacea*. Error bars represent SEs from at least 3 independent biological replicates, each with 21 seedlings. Statistical significance was determined by Duncan's multiple range test with p -value < 0.05, and indicated with lower-case alphabets.



Figure S2. Experimental set-up for fungi-*Arabidopsis* co-cultivation in a desiccator with shared headspace.



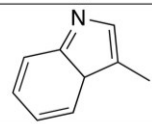
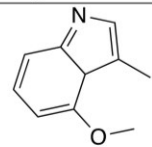
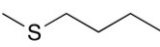
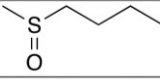
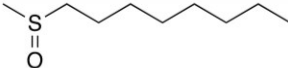
Name	R
3-Indolylmethyl glucosinolate (I3M)	
(4-Methoxy-3-indolylmethyl) glucosinolate (4MOI3M)	
4-Methylthiobutyl glucosinolate (4MTB)	
4-Methylsulfinylbutyl glucosinolate (4MSOB)	
8-Methylsulfinyloctyl glucosinolate (8MSOO)	

Figure S3. Structures of the different glucosinolates (GSLs). Left: core structure of GSL. Right: side-chain (R) of different GLS species.

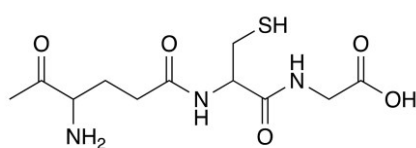


Figure S4. Structure of glutathione (GSH).

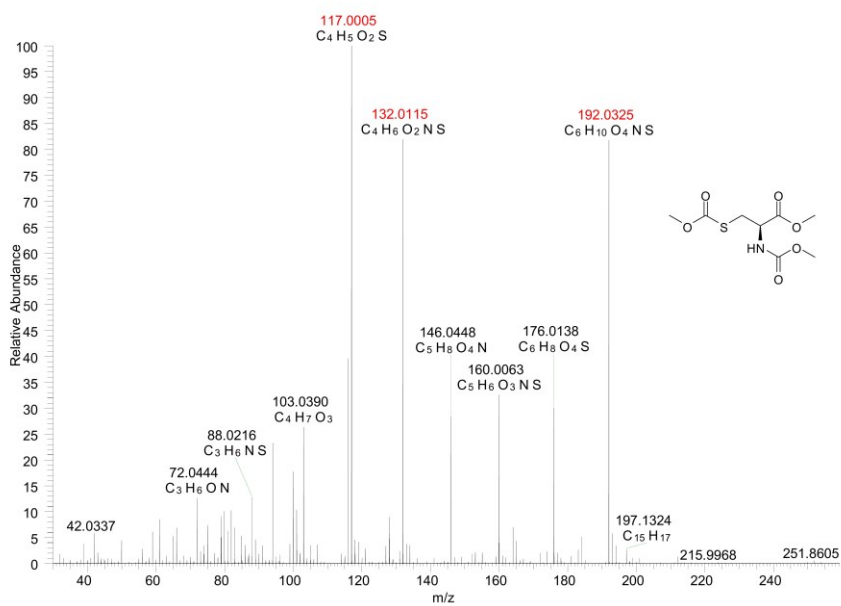


Figure S5. HR-MS spectrum for cysteine derivative. The structure of derived cysteine is shown on the right. Fragments used for the calculation of $^{34}\text{S}/^{32}\text{S}$ ratio are marked in red.

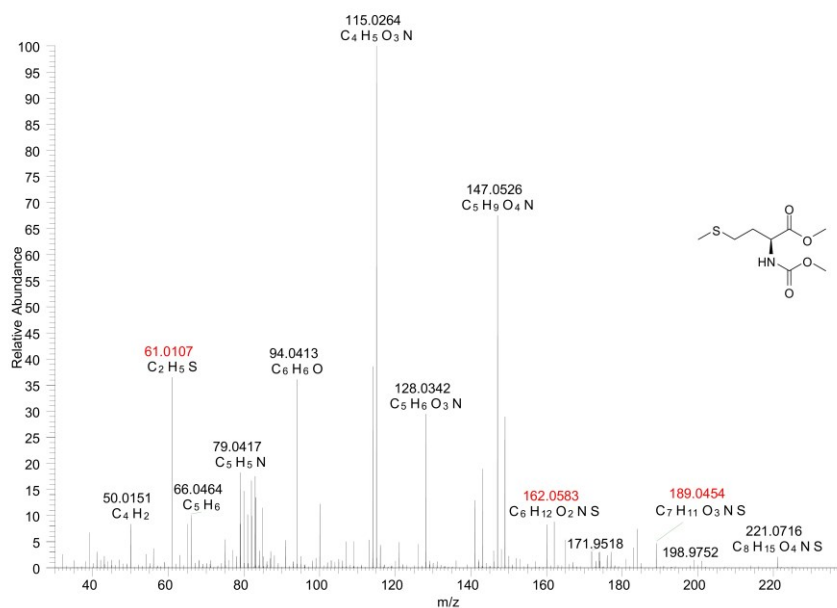


Figure S6. HR-MS spectrum for methionine derivative. The structure of derived methionine is shown on the right. Fragments used for the calculation of ³⁴S/³²S ratio are marked in red.

Supplementary Table 1. Primers used in this study.

Gene	Accession Number	Sequence (5'-3')
<i>RPS18B</i>	AT1G34030	RPS-qF-GTCTCCAATGCCCTTGACAT
		RPS-qR-TCTTTCCTCTGCGACCAGTT
<i>SULTR1.1</i>	AT4G08620	SULTR1.1-qF-GCCATCACAATCGCTCTCCAA
		SULTR1.1-qR-TTGCCAATTCCACCCATGC
<i>SULTR1.2</i>	AT1G78000	SULTR1.2-qF-GGATCCAGAGATGGCTACATGA
		SULTR1.2-qR-TCGATGTCCGTAACAGGTGAC
<i>SULTR2.1</i>	AT5G10180	SULTR2.1-qF-ATTGTTGCTCTAACCGAGGCGATT
		SULTR2.1-qR-TGTACCCTTTTATTCCGGCGAACG
<i>SDI1</i>	AT5G48850	SDI1-qF-TCAGAGCCAAACATGCTCAGTT
		SDI1-qR-ACAACAGCCATGTCCTTGAGG
<i>SDI2</i>	AT1G04770	SDI2-qF-CGAGCGAAGCATGTTTCAGTTG
		SDI2-qR-CGTCAATGGCTTCTTCAGCTCT
<i>BCAT4</i>	AT3G19710	BCAT4-qF-CAGAAGATGGTCGGATTCTGCTA
		BCAT4-qR-GGCAAAAAGCTGTGAAGGTGGT
<i>SOT16</i>	AT1G74100	SOT16-qF-CGAAGTCGTCGAACTCACAGAGTT
		SOT16-qR-AAAGACCTTCGAGGAGACATTCTTG
<i>SOT17</i>	AT1G18590	SOT17-qF-GGAATCCAAAACCATAAACGACG
		SOT17-qR-CGGATCTTTTGGTCTCCAGCC
<i>SOT18</i>	AT1G74090	SOT18-qF-CCCTACCGAGTCACGACGAGA
		SOT18-qR-GGTAGCCACCAGTAACCACCATACT
<i>GSH1</i>	AT4G23100	GSH1-qF-GACAGACTGACAAGGACCGC
		GSH1-qR-CAACATACTGCTCAAACCCAAAAGA
<i>GSH2</i>	AT5G27380	GSH2-qF-TTGGAGTACAGTAACCCAAGAGCGGTAGT
		GSH2-qR-CATCCTCTTGTACTCCCTTCTTTTCGACTT
<i>CYP79B2</i>	AT4G39950	CYP79B2-qF-AAATCAAACCCACCATTAAGGAG
		CYP79B2-qR-GAGAATCTCCGGTTTGTTCAC
<i>CYP79F2</i>	AT1G16400	CYP79F2-qF-CCCATAATAGACGAGAGGGTTCGAAA
		CYP79F2-qR-CGATCGCTGCTATACAAAATTCG

Supplementary Table 2. m/z values of extracted ion chromatogram traces of isotopologues of glucosinolates and glutathione for LC-ESI-Q-ToF-MS analysis for ³⁴S incorporation. 4MSOB GSL, 4-methylsulfinylbutyl glucosinolate; 4MTB GSL, 4-methylthiobutyl glucosinolate; 8MSOO GSL, 8-methylsulfinyloctyl glucosinolate; I3M GSL, indol-3-yl-methyl glucosinolate; 4MOI3M GSL, 4-methoxyindol-3-yl-methyl glucosinolate; GSH, glutathione (reduced form).

Isotopologue	Ionization Mode	m/z
4MSOB GSL [M-H] ⁻	neg	436.0411±0.002
4MSOB GSL isotopologue+1	neg	437.0446±0.002
4MSOB GSL isotopologue+2	neg	438.0379±0.002
4MSOB GSL isotopologue+3	neg	439.0422±0.002
4MSOB GSL isotopologue+4	neg	440.0348±0.002
4MTB GSL [M-H] ⁻	neg	420.0460±0.002
4MTB GSL isotopologue+1	neg	421.0490±0.002
4MTB GSL isotopologue+2	neg	422.0434±0.002
4MTB GSL isotopologue+3	neg	423.0484±0.002
8MSOO GSL [M-H] ⁻	neg	492.1038±0.002
8MSOO GSL isotopologue+1	neg	493.1068±0.002
8MSOO GSL isotopologue+2	neg	494.1017±0.002
8MSOO GSL isotopologue+3	neg	495.1020±0.002
I3M GSL [M-H] ⁻	neg	447.0541±0.002
I3M GSL isotopologue+1	neg	448.0566±0.002
I3M GSL isotopologue+2	neg	449.0512±0.002
I3M GSL isotopologue+3	neg	450.0558±0.002
4MOI3M GSL [M-H] ⁻	neg	477.0646±0.002
4MOI3M GSL isotopologue+1	neg	478.0676±0.002
4MOI3M GSL isotopologue+2	neg	479.0615±0.002
4MOI3M GSL isotopologue+3	neg	480.0669±0.002
GSH [M+H] ⁺	pos	308.0913±0.002
GSH isotopologue+1	pos	309.0943±0.002
GSH isotopologue+2	pos	310.0899±0.002

CORK1, a LRR-Malectin Receptor Kinase for Cellooligomer Perception in *Arabidopsis thaliana*

Yu-Heng Tseng, Sandra S. Scholz, Judith Fliegmann, Thomas Krüger, Akanksha Gandhi, Olaf Kniemeyer, Axel A. Brakhage, Ralf Oelmüller

Submitted to Plant Physiology (2022)

Because of the pandemic, there may be delays during peer review. We also understand that our authors might not be able to meet deadlines, so please contact us if you need an extension. The Editors-in-Chief of The Plant Cell, Plant Direct, Plant Physiology, The Plant Journal, Plant Biotechnology Journal, and the Journal of Experimental Botany have issued a joint statement about journal flexibility in the troubling times of COVID-19. Please read the statement [here](#).

Thank you!

Your submission is complete



(PP2022-RA-00601).

[Home Page for Yu-Heng Tseng](#)

[Use Modern Desktop](#)

Author Tasks

[Contact Coauthors for PP2022-RA-00601 - CORK1, a LRR-Malectin Receptor Kinase for Cel...](#)

[Submission Assistance](#)

[Submit Manuscript](#)

 [Live Manuscripts \(3\)](#)

General Tasks

[Modify Unavailability Dates](#)

[Modify Profile/Password](#)

[Download Copy of My Records](#)

[Log Out](#)

Because of the pandemic, there may be delays during peer review. We also understand that our authors might not be able to meet deadlines, so please contact us if you need an extension. The Editors-in-Chief of The Plant Cell, Plant Direct, Plant Physiology, The Plant Journal, Plant Biotechnology Journal, and the Journal of Experimental Botany have issued a joint statement about journal flexibility in the troubling times of COVID-19. Please read the statement [here](#).

Manuscript #	PP2022-RA-00601
Current Revision #	0
Submission Date	27-Apr-2022 07:39:45
Current Stage	Awaiting Contributing Author Confirmation
Title	CORK1, a LRR-Malectin Receptor Kinase for Cellooligomer Perception in Arabidopsis thaliana
Running Title	CORK1 for cellooligomer perception
Manuscript Type	Research Article
Focus Issue	Receptors and Signaling (OC)
Category	Signaling and Response
Corresponding Author	Mr. Yu-Heng Tseng (Friedrich-Schiller University)
Coauthors	Mr. Yu-Heng Tseng (Friedrich-Schiller University) (corr-auth) , Dr. Sandra S. Scholz (Friedrich-Schiller University) , Dr. Judith Fliegmann (ZMBP, University of Tuebingen) , Dr. Thomas Krüger (Leibniz Institute for Natural Product Research and Infection Biology - Hans Knöll Institute (Leibniz-HKI)) , Ms. Akanksha Gandhi (Friedrich-Schiller University) , Dr. Olaf Kniemeyer (Leibniz Institute for Natural Product Research and Infection Biology - Hans Knöll Institute (Leibniz-HKI)) , Prof. Axel A Brakhage (Leibniz Institute for Natural Product Research and Infection Biology - Hans Knöll Institute (Leibniz-HKI)) , Prof. Ralf Oelmüller (Friedrich-Schiller University)
Abstract	Cell wall integrity (CWI) maintenance is central for plant cells. Mechanical or chemical distortions, pH changes, or breakdown products of cell wall polysaccharides activate plasma membrane-localized receptors and induce appropriate downstream responses. Microbial interactions alter or destroy the structure of the plant cell wall, connecting CWI maintenance to immune responses. Cellulose is the major polysaccharide in the primary and secondary cell wall. Its breakdown generates short-chain cellooligomers which induce Ca ²⁺ -dependent CWI responses. We have shown here that these responses require the malectin domain-containing CELLOOLIGOMER-RECEPTOR KINASE 1 (CORK1) in Arabidopsis. CORK1 is required for cellooligomer-induced cytoplasmic Ca ²⁺ elevation, reactive oxygen species (ROS) production, mitogen associated protein kinase (MAPK) activation, cellulose synthase phosphorylation, and the regulation of CWI-related genes including those involved in biosynthesis of cell wall material, secondary metabolites and tryptophan. Phosphoproteome analyses identified early targets involved in signaling, cellulose synthesis, the endoplasmatic reticulum/Golgi secretory pathway, cell wall repair and immune responses. Two conserved phenylalanine residues in the malectin domain are crucial for CORK1 function. We propose that cellulose breakdown products bind to the malectin domain in CORK1, indicating its role as a novel receptor kinase for CWI maintenance.
One Sentence Summary	In this study, we discovered the malectin-domain containing receptor kinase CORK1 as a potential receptor for cellooligomers, and identified early phosphorylation targets and genes regulated through cellooligomer/CORK1.
Monitoring Editor	Not Assigned
Research Areas	cell walls - other aspects, defense/disease resistance/immunity - leucine-rich repeat receptor-like kinase/LRR/NBS-LRR, sugar-sensing/sugar sensing, calcium signaling/transport, signal transduction - crosstalk
Research Methods	genetics - genome-wide association study/GWAS, RNA-Seq, proteomics, chemical biology screening, quantitative PCR (qPCR), promoter activation assay, biochemistry - enzymology
Research Organisms	Arabidopsis
Conflict of Interest Statement	No, there are no conflicts of interest.
Acknowledgments	We thank Prof. Dr. Maria Mittag for providing the expression vector pGEX1AT and Prof. Georg Felix for discussions and comments on the work. We also thank Claudia Röppischer, Sarah Mußbach and Christin Weilandt for technical assistance. Special thanks to Yelyzaveta Zhyr for the help on plant transformation and the green house team at Max Planck Institute for Chemical Ecology for taking care of all the Arabidopsis transformants. This work was supported by the Deutsche Forschungsgemeinschaft (DFG, German Research Foundation) CRC1127 ChemBioSys (project ID: 239748522) and CRC/TR 124 FungiNet (project Z2; project ID: 210879364).
CrossCheck Manuscript	Never Processed / Send Manuscript for CrossCheck Analysis

Manuscript Items

- Cover Letter (last updated: 04/27/2022 07:45:37) [PDF \(70KB\)](#) [Source File \(DOCX\) 12KB](#)
- Merged File containing manuscript text and 3 Figure files. [PDF \(17684KB\)](#)

1. Manuscript Text File (last updated: 04/27/2022 07:45:36) [PDF \(299KB\)](#)  [Source File \(DOCX\) 352KB](#) 
2. Figure 1-7 (last updated: 04/27/2022 07:45:37) [PDF \(17124KB\)](#)  [Source File \(PDF\) 17124KB](#) 
3. Figure - Table 1 Editable (last updated: 04/27/2022 07:45:37) [PDF \(64KB\)](#)  [Source File \(XLSX\) 12KB](#) 
4. Figure - Table 2 Editable (last updated: 04/27/2022 07:45:37) [PDF \(75KB\)](#)  [Source File \(XLSX\) 18KB](#) 

3. Supplementary Figure S1-S5 and Supplementary Table S1 and S2 (last updated: 04/27/2022 07:45:37) [PDF \(4184KB\)](#)  [Source File \(PDF\) 4184KB](#) 
4. Supplementary Table S1 Editable (last updated: 04/27/2022 07:45:37) [PDF \(96KB\)](#)  [Source File \(DOCX\) 14KB](#) 
5. Supplementary Table S2 Editable (last updated: 04/27/2022 07:45:37) [PDF \(88KB\)](#)  [Source File \(DOCX\) 13KB](#) 
6. Supplementary Dataset S1 (last updated: 04/27/2022 07:45:37) [Dataset](#)  [Source File \(XLSX\) 47KB](#) 
7. Supplementary Dataset S2 (last updated: 04/27/2022 07:45:37) [Dataset](#)  [Source File \(XLSX\) 137KB](#) 
8. Parsed Citations (last updated: 04/27/2022 07:44:12) [Parsed Citations](#)  [Source File \(HTML\) 113KB](#) 

More Manuscript Info and Tools

[Contact Coauthors](#)

[Send Manuscript Correspondence](#)

CORK1, a LRR-Malectin Receptor Kinase for Celloligomer Perception in *Arabidopsis thaliana*

Yu-Heng Tseng¹, Sandra S. Scholz¹, Judith Fliegmann², Thomas Krüger³, Akanksha Gandhi¹, Olaf Kniemeyer^{3,4}, Axel A. Brakhage³, Ralf Oelmüller^{1*}

¹Matthias Schleiden Institute of Genetics, Bioinformatics and Molecular Botany, Department of Plant Physiology, Friedrich-Schiller-University Jena, Jena, Germany

²Center for Plant Molecular Biology (ZMBP), University of Tübingen, Tübingen, Germany

³Department of Molecular and Applied Microbiology, Leibniz Institute for Natural Product Research and Infection Biology - Hans Knöll Institute (Leibniz-HKI), Jena, Germany

⁴Department of Microbiology and Molecular Biology, Institute of Microbiology, Friedrich Schiller University, Jena, Germany

* Correspondence:

Ralf Oelmüller

b7oera@uni-jena.de

Abstract

Cell wall integrity (CWI) maintenance is central for plant cells. Mechanical or chemical distortions, pH changes, or breakdown products of cell wall polysaccharides activate plasma membrane-localized receptors and induce appropriate downstream responses. Microbial interactions alter or destroy the structure of the plant cell wall, connecting CWI maintenance to immune responses. Cellulose is the major polysaccharide in the primary and secondary cell wall. Its breakdown generates short-chain cellooligomers which induce Ca²⁺-dependent CWI responses. We have shown here that these responses require the malectin domain-containing CELLOOLIGOMER-RECEPTOR KINASE 1 (CORK1) in *Arabidopsis*. CORK1 is required for cellooligomer-induced cytoplasmic Ca²⁺ elevation, reactive oxygen species (ROS) production, mitogen associated protein kinase (MAPK) activation, cellulose synthase phosphorylation, and the regulation of CWI-related genes including those involved in biosynthesis of cell wall material, secondary metabolites and tryptophan. Phosphoproteome analyses identified early targets involved in signaling, cellulose synthesis, the endoplasmic reticulum/Golgi secretory pathway, cell wall repair and immune responses. Two conserved phenylalanine residues in the malectin domain are crucial for CORK1 function. We propose that cellulose breakdown products bind to the malectin domain in CORK1, indicating its role as a novel receptor kinase for CWI maintenance.

Introduction

The plant cell wall is mainly composed of the polysaccharide polymers cellulose, hemicellulose and pectin. Cellulose accounts for more than 30% of the total plant cell wall material (Lodish et al., 2000), and consists of β -(1,4)-bound D-glucose moieties, which form unbranched fibers with a paracrystalline structure. Hemicellulose is made of xylans, xyloglucans, mannans, glucomannans, and β -(1,3;1-4)-glucans. The backbone for xylans, xyloglucans and mannans is made of β -(1,4) linked monomer residues, while β -(1,3;1-4)-glucans contain β -(1-4)-linked glucose interleaved with β -(1,3) linkages. Unlike cellulose, hemicellulose has short branches and its amorphous structure is easily accessible to hydrolases (Scheller and Ulvskov, 2010; Gibson, 2012). Pectins are categorized into unbranched homogalacturonan (HG), branching rhamnose (Rha)-containing rhamnogalacturonan I (RG-I), and rhamnogalacturonan II (RG-II) with complex composition (Mohnen, 2008; Atmodjo et al., 2013). While HG is a monopolymer of α -(1,4)

galacturonic acid (GalA), RG-I has a disaccharide unit backbone of α -D-GalA-(1,2)- α -L-Rha, and RG-II possesses GalA linked with various sugars (Ridley et al., 2001; Harholt et al., 2010).

Fragments of these cell wall polysaccharides have been shown to act as damage-associated molecular patterns (DAMPs; Gust et al., 2017). Cellulose breakdown products, cellooligomers (COMs), trigger calcium influx, ROS production, MAPK phosphorylation, and defense-related gene expression, which eventually lead to higher pathogen resistance (Hu et al., 2004; Galletti et al., 2011; Souza et al., 2017; Claverie et al., 2018; Johnson et al., 2018; Mélida et al., 2020; Yang et al., 2021a). COMs with 2-7 glucose moieties induce cytoplasmic calcium ($[Ca^{2+}]_{\text{cyt}}$) elevation. The amplitude of the response depends on the length of the oligomer, and celotriose (CT) was the most active COM in *Arabidopsis thaliana* (Johnson et al., 2018). The defense responses induced by COMs are relatively mild when compared to those induced by the pathogen-associated molecular patterns (PAMPs) chitin or flg22 (Souza et al., 2017; Claverie et al., 2018; Johnson et al., 2018; Rebaque et al., 2021). However, in combination with chitin, flg22 or oligogalacturonic acid (OG), synergistic effects on calcium influx, ROS production, and MAPK phosphorylation indicate crosstalk between COM and PAMP responses (Souza et al., 2017; Johnson et al., 2018).

Plants rely on an array of membrane-associated pattern recognition receptors (PRRs) to recognize breakdown products of its cell wall. The wall-associated kinase 1 (WAK1) is activated by the pectin fragments OGs (He et al., 1996; Brutus et al., 2010). FERONIA, a membrane-localized receptor-like kinase with a malectin-like domain, is involved in monitoring cell wall integrity (CWI), pollen tube development, plant growth and perception of RALF peptides (Escobar-Restrepo et al., 2007; Haruta et al., 2014). Its extracellular region has been shown to interact with pectin (Feng et al., 2018; Tang et al., 2021). In rice, two species of mixed-linked β -1,3/1,4-glucans (MLGs) from hemicellulose, namely 3^1 - β -D-cellobiosyl-glucose and 3^1 - β -D-celotriosyl-glucose, bind to OsCERK1, and induce the dimerization of OsCERK1 and the chitin receptor OsCEBiP (Yang et al., 2021a). However, up to date, no receptor has been reported to perceive β -1,4 glucans. Here, we show that CORK1 (CelloOligomer Receptor Kinase 1) specifically recognizes COMs in *A. thaliana*. CORK1 is a functional LRR-malectin receptor kinase. Upon COM treatment, CORK1 mutants are impaired in $[Ca^{2+}]_{\text{cyt}}$ elevation, ROS production, regulation of genes involved in CWI maintenance and immune responses, including *WRKY30/WRKY40*. Two conserved phenylalanine residues in the malectin domain are crucial for COM-induced responses in *A. thaliana*. Phosphoproteome and transcriptome data identified protein and gene targets of the novel COM/CORK1 pathway and have shed light on the role of COMs in CWI maintenance.

Materials and Methods

Growth medium and conditions for seedlings

A. thaliana seeds were surface-sterilized for 8 minutes in sterilization solution containing lauryl sarcosine (1%) and Clorix cleaner (23%). Surface-sterilized seeds were washed with sterilized water 8 times and placed on Petri dishes with MS medium supplemented with 0.3% gelrite (Murashige and Skoog, 1962). After cold treatment at 4°C for 48 hours, plates were incubated at 22°C under long day conditions (16 hours light/ 8 hours dark; 80 $\mu\text{mol m}^{-2} \text{s}^{-1}$).

Wild-type (ecotype Columbia-0), the aequorin-containing wild-type [pMAQ2] line (AeqWT; Knight et al., 1991), and EMS (ethyl methanesulfonate)-induced mutant lines in AeqWT background (Johnson et al., 2018) were used in this study. In addition, two T-DNA insertion lines, *cork1-1* (N671776; SALK_099436C) and *cork1-2* (N674063; SALK_021490C), were obtained from Nottingham *Arabidopsis* Stock Centre (NASC). Homozygous seedlings of these insertion lines were crossed to the AeqWT. The corresponding segregated wild-type (SWT) and homozygous (HO) seedlings from the F3 generation were used for experiments.

EMS mutagenesis of *A. thaliana* seeds

2.5 g of AeqWT seeds were used for mutagenesis. According to Kim *et al.* (2006), seeds were soaked in 40 ml of 100 mM phosphate buffer (pH = 7.5) for 10 hours at 4°C. The next day, the buffer was replaced and EMS (Sigma-Aldrich, Germany) was added to a final concentration of 0.2 %. The

mixture was incubated at room temperature in a hood over night with gentle stirring. The seeds were washed twice in 40 ml of 100 mM sodium thiosulphate for 15 min to destroy the remaining EMS, followed by 18 wash steps with water (Leyser and Furner, 1993). Freshly mutagenized seeds were directly separated in different Eppendorf tubes, surface-sterilized and germinated as described above. Three-week old plants were transferred to soil to obtain the seeds of the individual mother plants.

Whole Genome Sequencing and SNP analysis

After screening ~100 independent EMS lines, we found a COM non-responsive mutant, named here as EMS71. From the F2 generation of the back-cross between EMS71 and AeqWT, two pools of seedlings were sorted out. One pool consisted of CT responsive individuals, while the other contained non-responsive individuals (50 seedlings in each pool). Whole genome sequencing of the two pools was performed on Illumina sequencing platform (PE150; Novogene Co., UK). The reads from both pools were mapped separately against the TAIR10 reference genome using Samtools v. 1.8 (Li et al., 2009). SIMPLE v. 1.8.1 (Wachsman et al., 2017) analysis was implemented to filter out single-nucleotide polymorphisms (SNPs) which appeared 90-100 % in the non-responsive population, while less than 70% in the responsive population. Putative candidate genes were selected based on whether the SNP causes non-synonymous mutation, or affects mRNA processing (e.g. mRNA splicing). SNP sites of candidate genes were confirmed in 3 different individuals from the EMS71 line. As a result, two candidate genes, *ARF1* (At1g59750) and *CORK1* (AT1G56145), were selected for further confirmation as described in the Result section.

Transcriptome analysis

16 roots of SWT or HO from *cork1-2* mutant line crossed to AeqWT were treated with 1 mL of either water or 10 μ M CT for 1 hour. Total RNA was extracted and purified as described, and sent to Novogene Co. (UK) for sequencing with Illumina NovaSeq instrument (poly-A enrichment; PE150). The raw reads were aligned to *Arabidopsis* TAIR10 reference genome using STAR v. 2.7.10a (Dobin et al., 2013). The aligned bam files were analyzed with featureCounts v. 2.0.1 (Liao et al., 2014), and the count table for all samples were analyzed with DESeq2 v. 1.34.0 (Love et al., 2014). GO enrichment and KEGG pathway analysis was performed on PANTHER (Mi et al., 2021) and KEGG PATHWAY (Kanehisa and Goto, 2000) database, respectively. Significantly regulated genes were defined with the criteria: $|\log_2 \text{ fold change}| \geq 1.33$ and adjusted p-value < 0.05 . The adjusted p-value was calculated by DESeq2 using the built-in Benjamini and Hochberg method. The default FDR cutoff value was set as 0.1.

Phosphoproteomic analysis

Sample collection

300 roots of SWT or HO from the *cork1-2* mutant line were collected at 0 minute, or after treatment with either water or 10 μ M CT for 5 or 15 minutes. Samples were immediately frozen in liquid nitrogen until further analysis.

In-solution digest

Tissues were disrupted by using mortar and pestle with liquid nitrogen. Debris were homogenized in lysis buffer (1% (w/v) SDS, 150 mM NaCl, 100 mM TEAB (triethyl ammonium bicarbonate)), one tablet each of cOmplete Ultra Protease Inhibitor Cocktail and PhosSTOP). After addition of 0.5 μ l Benzomase nuclease (250 U/ μ l) the samples were incubated at 37°C in a water bath sonicator for 30 min. Proteins were separated from unsolubilized debris by centrifugation (15 min, 18000 \times g). Each 1.5 mg of total protein per sample was diluted with 100 mM TEAB to gain a final volume of 1.5 ml. Subsequently, cysteine thiols were reduced and carbamidomethylated in one step for 30 min at 70°C by addition of 30 μ L of 500 mM TCEP (tris(2-carboxyethyl)phosphine) and 30 μ l of 625 mM 2-chloroacetamide (CAA). The samples were further cleaned up by methanol-chloroform-water precipitation using the protocol of Wessel and Flügge (1984). Protein precipitates were resolubilized in 5% trifluoroethanol of aqueous 100 mM TEAB and digested overnight (18

hours) with a Trypsin+LysC mixture (Promega) at a protein to protease ratio of 25:1. Each sample was divided in 3×0.5 mg used for the phosphopeptide enrichment and 150 μ g initial protein used for the reference proteome analysis. Samples were evaporated in a SpeedVac. The reference proteome sample was resolubilized in 30 μ L of 0.05% TFA in H₂O/ACN 98/2 (v/v) filtered through 10 kDa MWCO PES membrane spin filters (VWR). The filtrate was transferred to HPLC vials and injected into the LC-MS/MS instrument.

Phosphopeptide enrichment

Phosphopeptides were enriched by using TiO₂+ZrO₂ TopTips (Glygen Corp., Columbia, MD, USA). TopTips were loaded with 0.5 mg protein isolate using 3 TopTips per biological replicate after equilibration with 200 μ l Load and Wash Solution 1, LWS1 (1% trifluoroacetic acid (TFA), 20% lactic acid, 25% acetonitrile (ACN), 54% H₂O). TopTips were centrifuged at 1500 rpm ($\sim 200 \times g$) for 5 min at room temperature. After washing with 200 μ l LWS1, the TiO₂/ZrO₂ resin was washed with 25% ACN and subsequently the phosphopeptides were eluted with 200 μ l NH₃·H₂O (NH₄OH), pH 12. The alkaline solution was immediately evaporated using a SpeedVac. The phosphoproteome samples were resolubilized in 50 μ L of 0.05% TFA in H₂O/ACN 98/2 (v/v) filtered through 10 kDa MWCO PES membrane spin filters (VWR). The filtrate was also transferred to HPLC vials and injected into the LC-MS/MS instrument.

LC-MS/MS analysis

Each sample was measured in duplicate (2 analytical replicates of 3 biological replicates of a reference proteome fraction and a phosphoproteome fraction). LC-MS/MS analysis was performed on an Ultimate 3000 nano RSLC system connected to a QExactive HF mass spectrometer (both Thermo Fisher Scientific, Waltham, MA, USA). Peptide trapping for 5 min on an Acclaim Pep Map 100 column (2 cm \times 75 μ m, 3 μ m) at 5 μ L/min was followed by separation on an analytical Acclaim Pep Map RSLC nano column (50 cm \times 75 μ m, 2 μ m). Mobile phase gradient elution of eluent A (0.1% (v/v) formic acid in water) mixed with eluent B (0.1% (v/v) formic acid in 90/10 acetonitrile/water) was performed using the following gradient: 0-5 min at 4% B, 30 min at 7% B, 60 min at 10% B, 100 min at 15% B, 140 min at 25% B, 180 min at 45% B, 200 min at 65% B, 210-215 min at 96% B, 215.1-240 min at 4% B. Positively charged ions were generated at spray voltage of 2.2 kV using a stainless steel emitter attached to the Nanospray Flex Ion Source (Thermo Fisher Scientific). The quadrupole/orbitrap instrument was operated in Full MS / data-dependent MS2 Top15 mode. Precursor ions were monitored at m/z 300-1500 at a resolution of 120,000 FWHM (full width at half maximum) using a maximum injection time (IT_{max}) of 120 ms and an AGC (automatic gain control) target of 3×10^6 . Precursor ions with a charge state of $z=2-5$ were filtered at an isolation width of m/z 1.6 amu for further HCD fragmentation at 27% normalized collision energy (NCE). MS2 ions were scanned at 15,000 FWHM (IT_{max}=100 ms, AGC= 2×10^5) using a fixed first mass of m/z 120 amu. Dynamic exclusion of precursor ions was set to 30 s. The LC-MS/MS instrument was controlled by Chromeleon 7.2, QExactive HF Tune 2.8 and Xcalibur 4.0 software.

Protein database search

Tandem mass spectra were searched against the UniProt database (2022/01/06; <https://www.uniprot.org/proteomes/UP000006548>) of *Arabidopsis thaliana* using Proteome Discoverer (PD) 2.4 (Thermo) and the Sequest HT algorithm. Two missed cleavages were allowed for the tryptic digestion. The precursor mass tolerance was set to 10 ppm and the fragment mass tolerance was set to 0.02 Da. Modifications were defined as dynamic Met oxidation, phosphorylation of Ser, Thr, and Tyr, protein N-term acetylation with and without Met-loss as well as static Cys carbamidomethylation. A strict false discovery rate (FDR) $< 1\%$ (peptide and protein level) and an X_{corr} score > 4 was required for positive protein hits. The Percolator node of PD2.4 and a reverse decoy database was used for qvalue validation of spectral matches. Only rank 1 proteins and peptides of the top scored proteins were counted. Label-free protein quantification was based on the Minora algorithm of PD2.4 using the precursor abundance based on intensity and a signal-to-noise ratio > 5 .

Normalization was performed by using the total peptide amount method. Imputation of missing values was applied by using abundance values of 75% of the lowest abundance identified per sample. For the reference proteome analysis used for master protein abundance correction of the phosphoproteome data, phosphopeptides were excluded from quantification. Differential protein and phosphopeptide abundance was defined as a fold change of >2, ratio-adjusted pvalue <0.05 (pvalue/log4ratio) and at least identified in 2 of 3 replicates of the sample group with the highest abundance.

ROS and [Ca²⁺]_{cyt} measurements

Seedlings were grown vertically on Hoagland agar medium (Hoagland's No. 2 Basal Salt Mixture; Sigma-Aldrich, Germany) for 16 days before harvesting the leaf discs (about 1 mm in diameter), or approximately 70% of the roots for ROS and [Ca²⁺]_{cyt} measurements (Vadassery et al., 2009; Vadassery and Oelmüller, 2009; Johnson et al., 2011).

For ROS measurement, root tissue was incubated in sterile water in a 96-well plate in the dark at room temperature for 1 hour. Prior to the elicitor treatment, water was replaced by 150 µL of assay solution containing 2 µg/mL horseradish peroxidase (Sigma-Aldrich, Germany) and 100 µM luminol (FUJIFILM Wako Pure Chemical Corporation, Japan).

The [Ca²⁺]_{cyt} concentration was inferred from aequorin-based luminescence (Knight et al., 1991). Leaf discs and root tissue were incubated overnight in 150 µL of 7.5 µM coelenterazine solution (P.J.K. GmbH, Germany) in a 96-well plate in the dark at room temperature.

Bioluminescence counts from elicitor application were recorded as relative light units (RLU) with microplate luminometer (Luminoskan Ascent version 2.4, Thermo Electro Corporation, Germany or Mithras LB940, Berthold, Germany).

Cellulose (C7252, Sigma-Aldrich, Germany), cellotriose (C1167, Sigma-Aldrich, Germany, or 0-CTR-50MG, Megazyme, Ireland) and chitohexaose (OH07433, Carbosynth, United Kingdom) were used as elicitors. Concentration of elicitors, unless specified, is 10 µM for cellotriose and chitohexaose, and 1 mM for cellulose. All elicitors were dissolved and diluted with distilled water.

Nucleic acid isolation, PCR and qPCR

Plant tissue was homogenized in liquid nitrogen. DNA extraction was performed according to Doyle (1990). RNA extraction was done with Trizol™ reagent (Thermo-Fisher Scientific, Germany), treated with Turbo DNA-free™ Kit (Thermo-Fisher Scientific, Germany), and reverse transcribed with RevertAid Reverse Transcriptase (Thermo-Fisher Scientific, Germany) according to the manufacturer's instructions.

Genotyping of back-crossed F2 mutant population was achieved by PCRs with genomic DNA. PCRs were run with DreamTaq DNA Polymerase (Thermo Fisher Scientific, Germany) in a thermal cycler (Applied Biosystems SimpliAmp Thermal Cycler, Thermo Fischer Scientific, Germany). Quantitative PCRs (qPCRs) were performed with Dream Taq DNA Polymerase (Thermo-Fisher Scientific, Germany) with the addition of Evagreen® (Biotum, Germany). CFX Connect™ Real-Time PCR Detection System (Bio-Rad, Germany) was used for running and analyzing qPCRs. The expression of genes was normalized to the housekeeping gene encoding a ribosomal protein (RPS; AT1G34030). The resulting ΔCq values were used for statistical analysis. For the confirmation of SNP in the EMS mutant, a primer pair flanking the SNP site was designed, and the region was amplified with Phusion™ High-fidelity DNA polymerase (Thermo-Fisher Scientific, Germany). The PCR product was purified with NucleoSpin Gel and PCR Clean-up kit (Macherey-Nagel, Germany), and sequenced by Eurofins Genomics, Germany. All primers used are listed in Supplementary Table S1.

Multiple sequence alignment

Amino acid sequences of malectin RLKs and malectin-like RLKs were retrieved from Uniprot database and aligned with MEGA7 (Kumar et al., 2016) using default Clustal W algorithm (Thompson et al., 1994). The aligned sequences were edited for presentation using BioEdit v. 7.2.5

(<http://www.mbio.ncsu.edu/BioEdit/bioedit.html>). Accession number for all sequences are listed in Supplementary Table S2.

Plasmid construction

Full length coding regions of *ARF1* and of *CORK1* (AT1G56145.1) were amplified from the reverse-transcribed RNA (cDNA) using PhusionTM High-fidelity DNA polymerase (Thermo-Fisher Scientific, Germany). The fragments were cloned into entry vector pENTRTM/D-TOPOTM, and transferred to pB7FWG2.0 destination vector (Karimi et al., 2002) with GatewayTM LR ClonaseTM II (Thermo-Fisher Scientific, Germany). Site-directed mutagenesis was carried out to specifically mutate the amino acid residues of interest.

For the kinase activity assay, the cytoplasmic domain of CORK1 (residues 654-1039; CORK1^{KD}) was cloned and ligated into the expression vector pET28a using restriction enzymes *Bam*HI and *Eco*RI. Two stop codons were added before the *Eco*RI restriction site, generating a 6X His-Tagged protein at the N-terminus. The mutated form (CORK1^{KD-G748E}) was obtained by site-directed mutagenesis. The mutated PCR fragment for the kinase domain was cloned and ligated into the expression vector pGEX1 λ T using restriction enzymes *Bam*HI and *Eco*RI, generating a glutathione S-transferase (GST) fusion protein at the N-terminus.

To generate the luciferase reporter constructs with the *WRKY30* and *WRKY40* promoters, 2 kb-DNA fragments upstream of the respective start codons were cloned, and ligated into the pJS plasmid (Yoo et al., 2007) using *Nco*I and *Bam*HI restriction sites.

For every construct, the insert sequence was confirmed by Sanger sequencing (Eurofins Genomics). Primers used are listed in Supplementary Table S1.

Protein Expression, Extraction, Purification and Kinase assay

pET28a vector with CORK1^{KD} and pGEX1 λ T vector with CORK1^{KD-G748E} were transformed into *E. coli* strain BL21(DE3) pLysS (Novagen). For the expression of CORK1^{KD}, the transformed bacteria were grown directly in LB broth (Bertani, 1951) with 34 μ g/mL chloramphenicol and 50 μ g/mL kanamycin at 37°C for 16 hours with shaking. IPTG (isopropyl β -D-1-thiogalactopyranoside; Carl Roth, Germany) was added to the culture to a final concentration of 1 mM to induce protein expression for 3 hours. For the expression of GST-CORK1^{KD-G748E}, the overnight culture was inoculated into LB broth with 34 μ g/mL chloramphenicol and 100 μ g/mL ampicillin at 37°C with shaking. After O.D._{600nm} reached 0.6, IPTG was added to the broth to final concentration of 1 mM to induce protein expression for 3 hours at 25°C. Cells were collected by centrifugation for 10 minutes at 4°C, 5000 rpm.

Bacterial pellet for CORK1^{KD} was resuspended in extraction buffer containing 50 mM Tris-HCl, pH 8.0, 300 mM NaCl and 0.1% (w/v) CHAPS (3-[(3-cholamidopropyl)-dimethylammonio]-1-propansulfonate hydrate, Sigma-Aldrich, Germany). Sonication was applied to lyse the cells. Cell debris was pelleted by centrifugation for 10 minutes at 4°C, 12000 rpm. Cell lysate was incubated with ProBond Ni-NTA resin (Thermo-Fisher Scientific, Germany) for 0.5 – 1 hour. The resin was washed in the same buffer with 20 mM imidazole for 3 times to remove unbound protein. Finally, His-tagged protein was eluted with the same buffer containing 250 mM imidazole. For GST-CORK1^{KD-G748E}, purification was done with PierceTM GST Spin Purification Kit following manufacturer's instruction. Purified proteins were concentrated and buffer-exchanged in kinase assay buffer (25 mM Tris-HCl, pH 7.5, 10 mM MgCl₂) using Vivaspin[®] 20 ultrafiltration unit (3000 MWCO, Satorius, Germany).

Kinase activity assay was carried out by mixing 2 μ g of CORK1^{KD} or GST-CORK1^{KD-G748E} with 3 μ g of myelin basic protein (MBP; Sigma-Aldrich, Germany) in kinase reaction buffer (25 mM Tris-HCl, pH 7.5, 10 mM MgCl₂, 1 mM DTT and 100 μ M ATP). The reaction mixtures were incubated at 30°C for 30 min and terminated by adding SDS-PAGE loading buffer. The proteins were separated by SDS-PAGE. Protein phosphorylation was examined by staining with Pro-Q Diamond phosphoprotein gel stain (Thermo-Fisher Scientific, Germany) following manufacturer's instructions, or with morin hydrate (Wang et al., 2013), and visualized using AlphaImager HP system

(ProteinSimple, San Jose, California, USA). Coomassie blue staining (Roti-Blue, Carl Roth, Germany) was conducted to visualize the total protein.

Complementation of the COM receptor mutant

CORK1 or *ARF1* in pB7FWG2.0 vector were transformed into the COM non-responsive EMS mutant EMS71 using the floral dip method with *A. tumefaciens* strain GV3101 (Zhang et al., 2006). Complemented plants were selected on soil using a 0.1% (v/v) BASTA solution 14 and 18 days after sowing.

Transient expression in *A. thaliana*

Transient co-expression of the pFRK1::luciferase reporter (Yoo et al., 2007) with the receptor expression constructs in mesophyll protoplasts of *A. thaliana* Col-0 wild-type was performed as described (Wang et al., 2016). Luminescence was recorded for up to 5 hours in W5-medium containing 200 μ M firefly luciferin (Synchem UG) after overnight incubation for 14 hours and subsequent treatment with CT or control solutions. After the measurements, protoplasts were harvested by centrifugation and denatured in $2 \times$ SDS-PAGE loading buffer. The crude extracts were separated on 8% polyacrylamide gels and transferred to nitrocellulose membranes. Membranes were saturated with 5% milk powder in PBS with 0,05% Tween-20 (PBS-T) followed by immunostaining with anti-GFP antibodies (Torrey Pines Biolabs, 1:5000 in PBS-T) and secondary goat-anti-rabbit antibodies coupled to alkaline phosphatase (Applied Biosystems) using CDP-star as substrate.

Microscopy

Protoplast of *A. thaliana* were mounted on a glass slide with cover slip for microscopic inspection using Axio Imager.M2 (Zeiss Microscopy GmbH, Germany). The bright field and fluorescent images were recorded with a monochromatic camera Axiocam 503 mono (Zeiss Microscopy GmbH, Germany). Digital images were processed with the ZEN software (Zeiss Microscopy GmbH, Germany).

Statistical tests

Statistical tests were performed using R studio version 1.1.463 with R version 4.1.2. Figures were plotted using Python 3.7.4 and arranged with LibreOffice Draw 5.1.6.2.

Data availability

Raw sequences for the GWAS have been deposited in the Gene Expression Omnibus (GEO) database (accession no. GSE197891). For transcriptome analysis, raw sequences and the count tables after DESeq2 analysis have been deposited in the Gene Expression Omnibus (GEO) database (accession no. GSE198092). Lists of differentially expressed genes mentioned here are provided in Supplementary Dataset S1. The mass spectrometry proteomics data have been deposited to the ProteomeXchange Consortium via the PRIDE (Perez-Riverol et al., 2022) partner repository with the dataset identifier PXD033224. Lists of significantly changed phosphopeptides mentioned here are provided in Supplementary Dataset S2.

Results

Identification of the CelloOligomer Receptor Kinase 1 (CORK1)

To identify proteins involved in COM perception, an ethyl methanesulfonate (EMS)-treated seedling population generated from the wild-type pMAQ2 aequorin line (AeqWT) was screened. Roots from individual F2 seedlings were used to monitor $[Ca^{2+}]_{cyt}$ elevation upon 1 mM cellobiose (CB) application. One mutant (designated as EMS71) showed no $[Ca^{2+}]_{cyt}$ elevation in response to CB (1 mM) and CT (10 μ M). The non-responsive phenotype was confirmed in the F3 generation in both root and leaf tissues (Fig. 1A and 1B). Since $[Ca^{2+}]_{cyt}$ elevation induced by chitin was not affected (Fig. 1C), EMS71 is specifically impaired in COM perception.

EMS71 was back-crossed to AeqWT, and the F2 population was divided into responsive and non-responsive groups. DNA from these two groups were extracted, sequenced and analyzed as described in Materials and Methods. Finally, two candidate genes, At1g59750 (*ARF1*; A248V) and At1g56145 (*CORK1*; G748E), were selected for further confirmation.

The two candidate genes were over-expressed with CaMV 35S promoter in EMS71. Upon CT application, $[Ca^{2+}]_{\text{cyt}}$ elevation was only detected in EMS71 seedlings transformed with *CORK1* construct, but not in those with *ARF1*, suggesting *CORK1* is responsible for the $[Ca^{2+}]_{\text{cyt}}$ elevation induced by COMs (Fig. 1D).

In addition, two T-DNA insertion mutant lines, *cork1-1* and *cork1-2*, were crossed to AeqWT for $[Ca^{2+}]_{\text{cyt}}$ measurements. In the F2 generation, ~25% of the seedlings were non-responsive to CT (Fig. 2A). Genotyping showed that the responsive seedlings were either segregated wild-type (SWT) or heterozygotes, while non-responsive seedlings were all homozygous (HO) for the T-DNA insertion (Fig. 2B). The *CORK1* transcript level was significantly reduced in the HO seedlings compared to SWT seedlings (Fig. 2C). This demonstrates that *CORK1* is required for COM perception in *Arabidopsis*.

The gene model for *CORK1* predicts three RNA isoforms (Fig. 2D). At1g56145.1 (lacking an intron near the 3' end), At1g56145.2 (deduced from the complete DNA sequence) and At1g56145.3 (omitting the first 309 nucleotides from the 5' end). In the *cork1-1* and *cork1-2* mutants, the T-DNAs were inserted in the first exon and the exon located near the 3' end, respectively (Fig. 2D). The SNP for EMS71 is caused by a G→A exchange of the 2243rd nucleotide, converting the 748th glycine residue to a glutamic acid (Fig. 2D and 2E). Thus, the latter mutation affects all three predicted RNA isoforms.

Based on the sequence for the first isoform, *CORK1* is annotated as a leucine-rich repeat transmembrane protein kinase, with a predicted 24-amino acid long signal peptide at the N-terminus, followed by leucine-rich repeat (LRR) domains, and a malectin domain (MD). After the transmembrane domain, a Ser-Thr/Tyr kinase domain is predicted to reside in the cytoplasm (Fig. 2E).

***CORK1* encodes a functional receptor kinase**

To determine whether *CORK1* encodes a LRR receptor kinase, subcellular localization was first examined by transfecting *A. thaliana* protoplasts with a 35S::*CORK1*-GFP construct. The GFP signal at the plasma membrane confirmed that *CORK1* is a membrane-associated protein (Fig. 3A).

Next, the cytoplasmic region encompassing the kinase domain (*CORK1*^{KD}) was cloned into the expression vector pET28a to characterize its kinase activity. GST-*CORK1*^{KD-G748E} was also constructed into pGEX1λT to test whether the mutation found in the kinase domain of EMS71 affects the kinase activity. Figure 3B shows that the substrate myelin protein bovine (MBP) was only phosphorylated by *CORK1*^{KD} but not by the mutated form GST-*CORK1*^{KD-G748E}. At the same time, *CORK1*^{KD} exhibited strong autophosphorylation. This suggests that *CORK1* encodes a functional kinase domain, and the G748E mutation disrupted the kinase activity.

***CORK1* mutant failed to produce ROS upon COM perception**

Besides $[Ca^{2+}]_{\text{cyt}}$ elevation, COMs also induce ROS production, albeit less than classical PAMPs like chitin (Johnson et al., 2018). In SWT roots, but not those in HO, of *cork1-1* and *cork1-2* seedlings, ROS was produced after CT treatment. ROS production was detected upon chitin treatment in both SWT and HO (Fig. 4A and 4B). This suggests that *CORK1* is required for COM-, but not chitin-induced ROS production.

Up-regulation of *WRKY30* and *WRKY40* mRNA level by COMs is *CORK1*-dependent

Since CB activates *WRKY30* and *WRKY40* expression (Souza et al., 2017; Johnson et al., 2018), we checked whether the activation of these genes requires *CORK1*. CT and chitin were applied to roots of SWT and HO seedlings of *cork1-1* and *cork1-2*. After 1 hour, the *WRKY30* and *WRKY40* transcript levels in SWT of both T-DNA lines were up-regulated ~30- and ~15-fold, respectively (Fig.

5A and 5B). On the other hand, no significant response to CT was observed in the HO mutants (Fig. 5A and 5B). Chitin stimulated the *WRKY30* transcript level ~10-fold and that of the *WRKY40* ~2-fold in both genotypes (Fig. 5A and 5B). This demonstrates COM-mediated activation of *WRKY30* and *WRKY40* requires *CORK1*.

Two Phe residues in the malectin domain are important for CT response

Sequence alignment of the *Arabidopsis* LRR-MD RLKs demonstrated that two Phe residues within the MD (F520 and F539) are highly conserved in all MD RLKs (Fig. 6A and Supplementary Fig. S1) and Malectin-Like (MLD) RLKs (Supplementary Fig. S2). It has been suggested that aromatic rings of amino acids interact with the apolar side of carbohydrate (Boraston et al., 2004; Pires et al., 2004; Schallus et al., 2010). Therefore, we changed the two conserved Phe residues to Ala. In the EMS71 mutant transformed with a 35S::CORK1-GFP construct, the $[Ca^{2+}]_{cyt}$ elevation in response to CT application was restored. The $[Ca^{2+}]_{cyt}$ response in plants transformed with either of the two Phe mutant versions (F520A or F539A) was significantly reduced, and no $[Ca^{2+}]_{cyt}$ could be observed in plants transformed with the double mutated version (Fig. 6B). To further support the importance of the two Phe residues, mesophyll protoplasts of *A. thaliana* were co-transformed with the pFRK1::luciferase reporter and either the wild-type or the double-mutated version of *CORK1*. The co-expression of wild-type *CORK1* with the reporter gene conferred responsiveness to the treatment with 1 μ M CT, which was absent when the mutated form was expressed (Fig. 6C - 6F). This suggests that the two conserved Phe residues are important in COM perception in *Arabidopsis*.

Transcriptome analysis uncovered COM/CORK target genes

To identify the biological functions of COMs, we performed transcriptome analysis with the roots of *cork1-2* SWT and HO seedlings 1 hour after the application of either 10 μ M CT or water. Among the 23106 mapped genes, 561 genes were up- and 54 genes down-regulated by CT in a *CORK1*-dependent manner. On the contrary, only 2 genes were significantly up-regulated and no genes were down-regulated by CT in HO (Fig. 7A; Supplementary Dataset S1). This shows the high specificity of *CORK1* to COMs.

Gene ontology (GO) enrichment analysis showed a profound increase in genes involved in tryptophan biosynthesis, cell wall modification and secondary metabolite production (Supplementary Fig. S3). The genes for ASA1 (anthranilate synthase α subunit 1) and ASB1 (anthranilate synthase β subunit 1), which carry out the first step in the tryptophan biosynthesis from chorismate, were ~10 fold and for TSA1 (tryptophan synthase α chain), which catalyzes the last step in the biosynthesis, ~8 fold up-regulated by CT (Table 1 and Fig. 7B).

Among the first 15 categories for the most strongly regulated genes, 5 categories are related to "cell wall" functions. All of them center around callose deposition and cell wall thickening, and most of these genes/proteins are described in the context of defense (Supplementary Fig. S3). Genes in these categories include *FLS2* (~4 fold), *MYB51* (~13 fold), *UDP-glycosyltransferase 74B1* (~4.5 fold), the cytochrome P450 enzymes *CYP81F2* (~12 fold) and *CYP83B1* (~7 fold) as well as the ABC-transporter gene *ABCG36* (~3 fold). Similarly, genes involved in lignin biosynthesis (phenylpropanoid metabolism) were also up-regulated, such as those for cinnamate-4-hydroxylase (C4H, ~3 fold), 4-coumarate-CoA ligase 1 (4CL1, ~4 fold), phenylalanine ammonia lyase 1 (PAL1, ~3 fold), and for three enzymes important for lignin production, Caffeoyl-CoA 3-O-methyltransferase (CCoAOMT, ~13 fold), cinnamyl alcohol dehydrogenase 5 (CAD5, ~3 fold) and peroxidase 4 (PER4, ~5 fold; Fernández-Pérez et al., 2015; Barros et al., 2019). *PEN2* and *PMR4/GSL5*, encoding a myrosinase and a callose synthase, respectively, were only slightly up-regulated (~1.7 fold; Table 1 and Fig. 7B).

In addition to cell wall-related genes, *SOT16* and *SOT17*, which encode sulfotransferases for glucosinolate production, were up-regulated ~5.5 fold. Likewise, the transcript level for *CYP71B15* (*PAD3*), which is required for camalexin production, was ~3.5-fold up-regulated. In line with qPCR analyses and previous reports (Souza et al., 2017; Johnson et al., 2018), *WRKY30*, *WRKY40* and the lipoxygenase genes involved in jasmonic acid synthesis *LOX1* (~3.5 fold), *LOX3* (~11.5 fold) and

LOX4 (~5.5 fold) responded to COMs. Finally, genes for proteins in the FLS2 signaling pathway were up-regulated, such as *FRK1* (~4.5 fold) and *WRKY29* (~2.5 fold; Asai et al., 2002; Table 1 and Fig. 7B).

Interestingly, most of the down-regulated genes are involved in ion homeostasis, and a *PR-1 like* gene which mediates defense (At2g19990, ~0.16 fold; Fig. 7B and Supplementary Fig. S4).

In summary, COM perception by CORK1 induces cell wall reinforcement, defense-related secondary metabolite synthesis, and crosstalk with other signaling components.

COM/CORK-mediated changes in the phosphoproteome pattern in roots

To identify early COM/CORK1 targets, the phosphoproteomes of SWT and HO roots were analyzed 5 and 15 minutes after 10 μ M CT or water (control) application. Most of the proteins with a significantly altered phosphorylation state are related to (i) cellulose synthase complex (CSC) functions and translocation to the plasma membrane, (ii) the ER secretory pathway and protein sorting, (iii) proteins involved in signal transduction, or (iv) defense/stress responses (Supplementary Fig. S5 and Supplementary Dataset S2).

Cellulose synthases 1 and 3 (CESA1, -3) of the CSC are required for cellulose synthesis for the primary cell wall and the protein is rapidly phosphorylated at Ser24 and Ser176, respectively, in response to CT application. Mutations of CESAs phosphorylation sites modulate anisotropic cell expansion and bidirectional mobility of the cellulose synthase (Chen et al., 2010). Besides CESAs, we also identified Cellulose Synthase-Interactive 1 (CSII) as a phosphorylation target of CT at Thr37. Association of CSC with cortical microtubules is mediated by CSII and the protein contains multiple phosphorylation sites potentially involved in regulatory processes (Jones et al., 2016). Loss of function CSII mutants are impaired in the dissociation of the CSC from the microtubules during their passage to the plasma membrane which results in cellulose deficiency in the mutant cell walls (Li et al., 2015). The COMPANION OF CELLULOSE SYNTHASE 1 and 2 (CC1/CC2) and the N-terminal domain in CSI are responsible for the connection of the CSCs to the cortical microtubules and *csi1* mutants are impaired in microtubule stability under salt stress (Endler et al., 2015; Speicher et al., 2018), but also for CSC delivery to the plasma membrane and its recycling (Lei et al., 2012; Lei et al., 2015). In addition to its role in trafficking and mobility of CSCs, microtubules also influence the orientation and crystallinity of cellulose (Lei et al., 2015). Thus, CESA1 and CSII are two central players in cellulose repair mechanism, and are phosphorylated by COM/CORK.

Among the proteins involved in the endomembrane system and the secretory pathway are two GTPases which regulate membrane trafficking: AGD5, a GTPase-activating protein operating at the *trans*-Golgi network (Stefano et al., 2010) and RABA5C, a GTPase that specifies a membrane trafficking pathway to geometric edges of lateral root cells (Kirchhelle et al., 2019). The 1-phosphatidylinositol-3-phosphate 5-kinase is involved in maintenance of endomembrane homeostasis including endocytosis and vacuole formation (Hirano et al., 2011); the exocyst complex component SEC8 participates in the docking of exocytic vesicles with fusion sites on the plasma membrane and the formation of new primary cell wall; the vacuolar sorting protein 41 regulates vacuolar vesicle fusions and protein sorting together with phosphoinositides (Brillada et al., 2018); a SNARE protein as part of a complex **facilitates trafficking** in the endomembrane system including distinct secretory and vacuolar trafficking steps. The phosphorylated myosin mediates the organization of actin filament and vesicle transport along the filaments. Finally, MAPK 17 influences the number and cellular distribution of peroxisomes through the cytoskeleton-peroxisome connection (Frick and Strader, 2018). Not surprisingly, stimulation of membrane trafficking, protein sorting and secretion also affects enzymes involved in cellulose, callose and other polysaccharide biosynthesis, such as CESAs, CSII, callose synthase and a regulator of callose deposition, the PAMP-Induced coiled coil protein At2g32240 (Wang et al., 2019). The cytosolic UDP-glucuronic acid decarboxylases, At3g46440 and At5g59290, produce UDP-xylose, which is a substrate for many cell wall carbohydrates including hemicellulose and pectin. UDP-xylose is also known to feedback regulate several cell wall biosynthetic enzymes, many of them are associated with the endomembrane system (Pattathil et al.,

2005; Kuang et al., 2016; Zhong et al., 2017). Phosphorylated proteins with related functions control auxin translocation at the plasma membrane (At1g56220, ABCG36).

Inspection of target proteins at different time points uncovered that the canonical immunity-related mitogen-activated protein kinases MPK3 and MPK6 showed increased phosphorylation (Ser16 of MPK3 and Tyr223 of MPK6) at both time points after CT application in SWT roots. Likewise, the calmodulin-binding protein IQM4 (at Ser505, Ser509, Ser520 and Ser525) and the Ca²⁺-dependent protein kinase CPK9 (at Ser69) are among the most phosphorylated targets at both time points and link stress-induced Ca²⁺ signaling to abscisic acid (Zhou et al., 2018; Chen et al., 2019). On the other hand, phosphorylation of the plasma membrane-localized FERONIA (at Ser695), SERK1 (at Thr450 and Thr463) and MAPKKK3 which mediates MPK3/6 activation by at least four pattern-recognition receptors (FLS2, EFR, CERK1, and PEPRs; Bi et al., 2018) was only detectable at the early time point. On the other hand, phosphorylation at Ser716 of the Tumor Necrosis Factor Receptor-Associated Factor (TRAF) 1B, which involved in immune receptor turnover, was increased 5 minutes but decreased 15 minutes after CT treatment (Huang et al., 2016; Table 2).

Among the defense-related proteins, phosphorylation of RBOHD at Ser347 was significantly decreased at the early time point (Table 2). The MPK8 module negatively regulates ROS accumulation through controlling expression of the *RBOHD* gene and the phosphorylation state decreased 15 min after CT application. Takahashi *et al.* (2011) proposed that Ca²⁺/CaMs and the MAP kinase phosphorylation cascade converge at MPK8 to monitor or maintain ROS homeostasis. Likewise, phosphorylation of JOX2 at Ser369 which catalyzes the hydroxylation of jasmonic acid to 12-OH-jasmonic acid and thus restricts the generation of the active jasmonic acid-isoleucine, was only detectable at the early time point. Also EXA1 (Essential for potyvirus Accumulation 1) controlling virus infection was only phosphorylated at Ser1553 at the early time point (Hashimoto et al., 2016). In contrast, phosphorylation of EDR4 (Enhanced Disease Resistance 4) which represses salicylic-acid-mediated resistance, and ZAT10, a repressor of abiotic stress and jasmonic acid responses, was only stimulated 15 min after CT application (Wu et al., 2015; Xie et al., 2019). The ABC transporter G36 which controls pathogen entry into cells, was phosphorylated at both time points and its mRNA was upregulated in our expression analysis (Table 1). The identified targets of COM/CORK1 signaling show dynamic changes in the protein phosphorylation pattern. Considering the different roles of these proteins in activating or repressing signaling and defense responses, it can be speculated that COM/CORK1 signaling establishes a moderate immune response and maintains its homeostasis.

Discussion

We demonstrate that CORK1, a leucine-rich repeat-malectin receptor kinase, is required for COM-mediated rapid increase in [Ca²⁺]_{cyt} level and stimulation of ROS production in *Arabidopsis*. Transcriptome analyses uncovered CT-regulated and CORK1-dependent target genes of a proposed COM/CORK1 signaling pathway. Major CT/CORK1 target genes are involved in cell wall strengthening, secondary metabolite metabolism and Trp biosynthesis. Phosphoproteome analysis identified early COM/CORK1 target proteins involved in secretory pathways and vesicle trafficking, the plasma membrane-associated RBOHD, FER and SERK1, MPK3/6, novel MAPKs such as MAPKKK3, MPK17 and MPK8, as well as downstream proteins involved in plant immunity. Interestingly, the different phosphorylation patterns 5 and 15 min after the stimulus and phosphorylation of EXA1, TRAF1B, MPK8, JOX2 and EDR4 demonstrate that CT establishes a balanced defense response. For instance, CT stimulates ROS production. Simultaneously phosphorylation and thus activation of RBOHD was repressed at the early time point (Table 2), and MPK8, which is involved in establishing ROS homeostasis (Takahashi et al., 2011), is phosphorylated. Furthermore, expression of defense-related genes such as *WRKY30/40*, is stimulated by COM, while phosphorylation of EXA1, TFAF1B, JOX2 and EDR4 restrict or balance defense responses. A crosstalk to other receptor kinases is demonstrated by FER and SERK1, and potentially the up-regulation of *FLS2* at the mRNA level. The observed downstream responses are consistent with the idea that COM/CORK1 activates processes which maintain cell wall integrity.

LRR-Malectin receptors are the new players in cell wall surveillance

Malectins were first discovered in *Xenopus* (Schallus et al., 2008). They are located in the ER of animal cells, and bind to diglycosylated N-linked glycans to control glycoprotein quality (Galli et al., 2011; Takeda et al., 2014; Tannous et al., 2015). The ligands of malectins include the disaccharide maltose and nigerose (Schallus et al., 2008; Schallus et al., 2010). The structure of malectins are similar to the carbohydrate-binding modules found in enzymes which degrade the plant cell wall (Schallus et al., 2008; Gilbert et al., 2013; Duan et al., 2016). Although the two Phe residues conserved in all MDs in *A. thaliana* are not conserved in the maltose binding malectin from *Xenopus* (Schallus et al., 2010), the replacement of the two Phe with Ala eliminated CT-induced $[Ca^{2+}]_{cyt}$ elevation and reporter gene activation (Fig. 6). This suggests a functional divergent role of malectins in plants and animals. The two Phe residues in the plant MDs might be specifically involved in binding COs with β 1-4-bonds, while non-plant malectins bind maltose and nigerose with α 1-4-bonds.

Besides CORK1, there are 13 additional LRR-MD-RLKs in *Arabidopsis*. They have been shown to be involved in lipopolysaccharide perception (Hussan et al., 2020), pollen tube development (Lee and Goring, 2021) and control of cell death in leaves (Li et al., 2020). Several of them are up-regulated by brassinosteroids and participate in immune responses (Qutob et al., 2006; Hok et al., 2014; Xu et al., 2014). However, whether their MDs bind to sugars is not known. Due to structure and sequence similarity, they might interact with other sugars from cell wall polymers, since the *cork1* phenotype excludes their participation in COM responses.

Intriguingly, the phosphoproteomic study identified FER as a phosphorylation target after CT treatment (Table 2). It harbors a malectin-like domain (MLD), consisting of two tandem malectin domains. It has been shown to regulate CWI and pollen tube development, although known ligands for FER are RALF peptides and pectins (Escobar-Restrepo et al., 2007; Zhang et al., 2020; Tang et al., 2021; Yang et al., 2021b). Together with the phosphorylation of several members of CSC, it is likely that CORK1 controls cell wall repair mechanism, and may coordinate FER upon cell wall damage.

Crosstalk between CORK1 and other signaling pathways

Activation of *FLS2*, genes involved in FLS2 signaling and FLS2 targets, phosphorylation of MAPKs (MAPKKK3, MPK3 and MPK6), plasma membrane-localized SERK1 and FER by CT/CORK1 suggest crosstalk to other receptor kinases and PAMP-activated defense signaling (Fig. 7, Table 1 and Table 2). Souza *et al.* (2017) and Johnson *et al.* (2018) have shown that combined treatments of CB/CT with either flg22 or chitin trigger higher $[Ca^{2+}]_{cyt}$ levels, ROS production and MPK3/6 phosphorylation. CWI signaling and plant defense are tightly coupled, both operate via $[Ca^{2+}]_{cyt}$ elevation. Although their Ca^{2+} signatures might differ, the overlap is apparent by the large number of defense-related genes which respond to CT/CORK1 activation and PAMP-induced signaling. Likewise, *WRKY30* and *WRKY40* are downstream targets of COM/CORK1 activation and the transcription factors participate in various biotic and abiotic responses (Scarpeci et al., 2013; Wang et al., 2021). Understanding the crosstalk between CORK1 and other PRRs as well as their signaling components will provide a broader picture of how plants integrate different threats and developmental signals. CWI signaling is also important during many developmental processes, starting from growth, division and differentiation of cells, meristem development, senescence to fertilization. The tissue-specific expression of the different members of the MD-containing receptor kinases might reflect their different roles in monitoring cell wall alterations (Wu et al., 2016).

CT regulates metabolism of aromatic amino acids and secondary metabolites

Tryptophan-derived secondary metabolites have long been considered as important components for innate immunity, and Trp serves as the starting amino acid for the biosynthesis of camalexin and indolic glucosinolates (Bednarek, 2012). Up-regulation of Trp biosynthesis is crucial for plant defense against fungal pathogens and hemibiotrophs (Ishihara et al., 2008; Consonni et al., 2010; Hiruma et al., 2013).

Although several genes important for flagellin-induced callose deposition (Clay et al., 2009) are also up-regulated by CT, however, callose deposition could not be observed (Souza et al., 2017). This might be due to the low induction of *PEN2* and *PMR4* by CT (Fig. 7). Interestingly, *ABCG36* (*PEN3*) was up-regulated and the gene product, ABCG36/PEN3, was phosphorylated by CT after 5 minutes (Fig. 7 and Table 2). Phosphorylation of the transporter is important for pathogen defense, and it has been proposed that it participates in the deposition of defense-related secondary metabolites (Underwood and Somerville, 2017). Which components can be exported by ABCG36 (PEN3) are not known, but they might as well be important for cell wall repair. Besides differences between COM (DAMP) and flagellin (PAMP), our –omics analyses confirm crosstalks at the signaling levels. Besides COM/CORK1-induced investment into defense, it might play an important role in priming plant immune responses induced by other stimuli.

Another group of CT-stimulated genes involved in phenylpropanoid metabolism (Fig. 7) convert Phe through cinnamic acid (Phe-ammonia lyase), *p*-coumaric acid (cinnamate-4-hydroxylase) to *p*-coumaryl-CoA (**4-coumarate:CoA ligase 1**). From there, *p*-coumaryl-CoA can be used to synthesize lignin with cinnamyl alcohol dehydrogenase 5 (CAD5), caffeoyl-CoA O-methyltransferases and peroxidase 4 (Fernández-Pérez et al., 2015; Barros et al., 2019). These steps are important in secondary cell wall synthesis.

Apart from aromatic compounds, expression of lipoxygenases involved in jasmonic acid (JA) biosynthesis are up-regulated by CT (Table 1). Moreover, the gene for CML42, a negative regulator of JA signaling and biosynthesis, is down-regulated by CT (Vadassery et al., 2012; Table 1). Furthermore, JOX2, which converts JA to 12-hydroxyjasmonate, an inactive form of JA (Zhang et al., 2021), is phosphorylated at Ser369 in response to CT. The enzyme prevents over-accumulation of JA and its bioactive form JA-Ile under stress (Caarls et al., 2017; Smirnova et al., 2017) and thus, represses basal JA defense responses. These results show that JA is a target of COM signaling. However, it appears that COM treatment established moderate and balanced JA level in the cell. The comparative analysis of the regulated genes and phosphorylation targets suggest that the primary effect of COM/CORK1 signaling is activating cellular processes which strengthen the cell wall and not those promoting cytoplasmic immunity.

This work provides evidence for the first receptor for cellulose breakdown fragments, and demonstrates the importance of the malectin domain for COM sensing. With recent findings of other cell wall breakdown products acting as DAMPs (Claverie et al., 2018; Mélida et al., 2020; Rebaque et al., 2021; Yang et al., 2021a), closer inspection of the other LRR-MD RLK members might be a reasonable strategy to identify receptors for other polysaccharide breakdown products of the cell wall. Our transcriptome and phosphoproteome analyses provide a list of components which are potentially involved in COM signaling, might represent COM targets, or participate in CORK1 crosstalk.

Acknowledgement

We thank Prof. Dr. Maria Mittag for providing the expression vector pGEX1 λ T and Prof. Georg Felix for discussions and comments on the work. We also thank Claudia Röppischer, Sarah Mußbach and Christin Weilandt for technical assistance. Special thanks to Yelyzaveta Zhyr for the help on plant transformation and the green house team at Max Planck Institute for Chemical Ecology for taking care of all the *Arabidopsis* transformants. This work was supported by the Deutsche Forschungsgemeinschaft (DFG, German Research Foundation) CRC1127 ChemBioSys (project ID: 239748522) and CRC/TR 124 FungiNet (project Z2; project ID: 210879364).

Author Contributions

Y-HT and **RO** developed the idea and organized the project. **Y-HT**, performed the experiments, collected the samples and data, analyzed the results and plotted the figures. **SSS** generated the EMS mutant population. **JF** performed the protoplast assay and analyzed the data. **TK** carried out the phosphopeptide measurement and data analysis. **AG** assisted on sample collection and

protein extraction. **AAB** and **OK** provided the materials and equipment for protein extraction. **Y-HT** and **RO** wrote up the study. All authors contributed to the manuscript.

References

- Asai T, Tena G, Plotnikova J, Willmann MR, Chiu W-L, Gomez-Gomez L, Boller T, Ausubel FM, Sheen J** (2002) MAP kinase signalling cascade in Arabidopsis innate immunity. *Nature* **415**: 977–983
- Atmodjo MA, Hao Z, Mohnen D** (2013) Evolving views of pectin biosynthesis. *Annu Rev Plant Biol* **64**: 747–779
- Barros J, Escamilla-Trevino L, Song L, Rao X, Serrani-Yarce JC, Palacios MD, Engle N, Choudhury FK, Tschaplinski TJ, Venables BJ, et al** (2019) 4-Coumarate 3-hydroxylase in the lignin biosynthesis pathway is a cytosolic ascorbate peroxidase. *Nat Commun* **10**: 1994
- Bednarek P** (2012) Chemical warfare or modulators of defence responses - the function of secondary metabolites in plant immunity. *Curr Opin Plant Biol* **15**: 407–414
- Bertani G** (1951) Studies on lysogeny I.: The mode of phage liberation by lysogenic *Escherichia coli*. *J Bacteriol* **62**: 293–300
- Bi G, Zhou Z, Wang W, Li L, Rao S, Wu Y, Zhang X, Menke FLH, Chen S, Zhou J-M** (2018) Receptor-like cytoplasmic kinases directly link diverse pattern recognition receptors to the activation of mitogen-activated protein kinase cascades in Arabidopsis. *Plant Cell* **30**: 1543–1561
- Boraston AB, Bolam DN, Gilbert HJ, Davies GJ** (2004) Carbohydrate-binding modules: Fine-tuning polysaccharide recognition. *Biochem J* **382**: 769–781
- Brillada C, Zheng J, Krüger F, Rovira-Diaz E, Askani JC, Schumacher K, Rojas-Pierce M** (2018) Phosphoinositides control the localization of HOPS subunit VPS41, which together with VPS33 mediates vacuole fusion in plants. *Proc Natl Acad Sci* **115**: E8305–E8314
- Brutus A, Sicilia F, Macone A, Cervone F, De Lorenzo G** (2010) A domain swap approach reveals a role of the plant wall-associated kinase 1 (WAK1) as a receptor of oligogalacturonides. *Proc Natl Acad Sci* **107**: 9452–9457
- Caarls L, Elberse J, Awwanah M, Ludwig NR, de Vries M, Zeilmaker T, Van Wees SCM, Schuurink RC, Van den Ackerveken G** (2017) Arabidopsis JASMONATE-INDUCED OXYGENASES down-regulate plant immunity by hydroxylation and inactivation of the hormone jasmonic acid. *Proc Natl Acad Sci* **114**: 6388–6393
- Chen D-H, Liu H-P, Li C-L** (2019) Calcium-dependent protein kinase CPK9 negatively functions in stomatal abscisic acid signaling by regulating ion channel activity in Arabidopsis. *Plant Mol Biol* **99**: 113–122
- Chen S, Ehrhardt DW, Somerville CR** (2010) Mutations of cellulose synthase (CESA1) phosphorylation sites modulate anisotropic cell expansion and bidirectional mobility of cellulose synthase. *Proc Natl Acad Sci* **107**: 17188–17193
- Claverie J, Balacey S, Lemaître-Guillier C, Brulé D, Chiltz A, Granet L, Noirot E, Daire X, Darblade B, Héloir M-C, et al** (2018) The cell wall-derived xyloglucan is a new DAMP triggering plant immunity in *Vitis vinifera* and Arabidopsis thaliana. *Front Plant Sci* **9**: 1725

- Clay NK, Adio AM, Denoux C, Jander G, Ausubel FM** (2009) Glucosinolate metabolites required for an Arabidopsis innate immune response. *Science* **323**: 95–101
- Consonni C, Bednarek P, Humphry M, Francocci F, Ferrari S, Harzen A, Ver Loren van Themaat E, Panstruga R** (2010) Tryptophan-derived metabolites are required for antifungal defense in the Arabidopsis mlo2 mutant. *Plant Physiol* **152**: 1544–1561
- Dobin A, Davis CA, Schlesinger F, Drenkow J, Zaleski C, Jha S, Batut P, Chaisson M, Gingeras TR** (2013) STAR: ultrafast universal RNA-seq aligner. *Bioinforma Oxf Engl* **29**: 15–21
- Doyle JJ** (1990) Isolation of plant DNA from fresh tissue. *Focus* **12**: 13–15
- Duan C-J, Feng Y-L, Cao Q-L, Huang M-Y, Feng J-X** (2016) Identification of a novel family of carbohydrate-binding modules with broad ligand specificity. *Sci Rep* **6**: 19392
- Endler A, Kesten C, Schneider R, Zhang Y, Ivakov A, Froehlich A, Funke N, Persson S** (2015) A mechanism for sustained cellulose synthesis during salt stress. *Cell* **162**: 1353–1364
- Escobar-Restrepo J-M, Huck N, Kessler S, Gagliardini V, Gheyselinck J, Yang W-C, Grossniklaus U** (2007) The FERONIA receptor-like kinase mediates male-female interactions during pollen tube reception. *Science* **317**: 656–660
- Feng W, Kita D, Peaucelle A, Cartwright HN, Doan V, Duan Q, Liu M-C, Maman J, Steinhorst L, Schmitz-Thom I, et al** (2018) The FERONIA receptor kinase maintains cell-wall integrity during salt stress through Ca²⁺ signaling. *Curr Biol* **28**: 666-675.e5
- Fernández-Pérez F, Vivar T, Pomar F, Pedreño MA, Novo-Uzal E** (2015) Peroxidase 4 is involved in syringyl lignin formation in Arabidopsis thaliana. *J Plant Physiol* **175**: 86–94
- Frick EM, Strader LC** (2018) Kinase MPK17 and the peroxisome division factor PMD1 influence salt-induced peroxisome proliferation. *Plant Physiol* **176**: 340–351
- Galletti R, Ferrari S, De Lorenzo G** (2011) Arabidopsis MPK3 and MPK6 play different roles in basal and oligogalacturonide- or flagellin-induced resistance against Botrytis cinerea. *Plant Physiol* **157**: 804–814
- Galli C, Bernasconi R, Soldà T, Calanca V, Molinari M** (2011) Malectin participates in a backup glycoprotein quality control pathway in the mammalian ER. *PloS One* **6**: e16304
- Gibson LJ** (2012) The hierarchical structure and mechanics of plant materials. *J R Soc Interface* **9**: 2749–2766
- Gilbert HJ, Knox JP, Boraston AB** (2013) Advances in understanding the molecular basis of plant cell wall polysaccharide recognition by carbohydrate-binding modules. *Curr Opin Struct Biol* **23**: 669–677
- Gust AA, Pruitt R, Nürnberger T** (2017) Sensing danger: Key to activating plant immunity. *Trends Plant Sci* **22**: 779–791
- Harholt J, Suttangkakul A, Vibe Scheller H** (2010) Biosynthesis of pectin. *Plant Physiol* **153**: 384–395
- Haruta M, Sabat G, Stecker K, Minkoff BB, Sussman MR** (2014) A peptide hormone and its receptor protein kinase regulate plant cell expansion. *Science* **343**: 408–411

- Hashimoto M, Neriya Y, Keima T, Iwabuchi N, Koinuma H, Hagiwara-Komoda Y, Ishikawa K, Himeno M, Maejima K, Yamaji Y, et al** (2016) EXA1, a GYF domain protein, is responsible for loss-of-susceptibility to plantago asiatica mosaic virus in *Arabidopsis thaliana*. *Plant J Cell Mol Biol* **88**: 120–131
- He ZH, Fujiki M, Kohorn BD** (1996) A cell wall-associated, receptor-like protein kinase. *J Biol Chem* **271**: 19789–19793
- Hirano T, Matsuzawa T, Takegawa K, Sato MH** (2011) Loss-of-function and gain-of-function mutations in FAB1A/B impair endomembrane homeostasis, conferring pleiotropic developmental abnormalities in *Arabidopsis*. *Plant Physiol* **155**: 797–807
- Hiruma K, Fukunaga S, Bednarek P, Piślewska-Bednarek M, Watanabe S, Narusaka Y, Shirasu K, Takano Y** (2013) Glutathione and tryptophan metabolism are required for *Arabidopsis* immunity during the hypersensitive response to hemibiotrophs. *Proc Natl Acad Sci* **110**: 9589–9594
- Hok S, Allasia V, Andrio E, Naessens E, Ribes E, Panabières F, Attard A, Ris N, Clément M, Barlet X, et al** (2014) The receptor kinase IMPAIRED OOMYCETE SUSCEPTIBILITY1 attenuates abscisic acid responses in *Arabidopsis*. *Plant Physiol* **166**: 1506–1518
- Hu XY, Neill SJ, Cai WM, Tang ZC** (2004) Induction of defence gene expression by oligogalacturonic acid requires increases in both cytosolic calcium and hydrogen peroxide in *Arabidopsis thaliana*. *Cell Res* **14**: 234–240
- Huang S, Chen X, Zhong X, Li M, Ao K, Huang J, Li X** (2016) Plant TRAF proteins regulate NLR immune receptor turnover. *Cell Host Microbe* **19**: 204–215
- Hussan RH, Dubery IA, Piater LA** (2020) Identification of MAMP-responsive plasma membrane-associated proteins in *Arabidopsis thaliana* following challenge with different LPS chemotypes from *Xanthomonas campestris*. *Pathogens* **9**: 787
- Ishihara A, Hashimoto Y, Tanaka C, Dubouzet JG, Nakao T, Matsuda F, Nishioka T, Miyagawa H, Wakasa K** (2008) The tryptophan pathway is involved in the defense responses of rice against pathogenic infection via serotonin production. *Plant J Cell Mol Biol* **54**: 481–495
- Javorka P, Raxwal VK, Najvarek J, Riha K** (2019) artMAP: A user-friendly tool for mapping ethyl methanesulfonate-induced mutations in *Arabidopsis*. *Plant Direct* **3**: e00146
- Johnson JM, Sherameti I, Ludwig A, Nongbri P, Sun C, Lou B, Varma A, Oelmüller R** (2011) Protocols for *Arabidopsis thaliana* and *Piriformospora indica* co-cultivation – A model system to study plant beneficial traits. *Endocytobiosis Cell Res* **21**: 101–113
- Johnson JM, Thürich J, Petutschnig EK, Altschmied L, Meichsner D, Sherameti I, Dindas J, Mrozinska A, Paetz C, Scholz SS, et al** (2018) A Poly(A) ribonuclease controls the cellobiose-based interaction between *Piriformospora indica* and its host *Arabidopsis*. *Plant Physiol* **176**: 2496–2514
- Jones DM, Murray CM, Ketelaar KJ, Thomas JJ, Villalobos JA, Wallace IS** (2016) The emerging role of protein phosphorylation as a critical regulatory mechanism controlling cellulose biosynthesis. *Front Plant Sci* **7**: 684

- Kanehisa M, Goto S** (2000) KEGG: kyoto encyclopedia of genes and genomes. *Nucleic Acids Res* **28**: 27–30
- Karimi M, Inzé D, Depicker A** (2002) GATEWAYTM vectors for Agrobacterium-mediated plant transformation. *Trends Plant Sci* **7**: 193–195
- Kim Y, Schumaker KS, Zhu J-K** (2006) EMS mutagenesis of Arabidopsis. *Methods Mol Biol Clifton NJ* **323**: 101–103
- Kirchhelle C, Garcia-Gonzalez D, Irani NG, Jérusalem A, Moore I** (2019) Two mechanisms regulate directional cell growth in Arabidopsis lateral roots. *eLife* **8**: e47988
- Knight MR, Campbell AK, Smith SM, Trewavas AJ** (1991) Transgenic plant aequorin reports the effects of touch and cold-shock and elicitors on cytoplasmic calcium. *Nature* **352**: 524–526
- Kuang B, Zhao X, Zhou C, Zeng W, Ren J, Ebert B, Beahan CT, Deng X, Zeng Q, Zhou G, et al** (2016) Role of UDP-glucuronic acid decarboxylase in xylan biosynthesis in Arabidopsis. *Mol Plant* **9**: 1119–1131
- Kumar S, Stecher G, Tamura K** (2016) MEGA7: Molecular Evolutionary Genetics Analysis Version 7.0 for Bigger Datasets. *Mol Biol Evol* **33**: 1870–1874
- Lee HK, Goring DR** (2021) Two subgroups of receptor-like kinases promote early compatible pollen responses in the Arabidopsis thaliana pistil. *J Exp Bot* **72**: 1198–1211
- Lei L, Li S, Gu Y** (2012) Cellulose synthase interactive protein 1 (CSII) mediates the intimate relationship between cellulose microfibrils and cortical microtubules. *Plant Signal Behav* **7**: 714–718
- Lei L, Singh A, Bashline L, Li S, Yingling YG, Gu Y** (2015) CELLULOSE SYNTHASE INTERACTIVE1 is required for fast recycling of cellulose synthase complexes to the plasma membrane in Arabidopsis. *Plant Cell* **27**: 2926–2940
- Leyser HMO, Furner IJ** (1993) EMS mutagenesis of Arabidopsis. *Arab. Compleat Guide Electron.* V 14
- Li H, Handsaker B, Wysoker A, Fennell T, Ruan J, Homer N, Marth G, Abecasis G, Durbin R, 1000 Genome Project Data Processing Subgroup** (2009) The Sequence Alignment/Map format and SAMtools. *Bioinforma Oxf Engl* **25**: 2078–2079
- Li S, Lei L, Yingling YG, Gu Y** (2015) Microtubules and cellulose biosynthesis: the emergence of new players. *Curr Opin Plant Biol* **28**: 76–82
- Li X, Sanagi M, Lu Y, Nomura Y, Stolze SC, Yasuda S, Saijo Y, Schulze WX, Feil R, Stitt M, et al** (2020) Protein phosphorylation dynamics under carbon/nitrogen-nutrient stress and identification of a cell death-related receptor-like kinase in Arabidopsis. *Front Plant Sci* **11**: 377
- Liao Y, Smyth GK, Shi W** (2014) featureCounts: an efficient general purpose program for assigning sequence reads to genomic features. *Bioinforma Oxf Engl* **30**: 923–930
- Lodish H, Berk A, Zipursky SL, Matsudaira P, Baltimore D, Darnell J** (2000) *The Dynamic Plant Cell Wall*. *Mol. Cell Biol.* 4th Ed.

- Love MI, Huber W, Anders S** (2014) Moderated estimation of fold change and dispersion for RNA-seq data with DESeq2. *Genome Biol* **15**: 550
- Mélida H, Bacete L, Ruprecht C, Rebaque D, del Hierro I, López G, Brunner F, Pfrengle F, Molina A** (2020) Arabinoxylan-oligosaccharides act as damage associated molecular patterns in plants regulating disease resistance. *Front Plant Sci* **11**: 1210
- Mi H, Ebert D, Muruganujan A, Mills C, Albou L-P, Mushayamaha T, Thomas PD** (2021) PANTHER version 16: a revised family classification, tree-based classification tool, enhancer regions and extensive API. *Nucleic Acids Res* **49**: D394–D403
- Mohnen D** (2008) Pectin structure and biosynthesis. *Curr Opin Plant Biol* **11**: 266–277
- Murashige T, Skoog F** (1962) A revised medium for rapid growth and bio assays with tobacco tissue cultures. *Physiol Plant* **15**: 473–497
- Pattathil S, Harper AD, Bar-Peled M** (2005) Biosynthesis of UDP-xylose: characterization of membrane-bound AtUxs2. *Planta* **221**: 538–548
- Perez-Riverol Y, Bai J, Bandla C, García-Seisdedos D, Hewapathirana S, Kamatchinathan S, Kundu DJ, Prakash A, Frericks-Zipper A, Eisenacher M, et al** (2022) The PRIDE database resources in 2022: a hub for mass spectrometry-based proteomics evidences. *Nucleic Acids Res* **50**: D543–D552
- Pires VMR, Henshaw JL, Prates JAM, Bolam DN, Ferreira LMA, Fontes CMGA, Henrissat B, Planas A, Gilbert HJ, Czjzek M** (2004) The crystal structure of the family 6 carbohydrate binding module from *Cellvibrio mixtus* endoglucanase 5a in complex with oligosaccharides reveals two distinct binding sites with different ligand specificities. *J Biol Chem* **279**: 21560–21568
- Qutob D, Kemmerling B, Brunner F, Kűfner I, Engelhardt S, Gust AA, Luberacki B, Seitz HU, Stahl D, Rauhut T, et al** (2006) Phytotoxicity and innate immune responses induced by Nep1-Like proteins. *Plant Cell* **18**: 3721–3744
- Rebaque D, del Hierro I, López G, Bacete L, Vilaplana F, Dallabernardina P, Pfrengle F, Jordá L, Sánchez-Vallet A, Pérez R, et al** (2021) Cell wall-derived mixed-linked β -1,3/1,4-glucans trigger immune responses and disease resistance in plants. *Plant J* **106**: 601–615
- Ridley BL, O’Neill MA, Mohnen D** (2001) Pectins: structure, biosynthesis, and oligogalacturonide-related signaling. *Phytochemistry* **57**: 929–967
- Scarpeci TE, Zanol MI, Mueller-Roeber B, Valle EM** (2013) Overexpression of AtWRKY30 enhances abiotic stress tolerance during early growth stages in *Arabidopsis thaliana*. *Plant Mol Biol* **83**: 265–277
- Schallus T, Fehér K, Sternberg U, Rybin V, Muhle-Goll C** (2010) Analysis of the specific interactions between the lectin domain of malectin and diglucosides. *Glycobiology* **20**: 1010–1020
- Schallus T, Jaekch C, Fehér K, Palma AS, Liu Y, Simpson JC, Mackeen M, Stier G, Gibson TJ, Feizi T, et al** (2008) Malectin: a novel carbohydrate-binding protein of the endoplasmic reticulum and a candidate player in the early steps of protein N-glycosylation. *Mol Biol Cell* **19**: 3404–3414

- Scheller HV, Ulvskov P** (2010) Hemicelluloses. *Annu Rev Plant Biol* **61**: 263–289
- Smirnova E, Marquis V, Poirier L, Aubert Y, Zumsteg J, Ménard R, Miesch L, Heitz T** (2017) Jasmonic Acid Oxidase 2 hydroxylates jasmonic acid and represses basal defense and resistance responses against *Botrytis cinerea* Infection. *Mol Plant* **10**: 1159–1173
- Souza C de A, Li S, Lin AZ, Boutrot F, Grossmann G, Zipfel C, Somerville SC** (2017) Cellulose-derived oligomers act as damage-associated molecular patterns and trigger defense-like responses. *Plant Physiol* **173**: 2383–2398
- Speicher TL, Li PZ, Wallace IS** (2018) Phosphoregulation of the Plant Cellulose Synthase Complex and Cellulose Synthase-Like Proteins. *Plants* **7**: 52
- Stefano G, Renna L, Rossi M, Azzarello E, Pollastri S, Brandizzi F, Baluska F, Mancuso S** (2010) AGD5 is a GTPase-activating protein at the trans-Golgi network. *Plant J Cell Mol Biol* **64**: 790–799
- Takahashi F, Mizoguchi T, Yoshida R, Ichimura K, Shinozaki K** (2011) Calmodulin-dependent activation of MAP kinase for ROS homeostasis in *Arabidopsis*. *Mol Cell* **41**: 649–660
- Takeda K, Qin S-Y, Matsumoto N, Yamamoto K** (2014) Association of malectin with ribophorin I is crucial for attenuation of misfolded glycoprotein secretion. *Biochem Biophys Res Commun* **454**: 436–440
- Tang W, Lin W, Zhou X, Guo J, Dang X, Li B, Lin D, Yang Z** (2022) Mechano-transduction via the pectin-FERONIA complex activates ROP6 GTPase signaling in *Arabidopsis* pavement cell morphogenesis. *Curr Biol* **32**:508-517.e3
- Tannous A, Pisoni GB, Hebert DN, Molinari M** (2015) N-linked sugar-regulated protein folding and quality control in the ER. *Semin Cell Dev Biol* **41**: 79–89
- Thompson JD, Higgins DG, Gibson TJ** (1994) CLUSTAL W: improving the sensitivity of progressive multiple sequence alignment through sequence weighting, position-specific gap penalties and weight matrix choice. *Nucleic Acids Res* **22**: 4673–4680
- Underwood W, Somerville SC** (2017) Phosphorylation is required for the pathogen defense function of the *Arabidopsis* PEN3 ABC transporter. *Plant Signal Behav* **12**: e1379644
- Vadassery J, Oelmüller R** (2009) Calcium signaling in pathogenic and beneficial plant microbe interactions: what can we learn from the interaction between *Piriformospora indica* and *Arabidopsis thaliana*. *Plant Signal Behav* **4**: 1024–1027
- Vadassery J, Ranf S, Drzewiecki C, Mithöfer A, Mazars C, Scheel D, Lee J, Oelmüller R** (2009) A cell wall extract from the endophytic fungus *Piriformospora indica* promotes growth of *Arabidopsis* seedlings and induces intracellular calcium elevation in roots. *Plant J Cell Mol Biol* **59**: 193–206
- Vadassery J, Reichelt M, Hause B, Gershenzon J, Boland W, Mithöfer A** (2012) CML42-mediated calcium signaling coordinates responses to *Spodoptera* herbivory and abiotic stresses in *Arabidopsis*. *Plant Physiol* **159**: 1159–1175
- Wachsman G, Modliszewski JL, Valdes M, Benfey PN** (2017) A SIMPLE pipeline for mapping point mutations. *Plant Physiol* **174**: 1307–1313

- Wang L, Albert M, Einig E, Fürst U, Krust D, Felix G** (2016) The pattern-recognition receptor CORE of Solanaceae detects bacterial cold-shock protein. *Nat Plants* **2**: 16185
- Wang T-J, Huang S, Zhang A, Guo P, Liu Y, Xu C, Cong W, Liu B, Xu Z-Y** (2021) JM17-WRKY40 and HY5-ABI5 modules regulate the expression of ABA-responsive genes in Arabidopsis. *New Phytol* **230**: 567–584
- Wang X, Hwang S-Y, Cong W-T, Jin L-T, Choi J-K** (2013) Phosphoprotein staining for sodium dodecyl sulfate-polyacrylamide gel electrophoresis using fluorescent reagent morin hydrate. *Anal Biochem* **435**: 19–26
- Wang Z, Li X, Wang X, Liu N, Xu B, Peng Q, Guo Z, Fan B, Zhu C, Chen Z** (2019) Arabidopsis endoplasmic reticulum-localized UBAC2 proteins interact with PAMP-INDUCED COILED-COIL to regulate pathogen-induced callose deposition and plant immunity. *Plant Cell* **31**: 153–171
- Wessel D, Flügge UI** (1984) A method for the quantitative recovery of protein in dilute solution in the presence of detergents and lipids. *Anal Biochem* **138**: 141–143
- Wu G, Liu S, Zhao Y, Wang W, Kong Z, Tang D** (2015) ENHANCED DISEASE RESISTANCE4 associates with CLATHRIN HEAVY CHAIN2 and modulates plant immunity by regulating relocation of EDR1 in Arabidopsis. *Plant Cell* **27**: 857–873
- Wu Y, Xun Q, Guo Y, Zhang J, Cheng K, Shi T, He K, Hou S, Gou X, Li J** (2016) Genome-wide expression pattern analyses of the arabidopsis leucine-rich repeat receptor-like kinases. *Mol Plant* **9**: 289–300
- Xie M, Sun J, Gong D, Kong Y** (2019) The Roles of Arabidopsis C1-2i subclass of C2H2-type zinc-finger transcription factors. *Genes* **10**: 653
- Xu P, Xu S-L, Li Z-J, Tang W, Burlingame AL, Wang Z-Y** (2014) A brassinosteroid-signaling kinase interacts with multiple receptor-like kinases in Arabidopsis. *Mol Plant* **7**: 441–444
- Yang C, Liu R, Pang J, Ren B, Zhou H, Wang G, Wang E, Liu J** (2021a) Poaceae-specific cell wall-derived oligosaccharides activate plant immunity via OsCERK1 during Magnaporthe oryzae infection in rice. *Nat Commun* **12**: 2178
- Yang H, Wang D, Guo L, Pan H, Yvon R, Garman S, Wu H-M, Cheung AY** (2021b) Malectin/Malectin-like domain-containing proteins: A repertoire of cell surface molecules with broad functional potential. *Cell Surf* **7**: 100056
- Yoo S-D, Cho Y-H, Sheen J** (2007) Arabidopsis mesophyll protoplasts: a versatile cell system for transient gene expression analysis. *Nat Protoc* **2**: 1565–1572
- Zhang X, Henriques R, Lin S-S, Niu Q-W, Chua N-H** (2006) Agrobacterium-mediated transformation of Arabidopsis thaliana using the floral dip method. *Nat Protoc* **1**: 641–646
- Zhang X, Wang D, Elberse J, Qi L, Shi W, Peng Y-L, Schuurink RC, Van den Ackerveken G, Liu J** (2021) Structure-guided analysis of Arabidopsis JASMONATE-INDUCED OXYGENASE (JOX) 2 reveals key residues for recognition of jasmonic acid substrate by plant JOXs. *Mol Plant* **14**: 820–828
- Zhang X, Yang Z, Wu D, Yu F** (2020) RALF-FERONIA signaling: linking plant immune response with cell growth. *Plant Commun* **1**: 100084

- Zhong R, Teng Q, Haghighat M, Yuan Y, Furey ST, Dasher RL, Ye Z-H (2017)** Cytosol-localized UDP-xylose synthases provide the major source of UDP-Xylose for the biosynthesis of xylan and xyloglucan. *Plant Cell Physiol* **58**: 156–174
- Zhou YP, Wu JH, Xiao WH, Chen W, Chen QH, Fan T, Xie CP, Tian C-E (2018)** Arabidopsis IQM4, a novel calmodulin-binding protein, is involved with seed dormancy and germination in Arabidopsis. *Front Plant Sci* **9**: 721: 721.

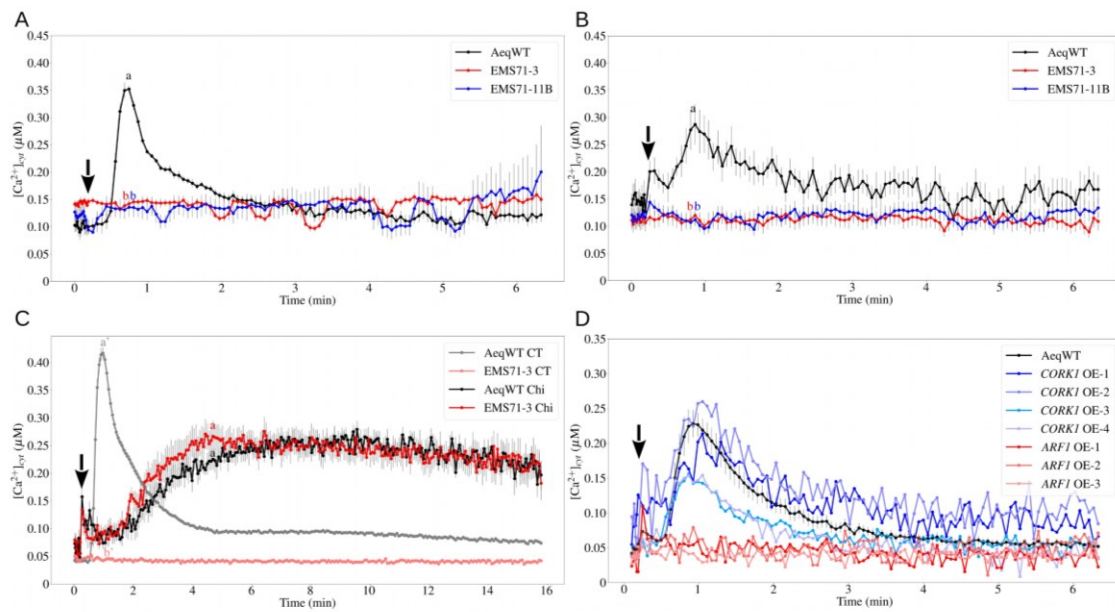


Figure 1. Identification of *CORK1* as COM receptor through EMS mutagenesis. A and B, Cytoplasmic calcium elevation by 10 μM CT in root (A) and leaf (B) tissues. Error bars represent SEs from at least 10 seedlings. C, Cytoplasmic calcium elevation by 10 μM CT or 10 μM chitohexaose (Chi) in root tissue. Error bars represent SEs from 8 seedlings. D, Cytoplasmic calcium elevation by 10 μM CT in leaf tissue of EMS mutant complemented with *CORK1* or *ARF1*. Error bars represent SEs from 12 seedlings for aequorin wildtype (AeqWT). Arrows indicate the onset of elicitor application. Statistical significance at the peak value was determined by Tukey's HSD test with $P < 0.05$, and is indicated by different lower-case letters. All experiments were repeated at least 3 times with similar results.

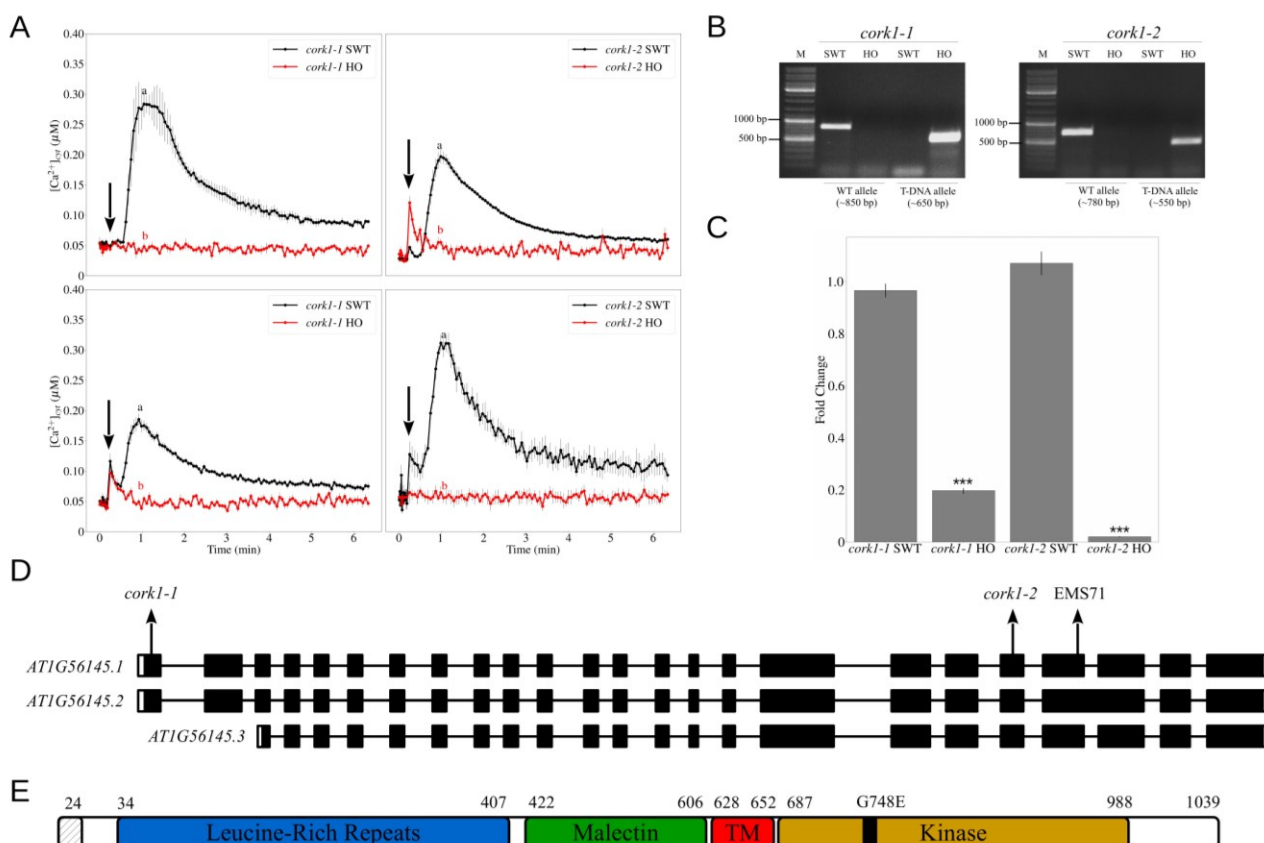


Figure 2. T-DNA mutants for *CORK1* do not respond to COM. **A**, Cytoplasmic calcium elevation by 10 μ M CT in root (upper panels) and leaf (bottom panels) tissues of T-DNA mutants crossed to aequorin wild-type. Error bars represent SEs from at least 5 seedlings. SWT/HO: segregated wild-type/homozygous mutant from the cross to aequorin wild-type. Arrows indicate the onset of elicitor application. Statistical significance at the peak value was determined by Tukey's HSD test with $P < 0.05$, and is indicated by different lower-case letters. The experiment was repeated at least 3 times with similar results. **B**, Genotyping of the SWT and HO seedlings. Wild-type allele is confirmed with the primer set LP and RP of the respective T-DNA insertion line. T-DNA allele is confirmed with the primer set LB_SALK and RP of the respective T-DNA insertion line. Annealing temperature for the PCR reactions is 58 $^{\circ}$ C. M: DNA marker (ladder); bp: base pair. **C**, *CORK1* expression in root tissue of SWT and HO seedlings. Error bars represent SEs from 3 independent biological replicates, each with 5 seedlings. Statistical significance was determined by Student's T-test based on Δ Cq values between the two genotypes (** $P < 0.001$). **D**, Gene model for *CORK1* (AT1G56145). Two T-DNA insertion mutants used in this study are named as *cork1-1* (SALK_099436C; N671776) and *cork1-2* (SALK_021490C; N674063). Position of the SNP induced by EMS mutagenesis is labeled as EMS71. Arrows indicate the approximate location of T-DNA insertions and SNP on the gene. **E**, Predicted protein structure of *CORK1*. Positions of amino acid residues are shown in numbers. The first 24 amino acids are predicted to be a signal peptide. G748E indicates the amino acid substitution from glycine to glutamate found in EMS71. TM: transmembrane domain.

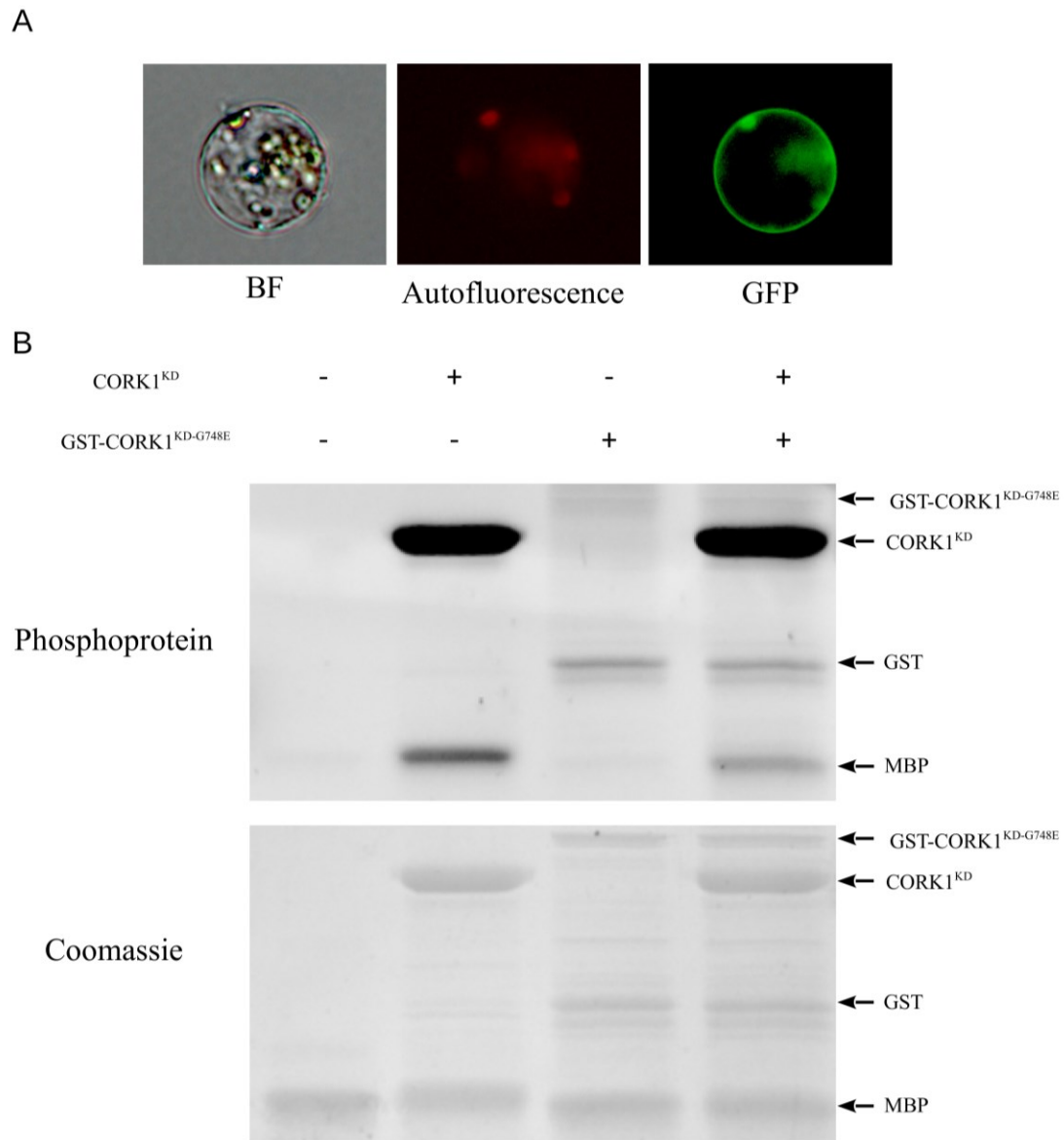


Figure 3. *CORK1* encodes a functional membrane-bound receptor kinase. **A**, Subcellular localization of GFP-tagged CORK1 in *Arabidopsis* mesophyll protoplast. BF: bright-field. **B**, Phosphorylation of the substrate MBP (myelin basic protein) by CORK1^{KD} but not by CORK1^{KD-G748E}.

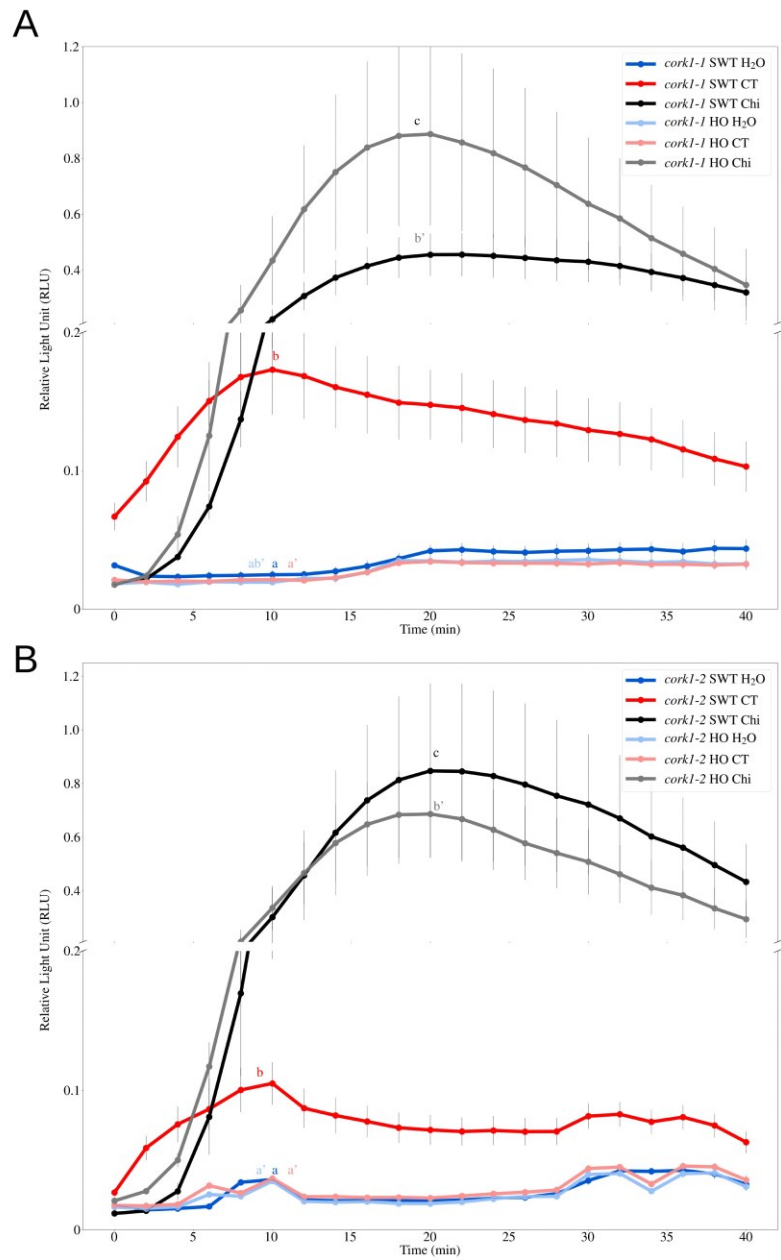


Figure 4. *cork1* mutants failed to induce ROS production upon COM perception. A and B, CT (10 μ M) triggers ROS production in root tissue in SWT but not in HO seedlings of *cork1-1* (A) and *cork1-2* (B). ROS production by application of 10 μ M chitohexaose (Chi) was not affected by the mutation. SWT/HO: segregated wild-type/homozygous mutant from the cross to aequorin wild-type. Error bars represent SEs from at least 6 seedlings for each treatment. Statistical significance at the peak value was determined by Tukey's HSD test with $P < 0.05$, and is indicated by different lower-case letters. The experiment was repeated 3 times with similar results.

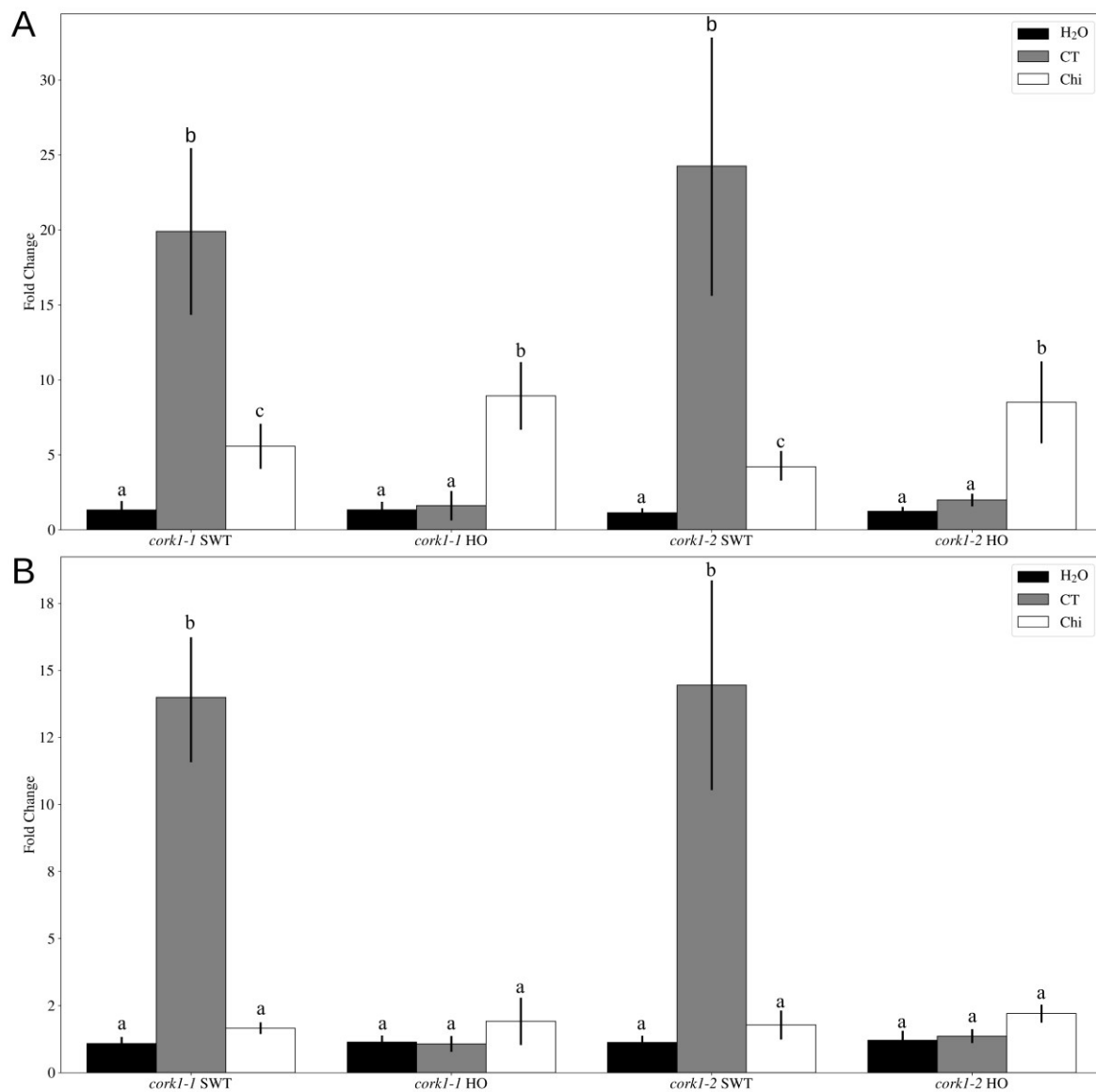


Figure 5. Up-regulation of *WRKY30* and *WRKY40* mRNA level in root tissue by COM is *CORK1*-dependent. A and B, *WRKY30* (A) and *WRKY40* (B) mRNA level 1 h after 10 μ M CT or 10 μ M chitohexaose (Chi) treatment in *cork1-1* and *cork1-2* SWT (segregated wild-type) and HO (homozygous mutant) from the cross to aequorin wild-type. Values were normalized to water treatment on the same genotype. Error bars represent SEs from at least 4 independent biological replicates, each with 16 seedlings. Statistical significance was determined by Tukey's HSD test based on ΔC_q values with p -value < 0.05, and indicated by different lower-case letters.

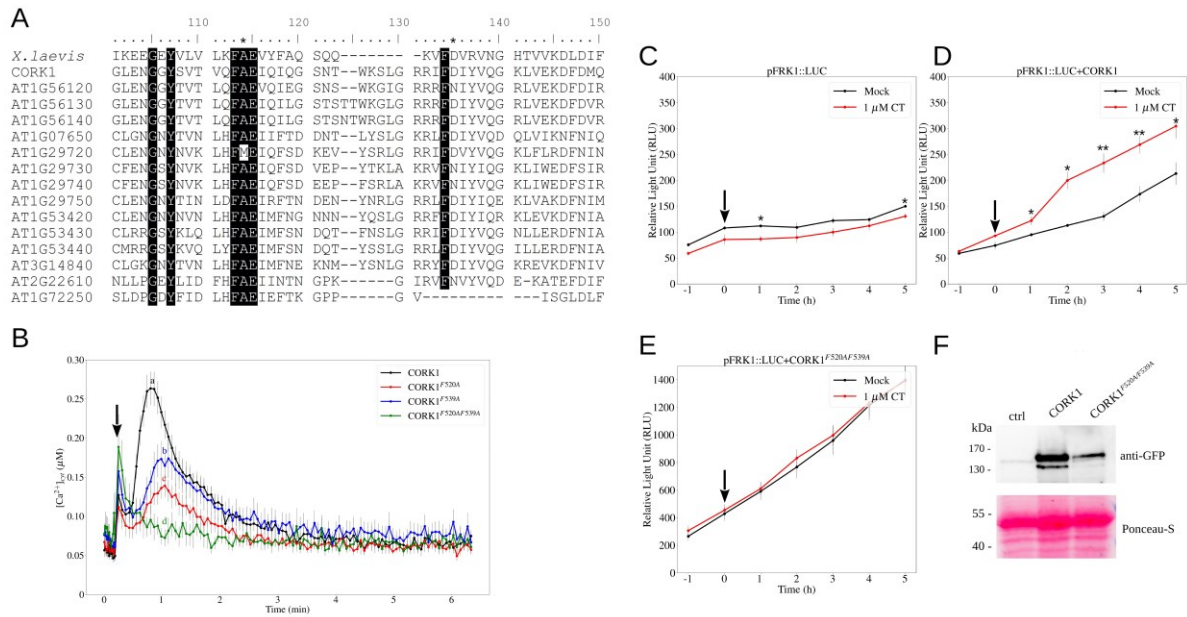


Figure 6. Two conserved phenylalanine residues in the malectin domain are important for COM perception. **A**, Alignment of the amino acid sequences from malectin of *X. laevis* and the malectin domains present in *A. thaliana* LRR-malectin RLKs. Shown here are amino acids from position 101-150 of the alignment. Black shade indicates conserved amino acid residues over 90% threshold. The two conserved phenylalanine residues are indicated with an asterisk. **B**, Cytoplasmic calcium elevation by 10 μM CT in leaf tissue of EMS71 complemented with CORK1, or with single (CORK1^{F520A}/CORK1^{F539A}) or double (CORK1^{F520AF539A}) mutation in the two conserved phenylalanine residues. Error bars represent SEs from 12 seedlings. Arrow indicates the onset of elicitor application. Statistical significance at the peak value was determined by Tukey's HSD test with $P < 0.05$, and is indicated by different lower-case letters. The experiment was repeated 3 times with similar results. **C-E**, Protoplasts from *A. thaliana* Col-0 were transfected with the pFRK1::Luciferase (pFRK1::LUC) reporter construct (**C**), or the reporter construct plus the CORK1 receptor (**D**), or the reporter construct plus the double mutated version CORK1^{F520AF539A} (**E**). Results show luciferin-dependent light emission over time after treatment with water (Mock) or 1 μM CT. Arrow indicates the onset of elicitor application at 0 h. Each data point represents the mean value from 4 technical replicates. Error bars represent SEs. Statistical significance was determined by Student's T-test between the two treatments (* $P < 0.05$; ** $P < 0.01$). The experiment was repeated 4 times with similar results. **F**, Western blot indicating the expression of both versions of GFP-tagged CORK1. ctrl: control, protoplast transfected with pFRK1::LUC reporter construct only.

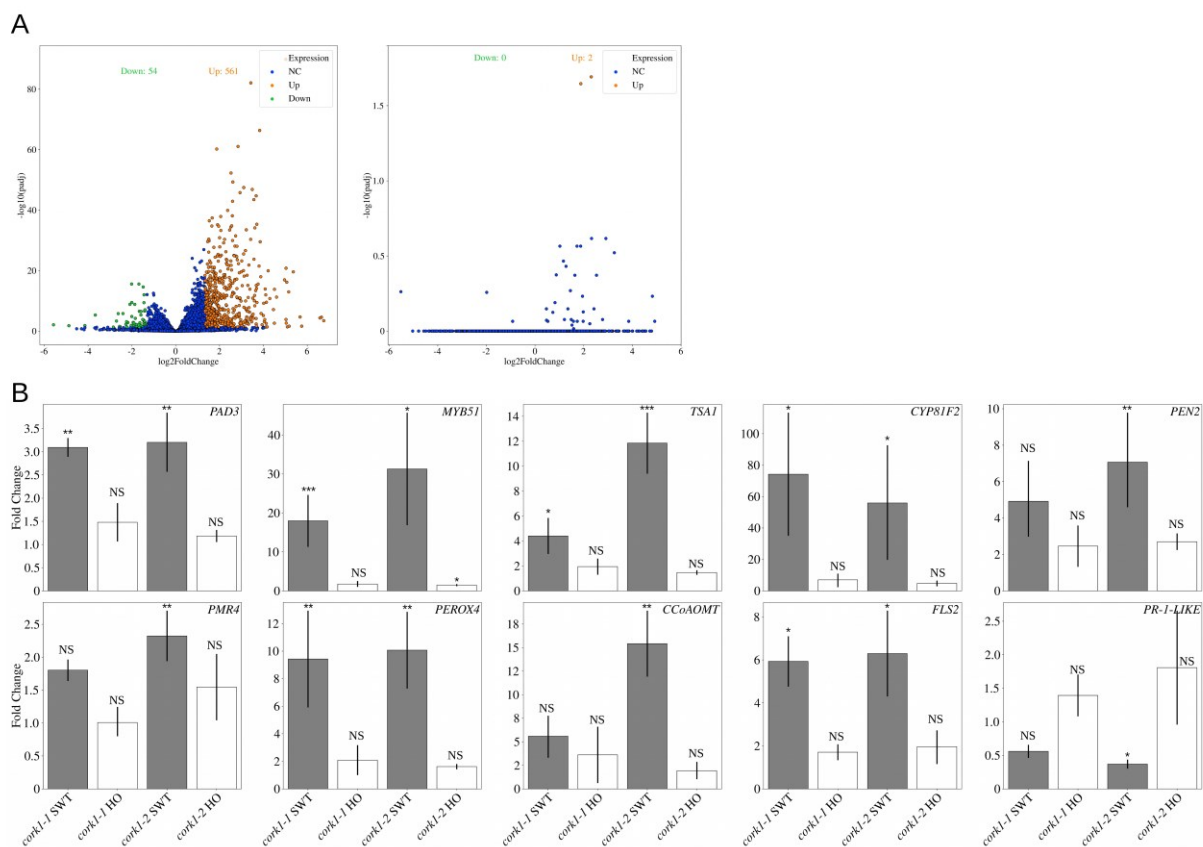


Figure 7. CT-regulated genes. A, Volcano plots showing the distribution of differentially expressed genes in root tissue. Left: 10 μ M CT treatment compared to water control in SWT. Right: 10 μ M CT treatment compared to water control in HO. NC: no change; Up: up-regulation; Down: down-regulation; padj: adjusted p-value using Benjamini and Hochberg method. The FDR cutoff value is set as 0.1. B, qPCR analysis of candidate genes regulated by 10 μ M CT in root tissue SWT and HO seedlings. Values were normalized to water treatment on the same genotype. SWT/HO: segregated wild-type/homozygous mutant from the cross of *cork1-2* to aequorin wild-type. Error bars represent SEs from 4 independent biological replicates, each with 16 seedlings. Statistical significance was determined by Student's T-test based on Δ Cq values (NS: not significant; *P < 0.05; **P < 0.01; ***P < 0.001).

Table 1. Differentially expressed candidate genes by 10 μ M CT compared to water control in root tissue of *cork1-2* segregated wild-type from the cross to aquorin wild-type.

Process	Accession No.	Annotation	log2FoldChange	padj	
Tryptophan biosynthesis	AT3G54640	<i>TSA1</i>	2.93	1.54E-46	
	AT5G05730	<i>ASAI</i>	3.83	4.27E-67	
	AT1G25220	<i>ASB1</i>	3.43	8.09E-83	
	AT5G46330	<i>FLS2</i>	1.93	6.18E-11	
	AT2G19190	<i>FRK1</i>	2.22	4.26E-15	
	AT4G23550	<i>WRKY29</i>	1.37	4.38E-10	
	AT1G18570	<i>MYB51</i>	3.67	1.76E-45	
	AT1G24100	<i>UGT74B1</i>	2.23	4.37E-31	
	AT5G57220	<i>CYP81F2</i>	3.59	8.92E-11	
	AT4G31500	<i>CYP83B1/SUR2</i>	2.79	8.38E-29	
Flagellin perception/callose deposition/wall thickening/indolic glucosinolate biosynthesis	AT1G59870	<i>ABCG36</i>	1.46	2.00E-09	
	AT2G44490	<i>PEN2</i>	0.89	2.35E-07	
	AT4G03550	<i>PMR4</i>	0.73	2.97E-04	
	AT3G26830	<i>CYP71B15/PAD3</i>	1.89	3.08E-04	
	AT1G55020	<i>LOX1</i>	1.87	5.91E-61	
	AT1G17420	<i>LOX3</i>	3.53	2.31E-06	
	AT1G72520	<i>LOX4</i>	2.44	1.69E-18	
	AT1G74100	<i>SOT16</i>	2.52	3.37E-35	
	AT1G18590	<i>SOT17</i>	2.78	2.18E-25	
	AT2G37040	<i>PAL1</i>	1.55	2.79E-15	
Phenylpropanoid metabolism/biosynthesis	AT2G30490	<i>C4H</i>	1.65	1.75E-20	
	AT1G51680	<i>4CL1</i>	2.08	7.53E-26	
	AT1G67980	<i>CCOAOMT</i>	3.67	6.47E-05	
	AT4G34230	<i>CAD5</i>	1.60	6.77E-10	
	AT1G14540	<i>PER4</i>	2.44	1.93E-22	
	AT5G24110	<i>WRKY30</i>	3.29	7.20E-16	
	AT1G80840	<i>WRKY40</i>	2.75	6.59E-09	
	AT2G19990	<i>PR-1-Like</i>	-2.62	1.59E-06	
	Camalexin biosynthesis				
Jasmonic acid biosynthesis					
Glucosinolate biosynthesis					
Leaf senescence					
ABA signaling					
Plant-pathogen interaction					

Table 2. Candidate proteins with significant alteration in phosphorylation upon 10 μM CT treatment compared to water control in root tissue of *cor1.2* SWT. Numbers in the parentheses indicate the probability of the modification on the amino acid residue. Calculation for the corrected fold change and the ratio-adjusted p-value is described in the Materials and Methods section. SWT: segregated wild-type from the cross to aquorin wild-type

Comparison	UniProt accession No.	Annotation	Peptide Sequence	Modifications	Modifiers in Proteins	Corrected Fold Change	Ratio-adjusted p-value
5 minutes	Q9XIE2	ABCG36	RTQSVNDDEEALK	1xPhospho [S4(100)]	Q9XIE2 1xPhospho [S45(100)]	10.64	1.74E-02
	Q9XIE2	ABCG36	IQSVNDDEEALK	1xPhospho [S3(100)]	Q9XIE2 1xPhospho [S45(100)]	6.97	8.76E-03
	Q9XIE2	ABCG36	NIEDFFSSGSR	1xPhospho [S10(99.4)]	Q9XIE2 1xPhospho [S40(99.4)]	4.32	9.41E-03
	Q9XIE2	ABCG36	NIEDFFSSGRR	1xPhospho [S10(99.7)]	Q9XIE2 1xPhospho [S40(99.7)]	2.50	4.26E-04
	Q9FL69	AGD5	MESAAIPVER	1xPhospho [T6(100)]	Q9FL69 1xPhospho [T206(100)]	17.18	1.18E-02
	Q9CG36	At1g45688	TDSEV TSLAASSTFAKSR	2xPhospho [S12(100); S16(100)]	Q9CG36 2xPhospho [S16(100)]; S20(100)]	2.36	4.08E-02
	Q9CG36	At1g45688	TDSEV TSLAASSTFAKSR	1xPhospho [S16(100)]	Q9CG36 1xPhospho [S20(100)]	2.24	2.01E-02
	F4HSU2	At2g32240	DIDL SFSPTKR	1xPhospho [S8(99.6)]	F4HSU2 1xPhospho [S1274(99.6)]	5.71	3.55E-03
	F4HSU2	At2g32240	SRDIDL SFSPTK	1xPhospho [S10(100)]	F4HSU2 1xPhospho [S1274(100)]	3.28	8.22E-03
	F4HSU2	At2g32240	DIDL SFSPTK	1xPhospho [S8(99.7)]	F4HSU2 1xPhospho [S1274(99.7)]	2.80	1.80E-02
	Q94L10	CESA3	RLPYSSDYNQSPNR	1xPhospho [S1(100)]	Q94L10 1xPhospho [S176(100)]	2.80	3.76E-03
	Q38868	CPK9	AAAAAAGLSR	1xPhospho [S9(100)]	Q38868 1xPhospho [S69(100)]	4.10	6.33E-03
	F4HM1	CSH1	MHDSPPPTHTTK	1xPhospho [T8(100)]	F4HM1 1xPhospho [T37(100)]	6.28	2.56E-02
	Q9FMM3	EXA1	VLSPPVTAQSHK	1xPhospho [S4(99.6)]	Q9FMM3 1xPhospho [S1553(99.6)]	4.87	3.21E-04
	Q9LJM0	FAB1B	VAYVPALPSK	1xPhospho [S6(100)]	Q9LJM0 1xPhospho [S132(100)]	15.97	4.24E-04
	Q9SCZ4	FER	TGPTLDHHTVTVVK	1xPhospho [S11(99.2)]	Q9SCZ4 1xPhospho [S695(99.2)]	6.69	4.92E-03
	O64851	IQM4	FPSPYGIPSPRSPR	2xPhospho [S10(100); S14(100)]	O64851 2xPhospho [S505(100); S509(100)]	921.45	2.27E-03
	F4VYX1; O64851	IQM4	LAYMGIPSPR	1xOxidation [M4]; 1xPhospho [S8(100)]	F4VYX1 1xPhospho [S520(100)]; O64851 1xPhospho [S525(100)]	45.79	1.31E-05
	Q9FF6	JOX2	SHVESHSR	1xPhospho [S8(100)]	Q9FF6 1xPhospho [S369(100)]	4.19	2.42E-04
	F4HRJ4	MAPKK3	VASTSLPK	1xPhospho [T/S]	F4HRJ4 1xPhospho [T/S]	2.32	1.68E-02
	B3H653	MPK3	EATNLIPSR	1xPhospho [S8(100)]	B3H653 1xPhospho [S16(100)]	17.07	1.53E-02
	Q39026	MPK6	VTSEDFMTEYVTR	1xOxidation [M8]; 1xPhospho [Y11(100)]	Q39026 1xPhospho [Y223(100)]	239.27	4.67E-03
	Q39026	MPK6	VTSEDFMTEYVTR	1xPhospho [T9(100)]	Q39026 1xPhospho [T221(100)]	29.15	3.22E-03
	P28187	RABA5C	QLNSDYKEELTVNR	1xPhospho [S6(100)]	P28187 1xPhospho [S186(100)]	2.21	2.47E-02
	Q9FT10	RHOH	ILSQLSQK	1xPhospho [S7(100)]	Q9FT10 1xPhospho [S347(100)]	-29.59	3.20E-03
	Q94F62; Q94AG2	SERK1	DTHTVAVR	1xPhospho [T6(99.5)]	Q94F62 1xPhospho [T450(99.5)]; Q94AG2 1xPhospho [T463(99.5)]	15.22	8.50E-04
	Q39233	SY21	MSFDLEAGTRSPAPNR	1xMet-loss+Acetyl [N-Term]; 1xPhospho [S12(99.2)]	Q39233 1xMet-loss+Acetyl [N-Term]; 1xPhospho [S12(99.2)]	65.82	1.67E-04
	ASMQL1	TRAF1B	STAVLSSPR	1xPhospho [S6(100)]	ASMQL1 1xPhospho [S716(100)]	9.72	1.53E-04
	F4KHL8	UX53	QNTTKPPSPPLR	1xPhospho [S9(100)]	F4KHL8 1xPhospho [S311(100)]	3.13	4.96E-03
	Q39160	XI-1	AGATGSITPR	1xPhospho [T9(100)]	Q39160 1xPhospho [T1195(100)]	5.97	2.31E-02
	Q9FL69	AGD5	MESAAIPVER	1xPhospho [T6(100)]	Q9FL69 1xPhospho [T206(100)]	16.41	6.12E-05
	F4HSU2	At2g32240	DIDL SFSPTKR	1xPhospho [S8(99.6)]	F4HSU2 1xPhospho [S1274(99.6)]	5.71	3.55E-03
	At2g32240	At2g32240	DIDL SFSPTKR	1xPhospho [S8(99.6)]	F4HSU2 1xPhospho [S1274(99.6)]	5.40	4.15E-02
	F4HSU2	At2g32240	DIDL SFSPTK	1xPhospho [S8(99.7)]	F4HSU2 1xPhospho [S1274(99.7)]	4.42	2.98E-02
	Q38868	CPK9	AAAAAAGLSR	1xPhospho [S9(100)]	Q38868 1xPhospho [S69(100)]	5.02	1.51E-02
	Q9FHK4	EDR4	SLQLEGGGR	1xPhospho [S1(100)]	Q9FHK4 1xPhospho [S322(100)]	5.44	7.39E-03
	Q9FMM3	EXA1	MTTSSHPSPVPTQK	1xPhospho [S10(100)]	Q9FMM3 1xPhospho [S1449(100)]	43.54	1.45E-02
	F4VYX1; O64851	IQM4	LAYMGIPSPR	1xPhospho [S8(100)]	F4VYX1 1xPhospho [S520(100)]; O64851 1xPhospho [S525(100)]	844.25	6.30E-05
	F4VYX1; O64851	IQM4	LAYMGIPSPR	1xOxidation [M4]; 1xPhospho [S8(100)]	F4VYX1 1xPhospho [S520(100)]; O64851 1xPhospho [S525(100)]	99.10	1.57E-03
	O64851	IQM4	FPSPYGIPSPRSPR	2xPhospho [S10(100); S14(100)]	O64851 2xPhospho [S505(100); S509(100)]	355.82	3.33E-05
	Q84M93	MPK17	LEHNDDEEHNSPPHQR	1xPhospho [S13(100)]	Q84M93 1xPhospho [S397(100)]	51.33	5.67E-03
	B3H653	MPK3	EATNLIPSR	1xPhospho [S8(100)]	B3H653 1xPhospho [S16(100)]	196.12	3.60E-02
	Q39026	MPK6	VTSEDFMTEYVTR	1xPhospho [T9(100)]	Q39026 1xPhospho [T221(100)]	33.63	6.00E-04
	Q9LM33	MPK8	HHAASLR	1xPhospho [S4(100)]	Q9LM33 1xPhospho [S495(100)]	-3.12	8.53E-03
	Q9LRP1	NPSN13	ELKDEEARNSEVVK	1xPhospho [S10(100)]	Q9LRP1 1xPhospho [S74(100)]	-184.99	1.13E-02
Q93YL5	SFC8	ASQHDINTPR	1xPhospho [T8(100)]	Q93YL5 1xPhospho [T482(100)]	88.63	1.71E-02	
ASMQL1	TRAF1B	STAVLSSPR	1xPhospho [S6(100)]	ASMQL1 1xPhospho [S716(100)]	-3.01	2.55E-02	
F4KHL8	UX53	QNTTKPPSPPLR	1xPhospho [S9(100); T/S]	F4KHL8 1xPhospho [S311(100)]	4.48	1.22E-02	
Q9SN95	UX55	QTSPPSPSPPIR	2xPhospho [S9(100); T/S]	Q9SN95 2xPhospho [S15(100); T/S]	3.13	1.18E-02	
P93043	VPS41	REDNRSFSQSR	1xPhospho [S8(99.7)]	P93043 1xPhospho [S860(99.7)]	351.09	7.54E-03	
Q9G289	ZAT10	MALEALTSR	1xMet-loss+Acetyl [N-Term]; 1xPhospho [S8(100)]	Q9G289 1xMet-loss+Acetyl [N-Term]; 1xPhospho [S8(100)]	2765.33	1.77E-04	


```

      10      20      30      40      50
X.jaervis -MLSIRTVLG PLATILLTVL GPGAHGSGL ADKVIWAVNA GGESHVDVHG
CORK1     FNFFVNCGR DIRSS---SG ALYEKDEGAL GPATFFVSK- TQRWAVSNVG
AT1G56120 YNFSINCGR EIRSV---SG ALFEKEDADL GPASFVVA- AKRWAASSVG
AT1G56130 SDFSINCGR EKRVS---TG ALFEREDEDL GPASFVVA- GQRWAASSVG
AT1G56140 SDFSINCGR EIRSV---TE AVFEREDEDL GPASFVVA- GQRWAASSVG
AT1G07650 YKLYINCGR EVKVDKEIT- --YQADDEPK G-ASMYVLGA NKRWALSSTG
AT1G29720 RFLHINCGR EVSIRNSLKG ITYQTDNSRQ TNAASNQ-- FDYWGVSNTG
AT1G29730 RSLHINCGR DVTIENSRRGR FLYEGDNYGL TGSATNYY-- RKNWGSNTG
AT1G29740 RSLHINCGR DVTIENSRRGR FLYEGDNYGL TGSATNYY-- GKNWGSNTG
AT1G29750 SCLHVNCGGS DMYVKEKTKK ELYEGDGNVE GGAAKYFLKP DANWGFSSSTG
AT1G53420 NALHINCGR EMSIN---G TIYESDKYDR LESWYESR-- -NGWFSNNVG
AT1G53430 SSLFINCGR RLKIG---K DTYTDDLNSR QSTFSSVS- -ERWGYSSSG
AT1G53440 SSLFINCGR RLKVD---K DEYADDLNKR GASTFSSVS- -ERWGYSSSG
AT3G14840 YGLHINCGR EITSN---E TKYDADTWDT PG-YYDSK-- -NGWVSSNTG
AT2G22610 TIMFINAGGD DSKVL----- DSELNISRDD
AT1G72250 PVISINSGSI STDVT----- VEDVTFLKDE

      60      70      80      90     100
X.jaervis IHYRKDPLEG RVGRASDYGM KLPILRSNPE DQVLYQTERY NEDSFGNDIP
CORK1     LFTGNSNQY IALSATQ--- ----FANTS DSELFQSARL SASSLRNYGL
AT1G56120 NFAGSSNNIY IATSLAQ--- ----FINTM DSELFQSARL SASSLRNYGL
AT1G56130 LFAGSSNNIY IATSQSQ--- ----FVNTL DSELFQSARL SASSVRNYGL
AT1G56140 LFAGSSNNIY ISTSQSQ--- ----FVNTL DSELFQSARL SASSLRNYGL
AT1G07650 NFMDDDDAD EYTVQNTS-- R-LSVNASSP SFGLYRTARV SPLSLTYGI
AT1G29720 DFTDDNSDHD EYTTSTN--- ----LTLSDG YPDLYKTARR SALSVMYAF
AT1G29730 DFMDAITED TYTVSSE--- ----SAVSAK YPDLYQNARR SPLSLMYAF
AT1G29740 DFMDAITED TYTVSSE--- ----SAVSAK YPDLYQNARR SPLSLMFAI
AT1G29750 DFMDNN--- ----FQNTR-- F-TMFVPASN QSDLYKSARI APVSLTFHA
AT1G53420 VFDVDDKHPVE RVTIESNS-- SELNV---V DFLGYTQARI SAI SLTYAL
AT1G53430 VFTGKEDAGY LATDRFN--- ----LINGS TPEYYKTARL SPQSLKMYGL
AT1G53440 AWLGNMGATY LATDTFN--- ----LINES TPEYYKTARL ASQSLKMYGL
AT3G14840 NFLDDDRTNK GSKWSNS-- SELKITNSSI DFRLYTQARL SAI SLTYAL
AT2G22610 YFEGGDVLR T EESIVEA--- ----GD FPFYQYARV G--NFCMQLN
AT1G72250 FFSGGESI-T TDAVVG--- ----ED EILLYQTARL G--NFAKFKQ

      110     120     130     140     150
X.jaervis IKEBGEVVLV LKFABVYFAQ SQQ----- -KVFDRVNG HTVVKDLDF
CORK1     GLENGGTSVT VQFABIQIQG SNT--WKS LG RRFEDIYVQG KLVEKDFDMQ
AT1G56120 GLENGGTVT LQFABVQIEG SNS--WKG LG RRFEDIYVQG RLVEKDFDIR
AT1G56130 GLENGGTVT LQFABIQILG STSTTWKLG RRFEDIYVQG RLVEKDFDVR
AT1G56140 GLENGGTVT LQFABIQILG STSNTWRGLG RRFEDIYVQG RLVEKDFDVR
AT1G07650 CLGNNTVTN LHFABIIFTD DNT--LYSLG KRIFDIYVQD QLVIKNFNIQ
AT1G29720 CLENGNNTVK LHFABIQFSD KEV--YSRLG RRFEDIYVQG KLFLRDFNIN
AT1G29730 CFENGSNVVK LHFABIQFSD VEP--YTKLA KRVENIYIQG KLIWEDFSIR
AT1G29740 CFENGSNVVK LHFABIQFSD EEP--FSRLA KRVENIYVQG KLIWEDFSIR
AT1G29750 CLENGNTIN LDFABIRFTN DEN--YNRLG RRFEDIYIQE KLVAKDFNIM
AT1G53420 CLENGNNTN LHFABIMFNG NNN--YQSLG RRFEDIYIQE KLEVDFNIA
AT1G53430 CLRRGSYKLQ LHFABIMFSN DQT--FNSLG RRFEDIYVQG NLLERDFNIA
AT1G53440 CMRRGSYKQ LHFABIMFSN DQT--YSSLG RRFEDIYVQG ILLERDFNIA
AT3G14840 CLGKNTVTN LHFABIMFNE KNM--YSNLG RRFEDIYVQG KREKDFNIV
AT2G22610 NLLPGEMLID FHFABIINTN GPK-----G IRVENVYVQD E-KATEFDIF
AT1G72250 SLDPGDFID LHFABIEFTK GPP-----G V----- ---ISGLDLF

      160     170     180     190     200
X.jaervis DRVGHSTAHD EIIPISIKKG KLSVQGEVST FTGKLSVEFV KGYDNPVKC
CORK1     KAANGSSIRV IQRVYKANVS ENYLEVHLFW AGKGTCCIPA QGTYG-PLVS
AT1G56120 RTAGGSSVRA VQREYKTNVS ENHLEVHLFW AGKGTCCIP I QGAYG-PLIA
AT1G56130 RTAGDSTVRA VQRVYKANVS ENHLEVHLFW AGKGTCCIP I QGAYG-PLIS
AT1G56140 RTAGDSTVRA VQREYKANVS QNHLEIHLFW AGKGTCCIP I QGAYG-PLIS
AT1G07650 EAARGSGKPI IKSP-L-VNVT DHTLKIQLR AGKGTGPII RGVY-PMIS
AT1G29720 KEANGMKPV IKEIN-ATVT NHMLEIRLYW AGKGTTLIPK RGVY-PLIS
AT1G29730 EEANGTHKEV IREVN-TTVT DNTLEIRLYW AGKGTMIIPQ RGVY-SLIS
AT1G29740 EEANGTHKEV IKEVN-TTVT DNTLEIRLYW AGKGTTLIPK RGVY-SLIS
AT1G29750 DEAKGAQTP I IKPLT-AVVT NHFLTIRLW AGKGTTRIP T RGVY-PIIS
AT1G53420 KEAKDVGNV IKTFF-VEIK DGKLEIRLYW AGKGTVIPK ERVY-PLIS
AT1G53430 ERAGGVGKPF IRQIDGVQVN GSTLEIHLQW TGRGTNVIPT RGVY-PLIS
AT1G53440 QRAGGVGKPF LRQVDEVQVN GSTLEIHLQW TGRGTNVIPT RGVY-PLIS
AT3G14840 DEAKGVKAV VKKFP-VMVT NGKLEIRLQW AGKGTQAIPT RGVY-PLIS
AT2G22610 SVVGANRPLL LVDLR----- -VMV MDDGLIRVRF EGINSPVVC
AT1G72250 SQVGANTPLV IEDLR----- -MLV GRBGEISIRL EGVTAAILC

```

```

                210          220          230          240          250
X.Jaevis  ALFIMKGTAD DVPMLQPHG LEKKEEEEE EEEEGSTSKK QINKNRVQSG
CORK1    AI-----
AT1G56120 AV-----
AT1G56130 AV-----
AT1G56140 AV-----
AT1G07650 AI-----
AT1G29720 AI-----
AT1G29730 AV-----
AT1G29740 AI-----
AT1G29750 AI-----
AT1G53420 AI-----
AT1G53430 AI-----
AT1G53440 AI-----
AT3G14840 AV-----
AT2G22610 GI-----
AT1G72250 GI-----

                260          270          280
X.Jaevis  PRTPNPYASD NSSLMFPILV AFGVFIPTLF CLCRL
CORK1    -----
AT1G56120 -----
AT1G56130 -----
AT1G56140 -----
AT1G07650 -----
AT1G29720 -----
AT1G29730 -----
AT1G29740 -----
AT1G29750 -----
AT1G53420 -----
AT1G53430 -----
AT1G53440 -----
AT3G14840 -----
AT2G22610 -----
AT1G72250 -----

```

Supplementary Figure S1. Alignment of malectin domains (MD) in *A. thaliana* and the malectin in *X. laevis*. Black shade indicates conserved amino acid residues over 90% threshold.

```

      10      20      30      40      50
X.laevnis ---MLSIRT VLGPLATILL TVLGPFGAHG SGLADKVIWA
CORK1 VNAGGESHV D-----
AT1G29750 -----
AT1G53430 -----
AT1G56120 -----
AT1G07650 -----
AT1G29720 -----
AT1G56140 -----
AT1G56130 -----
AT1G53440 -----
AT1G29740 -----
AT3G14840 -----
AT1G53420 -----
AT2G22610 -----
AT1G29730 -----
AT1G72250 -----
AT1G51860 LDCGLVPKET -TYTEKSTNI TYKSDVDYID SGLVKGINDA YKTQF----Q
AT3G46240 IDCGLSLPGV D----NNNL KVVGDQDFIT SG-DSATISS TTVEK-----
AT2G23200 VNCGSDSNVF YGGQTFVGD T NSSTNSVSFT NKGTEVINDQ SSVAP-----
AT2G14440 LYCGLP SNES -PYIEPLTNL TYISDVNFVR GGKTGNIKNN SDIDF---TS
AT1G30570 VDCGS-NATT EV-DGRTWVG DLSPNKSVTL QGPDAITAST ----SKGSS
AT3G05990 IDC GAS-SSS V----IDGR QWQPDETFVS SG-TPKNVSD QVLDE----
AT3G46420 VDCGLS PNEV SPYIEPFTGL QFTTDSNFIE TGKLGRIQAS LEPKY----R
AT1G25570 IDC GSPE-TS ----TDVFN R TWLPDQFYSG GSTAVVSEPL RFHLI-----
AT3G46370 -----
AT3G46270 IDC GTTGSYV D----SNNV TWVGDKG FVT TG-ESINIT- DVTTK-----
AT4G39110 IDC GSKSSSK TP-DGRVFKS DQET--IQYI EAKEDIQVSA ---PPSDKVA
AT1G07560 LDCGLQADES -PYTEPLTKL TFTSDADF I KSGKSGKI QNV PGM EY---I-
AT1G51820 VDCGLS LLES -PYDAPQTGL TYTSDADLVA SGKTGR LAKE FEPLV---D
AT1G24485 IDC GSSSSH I D----ADNR TWVGD TDFVA TGLTSKFVFP SKFPA-----
AT5G39030 INCG-ETDVP FDNHGR TW TQ EEK---NILP KNSDN-ASFS SVVSYKEESG
AT3G46290 INCGS-PTNG TL-MGRI FLS DKLS--SKLL T---SSKEIL ---ASVGGN
AT5G61350 IDC GSSDETK LS-DGRNFKS DQOS--VAF L QTDEDIKTSV DSIPI TDSNA
AT1G51805 VDCGLL PRDS -PYNALGTGL VYTS DVGLVS SGKTGR LAKE FEENN---S
AT5G59660 LDCGLPANEL SPYEE SFTGL RFSSDEK FIR SGKNGR IREN -PQG---YA
AT5G39000 FNCG-DTSNN VDVSGRNWTA ENQ---KILS SNLVN-ASFT AQASYQE-SG
AT3G04690 LSCG-TSEAS ADQDKKKWEP DTK---FLK T--GN--SIH ATATYQDPSL
AT1G51790 IDC GLQPENS -SYTETSTDI KYVSDSSYTD TGTSYFVAPE NRQN---MK
AT5G28680 LSCG-ASEPA VDQDKKKWEP DTK---FLK T--PN--TVH APATYQDPSL
AT2G19190 IDC GI-PDDS -SYNDETTGI KYVSDSAFVD SGTTRKRI AQ FQSSG---FD
AT2G04300 LDCGLS PNEP -PYVDAATDL TYTTDNDVFQ SGKTGTIDKE LESTY---N
AT5G59680 LDCGLPANEL SPYTEPRTGL QFSSDAAFIQ SGKIGRIQAN -LEAD---FL
AT2G19210 IDC GI-PEDS -SYNDETTDI KYVSDAAFVE SGTIHSIDPE FQTSS---LE
AT1G51890 LDCGLVPT E I -TYVEKSTNI TYRSDATYID SGVPGKINEV YRTQF----Q
AT1G51880 LDCGLVPKNA -TYTEKTTNI TYKSDANYID SGLVGRISAE YKAQL----Q
AT5G59616 -----
AT2G28970 LDCGFPIEES -PYSDFSTGL TFTSDSTFIQ TGESGRVDKE -LNKI---FR
AT5G54380 ISCGS-SQNI TF-QNRIFVP DSLH--SSLV LKIGNSSVAT ----STTSNN
AT5G48740 LSCGGSYTA -----AYNI SWVSDNDYIE TGNTT VTYA EGNST-----
AT2G28960 LDCGLPVNES -PYTDPRTGL TFSSDADFIL SGLRGEAGDD NT-----YIY
AT3G21340 LDCGLS PNEP -PYNDPSTGL TYSTDGDFVQ SGKTGR I QKA FESIF----S
AT3G46280 IDC GSTGSYV D----SNNV TWVGDKG FVT NG-EPMKIP- DVVKK-----
AT3G46260 IDC GTTGSYV D----SNNV TWVGDKG FVT TG-ESINIT- DVVKK-----
AT1G05700 IDC GI-PSGS -SYKDDTTGI NYVSDSFEVE TGVS KSI PPT AQ-----
AT3G46400 LDCGLS PNEQ SPYVELETGL QFLSDSSFIQ SGKIGRIDAS LESKY---P
AT5G38990 INCG-DTSNN MDYSGRNWTT ENP---KFMS SNAVDDASFT SSASYQE-SG
AT1G51800 LDCG-SPRET -SFREKTTNI TYISDANFIN TGVGGSIKQG YRTQF----Q
AT5G24010 INSGSNTNTS FF-TTRSFLS DSSEPGSSFL STDRSISISD ----TNPS P
AT2G28990 LDCGLPSDES -PYDDSFNGL TFTSDSTFIQ TGKIDSVDKD -LNIN---LS
AT4G20450 LDCGMPRNES -SYTDESTGL NFSSDADPIS SGKSGTIKTE DSDSGV-KYI
AT1G49100 LDCGLLPDGS -PYTNPSTGL TFTSDSSFIE SGKNGRVSKD SERNF---E
AT4G29450 IDC GI-PPYD -TPEDMTINI NYVDEAFIT TGVNFKVS EE YGYPKNPVLL
AT1G51840 VDCGLS PPEP -PYNAPQTGL TYTSDTGLIN TGKTGR IAKD FEPFV---D
AT5G59670 LDCGLPANEL SPYTETQTGL LFSSDATFIQ SGKTGRVQAN -QESK---FL
AT1G51850 VDCGLAPRES -PYNEAKTGL TYTSDDGLVN V GKPGRIAKE FEPLA---D
AT5G59700 INCGS-STNV TV-TSRVFIS DNLA--SNFL T---SPNEIL ----AASN RN
AT2G19230 IDC GI-PEDS -SYVDEKTDI KYISDAARVE SGTIHSIDSK FQKKN--LE
AT1G51870 LDCGLVPKET -TYVETSTNI TYKSDANYTD SGLVKGINDA HKTIV---Q
AT3G46330 LDCGLPLNEP -PYIESETGI QFSSDENFIQ SGKTGRIPKN -LESE---NL
AT2G29000 LDCGLPAKES -PYTESTTSL VFTSDANFIS SGISTKLPKH DD-----Y
AT3G46350 LDCGLAPTEP SPYTEPVTTL QYSSDSNFIQ SGKLGRI DTS LQTFE----L
AT2G37050 LDCG---GA EPFTD-ELGL KWSPDNHLIY -GETANISSV NETRT----
AT1G07550 LDCGLASNES -PYNEANSNL TYISDADFIQ GGKTGNVQKD LLMKL---R-
AT1G51810 LDCGLSIQGS -PYKESSTGL TYTSDGDFVQ SGKIGKITKE LESLY---K
AT4G29990 IDC GI-PDDS -SYTDEKTNM KYVSDLFVE SGTSHSIVSD LQTT S---LE
AT5G59650 LDCGLPMTEP SSYTESVTGL RFSSDAEFIQ TGESGKI QAS -MEND---YL
AT1G28340 ISCGARKNVR ----TPPTYA LWFKDIA YTG VGPANATTP T -YITP-----

```

AT3G51550	LNCGGGASNL	TTDNRIWIS	DVKS--KFLS	SSSED--SKT	SPALTQD-PS
AT2G21480	IDCGSKSSTK	TP-EGRVFKS	DSET--VQYI	EAKDDIQVSA	---PPSKLP
AT5G16900	LDCGLPSNEP	-PYIEPVTGL	VFSSDADHIP	SGISGRIQKN	-LEAV---HI
AT1G67720	IDCG----CS	SNYTDPRTGL	GWVSDSEI IK	QGKPVTLANT	NWNSM-----
AT3G19230	LNCGSS--SST	N-----LNEI	EYTPDEGFIS	VG-NTTTIKQ	KDLVP-----
AT1G51830					
AT5G39020	FNCG-DTSNN	VDNSGRNWTV	ESR---QILS	SNLVN-ASFT	SEASYQK-AG
AT4G00300	VNCGSDVDST	VD-NRR-FVG	DASSNVQFF	SSEGSIALKG	-----ENLPQ
AT4G29180	IDCGS-PPNI	-NYVDTDGTI	SYTDAPFIN	AGVNLNVSEE	YGPKNPVL P
AT1G51910	LDCGLIPKDT	-TYTBEQITNI	TYISDADYID	SGLTERISDS	YKSQL----Q
AT3G46340	LDCGLPPNEV	SPYIEPFTGL	RFSSDSSFIQ	SGKIGKVDKS	FEATT----L
AT2G14510	LDCGLPSKES	--YIEPSSNL	TFISDVNFIR	GGKTGNIQNN	SRTNF----IF

	60	70	80	90	100
X.Jaervis
VHGIHYRKDP	-----	---LEGRVG	RASDYGMKLP	ILRSNPE--	
CORKI	D-----				
AT1G29750					
AT1G53430					
AT1G56120					
AT1G07650					
AT1G29720					
AT1G56140					
AT1G56130					
AT1G53440					
AT1G29740					
AT3G14840					
AT1G53420					
AT2G22610					
AT1G29730					
AT1G72250					
AT1G51860	QQVWAVRSFP	----VGQR-	NCYNVNLV--	ANNKYLIRGT	FVYGNVD-GL
AT3G46240	-SLTTLRYFP	----TGDS-	NCYSNIPVT-	KGGKVLVTRM	FVYGNVDGKS
AT2G23200	EIYRTVRIFR	-----	HPSSYKFKLD	SLGLHFVRLH	FSVVSFRADL
AT2G14440	RPYKVLRYFP	----EGIR-	NCYLSVK--	QGTYLIRTL	FVYGNVD-GL
AT1G30570	VYABIYKTAR	-----VFD	AVLNVTFFGI	TQGNVYVRLH	FSPFAIEN-H
AT3G05990	-ILFTVRSFP	LSLDGTHHK-	FCYV-MSVS-	RGWKYMIRTT	YYYGGVNGKG
AT3G46420	KSQTTLRYPF	----DGIR-	NCYNLTVT--	QGTNYLIRAR	AIYGNVD-GL
AT1G25570	-AEKTIRYFP	----LSFGKK	NCY-VVPL--	PPGRYLRTF	TVYDNDY-GK
AT3G46370	-----MR-	NCYNLSVH--	KETKYLIRVT	SNYGNVD-GR	
AT3G46270	-PINTLRYFP	----TGQT-	NCYTNI PVT-	KGRKTLVTRK	YYYENYDDKF
AT4G39110	S--PIYLTAR	-----IFR	EATYKPHLT	RPGRHWVRLH	FLAFNDK-F
AT1G07560	KPYTVLRYFP	----DGVR-	NCYTLIVI--	QGTNYLIVAM	FTYGNVD-NL
AT1G51820	KPTTLRYFP	----EGVR-	NCYNLNVV--	SDTNYLIKAT	FVYGNVD-GL
AT1G24485	-ELTTLRYFP	----TGET-	NCYTNI PVE-	KGGKVLVTRR	FLYGDYDEES
AT5G39030	IPQVPYMTAR	-----IFR	SDFTYSPVVS	PG-WKFLRLY	FYPYSYKSGF
AT3G46290	SGSDIYHTAR	-----VFT	EVSSYKFSVT	R-GRHWVRLY	FNPFDYQN-F
AT5G61350	STLPLYL TAR	-----IFA	GKSTYSFYIS	RPGRHWIRLH	FYPLNHPL-Y
AT1G51805	TPNLTLYFPF	----DGAR-	NCYNLNVV--	RDNTYMIKAT	FVYGNVD-GH
AT5G59660	KP-----				FVYGNVD-GF
AT5G39000	VSQIPYMTAR	-----IFR	SEFTYSPVVT	PG-SNFLRLY	FYPTRYGSQF
AT3G04690	LSTVPYMTAR	-----IFT	APATYEIPIK	GDKRHLLRLY	FYPSTYTG-L
AT1G51790	QSMWSVRSFP	----EGIR-	NCYTI AVN--	SSTKYLIRAD	FMYGNVD-SR
AT5G28680	LSTVPYMTSR	-----IFT	APATYEIPVK	GDKRHMLRLH	FYPSTYTG-L
AT2G19190	RHLLNVRSEF	----QSKR-	SCYDVTPRPG	KGPKYLIRTR	FMYGNVD-DL
AT2G04300	KPILQLRYFP	----EGVR-	NCYTLNVV--	LGTNYLIRAS	FVYGNVD-GL
AT5G59680	KPSTTMYFPF	----DGKR-	NCYNLNVV--	KGRNHLIRAR	FVYGNVD-GR
AT2G19210	KQFQNVRSFP	----EGNR-	NCYDVKPPQG	KGPKYLIRTR	FMYGNVD-NL
AT1G51890	QI WALRSFP	----EGQR-	NCYNFSLT--	AKRKYLIRGT	FVYGNVD-GL
AT1G51880	QQTWTVRSFP	----EGER-	NCYNFNLV--	AKSRYLIRAT	FTYGNVD-GL
AT5G59616					
AT2G28970	KPYLTLRYFP	----EGKR-	NCS-----		
AT5G54380	STNSIYQTAR	-----VFS	SLASYRPFKIT	SLGRHWIRLH	FSPINNST-W
AT5G48740	-SSVPIRLFP	----DPQGR	QCYKLPVR-K	DLSSVLIRAT	FVYRNYD-SQ
AT2G28960	ROYKDLRYFP	----DGIR-	NCYNLKVVE--	QGINYLIRAG	FGYGNVD-GL
AT3G21340	KPSLKLRYFP	----DGFR-	NCYTLNVV--	QDTNYLIKAV	FVYGNVD-GL
AT3G46280	-PINTLRYFP	----TGQT-	NCYTNI PVT-	KGQKTLVTRK	FYYENYDAKF
AT3G46260	-PINTLRYFP	----TGQT-	NCYTNI PAT-	KGRTLVTRK	FYYKNYDENV
AT1G05700	RQLQNLRSFP	----EGSR-	NCYTLPIQGG	KGKYLIRAS	FMYGNVD-GE
AT3G46400	RSQTTLRYPF	----DGIR-	NCYNVNVY--	KGTNYLIRAT	INYGNVD-GL
AT5G38990	IPQVPYLKAR	-----IFR	YDFTYSPVVS	PG-WKFLRLY	FYPTRYGSDF
AT1G51800	QQTWNLRSFP	----QGIR-	NCYTLNLT--	IGDEYLIRAN	FLHGGYD-DK
AT5G24010	DSPVLNTAR	-----VFP	VGGSYKQVVT	TKGTHFIRLH	FAPFKASR-F
AT2G28990	KOYLTLRYFP	----EGKR-	NCYSLDVK--	RGTYLIVVS	FVYGNVD-GL
AT4G20450	KPYKQLRYFP	----EGAR-	NCYNLTVM--	QGTNYLIRAV	FVYGNVD-LK
AT1G49100	KAFVTLRYFP	----DGER-	NCYNLNVV--	QGTNYLIRAA	FLYGNVD-GL
AT4G29450	STLAEVRAFP	----QGNR-	NCYTLKLSQG	KDHLYLIRAS	FMYGNVD-GK
AT1G51840	KPALTMYFPF	----DGIR-	NCYNLNVV--	RDNTNYLIKAT	FVYGNVD-GL
AT5G59670	KPYRTLYFPF	----EGVR-	NCYNLSVF--	KERKYLIAAS	FLYGNVD-GH

AT1G51850	KPTLLTRYFP	----EGVR-	NCYNLNV	--SDTNYLIKAT	FVYGNVD-GL
AT5G59700	SNSDIYQTAR	-----IFT	GISKYRFSVA	R-GRHWIRLH	FNPFOYQN-F
AT2G19230	KQFKQVRSFP	----EGKK-	NCYDVQPPQG	KGPKYLIRTR	FMYGNYD-NL
AT1G51870	QPLWALRSFP	----EGER-	NCYNFNLT--	VNSTYLIRGT	FLYGNVD-GL
AT3G46330	KQYATLRYFP	----DGIR-	NCYDLRVE--	EGRNYLIRAT	FFYGNFD-GL
AT2G29000	KPYNFLRYFP	----DGTR-	HCYDLSVK--	QGTNYLIRAS	FVYGNVD-GR
AT3G46350	KQQTLLRYFP	----DGIR-	NCYNLTVK--	QGTNYLIRAR	FTYGNVD-GR
AT2G37050	-QYTTLRHFP	----ADSRK	YCYTLNV	--SRNRYLIRAT	FLYGNFDNSN
AT1G07550	KPYTVLRYFP	----DGIR-	NCYSLNVK--	QDTNYLIRVM	FRYGNVD-GL
AT1G51810	KPERTLRYFP	----DGV-	NCFSLNV	--RGTKYLIKPT	FLYGNVD-GR
AT4G29990	RQFQNVRSFP	----EGKR-	NCYDIRPQQG	KGPKYLIRTR	FMYGNYD-GF
AT5G59650	KPYTRLRYFP	----EERR-	NCYLSVD--	KNRKYLIRAR	FIYGNVD-GR
AT1G28340	-PLKTLRYFP	----ISEGPN	NCYNIVRV--	PKGHYSVRIF	FGLVDQP-SF
AT3G51550	VPEVPYMTAR	-----VFR	SPFTYTFPVA	SG-RKFVRLY	FYPNSYDG-L
AT2G21480	S--PIYLTA	-----IFR	EELYKPHLT	RPGWVWVRLH	FFAFPNDK-F
AT5G16900	KPYLFLRYFP	----DGLR-	NCYTLDVL--	QNRRYMIKAV	FVYGNVD-GY
AT1G67720	-QYRRRDFP	----TDNKK	YCYRLSTK--	ERRRYIVRTT	FLYGGG-SE
AT3G19230	-ILSTLRYFP	---DKSSRK-	HCYN-FPVA-	KTSKYLIRTT	YYYGNFDGKN
AT1G51830					
AT5G39020	VSRIPIYMKAR	-----IFR	SEFTYSFPVT	PG-SIFLRLY	FYPTQYKSGF
AT4G00300	NVPQIYRTAR	-----IFA	QOAKYKFNVN	EKGTHMVRHL	FNRLYSSR-I
AT4G29180	FPLADVRSFP	----QGNR-	NCYTLTPSDG	KGNLYLIRAS	FMYGNYD-GK
AT1G51910	QQTWTLRSFP	----EGQR-	NCYNFNLK--	ANLKYLIRGT	FVYGNVD-GL
AT3G46340	KSYMTRLRYFP	----DGKR-	NCYNLIVK--	QGKTYMIRAT	ALYGNVD-GL
AT2G14510	KPFKVLRYFP	----DGIR-	NCYLSVK--	QGTKYLIRTL	FYGNVD-GL

		110	120	130	140	150

X. Jaervis	QVLYQTERYN	EDSFGYDIPI	K-----	-----	-----	EEGE
CORKI	-----	-----	-----	-----	-----	FN
AT1G29750	-----	-----	-----	-----	-----	SC
AT1G53430	-----	-----	-----	-----	-----	SS
AT1G56120	-----	-----	-----	-----	-----	YN
AT1G07650	-----	-----	-----	-----	-----	YK
AT1G29720	-----	-----	-----	-----	-----	RF
AT1G56140	-----	-----	-----	-----	-----	SD
AT1G56130	-----	-----	-----	-----	-----	SD
AT1G53440	-----	-----	-----	-----	-----	SS
AT1G29740	-----	-----	-----	-----	-----	RS
AT3G14840	-----	-----	-----	-----	-----	YG
AT1G53420	-----	-----	-----	-----	-----	NA
AT2G22610	-----	-----	-----	-----	-----	-----
AT1G29730	-----	-----	-----	-----	-----	RS
AT1G72250	-----	-----	-----	-----	-----	-----
AT1G51860	NQPPSPDLHI	GPNKWSSVKI	LGVTNT---	-----	-----	SMHEII
AT3G46240	STP-SFSVVF	ECKHRGTLISI	S--SAFEP--	-----	-----	YLLELI
AT2G23200	LTARFTVSAT	SGSNHHLKSF	SPQNLTN---	-----	-----	TPRVEEFL
AT2G14440	NTSPRFDLFL	GPNIWTSVDV	QKVDG----	-----	-----	GDVIEEII
AT1G30570	NVNESSFSVF	ADGLRLMLDI	NIAGEIAHKN	LILESTGHNA	-----	TASSLVKEFL
AT3G05990	TPPPVFDQIV	DGTLWGIWNT	T--ADYAD-	-----	-----	GLASYIEGV
AT3G46420	NIYPKFDLYI	GNPFWTIDL	GKYVNG---	-----	-----	TWEEII
AT1G25570	SHSPSPDVS	EGTLVFSWRS	PWPESLLRDG	-----	-----	SYSDLF
AT3G46370	NEPPRFDLYL	GNPFWTIDL	GKHVNGD---	-----	-----	TWKEII
AT3G46270	SPP-SFDIVY	DGKHRDSVDI	T-ESLLDDE-	-----	-----	DTFYFSEVI
AT4G39110	DLQATFVSVL	TEKYVLLHNF	KISNNNDS-	-----	-----	QAAVQKEYL
AT1G07560	NTHPKFDLYL	GNPIWTTVDL	QRN-----	-----	-----	VNGTRAEII
AT1G51820	NVGNPNFLYL	GNPLWTTVSS	ND-----	-----	-----	TIEEII
AT1G24485	TYP-TFDVY	DGKHRSVVT	T-----TF-	-----	-----	ETVTESEAI
AT5G39030	DAVNSFVSVT	VNDFTLLQNF	SADLTVKASI	PE-----	-----	SKSLIKEF-I
AT3G46290	KMGSAKFAVS	SQSHVLLSDF	TVTSS-----	-----	-----	KVVKEYS
AT5G61350	NLTNSVFSVT	TDTTVLLHDF	SAG---DT-	-----	-----	SSIVFKEYL
AT1G51805	KDEPNFDLYL	GNPLWATVSR	SE-----	-----	-----	TVEEII
AT5G59660	DLKPKFDLYL	GNPLWATVDL	QTE-----	-----	-----	VNDWGNMTA
AT5G39000	NAVKSFFSVK	VNGFTLLMNF	SADLTVKASK	PQ-----	-----	TEFIIKEF-I
AT3G04690	NISNSYFTVE	ANDVTLLSNF	SAAITCQALT	-----	-----	QAYLVKEYSL
AT1G51790	NEIPGFDLHL	GNPKWDTVEL	VSPLQ-----	-----	-----	TVSKEII
AT5G28680	NILDSYFSVA	ANDLTLNLF	SAAITCQALT	-----	-----	QAYLVREYSL
AT2G19190	GRVPEFDLYL	GVNFWDSVKL	DDATT-----	-----	-----	ILNKEII
AT2G04300	NKELEFDLYL	GNPLWANVNT	AVYLMNG---	-----	-----	VTTEEII
AT5G59680	DTGPKFDLYL	GNPFWATIDL	AKQ-----	-----	-----	VNGTRPEIM
AT2G19210	GKAPDFDLYL	GNPIWDSVTI	DNATT-----	-----	-----	IVTKEII
AT1G51890	NQLPSFDLYI	GNPKWTSVSI	PGVRNG---	-----	-----	SVSEMI
AT1G51880	RQVPKFDIHI	GPSKWTSVKL	DGVGNG---	-----	-----	AVLEMI
AT5G59616	-----	-----	-----	-----	-----	-----
AT2G28970	-----	-----	-----	-----	-----	-----
AT5G54380	NLTSASITVV	TEDEVLLMNF	SPNNFN---	-----	-----	GSYIFKEYT
AT5G48740	NSPPAFHVSL	GRRITSTVDL	RTNDP-----	-----	-----	WIEELV
AT2G28960	NVYPKFDLHV	GPNMWIAVDL	EFG-----	-----	-----	KDREII
AT3G21340	NNPPSPFDLYL	GNPLWVTVDM	NGRTNG---	-----	-----	TIQEII

AT3G46280 SPP-SFDVIY DGKHRDSIVI T-ESLLNDE- ----- -ETFYFSEVI
 AT3G46260 SPP-SFDVVY DGKHRNSIAM TVDSLFSDE- ----- -ETFHYSEVI
 AT1G05700 NGSPEFDLFL GGNLWDTVLL SNGSS----- ---IVSKEVV
 AT3G46400 NISPRFDLYI GPNFWVTIDL EKHVGGD--- ----- --TWEEII
 AT5G38990 DAVKSPFSVN VNRFTLLHNF S----VKASI PE----- SSSLIKEF-I
 AT1G51800 -PSTQFELYL GPNLWSTVTT TNTEA----- ---SIFEMI
 AT5G24010 NLRSAKFRVL INGFSVINSF STSS----- ---VVVKEFI
 AT2G28990 NRDPNFDIHL GPNKWKRIDL DGE----- -KEGTREEII
 AT4G20450 -QRPKFDLYL GPNFWTTINL QDPSGGFYR IWL----- -QDGTVEEVI
 AT1G49100 NTVPNFDLFI GPNKVTTVNF NATGGG--- ----- ---VFVEII
 AT4G29450 KALPEFDLYV NVNFWSTVKF KNASD----- ---QVTKEIL
 AT1G51840 NVDPNFDLYL GPNLWTTVSS ND----- ---TTEEII
 AT5G59670 NIAPVFDLYL GPNLWAKIDL QD----- ---VNGTGEEIL
 AT1G51850 NVGPNFDLYF GPNLWTTV-- ----- ---VNGTGEEIL
 AT5G59700 QMVSASFVS SETHVLLSDF TVSS----- ---RVMKEYS
 AT2G19230 GKAPDFDLYL GVNLDWSVTL ENSTT----- ---IVTKEII
 AT1G51870 NQSPSFDLHI GASKWTSVNI VGVTD----- ---VMPEII
 AT3G46330 NVSPEFDMHI GPNKWTIDL QIV----- -PDGTVKEII
 AT2G29000 NIMPRFDLYI GPNIWAVVSE LD----LYS- ----- -PEEETI
 AT3G46350 NMSPTFDLYL GPNLWKRIDM TKLQNKVS-- ----- -TLEETI
 AT2G37050 NVYPKFDISL GATHWATIVI SETYI----- ---IETAELV
 AT1G07550 NNSPRFDLYL GPNWTTIDM GKS----- -GDGVLEEII
 AT1G51810 NVIPDFDLYI GPNMWTVNT DN----- ---TIKEII
 AT4G29990 SKTPEFDLYI GANLWESVVL INETA----- ---IMTKEII
 AT5G59650 NSNPIFELHL GPNLWATIDL QKF----- -VNGTMEEIL
 AT1G28340 DKEPLFDISI EGTQISSLSK GWSS--QDDQ ----- -VFAEAL
 AT3G51550 NATNSLFSVS FGPYTLKKNF SASQTAEALT ----- YAFIIKEF-V
 AT2G21480 DLQQATFSVL TEKYVLLHNF KLSNDNDS- ----- -QATVQKEYL
 AT5G16900 NDYPSFDLYL GPNKVVVDL EGK----- -VNGSVEEII
 AT1G67720 EAYPKFQLYL DATKWATVTI QEVSR----- ---VYVEELI
 AT3G19230 NPP-VFDQII GGTKWSVVNT S---EDYAK- ----- -GQSSYYEII
 AT1G51830 -----
 AT5G39020 DAVNSFFSVK VNGFTLLRNF NADSTVQASI PL----- SNSLIKEF-I
 AT4G00300 DLNDALFHVH VNGHVLLRNF SGDSS--D- ----- -FESRVREFL
 AT4G29180 MALPEFDLYV NVNFWTSVKL RNASE----- ---NVIKEIL
 AT1G51910 NQMPKFDLHI GPNKWTSVIL EGVANA---- ----- ---TIFEII
 AT3G46340 NISPKFDLYI GANFWTTLDA GEYLSG---- ----- ---VVEEIV
 AT2G14510 NTSRPFDFLF GPNIWTSVDV LIADV----- -GDGVVEEIV

.....|||||
 X.Jaevis YVLVLKFAEV YFAQ----SQ QKVFDRVNG HTVVKD----
 CORK1 FVVCNCGGRDI RSS-----S GALYEKDEGA LGPATFFVSK
 AT1G29750 LHVNCGGSDM YVKEK---KT KELYEGDGNV EGGAAKYFLK P-----
 AT1G53430 LFVNCGGSR L KIG----- KDTYDDLNS RGQSTFSSVS
 AT1G56120 FSVNCGGPEI RSV-----S GALFEKEDAD LGPASFVVA
 AT1G07650 LYVNCGGGEV KVDKE---IT ---YQADDEP KG-ASMYVLG A-----
 AT1G29720 LHVNCGGEEV SIRNS---LG KITQYTDNSR QTNAASNQQ-
 AT1G56140 FSVNCGGPEI RSV-----T EAVFEREDED LGPASFVVA
 AT1G56130 FSVNCGGPEK RSV-----T GALFEREDED FGPASFFVSA
 AT1G53440 LFVNCGGNRL KVD----- KBEYADDLNK RGASTFSSVS
 AT1G29740 LHVNCGGPDV TIENS---RG RFLYEGDNYG LTGSATNY-
 AT3G14840 LHVNCGGNEI TSN----- ETKYDADTWD TPG-YYDSK-
 AT1G53420 LHVNCGGDEM SIN----- GTIYESDKYD RLESWYESR-
 AT2G22610 -----TI MFIN---AGG DDSKVLDSLEL NISRDD----- YFEG--
 AT1G29730 LHVNCGGPDV TIENS---RG RFLYEGDNYG LTGSATNY-
 AT1G72250 -----PV ISIN---SGS ISTDVTVEDV TFLKDE---- FFSG--
 AT1G51860 HVVPQDSLEV CLVK---TGP TTPFISLLEV RPLNNE---- SYLTQS
 AT3G46240 FSPAGGETSV CFVR--TSSS SNPFVSSIEV VDLDDGMY-- AELGPG
 AT2G23200 LMMSLEFEI RFVP---DHS SLALINAIEV FSAPDD---- LEIPSA
 AT2G14440 HVTRCNILDI CLVK---TGT TTPMISAIEL RPLRYD---- TYTART
 AT1G30570 LPTGPGLLVL SFIFE--KGS -FGFVNAIEI VSVDDKLFKE S--VTKVGS
 AT3G05990 FLAQGKSISV CVASNSYTT S -DFFISALEL VRLDGTLYNS ---TDTTV
 AT3G46420 YIPKSNMLDV CLVK---TGP STPLISSLVL RPLANA---- TYITQS
 AT1G25570 AFVIGDELDEL CFYS---IAT DPPVIGSLEV LQVDPS---- SYDA-D
 AT3G46370 HIPKSNLVDV CLIK---TGT TPPIISTLEL RSLPKY---- SYNALS
 AT3G46270 FAPASENISV CLLR--TSPS DNPFISSIEV YSFDGMY-- KDLGPE
 AT4G39110 VNMTRDAQFAL RFRPM--KSS -AAFVNAIEV VSAPDELISD S--GTALFPV
 AT1G07560 HIPRSTSLQI CLVK---TGT TPPLISALEL RPLRNN---- TYIPQS
 AT1G51820 LVTRSNLSQV CLVK---TGI SIPPINMLEL RPKMKN---- MYVTQS
 AT1G24485 FIPENGNISV CFFR--TLSS KTFPVSTIEV RRLDSSMY-- TDLGPK
 AT5G39030 VPVY-LTLNL TFRPS---NN SLAFVNGIEI VSMPDFRYSK GGFDDLLTNV
 AT3G46290 LNVTTNDLVL TFTP S--SGS -FAFVNAIEV ISIPDTLITG S--PRFVGNP
 AT5G61350 I-YAAEKLSL YFKPH--KGS -TAFVNAIEV VSVDELVPD S--ASSVPQA
 AT1G51805 HVTKSDSLQV CLAK---TGD FIPFINILEL RPLKKN---- VYVTES
 AT5G59660 NIGFG----- -IMNG----- SYITKS
 AT5G39000 IPVY-QTLNL TFTP S--LD SLAFVNGIEI VSIPNRFYSK GGFDDVITNV
 AT3G04690 APTDKVLSI KFTPSDKYRD AFAFVNGIEV IQMPELFDTA ---ALVGT
 AT1G51790 YVVLTDTIQV CLVN---TGN GTFPISVLEL RQLPNS---- SYAAQS

AT5G28680 APSEKDVLSI IFTPSDKHPK AFATINGIEV IPPELFDTA ---SLVGFS
 AT2G19190 TIPLLDNVQV CVVD---KNA GTPFLSVLEI RLLLNT---- --TYETPY
 AT2G04300 HSTKSKVLQV CLIK---TGE SIIPIINSLEL RPLIND---- --TYNTQS
 AT5G59680 HIPTSNKLQV CLVK---TGE TPPLISVLEV RPMGSG---- --TYLTKS
 AT2G19210 HTLRSDHVHV CLVD---KNR GTPFLSALEI RLLKSN---- --TYETPY
 AT1G51890 HVLRQDHLQI CLVK---TGE TTPFISSLEL RPLNNN---- --TYVTKS
 AT1G51880 HVLTQDRLQI CLVK---TGK GIPFISSLEL RPLNNN---- --TYLTQS
 AT5G59616 -----
 AT2G28970 ----- --LRN-----
 AT5G54380 VNVTSSEPLTL SFIPS--NNS -VVFVNAIEV VSVPDNLIPD Q--ALALNPS
 AT5G48740 WPVNNDLSLL CLLAVK--GR GIPVISSLEV RPLPLG---- --SYKYSL
 AT2G28960 YMTTSNLLQI CLVK---TGS TIPMISTLEL RPLRND---- --SYLTQF
 AT3G21340 HKTISKSLQV CLVK---TGT SSPMINTLEL RPLKNN---- --TYNTQS
 AT3G46280 YVPENKNISV CLLR--TSPS DNPFISSIEV YSLDTGMY-- --DDLGNP
 AT3G46260 FAPANENISV CLVR--TSPS DNPFISSIEV YRFDAGMY-- --DDLGPE
 AT1G05700 YLSQSENI FV CLGN---KKG GTPFISSLEL RFLGNDNT-- --TYDSPN
 AT3G46400 HIPKNSLDV CLIK---TGT STPIISVLEL RSLPNN---- --TYITES
 AT5G38990 VPVN-QTLDL TFTP---PN SLAFVNGIEI ISMPDRFYSK GGFDDVVRNV
 AT1G51800 HILTTDRLQI CLVK---TGN ATPFISALEL RKLMMT---- --TYLTRQ
 AT5G24010 LKIDDPVLEI SFLPF--KAS GGFVNAIEV FSAPKDYIMD Q--GTLKLVIP
 AT2G28990 HKARNSLDI CLVK---TGE TLPFISALEI RPLRNN---- --TYVTKS
 AT4G20450 HMPKSNLNDI CLVK---TGT TTPFISSLEL RPLRND---- --TYTTTT
 AT1G49100 HMSRSTPLDI CLVK---TGT TTPMISTLEL RPLRSD---- --TYISAI
 AT4G29450 SFAESDTIYV CLVN---KKG GTPFISGLEL RPNVSS---- --IYGTEF
 AT1G51840 HVTKFNSLQI CLVK---TGI SIPPINLEL RPLKKN---- --VYATQS
 AT5G59670 HIPTSNSLQI CLVQ---TGE TTPLISSLEL RPLRMTG-- --SYTTVS
 AT1G51850 ----- CLIK---TGI SIPPINLEL RPKMKN---- --MYVTQG
 AT5G59700 LNVATDHLEL TFTP---GDS -FAFLNAIEV VSVPTLFSG D--PSFAGS
 AT2G19230 YTLRSDKHVH CLVD---KER GTPFLSVLEL RLLKNN---- --IYETAS
 AT1G51870 HVLTQKRLQV CLVK---TGK TTPFISSLEL RPLINN---- --IYIAES
 AT3G46330 HIPRSNSLQI CLVK---TGA TIPMISALEL RPLAND---- --TYIAKS
 AT2G29000 HMKTSTSLQI CLVK---TGP TTPFISSLEL RPLRND---- --NYITQS
 AT3G46350 YIPLNSLDV CLVK---TNT TIPFISALEL RPLPSN---- --SYITTA
 AT2G37050 FLASSPTVSV CLSN---ATT GQPFISTLEL RQLSGS-M-- --YGSMLS
 AT1G07550 HITRSNLDI CLVK---TGT STPMISSIEI RPLLYD---- --TYIAQT
 AT1G51810 HVSKNSLQV CLVK---TGT SIPYINTLEL RPLADD---- --IYTNES
 AT4G29990 YTPPSDHIHV CLVD---KNR GTPFLSVLEI RFLKND---- --TYDTPY
 AT5G59650 HTPTSNSLNV CLVK---TGT TTPFISALEL RPLGNN---- --SYLT-D
 AT1G28340 IFLLGGTATI CFHS---TGH GDPAIIISLEI LQVDDK-- --AYSFGE
 AT3G51550 VNVVEGGTLNM TFTPESAPSN AYAFVNGIEV TSMPPMYSST --DGLTMM
 AT2G21480 LNMTDAQFAL RPKPM--KGS -AAFINGIEI VSAPDELISD A--GTSLEPV
 AT5G16900 HIPSSNSLQI CLVK---TGN SLPFISALEL RLLRND---- --TYVTKS
 AT1G67720 VRATSSVVDV CVCC---AIT GSPFMSTLEL RPLNLS-M-- --YATDY-
 AT3G19230 VGVPGNRLSV CLAKNAHTLS SSPFISSLDV QSLEDTMYNS ----TDLGSY
 AT1G51830 -----
 AT5G39020 IPVH-QTLNL TFTP---KN LLAFAVNGIEI VSMPPDRFYSK GGFDNVLRNV
 AT4G00300 LWVDVGEVVI REVPS--KDS NFAFVNAIEV ISAPKDLIGD V--ATS-VSH
 AT4G29180 SFAESDTIYV CLVN---KKG GTPFISALEL RPMNSS---- --IYGTEF
 AT1G51910 HVLTQDRLQV CLVK---TGQ TTPFISSLEL RPLMND---- --TYVTKS
 AT3G46340 YIPRSNSLDV CLVK---TDT STPFISLLEL RPLDND---- --SYLTGS
 AT2G14510 HVTRSNILDI CLVK---TGT STPMISALEL RPLRYD---- --TYTART

..... 210 220 230 240 250
 X. Jaelvis
 CORK1 ----- --LDIFDRVW HST-----
 AT1G29750 ----- --DANW AVSNVGL--F
 AT1G53430 ----- --ERW GYSSSGV--W
 AT1G56120 ----- --AKRW AASSVGN--F
 AT1G07650 ----- --NKRW ALSSTGN--F
 AT1G29720 ----- --FDYW GVSNTGD--F
 AT1G56140 ----- --GQRW AASSVGL--F
 AT1G56130 ----- --GQRW AASSVGL--F
 AT1G53440 ----- --ERW GYSSSGA--W
 AT1G29740 ----- --GKNW GFSNTGD--F
 AT3G14840 ----- --NCW VSSNTGN--F
 AT1G53420 ----- --NCW FSNNVGV--F
 AT2G22610 -----
 AT1G29730 ----- --RKNW GYSNTGD--F
 AT1G72250 -----
 AT1G51860 GS---LMLFA RVYFPSSSSS FIR----- YDEDIHDRVW NSF-----
 AT3G46240 E----- --GRW LP-----
 AT2G23200 SD---KNLH TIYRLNVGGE KITP----- -DNDTLGRW LPDDDDFLYR
 AT2G14440 GS---LKKIL HFYF-TNSGK EVR----- YPEDVYDRW IPH-----
 AT1G30570 E---VELGLG GRGIETMYRL NVGGPKLGPS KDL-KLYRTW ETDLSYM--V
 AT3G05990 GM----SLV ARHAFGYSGP IIR----- FPDDQFDRW EPYS-----
 AT3G46420 GW---LKTYY RVYL-SDSND VIR----- YPDDVYDRW GSY-----
 AT1G25570 GTGQNVLLVN YGRLSGSDQ WGPFFT--NH TDNFG--RSW QSDEDFRS--
 AT3G46370 GS---LKSTL RAFL-SESTE VIR----- YPNDFYDRW VPH-----

AT3G46270 EG-----LIL YQRITYGAKK LIS----- YPLDPFGRW SPSA-----
 AT4G39110 I---GFSGLS DYAYQSVYRV NVGGPLIMPQ ND--TLGRW IPDKEFL--K
 AT1G07560 GS---LKTLF RVHL-TDSKE TVR----- YPEDVHDLR SPF-----
 AT1G51820 GS---LKLYF RGYI-SNSST RIR----- FPDDVYDRW YP-----
 AT1G24485 EG-----FIL QQRIAYGAQE LVR----- FPYDPYDRW MP-----
 AT5G39030 GSLIDFEIDN STAFETVHRL NVGGHMVDEV NDSG-MFRW LSDDYEF--L
 AT3G46290 A---QFPDMS MQGLETIHRV NMGGPLVASN ND--TLTRW VPDSEFL--L
 AT5G61350 P---DFKGLS SFSLEILHRI NIGGDLISPK ID--PLSRW LSDKPYN--T
 AT1G51805 GS---LKLFL RKYF-SDSQ TIR----- YPDDIYDRW HA-----
 AT5G59660 GS---LNLLS RTYL-SKSGS DLR----- YMKDVYDRW VSYG-----
 AT5G39000 GSSVDFHIEN STAFETVYRL NVGG---KTV GDSG-MFRW VSDDEII--L
 AT3G04690 DQTMDAKTAN ---LQSMFRL NVGGQDIPGS QDSGGLTRW YNDAPYI--F
 AT1G51790 E---SLQLFQ RLDGFGSTNL TVR----- YPNDVFDRI FPA-----
 AT5G28680 DQTSDDTKTAN ---LQTMFRL NVGGQDIPGS QDSGGLTRW YNDAPYI--F
 AT2G19190 D---ALTLR RLDYSKTGKL PSR----- YKDDIYDRW TPR-----
 AT2G04300 GS---LKLYF RNYF-STSR IIR----- YPNDVNDRI YP-----
 AT5G59680 GS---LKLYY REYF-SKSDS SLR----- YPDDIYDRW TSF-----
 AT2G19210 D---SLILFK RWDLGGGLGAL PVR----- YKDDVFDRI IP-----
 AT1G51890 GS---LIVVA RLYF-SPTPP FLR----- YDEDVHDLR IPF-----
 AT1G51880 GS---LIGFA RVFF-SATPT FIR----- YDEDIHDLR VRQ-----
 AT5G59616 -----
 AT2G28970 -----SF RVHC-STSDS EIR----- YDDSYDRW YPF-----
 AT5G54380 T---PFSGLS LLALETYVRL NMGGPLLSQ ND--TLGRW DNDAEYL--H
 AT5G48740 EGSPDIILRR SYRINSGYTN GTIR----- YPSDPFDRW DPDQ-----
 AT2G28960 GP---LDLIY RRAY-SSNST GFIR----- YPDDIYDRW DR-----
 AT3G21340 GS---LKYFF RYF-SGSGQ NIR----- YPDDVNDRI YP-----
 AT3G46280 EG-----LIL HDRIAYGAKE LIS----- YPLDPYGRW LALG-----
 AT3G46260 EG-----FIL YKRWAYGATK LIS----- YPLDPYGRW SPKG-----
 AT1G05700 G---ALFSSR RWDLRSLMGS PVR----- YDDVYDRW IP-----
 AT3G46400 GS---LKSIL RSYL-SVSTK VIR----- YPDDYDRW VPY-----
 AT5G38990 GRDVDFEIDN STAFETVYRV NVGGKVVGDV GDSG-MFRW LSDEGFL--L
 AT1G51800 GS---LQTFI RADVGATVNO GYR----- YGIDVFDRI TPY-----
 AT5G24010 NSAQIFSNLS SQVLETVHRI NVGGSKLTPF ND--TLWRW VVDDNYL--L
 AT2G28990 GS---LMMSF RVYL-SNSDA SIR----- YADDVHDLR SPF-----
 AT4G20450 GS---LKLIS RWFY-RKFP TLESII--R HPDDVHDLR DVY-----
 AT1G49100 GSS---LLLYF RGYL-NDSGV VLR----- YPDDVNDRI FP-----
 AT4G29450 GRNVSLVLYR RWDIGYLG- TGR----- YQDDRFDRW SPY-----
 AT1G51840 GS---LKLYF RMYV-SNSSR RIR----- -----
 AT5G59670 GS---LKYTY RLYF-KKSGS RLR----- YSKDVYDRW FPR-----
 AT1G51850 ES---LNYLF RYVI-SNSST RIR----- FPDDVYDRW YP-----
 AT5G59700 G---KFQGLS WQALETVYRV NMGGPRVTPS ND--TLSRW EPDSEFL--V
 AT2G19230 D---SLMLYR RWDLGATGDL PAR----- YKDDIYDRW MP-----
 AT1G51870 GS---MVLQN RYVFPDSDS IVR----- YDEDIHDLR NFV-----
 AT3G46330 GS---LKYF RMYL-SNATV LLR----- YPKDVYDRW VPY-----
 AT2G29000 GS---LKLMO RMCN-TETVS TLR----- YPDDVYDRW YT-----
 AT3G46350 GS---LRTFV RCFE-SNSVE DIR----- FPMVHDLR ESY-----
 AT2G37050 EDRFYLVA VAA RINFGAESA SVR----- YPDDVYDRW ESDLQKKNY
 AT1G07550 GS---LRNRY RYF-TDSNN YIR----- YPQDVHDLR VPL-----
 AT1G51810 GS---LNYLF RYVY-SNLKG YIE----- YPDDVHDLR KQ-----
 AT4G29990 E---ALMLGR RWDGATATNL QIR----- YKDDYDRW MP-----
 AT5G59650 GS---LNLFV RIYL-NKTG FLR----- YPDDIYDRW HNY-----
 AT1G28340 GWGQGVILRT ATRLTCGTGK SRFDED--YR GDHWGGDRW NRMRSFG---
 AT3G51550 GSSGVSVIDN STALENVYRL NVGGNDISPS ADTG-LYRSW YDQPYI--F
 AT2G21480 N---GFSGLS DYAYQSVYRV NVGGPLITPQ ND--TLGRW TPDKEYL--K
 AT5G16900 VS---LKHFL RRYV-RQSDR LIR----- YPDDVYDRW SPF-----
 AT1G67720 EDNFFLKVAA RVNFGAPND ALR----- YPDDVYDRW ESDINKRPNY
 AT3G19230 KL-----SLI ARNSFGGDGE IIS----- YPDDKYNRI QPFS-----
 AT1G51830 -----FFI-NDC-- -VR----- FPDDVYDRW YP-----
 AT5G39020 SSDVDFQIDN STAFESVHRL NVGGQIVNEV DDSG-MFRW LSDD-----S
 AT4G00300 DGTEKFNGLA KQAMEVYRV NVGGGRKVTFF ND--TLWRW VTDEGFL--K
 AT4G29180 GRNVSLVLYQ RWDTGYLNG- TGR----- YQKDYDRW SPY-----
 AT1G51910 GS---LMSFA RIYF-PKTAY FLR----- YSDDLDRW VPF-----
 AT3G46340 GS---LKTFR RYLL-SNSES VIA----- YPEDVKDRW EPT-----
 AT2G14510 GS---LKSMA HFYF-TNSDE AIR----- YPEDVYDRW MPY-----

260 270 280 290 300
 X.Jaevis
 ---AHDEIIP ISIKKGLSV QGEVSTFTGK LSVEFVKGY DN-----
 CORK1 TGSNS--NQY IALSATQ---FANTS DSE LQFQARL---SAS
 AT1G29750 MDDNN----FQNTRF-TM FVPASNQSD LYKSARI---APV
 AT1G53430 LGKED--AGY LATDRFN---LINGSTPE YYKTARL---SPQ
 AT1G56120 AGSSN--NIY IATSLAQ---FINTMDSE LQFQARL---SAS
 AT1G07650 MDNDDDADEY TVQNTSR-LS VNASSPSFG LYRTARV---SPL
 AT1G29720 TDDNSDHDEY YTSTNL---TLSGDYPD LYKTARR---SAL
 AT1G56140 AGSSN--NIY ISTSQSQ---FVNTLDSE LQFQARL---SAS
 AT1G56130 AGSSN--NIY IATSQSQ---FVNTLDSE LQFQARL---SAS
 AT1G53440 LGNDG--ATY LATDTFN---LINESTPE YYKTARL---ASQ
 AT1G29740 MDDAITEDTY TVSSES---AVSAKYPD LYQNARR---SPL
 AT3G14840 LDDDRNTNGK SKWSNSSELK ITNSSIDFR LYTQARL---SAI

AT1G53420 VDDKHVPERV TIESNSSELN V---VDFG- LYQARI--- -----SAI
 AT2G22610 -----GDV LRTEESIVEA GDFP-----F IYQARVGN-----
 AT1G29730 MDDAITEDTY TVSSES---- -AVSAKYPD- LYQNARR--- -----SPL
 AT1G72250 -----GES I-TTDAVVG N EDEI-----L LYQTARLGN-
 AT1G51860 ---TDDVTVW ISTDLPIDTS -NS-YDMPQS VMKTAAPVKN AS-----
 AT3G46240 ---SEINILVT GIQSTAVSID TSGASNKPPE SVLRNSWTG- --E-----
 AT2G23200 KDSARNINST QTPNYVGGLS SATDSTAPDF VYKTAKAMNR SSNE-QVGML
 AT2G14440 ---SQPEWTQ INTTRNVSGF SD-GYNPPQD VIKTASIPTN VS-----
 AT1G30570 IENAGVEVKN S-SNITYALA DDS-PVAPLL VYETARMSN TEV--LEKRF
 AT3G05990 ---LNSTVP ---NRRKLE VSGFNLPPS RIFNTDLRAT QVQ-----
 AT3G46420 ---FEPEWKK ISTDLVGN-S SSG-FLPPLK ALMTAASPN AS-----
 AT1G25570 -EDSRVARS LSTLEKIKGV DQAPNYFPMK LYQTAVTVSG GG-----
 AT3G46370 ---FETEWKQ ISTDLVGN-S SNG-YLLPQD VLMTAAIPVN TS-----
 AT3G46270 ---SGDNALT DLSTSAID ITGASNKPPE IVMSKALSG- --D-----
 AT4G39110 DENLAKDVKT TPSAIKYPP- EVTPLIAPQT VYATAVEMAN SLT--IDPNF
 AT1G07560 ---FMPEWRL LRTSLTVNTS DDNGYDIPED VVVTAAIPAN VS-----
 AT1G51820 -LFD-DSWTQ VTTNLKVNTS IT--YELPQS VMAKAATPIK AN-----
 AT1G24485 ---ASVFAS HLTSSATSID TTGADNRPE IILRTSWSQ- --K-----
 AT5G39030 IG--GVSPYM P-DVNI SYTE KTPAYVAPAY VYSTRMGMN AQDTYLNLFN
 AT3G46290 EKN-LAKSMS KFTVNVFVPG YATEDSAPRT VYGSCTEMNS ADN--PNSIF
 AT5G61350 FPEGSRNVTV DPSTLTYPDG GATALIAPNP VYATAEMAD AQT--SQPNF
 AT1G51805 -SFLENNWAQ VSTTLGVNVT DN--YDLSQD VMATGATPLN DS-----
 AT5G59660 -ASFRTGWTQ IYTALEVNNS NN--YAPPKD ALRNAATPTN AS-----
 AT5G39000 SESSGISPIV P-DIKINYTE KTPSYVAPDD VYATSRSMGN ADHPEQNLNF
 AT3G04690 SAGLGVTLQA SNNFRIN-YQ NMPVSIAPAD IYKTARSQGP N--GDINLKS
 AT1G51790 ---TPNGTKPL SDPSTSLTSN STGNFRLPQV VMRTGIVPDN PR-----
 AT5G28680 SAGLGVTLQA SNNFRIDY-Q KMPVSTAPAD VYKTARSQGP N--GDINMKS
 AT2G19190 --IVSSEYKI LNTSLTVDQF LNNGYQAPST VMSTAETARN ES-----
 AT2G04300 -FFDEDATWE LTTNLVNVSS NG--YDPPKF VMASASTPIS KN-----
 AT5G59680 --FDT-EWTQ INTTSDVGN ND--YKPPKV ALTTAAIPTN AS-----
 AT2G19210 --LRFPKYTI FNASLTIDSN NNEGQPARF VMNTATSPED LS-----
 AT1G51890 ---LDNKNLS LSTELSDVTS -NF-YNVPT VAKTAAVPLN AT-----
 AT1G51880 ---FGNLKLS ISTDLLVDTN -NP-YDVPQA VAKTACVPSN AS-----
 AT5G59616 -----
 AT2G28970 ---FSSFSY IITSLNINNS DT--FEIPKA ALKSAATPKN AS-----
 AT5G54380 VNSSVLVVTA NPSSIKYSP- SVTQETAPMN VYATADTMGD ANV--ASPSF
 AT5G48740 -SYSPPHAW SFNGLTKLNS FNITENPPAS VLKTARILAR KE--ASPSF
 AT2G28960 ---YNEFETD VNTTLNVR-S SSP-FQVPEA VSRMGITPEN AS-----
 AT3G21340 -FFDAKEWTE LTTNLNINSS NG--YAPPEV VMASASTPIS TF-----
 AT3G46280 ---SQD-STLT DLTTSAPSID ITGASNKPPE IVMSKALSG- --V-----
 AT3G46260 ---SQDYPLGI DLTTSAPSID ITGALNKPPE IVMTKAMSG- --D-----
 AT1G05700 ---RNFYCRE INTSLPVTS- DNNSYLSLSS VMSTAMPIN TT-----
 AT3G46400 ---FESEWRQ ISTDLVNNT ING-FLAPQE VLMTAAVPSN AS-----
 AT5G38990 GINSGAIPNI T-GVKINYTE KTPAYVAPED VYTTCLRMGN KDSPELMLNF
 AT1G51800 ---NFGNWSQ ISTDVSNIN -ND-YQPEI AMVTSVPTD PD-----
 AT5G24010 LR-AAARRAW TTHSPNYQNG GATREIAPDN VYMTAQEMDR DNQE-LQARF
 AT2G28990 ---NGSSHHT ITDDLINNS NA--YEIPKN ILQTAAPRN AS-----
 AT4G20450 --HADEWTD INTTTPVNTT VNA-FDLPOA IISKASIPQV AS-----
 AT1G49100 -FSY-KEWKI VTTTLNNTS NG--FDLPQG AMASAATRVN DN-----
 AT4G29450 --SSNISWNS IITSGYIDVF QNG-YCPPDE VIKTAAAPEN VD-----
 AT1G51840 -----
 AT5G59670 ---FMD-EWTQ ISTDLVNNT NI--YQPPED ALKNAATPTD AS-----
 AT1G51850 -YFD-NSWTQ VTTTLVNTS LT--YELPQS VMAKAATPIK AN-----
 AT5G59700 EKN-LVKSVS KIASVDYVPG FATEETAPRT VYGTCTEMNS ADN--PSSNF
 AT2G19230 ---LMFPNFI LNTSLMIDPT SSGFLPPSV VMSTAVAPMN SSI-----
 AT1G51870 ---SDDSSS ISTDLVQTN -NL-YDVPQF VMKTAAPKD AS-----
 AT3G46330 ---IQPEWQ ISTDVSNVSNK NH--YDPPQV ALKMAATPTN LD-----
 AT2G29000 ---DGIYETKA VKTALSVN-S TNP-FELPQV IIRSAATPVN SS-----
 AT3G46350 ---FDDWDTQ ISTDLVN-T SDS-FRLPQA ALITAAIPAK DG-----
 AT2G37050 LVDVAAGTVR VSTTLPIESR VDD--RPPQK VMQTAVVGTN GS-----
 AT1G07550 ---ILPEWTH INTSHHVIDS ID-GYDPPQD VLRTGAMPAN AS-----
 AT1G51810 -ILPYQDWQI LTTNLQINVS ND--YDLPQR VMKTAATPIK AST-----
 AT4G29990 --YKSPYQKT LNTSLTIDET NHNGFRPASI VMRSIAPGN ES-----
 AT5G59650 ---FMVDDWTQ IFTTLEVIND NN--YEPPKK ALAAAATPSN AS-----
 AT1G28340 ---KSADSP RSTETIKKA SVSPNFYPEG LYQSALVSTD DQ-----
 AT3G51550 GAGLGI PETA DPNMTIKYPT GTPTVAVPD VYSTARSMGP T--AQINLNY
 AT2G21480 DENLAKDVKT NPTAIYPP- GVTPLIAPQT VYATGAEMAD SQT--IDPNF
 AT5G16900 ---FLPEWTQ IITSLDVNNS NN--YEPPKA ALTTAAIPGD NG-----
 AT1G67720 LVGVAPGTR INTSKINTL TRE--YPPMK VMQTAVVGTQ GL-----
 AT3G19230 ---DQKHLTVT ---SRSRIN PSNFWNIPPA EAFVEGFTAS KGK-----
 AT1G51830 -IFQ-NSWTQ VTTNLNINIS TI--YELPQS VMSTAATPLN AN-----
 AT5G39020 FGNSSGIVNV P-GVKINYTE KTPAYVAPYD VYATSRMGMN S----SNLMF
 AT4G00300 TGDGSSSEKSY FTGRIKYRRG GASREVGPDN VYNTARVGRK SN-----GLV
 AT4G29180 ---SP-VSWNT TMTTGIDIF QSG-YRPPDE VIKTAAAPSKS DD-----
 AT1G51910 ---SQNETVS LSTNLVVDTS SNS-YNVQPN VANSIIPAE AT-----
 AT3G46340 ---FDSPEWKQ IWTTLKPN-N SNG-YLVKPN VLMTAAIPAN DS-----
 AT2G14510 ---SQPEWTQ INTTRNVSGF SD-GYNPPQD VIQTASIPTN GS-----

```

310          320          330          340          350
X.Jaevis    PKVCALFIMK GTADDPMLQ  PHPGLEKKEE EE-----
CORK1      SLRYYGLGLE --NGGYSVTV QA AEIQIGS  NT---WKS LG  RRI EDIYVQG
AT1G29750  SLTYFHACLE --NGNYTINL DA AEIRFTND  EN---YNR LG  RRI EDIYIQE
AT1G53430  SLKYYGLCLR --RGSYKQLL HA AEIMFSND  QT---FNS LG  RRI EDIYVQG
AT1G56120  SLRYYGLGLE --NGGYVTTL QA AEVQIEGS  NS---WKG LG  RRI EDIYVQG
AT1G07650  SLTYYGICLG --NGNYTVNL HA AEIIFTDD  NT---LYS LG  RRI EDIYVQD
AT1G29720  SLVYYAFCLE --NGNYNVKL HA AEIQFSDK  EV---YSR LG  RRI EDVYVQG
AT1G56140  SLRYYGLGLE --NGGYVTTL QA AEIQILGS  TSNT-WRGLG  RRI EDIYVQG
AT1G56130  SVRYYGLGLE --NGGYVTTL QA AEIQILGS  TSNT-WRGLG  RRI EDIYVQG
AT1G53440  SLKYYGLCMR --RGSYKVLQ HA AEIMFSND  QT---YSS LG  RRI EDIYVQG
AT1G29740  SLAYFAICFE --NGSYNVKL HA AEIQFSDE  EP---FSR LA  KRVI EDIYVQG
AT3G14840  SLTYQALCLG --KGNYSVNL HA AEIMFNEK  NM---YSN LG  RRY EDIYVQG
AT1G53420  SLTYIALCLE --NGNYNVNL HA AEIMFN GN  NN---YQS LG  RRI EDIYIQR
AT2G22610  ---FCYQLNN LLPGEYLIDF HA EIINTNG  PK-----G  IRV EDVYVQ
AT1G29730  SLAYYAFCFE --NGSYNVKL HA AEIQFSDV  EP---YTK LA  KRVI EDIYIQ
AT1G72250  ---FAYKFQS LDPGDYFIDL HA AEIEFTKG  PP-----G  V-----
AT1G51860  EPWLLWTTLD ENTAQSYVYM HA AEVQNLTA  NE-----T  RE EDNITYNG
AT3G46240  GLSLVDPTLP SAGVFPYLAM YSE P---LE  SS-----L  RS EDNIFFGG
AT2G23200  MNVTWSFKVK -SNHRHFIRI HA SDILSNLS  NS-----D  SD EYL FVNG
AT2G14440  EPLTFTW MSE SDD ETYAYL YAEIQQLKA  NE-----T  ROK ILLV N-
AT1G30570  NIS-WKFEVD -PNFDYLVRL HA CELLV---  -----DK  QN QR IRIYINN
AT3G05990  PLEPTWPPMP LKMATYIYAL YAHDSDSMG  DG-----S  RV EDVSVNG
AT3G46420  APLAIPGVLD FPSDKLYLFL HA SEIQVLKA  NE-----T  RE EIFW NK
AT1G25570  -S-LVYELEV DAKLDYLWLF HA SEIDSTVK  KA-----G  QRV EDLVV N-
AT3G46370  ARLSFTENLE FPHDEL YLYF HA SEVQLVQA  NQ-----S  RE SILWNG
AT3G46270  GLIISDLPLP STATLVYLAL YSE PQSLGR  TQ-----K  RS EDVFLDD
AT4G39110  NVS-WNFPSN -PSFN YLRL HA CDIVS---  -----K  SLN DLY EDVYING
AT1G07560  SPLTISWNLE TPDDL VYAYL HA EIQLSRE  ND-----T  RE NISAGQ
AT1G51820  DTLNITWTV E PPTTQFYSYV HIAEIQLALR  NE-----T  RE EDVTLNG
AT1G24485  DMAFYDIKLP FSGVTFYIVI YSE PLSLGS  DQ-----K  RS EDVYED
AT5G39030  NLT-WLFTVD -AGFSYLVR L HA FEKY---  -----LN  KAN QRV ESIPLGN
AT3G46290  NVT-WDFD VD -PGFY YFRF HA CDIVS---  -----L  SLN QLY EDLVDS
AT5G61350  NLS-WRMSVD -FGHDYFIR L HA CDIVS---  -----K  SLN DLY EDVFINK
AT1G51805  ETLNITWVVE PPTTKVYSYM HA AELET LRA  ND-----T  RE EDVMLNG
AT5G59660  APLTIEWP SG SPS-----  -----Q  E VPG TN-----I  TE
AT5G39000  NLT-WLFTVD -AGFSYLVR L HA CETLSE--  -----V  NKEG QRV ESIPIEN
AT3G04690  NLT-WMFQID -KNFTYLR L HA CEFP---  -----L  SKIN QKV EDN IYNN
AT1G51790  GFVDFGWI PD DPSLEFFFY L YTELQPQNS  GT-----V  E TR EDVILLN-
AT5G28680  NLT-WMFQVD -TNFTYIMR L HA CEFP---  -----L  AKIN QKV EDN IFINN
AT2G19190  LYLTLSFR PP DPNAKFYVYM HA AEIEVLKS  -----N  Q TR EDI SWLNG
AT2G04300  APFNFTWSLI PSTAKFYSYM HA ADIQT LQA  NE-----T  RE EDMLNG
AT5G59680  APLTNEWSSV NPDEQYVYA HA SEIQELQA  NE-----T  RE EDMLLNG
AT2G19210  QDIIFSWEPK DPTWKYFVYM HA AEVVELPS  -----N  E TR EDVLLNE
AT1G51890  QPLKINWSLD DITSQSYIYM HA AEIENLEA  NE-----T  RE EDNITYNG
AT1G51880  QPLIFDWTLD NITSQSYVYM HA AEIQLTKD  ND-----I  RE EDNITYNG
AT5G59616  ---MEWSSS NVNNQYLYG HA AEIQELQT  ND-----T  RE EDNMFWRN
AT2G28970  APLITWKPR  PSNAEVYFYL HA EIQT LAA  NE-----T  RE EDVFKG
AT5G54380  NVT-WLFPVD -PDRFYFVR V HA CDIVS---  -----Q  ALN TLV EDLVND
AT5G48740  -SLSYTL SLH TPG-DYYIIL YAGILSLSP  -----S  SVTIND
AT2G28960  LPLRFYVSLD DDSDKVNYF HA AEIQLALR  NE-----T  RE EDIELEE
AT3G21340  GTWNFSWLLP SSTTQFVYM HA EIQT LRS  LD-----T  RE EDVTLNG
AT3G46280  GLVLSDTLP LTGVFVYLVL YSE PQSLGR  TQ-----R  RS EDVFLDN
AT3G46260  GFIMSGNLPL STL LFPY LAL YSE PQSLGR  TQ-----K  RS EDVFLDG
AT1G05700  RPI TMTLENS DPNVRYFVYM HA AEVEDSL  KP-----N  Q TR EDI SIN-
AT3G46400  VPLSFTK DLE FPKDKLYFYF HA SEIQPLQA  NQ-----S  RE SILWNG
AT5G38990  NLT-WLFEVD -AGFAYIVRL HA CETQPE--  -----V  NKTG DRV ESIFFGY
AT1G51800  AAMNISLVGV ERTVQFYVFM HA AEIQELKS  ND-----T  RE EDNIMYNN
AT5G24010  NIS-WGFQVD EKRVLHLVRL HA CDIVS---  -----S  SLN QLY EDVFINE
AT2G28990  APLITWDPL  PINAEVLYM HA EIQTLEA  NE-----T  ROK EDVLLRG
AT4G20450  DTWSTTWSIQ NPDDDVH VYL HA EIQLKLP  SD-----T  RE EDLW NK
AT1G49100  GTWEPFWSLE DSTTRFHIYL HA AEQTLLA  NE-----T  RE EDVLLNG
AT4G29450  DPLELFWTSD DPNVRYAYL YAELETLEK  -----N  E TRKIKILWN-
AT1G51840  -----
AT5G59670  APLTFKWNSE KLDVQYFYFA HYAEIQDLQA  ND-----T  RE EDNILLNG
AT1G51850  DTLNITWTV E PPTTKFYSYM HA AEQLTRA  ND-----A  RE EDVMTNG
AT5G59700  NVT-WDFD VD -PGFYFLRF HA CDIVS---  -----K  ALN QLY EDLVDS
AT2G19230  EQIMVYWEPR DPNWKFYIYI HA AEVEK LPS  -----N  E TR EDVFLNK
AT1G51870  APWSLVWTID NTTALSYVYM HA EIQLKA  ND-----L  RE EDITYNG
AT3G46330  AALTMWRLE  NPDDQIYLYM HA SEIQVLKA  ND-----T  RE EDILNG
AT2G29000  EPITVEYGGY SSGDQVLYL HA AEIQLKA  SD-----N  RE EDIVWAN
AT3G46350  PSYIGITFST SSEERFFIYL HA SEVQALRA  NE-----T  RE EDISING
AT2G37050  --LTYRNL D GFPFGWAF T YAEIEDLAE  DE-----S  RK EDVLP E
AT1G07550  DPMTITWNLK TATDQVYGYI YAEIMEVQA  NE-----T  RE EDVVNN
AT1G51810  TTMEFPWNLE PPTSQFYLF L HA ELQSLQA  NE-----T  RE EDVNLNG
AT4G29990  NPLKFNWAPD DPRSKFYIYM HA AEVRELQR  -----N  E TR EDIYIN-
AT5G59650  APLTISWPPD NPGDQYLYS HA SEIQDLQT  ND-----T  RE EDILWDG
AT1G28340  -PDLTYSLDV EPNRNYSVWL HA EIDNTIT  AE-----G  KRV EDVING
AT3G51550  NLT-WIFSID -SGFTYLVRL HA CEVSSN--  -----I  TKIN QRV EDIYLN

```

AT2G21480	NVT-WNFPNS	-PSFHYFIRL	HCCDIIS---	-----KSLN	DLYENVYING
AT5G16900	TRLTIIWTLD	NPDEQIHLYV	HAELEPVGE	NTDEALRTL	TRTYFVVG
AT1G67720	--ISYRLNLE	DFPANARAYA	YAEIEELGA	NE-----	TRKIKLVQPY
AT3G19230	PLELQWPPFP	LPATKYVAL	YQDNRSPPG	MS-----	WRADVSVNG
AT1G51830	ATLNIWTIE	PPTPFYSYI	HAEQLSLRA	ND-----	TRBNVTLNG
AT5G39020	NLTGMFLTVD	-AGYNYLVR	HCCETLPQ--	-----VTKAG	QRVMSIFVED
AT4G00300	DMS-WGFKVN	-VGYKYLIRM	HCCDIAS---	-----KSLG	RLYENVYING
AT4G29180	EPLELSTWSS	DPDTRFYAYL	YAELENLKR	-----NE	SREIKIFWN-
AT1G51910	HPLNIWDDLQ	NINAPSYVYM	HAEIQNLKA	ND-----	IREFNITYNG
AT3G46340	APPRFTEELD	SPTDELYVYL	HSEVQSLQA	NE-----	SREIDILWSG
AT2G14510	EPLTFTWNLE	SSDDETYAYL	HAEIQQLKV	NE-----	TRBKILAN-

	360	370	380	390	400

<i>X.jaevis</i>	-----	-----	-----	-----	-----
CORK1	KLVEKDFD--	-MQKAANGSS	IRVIQRVYKA	NVSE---NYL	EVHLFWAGKG
AT1G29750	KLVAKDFN--	-IMDEAKGAQ	TPIIKPLT-A	YVTN---HPL	TIRLSWAGKG
AT1G53430	NLLERDFN--	-IAERAGGVG	KPFIRQIDGV	QVNG---STL	EIHLQWTGKG
AT1G56120	RLVEKDFD--	-IRRTAGGSS	VRAVQREYKT	NVSE---NHL	EVHLFWAGKG
AT1G07650	QLVIKDFN--	-IQEAARGSG	KPIIKSFL-V	NVTD---HTL	KIGLRWAGKG
AT1G29720	KLFLRDFN--	-INKEANGNM	KPVIKEIN-A	TVTN---HML	EIRLYWAGKG
AT1G56140	RLVEKDFD--	-VVRTAGDST	VRAVQREYKA	NVSQ---NHL	EIHLFWAGKG
AT1G56130	RLVEKDFD--	-VVRTAGDST	VRAVQRYKA	NVSE---NHL	EVHLFWAGKG
AT1G53440	ILLERDFN--	-IAQRAGGVG	KPFLRQVDEV	QVNG---STL	EIHLKWTGKG
AT1G29740	KLIWEDFS--	-IREEANGTH	KEVIKEVN-T	TVTD---NTL	EIRLYWAGKG
AT3G14840	KREVKDFN--	-IVDEAKGKV	KAVVKKFP-V	MVTN---GKL	EIRLQWAGKG
AT1G53420	KLEVKDFN--	-IAKEAKDVG	NVVIKTFP-V	EIKD---GKL	EIRLYWAGRG
AT2G22610	DE-----	---KATEFDI	FSVVGANRPL	LLVD-LRVMV	MDDGLIRVRF
AT1G29730	KLIWEDFS--	-IREEANGTH	KEVIKEVN-T	TVTD---NTL	EIRLYWAGKG
AT1G72250	-----	---ISGLDL	FSQVGANTPL	VIED-LRMLV	GREGELSIRL
AT1G51860	G-----	---LRWFSYL	RPPNLSISTI	FNPR--AVSS	-SNGIFNFTF
AT3G46240	K-----	---QVGRGP	VVPLFGKATQ	VVVR---DV	VASSSTLLTL
AT2G23200	YWR-----	---VDVKPSE	QPRLASPFK	DDVN---VS	DGSGLLNISI
AT2G14440	-----	---GVYIDY	IPRKFEBTL	ITPA---ALK	GGGV-CRVQL
AT1G30570	QTAAGNFD--	IFAHAGGKKN	GIYQDYLDV	SSK-----	N DVLVIQLGPD
AT3G05990	I-----	---TYKEL	SVTPAGAVIF	ASRW---PL	EG--LTTLAL
AT3G46420	K-----	---LVYNAY	SPVYLQTKI	RNPS--PVC	ERGE-CILEM
AT1G25570	DN-----	---NVSrvDV	FHEVGG-FAA	YSLN-YTVKN	LSSTIVTVKL
AT3G46370	M-----	---VIYPDF	IPDYLGAAATV	YNPS--PSLC	EVGK-CLELE
AT3G46270	M-----	---QVGSHP	IVPVFGKATQ	LVLRL---DV	EATSGSQIVL
AT4G39110	KTAISGLD--	LST-VAGNLA	APYKIDIVVN	ATL---MGP	-ELQVQIGPM
AT1G07560	-----	---DvNYGPV	SPDEFIVGTL	FNTS--PVK	EGGT-CHLQL
AT1G51820	E-----	---YTFGPF	SPIPLKTASI	VDLS--PGQC	DGGR-CILQV
AT1G24485	K-----	---QVGSDL	IVPPFGAVTQ	ASLR---DV	VKTELAYLTF
AT5G39030	QMAREEM--	DVIRLSGGGR	IPIYLDPRIY	VGSE-SGPRP	-DLRLDLHPL
AT3G46290	MVAATDID--	LSTLVDNTLA	GAYSMDFVT-	QTP---KGS	NKVRVSIIGS
AT5G61350	LSAISALD--	LSS-LTSALG	TAYYADFVLN	AST---ITN	GSIILVQVGT
AT1G51805	N-----	---DLFGPY	SPIPLKTETE	TNLK--PEEC	EDGA-CILQL
AT5G59660	-----	---SDPI	IPKKLDITSV	QSVT--PKTC	QEGK-CSLQL
AT5G39000	QTATLEM--	DVFRMSGGSW	IPMYLDYTVI	AGSG-SGRRH	-DLRLDLHPL
AT3G04690	RTAQADTPA	DIIGWTGEGK	IPMYKDYAIY	VDAN-NGG--	EETLQMTPS
AT1G51790	G-----	---KSFGPEL	SLNYFRTLAL	FTSN-----	P LKAESFQFSL
AT5G28680	RTAQGDTPA	DILGWTGGKG	IPYKDYAIY	VDAN-TGGGG	EESLQMTPS
AT2G19190	DV-----	---IS--PSF	KLRYLLTDTF	VTPD-----	P VSGITINFSL
AT2G04300	N-----	---LALERY	RPKTFATGTI	YFIK--PQIC	EGGQ-CIIELE
AT5G59680	K-----	---LFFGVP	VPPKLAISTI	LSVS--PNTC	EGGE-CNLQL
AT2G19210	KE-----	---IN-MSSF	SPRYLYTDTL	FVQN-----	P VSGPKLEFRL
AT1G51890	G-----	---ENWFSYF	RPPKFRITTV	YNPA--AVSS	-LDGNFNFTF
AT1G51880	G-----	---QNVYSYL	RPEKFEISTL	FDSK--PLSS	-PDGFSLSLF
AT5G59616	Q-----	---VIADPL	IPPKFTIYTI	FSQS--PSTC	EGGK-CSFQL
AT2G28970	N-----	---FNYSAF	SPTKLELLTF	FTSG--PVQC	DSDG-CNLQL
AT5G54380	DLALGSLD--	LST-LTNGLK	VPYKDFISN	GSV---ESS	GVLTVSVGPD
AT5G48740	EVK-----	---QSDY	TVTSSBAGTL	YFTQ-----	KGISKLNITL
AT2G28960	D-----	---IIQSAY	SPTMLQSDTK	YNLS--PHKC	-SSGLCYLKL
AT3G21340	K-----	---LAYERV	SPKTLATETI	FYST--PQQC	EDGT-CLELE
AT3G46280	T-----	---QVGSRP	IVPVFGKATQ	FILR---DV	VATSASQIVF
AT3G46260	M-----	---QVGSHP	IVPVFGKATQ	VVLR---DI	MASSESQIVF
AT1G05700	-G-----	---VTVAAGF	SPKYLQNTNF	FLN-----	P ESQSKIAFSL
AT3G46400	E-----	---IIIPTL	SPKYLKASTL	YSVS--PFVC	EVGK-CLELE
AT5G38990	QLAMREM--	DVFRLSGGFR	LPMYLDFKVL	VDAD-GTSQR	PSLRVDLTPY
AT1G51800	-----	---KHLYGPF	RPLNFTSSV	FTPT--EVVA	DANGQYIFSL
AT5G24010	YLAFKVDV--	LSTLTFHVLVLA	SPLYIDFVAE	S-----DRSG	-MLRISVGP
AT2G28990	N-----	---FNHSGF	SPTKLVFTL	YTEE--PMKC	GSEG-CYLQL
AT4G20450	NT-----	---IIRDY	SPLEFMADTV	PIRT--SSK	GDDGFCSDL
AT1G49100	K-----	---VYGYPY	SPKMLSIDTM	SPQDSTLTC	KGGS-CLLQL
AT4G29450	GS-----	---PVSETSF	EPSSKYSTTF	SNPR----A	FTGKDHWSI
AT1G51840	-----	-----	-----	-----	-----
AT5G59670	QN-----	---LSVTGPE	VPDKLSIKTF	QSSS--PISC	NGWA-CNFQL
AT1G51850	I-----	---YTYGYP	SPKPLKTETI	YDKI--PEQC	DGGA-CLLQV

AT5G59700 MDVVENLD-- LSSYLSNTLS GAYAMDFTV- GSA---KLT KRIRVSIGRS
 AT2G19230 EQ----- ---IDTTSVF RPSYLYDTL YVQN----P VSGPFLFVL
 AT1G51870 G----- ---KLWFSQF RPNKLSILTM FSQV--PLTS -SNGEYNTFF
 AT3G46330 ET----- ---INTRGV TPKYLEIMTW LTTN--PRQC NGGI-CRMQL
 AT2G29000 N----- ---IKKLAY KPKVSQIDTL LNTS--PNKC -DNTFCKAFL
 AT3G46350 E----- ---SVADLY RPVYL---VI YSPR--RKLS SKG-----L
 AT2G37050 QP----- ---EYSKSVV NIKENTQRPY RVYAPGYPNI TLPFVLNFRF
 AT1G07550 N----- ---KVHFDPF RPTRFEAQM FNNV--PLTC EGGF-CRLQL
 AT1G51810 N----- ---VTFKSY SPKFLEMQTV YSTA--PKQC DGGK-CLLQL
 AT4G29990 -D----- ---VILAENF RPFYLFDTDR STVD----P VGRKMNEIVL
 AT5G59650 A----- ---VVEEGF IPPKLGVTTI HNLS--PVTC KGEN-CIYQL
 AT1G28340 DT----- ---FFEDVDI IKMSGGRYAA LVLN-ATVTV SGRLLTVVLQ
 AT3G51550 QTAEPEA--- DVIAWTSSNG VPFHKDYVVN PPEG-NGQOD --LWLALHPN
 AT2G21480 KTAISGLD-- LST-VAGDLS APYKDIVVN STL---MTS -ELQVQIGPM
 AT5G16900 K----- ---ISYDESI TPLDLAVSTV ETVV--N-KC DGGN-CSLQL
 AT1G67720 FP----- ---DYSNAV NIAENANGSY TLYEPSYMN V TLDVLTFSF
 AT3G19230 L----- ---SFLRKL NVSTNGVMVY SGQW---PL SG--QTQITL
 AT1G51830 E----- ---YTIGPY SPKPKLTETI QDLS--PEQC NGGA-CILQL
 AT5G39020 KMAKKET--- DVIRLSGGPR IPMYLDFSVY VGFE-SGMTQ PELRLDLVPL
 AT4G00300 NLAYEFD-- ISYAADNVLA SPYIDFVVD ATADDNPNPSG SSIIVSVGVS
 AT4G29180 GS----- ---PVSG-AF NPSPEYSMTV SNSR-----A FTGKDHWSV
 AT1G51910 G----- ---QWESSI RPHNLSITTI SSPT--ALNS -SDGFNFMTF
 AT3G46340 E----- ---VAYEAF IPEYLNITTI QTNT--PVTC PGGK-CNLEL
 AT2G14510 ----- ---GVDYIDY TPWKFEARTL SNPA--PLKC EGGV-CRVQL

410 420

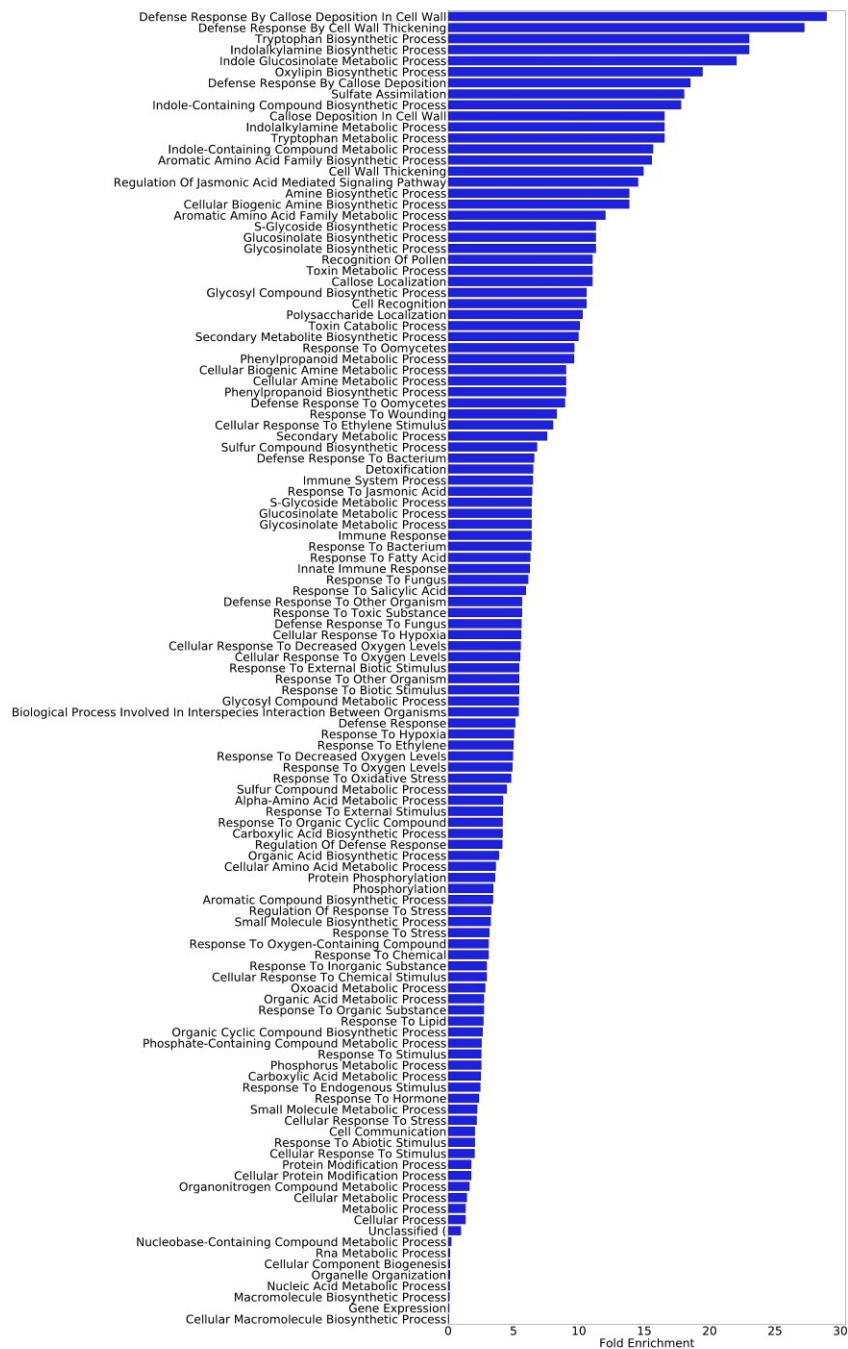
X.Jaevis | | . . .
 CORK1 SLMFPILVAF GVFIPTLFCL CRL
 AT1G29750 TTRIPTRGVY GPIISAI --- ---
 AT1G53430 TNVIPTRGVY GPLISAI --- ---
 AT1G56120 TCCPIQAGAY GPLIAAV --- ---
 AT1G07650 TTGIPIRGVY GPMISAI --- ---
 AT1G29720 TTLIPKRGNY GPLISAI --- ---
 AT1G56140 TCCPIQAGAY GPLISAV --- ---
 AT1G56130 TCCPIQAGAY GPLISAV --- ---
 AT1G53440 TNVIPTRGVY GPLISAI --- ---
 AT1G29740 TTIIIPKRGNY GSLISAI --- ---
 AT3G14840 TQAI PVRGVY GPLISAV --- ---
 AT1G53420 TTVIPKERVY GPLISAI --- ---
 AT2G22610 EGINGS---- -PVVCGI --- ---
 AT1G29730 TMIIIPQRGY GSLISAV --- ---
 AT1G72250 EGV TGA---- -AILCGI --- ---
 AT1G51860 AMTGNS--TL PPLLNALEIY TV-
 AT3G46240 WSTSSA--LL PPMINAELY VI-
 AT2G23200 GTKEAN--KD AGFLNGLEMM EV-
 AT2G14440 SKTPKS--TL PPQMNALIEIF SV-
 AT1G30570 SSVGASG--- DALLSGLEIF KL-
 AT3G05990 SPRSGS--NL PPLINGGEMF EL-
 AT3G46420 IKTERS--TL PPLLNAVEVF TV-
 AT1G25570 SSVSGA---- -PIISGLENY AI-
 AT3G46370 ERTQKS--TL PPLLNAIEVF TV-
 AT3G46270 KSTDDS--VL PTMINGLELY SI-
 AT4G39110 G-EDTGT--K NAILNGVEVL KM-
 AT1G07560 IKTPKS--TL PPLLNAIEAF IT-
 AT1G51820 VKTLKS--TL PPLLNAIEAF TV-
 AT1G24485 EATPDS--TL DPLINALELY VI-
 AT5G39030 VKDNPEY--Y EAILNGVEIL KL-
 AT3G46290 T-VHTDY--P NAIVNGLEIM KM-
 AT5G61350 PNLQSGK--P NAILNGLEIM KL-
 AT1G51805 VKTSKS--TL PPLLNAIEAF TV-
 AT5G59660 TRTNRS--TL PPLLNALEIY AV-
 AT5G39000 VSINPKY--Y DAILNGVEIL KM-
 AT3G04690 TFGQPEY--Y DSSLNGLEIF KM-
 AT1G51790 RQTQ-S-SSL PPLINAMETY FV-
 AT5G28680 TFGQPEY--Y DSQNLGIEIF KI-
 AT2G19190 LQPPGE-FVL PPIINALEVY QV-
 AT2G04300 LKTSKS--TL PPLCSALEVF TV-
 AT5G59680 IRTNRS--TL PPLLNAIEVY KV-
 AT2G19210 QQTP-R-STL PPIINAIETY RV-
 AT1G51890 SMTGNS--TH PPLINGLEIY QV-
 AT1G51880 TKTGNS--TL PPLINGLEIY KV-
 AT5G59616 RRTNRS--TL PPLLNAIEVY TV-
 AT2G28970 VRTPNs--TL PPLINALEAY TI-
 AT5G54380 S--QADI--T NATMNGLEVL KI-
 AT5G48740 RKIKFN---- -PQVSALEVY EI-
 AT2G28960 VRTPRS--TL PPLISAIEAF KV-
 AT3G21340 TKTPKS--TL PPLMNAIEVF TV-
 AT3G46280 QSTDDS--VL PPLINGLELY SI-

```

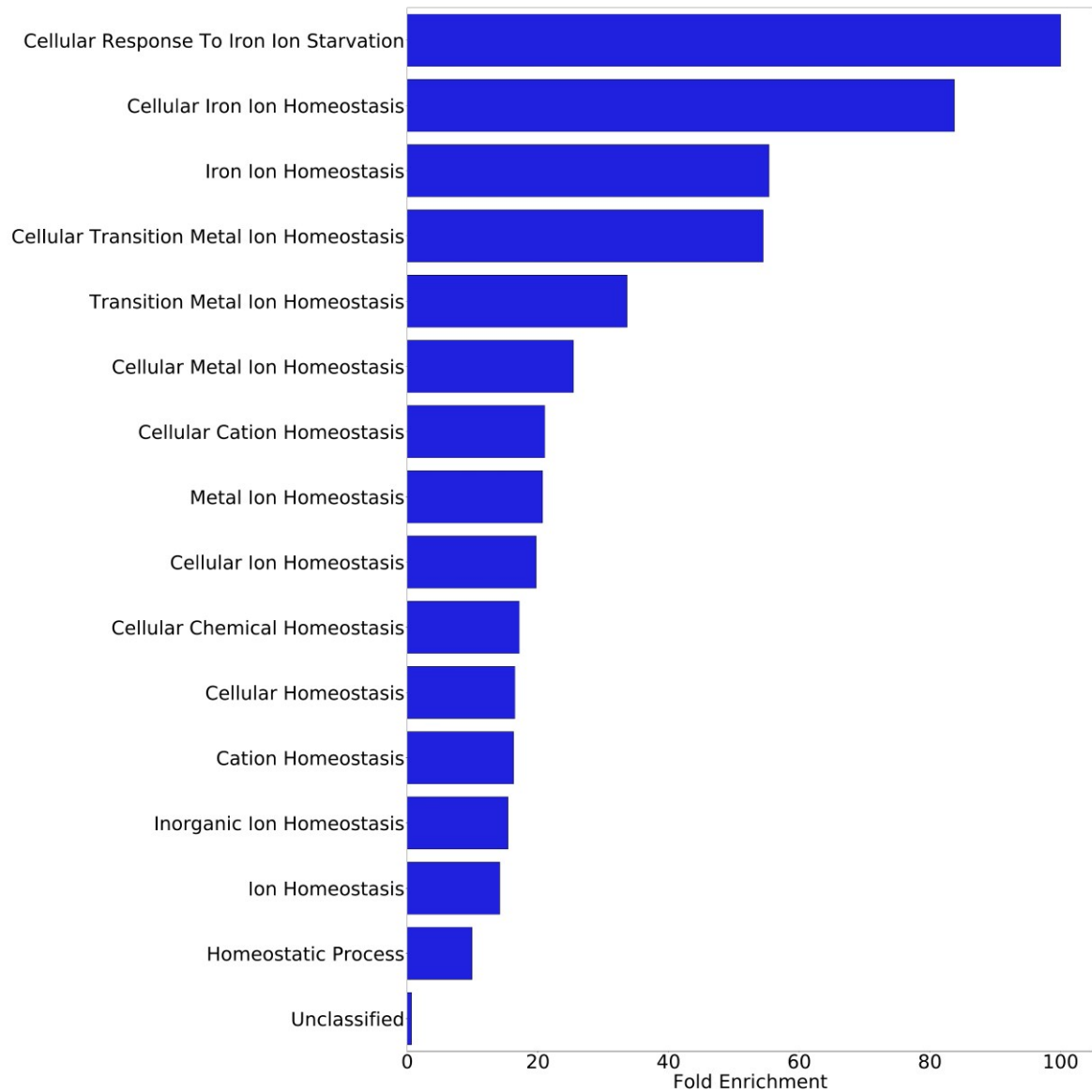
AT3G46260 KSTDDS--GL PTIISGLEVY SI-
AT1G05700 VRTP-K-STL PPIVNALEIY VA-
AT3G46400 KRTQNS--TL PPLLTAEIVF TV-
AT5G38990 KEDYPTY--Y DAILSGVEIL KL-
AT1G51800 QRTGNS--TL PPLLNAMEIY SV-
AT5G24010 DLSNPAR--V NALLNGVEIM RI-
AT2G28990 VKTPNS--TL PPLINAIEAY SV-
AT4G20450 TRTKSS--TL PPYCNAMEVF GL-
AT1G49100 VKTTKS--TL PPLINAIELF TV-
AT4G29450 QKTV-D-STL PPLINAIEIF TA-
AT1G51840 -----
AT5G59670 IRTKRS--TL PPLLNALEVY TV-
AT1G51850 VKTLKS--TL PPLLNAIEAF TV-
AT5G59700 S-VHTDY--P TAILNGLEIM KM-
AT2G19230 RQGV-K-STR PPIMNAIETY RT-
AT1G51870 EMTSNS--TL PPLLNALEIY TG-
AT3G46330 TKTQKS--TL PPLLNAFEVY SV-
AT2G29000 VRTQRS--TL PPLLNAIEVY IL-
AT3G46350 TGTIAA--DI QY-----
AT2G37050 AKTADS--SR GPILNAMEIS KY-
AT1G07550 IKTPKS--TL PPLMNAIEIF TG-
AT1G51810 VKTSRS--TL PPLINAMEAY TV-
AT4G29990 QRTG-V-STL PPIINAIEIY QI-
AT5G59650 IKTSRS--TL PSLLNALIEIY TV-
AT1G28340 PKAGGH---- -AIIINAIEVF EI-
AT3G51550 PVNKPEY--Y DSSLNGVEIF KM-
AT2G21480 G-EDTQK--K NALLNGVEVL KM-
AT5G16900 VRSEASPGVR VPLVNAMEAF TA-
AT1G67720 GKTKDS--TQ GPLLNALIEIS KY-
AT3G19230 TPAKDA--PV GPFINAGEVF QI-
AT1G51830 VETLKS--TL PPLLNAIEAF TV-
AT5G39020 KDTNQTY--Y DAILSGVEIL KL-
AT4G00300 NKTSVDGNGV DAILNGVEIM KM-
AT4G29180 QKTA-E-STR PPLINAIEIF SA-
AT1G51910 TMTTTS--TL PPLLNALEVY TL-
AT3G46340 KRTKNS--TH PPLINAIEFY TV-
AT2G14510 SKTPKS--TL PPLMNAIEIF SV-

```

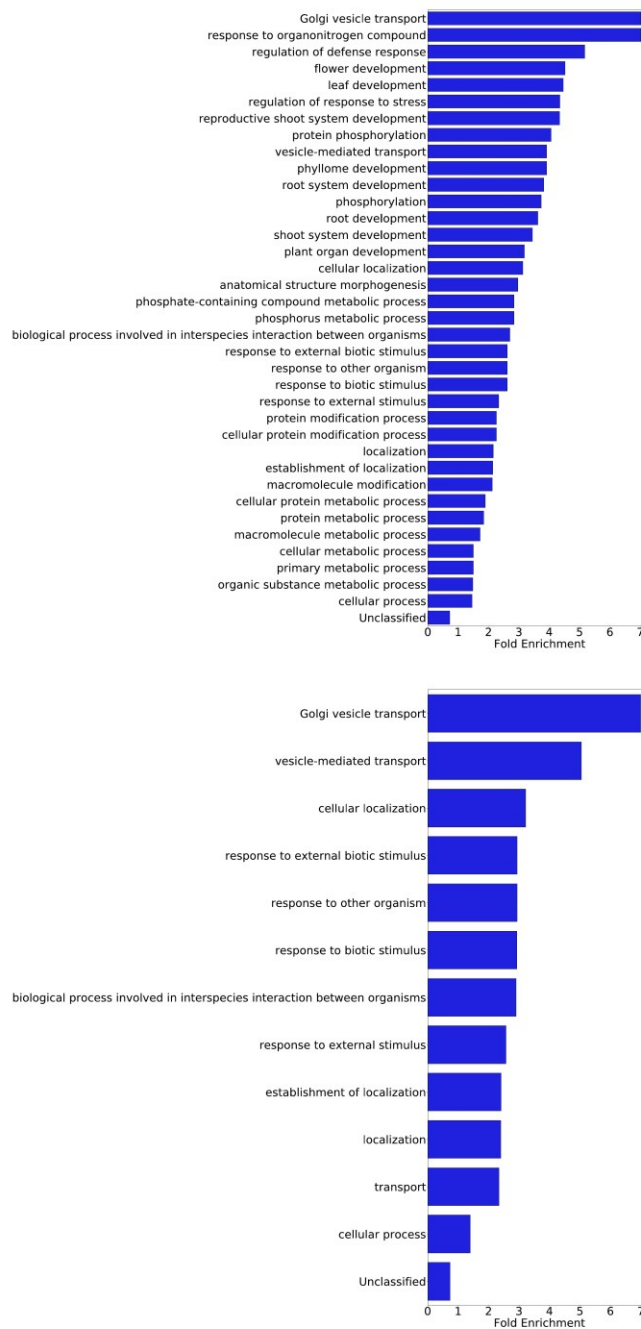
Supplementary Figure S2. Alignment of malectin domains (MD) and malectin-like domains (MLD) in *A. thaliana*, and the malectin in *X. laevis*. Black shade indicates conserved amino acid residues over 90% threshold.



Supplementary Figure S3. Biological functions enriched from up-regulated genes by 10 μ M CT compared to water control in root tissue of *cork1-2* segregated wild-type from the cross to aequorin wild-type.



Supplementary Figure S4. Biological functions enriched from down-regulated genes by 10 μ M CT compared to water control in root tissue of *cork1-2* segregated wild-type from the cross to aequorin wildtype.



Supplementary Figure S5. Biological functions enriched from phosphoproteomic analysis between 10 μ M CT compared to water control in root tissue of *cork1-2* segregated wild-type from the cross to aequorin wild-type. Top: 5 minutes after treatment; Bottom: 15 minutes after treatment.

Supplementary Table S1. Primers used in this study (5'→3').

Primers for genotyping:		
cork1-1 LP		TCTATTTAACCCGGTTCCACC
cork1-1 RP		GAATCGACAAAAGAGCAGTCCG
cork1-2 LP		CTGCTGTATTCTGCTCAAGG
cork1-2 RP		TGATATAGTGGCAATCTCCGC
LB SALK		GACCGCTTGCTGCAACTCTCTCAGG
Primers for gene expression analysis by quantitative PCR (qPCR):		
RPS (AT1G34030)	RPS-qF	GTCTCCAATGCCCTTGACAT
	RPS-qR	TCTTTCCTCTGCGACCAGTT
<i>PER4</i> (AT1G14540)	PER4-qF	ATGTGAAGTTGGTCTGAAGAG
	PER4-qR	ATGTGTGAGCTCCTGAGAGAG
<i>MYB51</i> (AT1G18570)	MYB51-qF	CTACAAGTGTTCCTGACTCTGAA
	MYB51-qR	ACGAAATTATCGCAGTACATTAGAGGA
<i>CORK1</i> (AT1G56145)	CORK1-qF	ACCAGAGTACGTGATGCTTG
	CORK1-qR	TCCATGCCCATTCGAGAAG
<i>CCOAO</i> (AT1G67980)	CCOAO-qF	TGGTGAACGACAAATGTGAGTTTG
	CCOAO-qR	ACAAAACCAAACCACAAGGTGTTG
<i>WRKY40</i> (AT1G80840)	WRKY40-qF	AGCCCTCCCAAGAAACGCAAATC
	WRKY40-qR	GCTTGGAGCACAAGCACATTTGAAG
<i>PR-1-Like</i> (AT2G19990)	AT2G19990-qF	ACGATTATGATAGTAACACGTGTG
	AT2G19990-qR	AGGATCATAGCTACAAATCACC
<i>PEN2</i> (AT2G44490)	PEN2-qF	AAGCCATCCATGAAGATGGAG
	PEN2-qR	ACCATATCCACTGTTCCACTC
<i>CYP71B15/PAD3</i> (AT3G26830)	PAD3-qF	ACGAGCATCTTAAGCCTGGA
	PAD3-qR	TCGGTCATCCCCATAGTGT
<i>TSA1</i> (AT3G54640)	TSA1-qF	TCAGTCGCTCTGAAGGATATC
	TSA1-qR	TCCAGCTATCTGTTTACATGC
<i>PMR4</i> (AT4G03550)	PMR4-qF	CTGGAATGCTGTTGTCTCTGTTG
	PMR4-qR	TCGCCTTTTGATTCTTCCCAGT
<i>WRKY30</i> (AT5G24110)	WRKY30-qF	CGGAGCCAAATTCOAAGAGG
	WRKY30-qR	GACGGAGAGTTTGATGCTGAG
<i>FLS2</i> (AT5G46330)	FLS2-qF	CGCAGACAATCTCTCGGGT
	FLS2-qR	CGTCATGTTCCCGAAGCTCT
<i>CYP81F2</i> (AT5G57220)	CYP81F2-qF	GTGAAAGCACTAGGCGAAGC
	CYP81F2-qR	ATCCGTTCCAGCTAGCATCA
Primers for plasmid construction:		
35S::CORK1 in pB7FWG2.0	CORK1-caccF	CACCATGCTGAGATTAATTCTCTCCTTG
	CORK1-R	TCATCAATGTCGTCGTCATGTTCTTC
	CORK1-NoSTOP	ATGTCGTCGTCATGTTCTTC
35S::ARF1 in pB7FWG2.0	ARF1-caccF	CACCATGGCAGCTTCCAATCATTATC
	ARF1-R	TCATCATCTTGATCCCGCCATAGATG
CORK1 ^{KD}	BamHI-KD-F	AAAAAAGGATCCAGGAAAAGAAAAGGGCGGCT
	EcoRI-KD-R	AAAAAAGAATTCTCATCAATGTCGTCGTCATGTTCTTCAAC
Primers for site-directed mutagenesis:		
G748E-F		TTGTATGAATGCTGCATTGAGG
G748E-R		TGCAGCATTCATACAATTTTACAAGG
F520A-F		TGTAACGGTTCAGGCGCTGAGATACAAATAC
F520A-R		GTATTTGTATCTCAGCCGCTGAACCGTTACA
F539A-F		CTTGAAGGCGAATTGCGGACATATATGTCCAG
F539A-R		CTGGACATATATGTCGCAATTCGCCTTCCAAG

Supplementary Table S2. UniProt accession number of amino acid sequences used in the multiple alignment for the *Arabidopsis* MD/MLD domains.

F4HSE1	Q9ASQ6	F4I336	F4I337	Q9FXF2	C0LGG7	F4HRH4	C0LGG9	F4I3K0
C0LGH2	C0LGH3	F4I3K4	F4IBQ9	F4IJK6	C0LGN2	C0LGD6	C0LGD8	C0LGD9
F4I9A5	F4ICJ5	F4HWL3	Q9SA72	F4I065	F4IB60	Q9C8I6	F4IB63	Q9FZB8
C0LGG3	Q9FZB6	F4IB68	F4IB69	C0LGG4	F4IB71	Q9FZB1	C0LGG6	F4IB76
C0LGI2	Q9SI06	Q9ZQQ7	Q9ZQR3	O64483	O65924	O64556	Q9SJT0	O22187
C0LGL4	O81067	O81069	F4IJP7	F4IPZ3	O80623	Q9SR05	Q9SFG3	F4JB46
Q9LIG2	F4J800	F4J801	Q67ZF1	Q8GYH9	Q9LX66	C0LGP2	Q9SNA3	F4J810
Q9SNA0	F4J927	Q9SN97	Q9SCZ4	Q0WQL0	C0LGQ7	F4JMW3	Q9M0D8	Q9SZV2
Q9T020	C0LGT5	Q9FLW0	Q3E8W4	Q9FID9	Q9FID8	Q9FID6	Q9FID5	C0LGV0
Q9LK35	F4KJ89	C0LGW2	F4KJ91	Q9FN94	Q9FN93	Q9FN92	Q9FLJ8	Q6INX3

5. Unpublished Results

5.1 Supplemental experiment for Manuscript 1

***Trichoderma* cell wall preparation induces cytoplasmic Ca²⁺ elevation in *Arabidopsis* roots**

As the *Trichoderma* mycelium did not possess detectable amounts of JA, ABA or JA-isoleucine (JA-Ile), I assumed that the fungus induces these phytohormones in the *Arabidopsis* roots by releasing (an) elicitor(s). Anderson-Prouty and Albersheim (1975) established a protocol for the enrichment of nonproteinous compounds from mycelial cell wall which are potentially involved in the chemical communication with their hosts (Johnson et al., 2018). Application of such cell wall preparation from *Trichoderma* (CWP-Th) to roots from *A. thaliana* seedlings expressing apoaequorin induced [Ca²⁺]_{cyt} elevation. After 30 to 40 seconds, the [Ca²⁺]_{cyt} level in the root cells reached its maximum before it declined to the level before CWP-Th application (Figure S1A). To test whether the Ca²⁺ response is induced by known elicitors, we performed the test with the *cerk1*, *bak1*, *fls2* and *cycam* mutants in the aequorin background. The *cerk1* mutant is impaired in chitin perception; the *fls2* and *bak1* defect in flagellin perception or response, and *cycam* does not respond to cellooligomers (Chinchilla et al., 2006, 2007; Miya et al., 2007; Wan et al., 2008; Johnson et al., 2018). CWP-Th induced [Ca²⁺]_{cyt} elevation in the *cerk1*, *fls2* and *bak1* mutants, but the response in the *cycam* mutant was strongly reduced (Figure S1A). This suggests that [Ca²⁺]_{cyt} elevation induced by the CWP-Th requires the poly(A) ribonuclease CYCAM, which is also required for cellooligomer signaling (Johnson et al., 2018).

CWP-Th contains at least two compounds responsible for [Ca²⁺]_{cyt} in *A. thaliana* roots

The CWP-Th was separated by HPLC. The obtained fractions were tested for their Ca²⁺-inducing activities. Two fractions induced [Ca²⁺]_{cyt} elevation in *A. thaliana* roots. The response pattern of fraction 2 resembled that of the total CWP-Th. The [Ca²⁺]_{cyt} level rose to ~ 0.2 μM within 30 seconds before decline to the baseline level (Figure S1B). Fraction 6 induced the [Ca²⁺]_{cyt} level to ~ 0.4 μM, but the response started less than 1 minute after application (Figure S1B). This suggests that the CWP-Th contains two different [Ca²⁺]_{cyt}-inducing compounds.

If the two fractions were applied to the *cycam*, *cerk1*, *fls2* or *bak1* mutants, fraction 2 failed to induce proper [Ca²⁺]_{cyt} elevation in the *cycam* mutant while all other responses were comparable to those in wild-type (Figure S1C - S1D). This confirms that fraction 2 contains compounds which require CYCAM for Ca²⁺-induction, whereas fraction 6 contains a different compound.

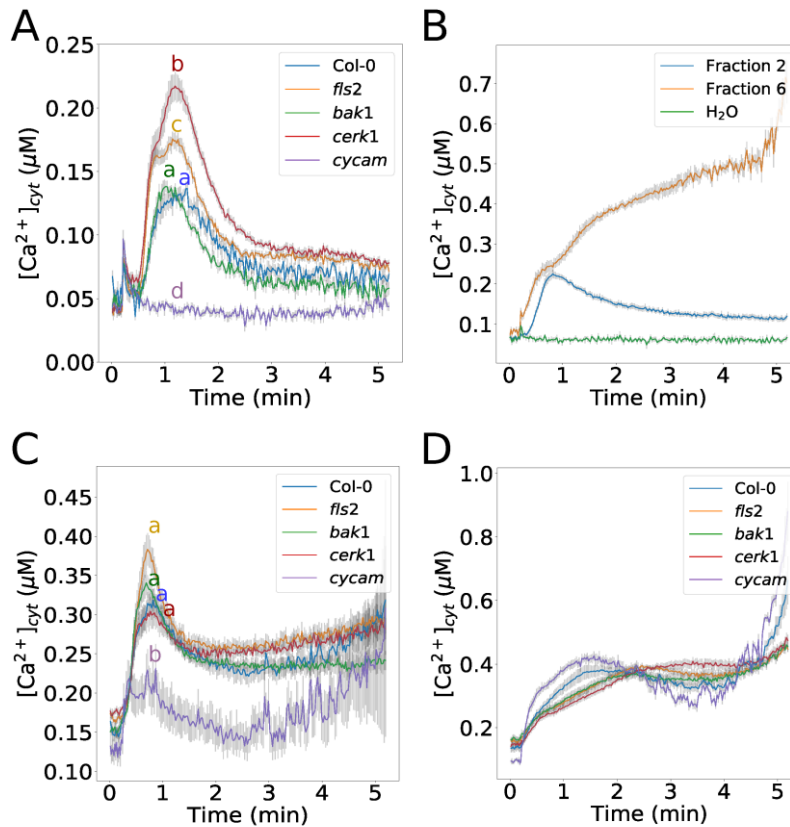


Figure S1. Mycelial cell wall material from the new *Trichoderma* strain (CWP-Th) elevates $[Ca^{2+}]_{cyt}$ in *A. thaliana* roots. **(A):** $[Ca^{2+}]_{cyt}$ measurement was carried out with wild-type (Col-0), *cerk1*, *fls2*, *bak1* and *cycam* mutants expressing cytosolic aequorin. Error bars represent SEs from 11 independent biological replicates for each genotype. Statistical significance was determined by Tukey's HSD test with $P < 0.05$, and is indicated by different lower-case letters with corresponding color. **(B):** Two fractions from the CWP-Th induced $[Ca^{2+}]_{cyt}$ in *A. thaliana* roots. Error bars represent SEs from at least 8 independent biological replicates for each treatment. **(C) and (D):** Elevation of $[Ca^{2+}]_{cyt}$ in *A. thaliana* root of wild-type (Col-0), *cerk1*, *fls2*, *bak1* and *cycam* mutants treated with fraction 2 **(C)** or with fraction 6 **(D)**. Error bars represent SEs from at least 8 independent biological replicates. Statistical significance was determined by Tukey's HSD test with $P < 0.05$, and is indicated by different lower-case letters.

Materials and Methods

Elicitor preparation from the mycelial cell walls

The preparation was done according to Anderson-Prouty and Albersheim (1975) with modifications (Johnson et al., 2014; Lee et al., 2011). The *Trichoderma* strain was cultured in potato-dextrose broth for 2 - 3 weeks at 22 °C, and mycelia were harvested by filtration through four layers of nylon membrane. After five washes with sterile H₂O, the mycelia were homogenized in sterile H₂O (1:5, w/v) with a Waring blender. The homogenate was filtered through four layers of nylon membrane. The residue was collected and washed with sterile H₂O three times, twice with chloroform/methanol (1:1, vol/vol), and twice with acetone. The material was air-dried for at least 2 hours under a sterile bench. The dried material was suspended in sterile H₂O (1 g/ 100 mL), filtered through four layers of nylon membrane followed by two layers of Whatman filter paper. Finally, the material was filter-sterilized through a 0.22 µm filter. The final preparation was named cell wall preparation-*T. harzianum* (CWP-Th).

HPLC analysis of CWP-Th and fraction collection

45 mL of CWP were concentrated to about 4 mL by rotary evaporation. Aliquots of this concentrated extract were repeatedly injected for fraction collection into an HPLC (Agilent 1100 system) using a Nucleodur Sphinx RP column (250 mm × 4.6 mm, 5 µm; Macherey-Nagel, Düren, Germany). The mobile phase consisted of 0.05% (v/v) formic acid in water as solvent A and acetonitrile as solvent B, with the flow rate set at 1 mL/min. The gradient was as follows: 0 - 15.0 min, 10 - 90% B; 15.0 - 15.1 min, 90% - 100% B; 15.1 - 16.0 min, 100% B, 16.0 - 16.1 min, 100% B - 10% B and 16.1 - 20.0 min 3% B. Eluent was monitored by a UV detector at 261 nm. The following fractions were collected: F1: 2.4 - 3.3 min, F2: 3.3 - 4.0 min, F3: 4.0 - 6.5 min, F4: 6.5 - 10.0 min, F5: 10.0 - 12.5 min, F6: 12.5 - 15.0 min. The fractions were evaporated to dryness by a rotary evaporator and resuspended in 2 mL of distilled water.

6. General discussion

Plants and microbes communicate with each other by various means. The mediating chemical elicitors exist in the cell wall material, secretome, or as volatile compounds. Upon perception of these chemical mediators, they elicit physiological response in plants, shaping the interaction. Once the plant-microbe interaction is established, in case of PGPMs, both partners gain benefits. On the other hand, pathogenic microbes take advantage of their host, resulting in loss of fitness of the host. This study covered the multifaceted mode of actions involved in this process. Characteristics of the new *Trichoderma* strain and the advantages it provided to plants were demonstrated. Potential elicitors from both partners and environmental factors which shape the interaction were examined. Next, TMTM, the fungal VOC from *M. hyalina* headspace, was unveiled. Its role in providing S nutrition to plants under S deficiency was indicated. Finally, to understand the perception system of elicitors in plants, a novel receptor kinase for COMs was identified and analyzed.

6.1 The new *Trichoderma* strain promoted plant fitness against pathogens

The new *Trichoderma* strain from this study was first isolated from the leaf of *Leucas aspera* (Willd.) Link (*Lamiaceae*). It was selected for further characterization because it promoted growth of several crop species in preliminary field experiments. In a co-cultivation system on petri-dish with *A. thaliana*, it colonized the root tissue and resided in root hairs (Manuscript 1, Figure 2E – 2G). Although *Trichoderma* species has been discovered to be endophytes in woody trees, this endophytic behavior has not been observed on other hosts (Chaverri and Samuels, 2013).

Trichoderma species are well-known for their mycoparasitism (Brotman et al., 2010). The new strain exhibited similar behavior on the pathogen *A. brassicicola* (Manuscript 1, Figure 6). Interestingly, this aggressiveness was not due to its fast growing behavior, since the fungus could out-grow *A. brassicicola* even when *A. brassicicola* had already occupied 80% of the agar medium (Manuscript 1, Figure 6D – 6E). This could be due to its abundant cell-wall degrading enzymes (Druzhinina et al., 2018). Although mycoparasitism against pathogenic fungi could be one mechanism to protect plants, it might affect the interaction between the host and other PGPMs. Several reports have indicated that some *Trichoderma* species negatively influenced AMF colonization on plants (Martinez et al., 2004; De Jaeger et al., 2010). On the other hand, other strains could be applied together with AMF to enhance plant growth (Chandanie et al., 2009; Baldi et al., 2016; Poveda et al., 2019). The new strain analyzed in this study did not affect AM formation in *N. attenuata* (Manuscript 1, Figure 8). This indicates its potential to be applied together with AMF to protect host plants without eradicating the growth promoting effect and other benefits from AMF.

Another aspect of this strain lies in its ability to redistribute phytohormone in its host (Manuscript 1, Figure 9 and Supplementary Figure 6). Redistribution of defense-related SA and JA

likely primed the plants against subsequent pathogen attack by *A. brassicicola* (Manuscript 1, Figure 7). Together with the observation on its interaction with AMF, this new strain has the potential to be developed as a new BCA in the field.

6.2 Novel elicitors from the fungal cell wall material triggered calcium response

Fungal mycelia possess phytohormones that can influence phytohormone distribution in plants, adjusting plant defense and growth (Meents et al., 2019). In the mycelium of the *Trichoderma* strain, only SA and IAA were found, while JA, JA-Ile and ABA were undetectable (Manuscript 1, Figure 7A). Therefore, there must be chemical elicitors other than phytohormones which mediate plant responses, alter the phytohormone distribution in the host after colonization, and consequently enhance plant defence. In deed, several chemicals that are involved in plant-microbe interaction have been shown to trigger plant defence *via* phytohormones (Pršić and Ongena, 2020). One strategy to discover potential elicitors is to look into the cell wall material, as non-proteinaceous components in the cell wall can induce plant defense (Anderson-Prouty and Albersheim, 1975; Johnson et al., 2018). In the cell wall preparation (CWP) of the *Trichoderma* strain, at least two fractions with potential elicitor functions were found (unpublished results, Figure 1), since they induced different calcium responses in *Arabidopsis* roots. While the $[Ca^{2+}_{\text{cyt}}]$ elevation by fraction 2 depends on the the poly(A) ribonuclease PARN, similar to the COM signaling (Johnson et al., 2018), fraction 6 might contain elicitors other than the well-known MAMPs such as COM and chitin (unpublished results, Figure 1C and 1D). Determination of the key constituents in these two fractions can strengthen our knowledge on the *Trichoderma* strain.

6.3 Environmental factors affected the growth-promotion effect by *Trichoderma*

Root architecture is often altered by microbe colonization. A typical feature of AMF is reprogramming of root development, inhibition of root growth and stimulating root branching (Bonfante and Genre, 2010; Paszkowski and Gutjahr, 2013). This was also observed on *Trichoderma*-colonized *Arabidopsis* roots (Contreras-Cornejo et al., 2015). On petri-dishes with synthetic agar medium, root growth of *N. attenuata* seedlings decreased upon fungal colonization, although more root hairs were observed (Manuscript 1, Figure 3E and 3F), showing similar effects.

However, at initial stage, the growth of *Arabidopsis* and *Nicotiana* plants was stimulated when they were grown on soil with *Trichoderma* (Manuscript 1, Figure 3A – 3D). To achieve a similar result on petri-dish for *Arabidopsis*, the medium must contain 50 mM NaCl (Manuscript 1, Figure 5A and 5B). A possible scenerio is that mild salt application enhanced fungal colonization, therefore strengthened the fungal effect on the plant (Manuscript 1, Figure 5C).

In contrast, under high salt stress (150 mM NaCl), fungal colonization occurred on both root and shoot (Manuscript 1, Figure 5C; Manuscript 3, Figure 4). This observation was not specific to this strain, as other reports also mentioned high salinity increased fungal colonization rates, and beneficial effects for the host were only observed under moderate salt conditions (Farias et al., 2020; Scharnagl et al., 2018). This indicates the PGPM function is subjected to salt.

6.4 Secretome provided new insight into the dynamics of symbiosis under different salt concentrations

During the symbiosis, both partners secrete various compounds to communicate with each other (Vincent et al., 2020). To understand how salt conditions affect root colonization by *Trichoderma* and the response of the host to the fungus, the secretomes from both partners were investigated in co-culture and alone.

Trichoderma sp. are the most successful fungi in producing lignocellulolytic enzymes for biomass conversion (Bischof et al., 2016). They acquired a large collection of these enzymes through evolution, which resulted in their pivotal role in industrial applications (Druzhinina et al., 2018). In co-culture with increasing NaCl concentration, increased lytic polysaccharide monoxygenases were found in the secreted fungal proteins (Manuscript 3, Figure 1). Conversely, the plant secreted more stress- and defense-related proteins under high salt in co-cultivation (Manuscript 3, Table 1). The high level of colonization under 150 mM NaCl indicates that the fungus tries to escape from the high salt stress. This results in an increased demand for energy, which is reflected by the increase in the digestion of plant material (Manuscript 1, Figure 5C and Manuscript 3, Figure 4).

Under mild salt stress (50 mM NaCl), fungal colonization reduced the secreted plant proteins involved in antioxidant activity. This suggests lower oxidative stress in the symbiosis (Manuscript 3, Figure 3C and Figure 5). However, in the fungal secretome, enzymes involved in carbohydrate catabolism and a prenylcysteine lyase were found (Manuscript 3, Table 1). The presence of these degradation enzymes might allow fungal colonization, and the released free sugar might also contribute to increase plant growth (Souza et al., 2017). Nevertheless, since defense proteins do not accumulate under 50 mM NaCl conditions, and the host profits from the interaction as shown by the growth promoting effect, the symbiotic interaction appears to be stable. Only under these conditions, we observed 3 secreted plant proteins (Manuscript 3, Table 1). One of them is the β -glucosidase PYK10, which is the major component in the endoplasmic reticulum (ER) body (Matsushima et al., 2003). Mutation in the basic helix–loop–helix (bHLH)-type transcription factor gene *NAIL* resulted in no ER body formation, or abnormal ER body accumulation upon JA application (Matsushima et al., 2004). *NAIL* controls the transcription of *PYK10*, and *nail* mutant resulted in over-colonization in plants, leading to reduced plant fitness (Sherameti et al., 2008). Upon tissue damage, the β -

glucosidase activity from PYK10 increased, and accumulated with its substrates (Yamada et al., 2011). It is likely that PYK10 activated proper defense to balance fungal colonization, maintaining the symbiosis at beneficial level.

6.5 Environmental factors shape the plant-*Trichoderma* interaction

The new *Trichoderma* strain possesses P solubilization ability to provide P nutrition for its host, enhancing its fitness under P deficiency (Manuscript 2, Figure 1, Figure 4 and Figure 5). However, a transition from a beneficial to a more saprotrophic life-style was observed, as under prolonged P deficiency, *Trichoderma* colonization propagated to the shoot as well (Manuscript 2, Figure 3). It seems that when the fungus experiences high level of stress in its environment, it tries to avoid it by taking advantage of the host which provides a habitat with a less hazardous environment (see also Manuscript 3, Figure 3).

Pathogenic fungi are efficient in taking advantage from their host by means of sugar acquisition (Breia et al., 2021). In plants, sugar mobilization is regulated by sugar transporters, such as SWEETs (Jeena et al., 2019). *Xanthomonas* sp. could secrete transcription activator-like (TAL) effectors to enhance the transcription of *SWEET11*, *13*, *14* in rice to increase sugar release (Chen et al., 2010). In contrast, the vacuolar type SWEET transporters in *Arabidopsis* root, SWEET2, 16, 17, played different role (Guo et al., 2014; Chen et al., 2015). *Pythium* sp. infection highly up-regulated SWEET2 expression in *Arabidopsis* (Chen et al., 2015). Instead of losing sugar to pathogen, more sugars were sequestered in the vacuole, and *sweet2* mutants demonstrated higher susceptibility towards the pathogen (Chen et al., 2015). This indicates that the regulation of sugar transporter genes might be a protective mechanism of the plant against massive hyphal propagation in the host tissue.

In the gene expression analysis of *Trichoderma* colonization upon P deficiency, *SWEET11* and *-12* were largely down-regulated, while *SUC1* and *SWEET2* were up-regulated (Manuscript 2, Figure 7). As SWEET11 and -12 are involved in pholem unloading and SUC1 is involved in transport of sugar from apoplast into root cells, respectively, the change in their transcript indicates that plants try to restrict sugar loss to the fungus (Milne et al., 2017; Sauer and Stolz, 1994); Manuscript 2, Figure 8).

The isolation and molecular characterization of the new *Trichoderma* strain, as well as its physiological effects on plants under different stress conditions, revealed that the strain could be interesting for practical application. Analysis of elicitors from the fungal cell wall and the secretomes of both partners under changing environmental threat conditions showed the potential mechanism involved in the interaction, and how the symbionts respond to environmental changes.

6.6 Effect of *M. hyalina* VOCs on plant

Microbial VOCs are involved in numerous aspects in plant-microbe interaction, from growth promotion to activating the plant defense machinery (Li et al., 2018b; Ameztoy et al., 2019; Chen et al., 2016). The volatiles from *M. hyalina*, *M. alpina* and *M. turficola* increased growth of *Arabidopsis* seedlings and induced flowering (Manuscript 4, Supplementary Figure 1). A common characteristic of the headspace of the plant growth-promoting *Mortierella* strains was their garlic-like smell. Two other *Mortierella* strains, *M. vinacea* and *M. longicolis*, did not promote plant growth nor flowering, and did not have the garlic-like smell (Manuscript 4, Supplementary Figure 1). This suggests that the distinct VOCs of the first three strains could be responsible for or involved in the growth promoting effects.

From *M. hyalina*, TMTM was found to be the major compound, while two other S-containing volatiles, dimethyl trithiocarbonate and bis(methylthio)methane, contributed only to ~4% of the total headspace (Manuscript 4, Table 1). It is known that microbial VOCs can trigger growth promotion at low concentration, while high concentrations have inhibitory effects (Blom et al., 2011; Park et al., 2015; Choi et al., 2016). Under our conditions, TMTM did not promote plant growth on full media, while co-cultivation with the fungus did. Therefore, additional factors, such as the two low abundant VOCs and/or additional unknown compounds, participate in the growth response. Concentration of each components may also play a role in growth promotion.

However, under S deficiency, TMTM treatment sustained plant growth (Manuscript 4, Figure 3 and Figure 4). This was achieved by the incorporation of TMTM into plant metabolites such as cysteine, methionine, GSH and GSLs (Manuscript 4, Figure 2). We observed a shift in the S homeostasis (Manuscript 4, Figure 5 and Figure 6). The dynamics of TMTM incorporation was also inferred from the expression of *SDI1* and *SDI2*, two marker genes for S deficiency (Aarabi et al., 2016). Under S deficiency, *SDI1* down-regulated the activity of the transcription factor MYB28 by forming a complex with it, and reduced GSL biosynthesis to preserve available S for growth (Gigolashvili et al., 2007; Aarabi et al., 2016). The changes in *SDI1* and *SDI2* expression can be explained by available S in the plant, which is higher upon TMTM treatment (Manuscript 4, Figure 5).

On the other hand, high dosage of TMTM induced GSH and GSLs accumulation (Manuscript 4, and Figure 6). High amount of TMTM may redirect plant to synthesize the defense-related secondary metabolites GSLs, while seedling's growth is reduced (Manuscript 4, Figure 1). GSLs are known to be involved in defense against herbivores (Jeschke and Burow, 2018), while GSH possesses antioxidant ability (Tausz et al., 2004). Thus high doses of TMTM may stimulate the biosynthesis of S-containing secondary defense compound as well as strengthen the antioxidant capacity of the plant. Exploring whether TMTM contributes to biotic/abiotic stress resistance in natural environments would

be another direction to understand the role of the volatile for the performance of the plants. Recently, a S-containing volatile from bacteria was shown to protect potato plants against pathogens (Chinchilla et al., 2019). It would be interesting to know whether TMTM can also act as pesticide.

6.7 Incorporation pathway of S-containing VOCs into plant metabolism

The first hypothesis for TMTM incorporation is that the organosulfide could be a substrate for O-acetylserine(thiol)lyases (OASTLs), since the assimilated sulfate is first transformed to sulfide for OASTLs to produce cysteine (Mugford et al., 2011). However, this does not occur in our case (Manuscript 4, Figure 7). Studies on the garlic S-containing volatile diallyl disulfide (DADS) showed that the organosulfide also affected sulfur metabolism genes and metabolites in plants (Cheng et al., 2016, 2020; Yang et al., 2019). The involvement of GSH and cysteine were suggested to be involved in DADS incorporation (Bolton et al., 2019; Liang et al., 2015; Cai and Hu, 2017). GSH reacted with DADS to generate S-allyl GSH and a short-lived intermediate allyl perthio, through α -carbon nucleophilic substitution. The allyl perthio reacted with another GSH molecule, releasing H₂S and S-allyl GSH disulfide (Liang et al., 2015). This mechanism could be another path for the incorporation of TMTM. Accumulation of GSH is consistent with its requirement for the biochemical reaction. Therefore, unlike sulfate assimilation, the GSH/GSSG (glutathione disulfide) system might play a crucial part in organosulfide assimilation. A detailed metabolomic analysis of early sulfur-containing compounds after TMTM treatment might elucidate the early steps in the mechanism.

6.8 Synthetic pathway of S-containing VOCs in microbes

Since microbes can produce VOCs that have potential to improve plant nutrition, understanding how these VOCs are produced can allow us to engineer strains for their production. Catabolic processes such as glycolysis, proteolysis, and lipolysis are the major pathways for microbial VOC synthesis (Peñuelas et al., 2014; Veselova et al., 2019). The isoprenoid pathway gives rise to isoprene, monoterpenes and sesquiterpenes (Schmidt et al., 2015). From amino acids, N- and S-containing volatiles, such as benzonitrile or dimethyl disulfide, can be generated (Schmidt et al., 2015). Finally, alkanes and alkenes can be generated from fatty acids (Schmidt et al., 2015).

For S-containing VOCs, it is known that lactic acid bacteria can produce methanethiol, dimethyl sulfide (DMS) and DMDS. The biosynthetic pathway starts by L-methionine γ -lyase to process L-methionine or by transamination and subsequent reductive demethylation of L-methionine. Cystathionine β -lyase and cystathionine γ -lyase are also proposed to be involved in VOC production, which utilize thiol-containing amino acids (Schulz and Dickschat, 2007). Co-cultivation of VOC-producing microbes with crops could be a new direction for future agricultural research.

6.9 Receptor perception of chemical mediators

Receptor kinases have been shown to perceive various MAMPs and DAMPs (CERK1, FLS2, WAK1). To understand how chemical elicitors are recognized and how they trigger plant response, the receptor of COMs, named CORK1, was identified and characterized (Manuscript 5). So far, this is the first receptor for cellulose fragment perception, and is the second receptor recognizing cell wall fragments after pectin and its OG fragments (Brutus et al., 2010; Tang et al., 2022).

Mitogen-activated protein kinase (MAPK) cascades play a pivotal role in signal transduction of these MAMPs and DAMPs. Bacterial flagellin triggered phosphorylation of MAPKKK8 (MEKK1), MKK4/MKK5 and MPK3/MPK6, leading to up-regulation of *WRKY22/WRKY29* in *Arabidopsis* (Asai et al., 2002). In turn, chitin triggered phosphorylation of PBL27, MAPKKK5, MKK4/MKK5 and MPK3/MPK6 in *Arabidopsis*, and OsMAPKKK18, OsMKK4 and OsMPK3/OsMPK6 in rice (Yamada et al., 2016, 2017). Application of COMs induced MPK3/MPK6 phosphorylation in *Arabidopsis*, as also reported for other cell wall breakdown products (Manuscript 5, Table 2; Johnson et al., 2018; Souza et al., 2017; Claverie et al., 2018; Mélida et al., 2020; Rebaque et al., 2021; Yang et al., 2021a). It appears that MPK3/MPK6 are situated at the converging point for MAMPs and DAMPs signalling. However, other phosphorylation targets for DAMPs have not yet been reported.

In our phosphoproteomic study using the *cork1* mutant, we identified the early (5 min) and the late (15 min) phosphorylation target proteins of CORK1 after CT perception (Manuscript 5, Table 2 and Supplementary Dataset 2). Most of the targets are related to CSC, the ER secretory pathway, signal transduction, or defense/stress responses. For example, Cellulose synthase 1 (CESA1) and Cellulose Synthase-Interactive 1 (CSII) were phosphorylated after CT treatment, and phosphorylation of CESA1 and CSII affects the mobility of the CSC (Chen et al., 2010; Li et al., 2015). Interestingly, phosphorylation of FERONIA (FER) was also observed, which indicates that CORK1 may communicate with FER about cell wall integrity (CWI). Considering the observation that CORK1 specifically perceive COMs, it is likely a new player in monitoring and regulating CWI.

Besides phosphorylation events, perception of chemical mediators also modulate gene expression. For example, COM treatment led to up-regulation of *WRKY30* and *WRKY40* in a receptor-dependent fashion (Manuscript 5, Figure 5). From our transcriptomic analysis (Manuscript 5, Figure 7, Table 1 and Supplementary Dataset 1), we also discovered an up-regulation of genes involved in tryptophan biosynthesis (eg. *TSA1*, encoding tryptophan synthase α chain) and secondary metabolite biosynthesis (eg. *PER4*, encoding a peroxidase involved in lignin biosynthesis). Unexpectedly, genes indispensable for proper callose deposition after flagellin treatment were also up-regulated by CT (such as *MYB51*, *UDP-glycosyltransferase 74B1*, *ABCG36* and *CYP81F2*; Clay et al., 2009). Although callose deposition was not detected after COM application (Souza et al., 2017), this could

be explained by the low induction of callose synthase *PMR4*. Nevertheless, this result demonstrates an overlap of signaling events between PAMPs and DAMPs, and treatment of COM can likely prepare the plants for faster or stronger response towards PAMPs, as the synegetic effects by pre- or co-treatment of COMs and other elicitors trigger faster or higher calcium signaling, ROS production and MPK3/MPK6 phosphorylation (Souza et al., 2017; Johnson et al., 2018).

6.10 Lectin receptor-like kinases (LecRLKs)

Lectins are carbohydrate-binding proteins prevalent in both animal and plant kingdom. The first discovered member was ricin, a highly toxic protein reside in seeds of castor bean (*Ricinus communis* L.) owing to its hemagglutination activity (Stillmark, 1888). It is now known that animals and plants possess more than 20 different types of lectins (Tsaneva and Van Damme, 2020). They can be localized in different subcellular compartments, from the nucleus, ER, vacuole to the cell membrane. Each of them recognizes different sugars, and most of them are involved in the immune system (Tsaneva and Van Damme, 2020).

According to protein sequence homology and function, lectins can be categorized into C-, G-, L-type lectins, and proteins with lysine motives (LysM) or malectin/malectin-like carbohydrate-binding modules (CBMs). C-type lectins require calcium for substrate binding, and can be further categorized into 17 subgroups according to their domain structure (Zelensky and Gready, 2005; Bellande et al., 2017). G-type lectins contain a *Galanthus nivalis* agglutinin mannose-binding motif. They are also called B-type lectin, because they are commonly found in the bulb of *Galanthus nivalis* in high amount (Teixeira et al., 2018; Bellande et al., 2017). L-type lectins are found in legume seeds (hence L-type). Several of the L-type LecRLKs has been demonstrated in bacterial defense mechanism in plants (Balagué et al., 2017; Huang et al., 2014). LysM-RLKs (LYKs) have been found to perceive Nod factors, and recognize chitin in cooperation with CERK1 to induce immunity (Arrighi et al., 2006; Fliegmann et al., 2013; Willmann et al., 2011; Cao et al., 2014).

6.11 Malectin/malectin-like domain receptor kinases (MD-/MLD-RLKs)

The last group of carbohydrate-binding proteins are malectins, first described in *Xenopus* (Schallus et al., 2008). It is a highly conserved sugar-binding protein in animals, and localized on the ER membrane important for protein glycosylation (Schallus et al., 2008; Galli et al., 2011). The distribution of malectin-domain containing proteins is widely found in plants, but not in fungi (Yang et al., 2021b).

In *Arabidopsis*, most of the malectin domains are found to be coupled with receptor-like proteins RLPs or RLKs, while two proteins have a MD-kinesin-like structure. MLD proteins contain two MD domains. It can be in combination with RLKs (MLD-RLKs), RLPs (MLD-RLPs), or with

LRR domains after the MLD (MLD-LRR-RLKs). However, all MD-RLKs found so far have a N-terminal LRR domain (LRR-MD-RLKs; Yang et al., 2021b).

Biological function of several MLD-LRR-RLKs has been demonstrated. FRK1 (Flg22-Induced Receptor-Like Kinase 1; AT2G19190) is a MLD-LRR-RLK and the gene is one of the early responsive gene for flagellin perception (Asai et al., 2002). Another protein with the same structure is IOS1 (Impaired Oomycete Susceptibility 1; AT1G51800). It can interact with BAK1 to mediate immunity against pathogens such as *Oomycetes* and *Pseudomonas syringae* (Hok et al., 2014; Yeh et al., 2016). In legume plants, MLD-LRR-RLKs play a decisive role in the nodulation by rhizobia. This feature gives them the name symbiosis receptor-like kinase (SYMRK; Stracke et al., 2002; Ané et al., 2002; Antolín-Llovera et al., 2014b; Gherbi et al., 2008). Upon perception of Nod factors, the MLD is cleaved from the GIPC sequence, leaving only the LRR domain outside of the cell membrane (Antolín-Llovera et al., 2014b). The cleaved SYMRK can then interact with Nod factor receptors (NFRs) to pass on the signal cascades (Antolín-Llovera et al., 2014b, 2014a). Through domain-swap experiments, it has recently been found that the cytoplasmic domain of the SYMRK is important for the proper signaling for nodule formation (Li et al., 2018a).

The MLD-RLKs are well known for their involvement in CWI signaling and in development of reproductive organs. *FERONIA* (*FER*), one of the the first characterized member in the *Catharanthus roseus* RLK1-like (CrRLK1L) protein family, is involved in pollen tube development (Escobar-Restrepo et al., 2007; Duan et al., 2014). The *fer* knock-out mutants showed severed female fertility due to incompetence in pollen tube rupture and sperm release (Escobar-Restrepo et al., 2007). Four more members in this group, *ANXURI/ANXUR2* (*ANX1/ ANX2*) and *Buddha's Paper Seal /Buddha's Paper Seal 2* (*BUPSI/BUPS2*), were shown to interact with each other to prevent precocious pollen tube rupture (Miyazaki et al., 2009; Ge et al., 2017; Boisson-Dernier et al., 2009). Furthermore, *FER* is involved in mechano sensing and binding to pectin (Shih et al., 2014; Feng et al., 2018; Tang et al., 2022). *THESEUS* (*THE1*) is another member found as CWI sensor, as it was first identified in screening in the cellulose deficient mutant *procuste1-1* (Hématy et al., 2007). Furthermore, the RALF (rapid alkalization factor) peptides are ligands for the MLD-RLKs mentioned here (Ge et al., 2017; Gonneau et al., 2018; Zhang et al., 2020). The last clade consists of MLD-RLPs. Some of them have been expressed in *Arabidopsis*, but their functions remain unknown (Sultana et al., 2020).

In contrast, proteins in the group LRR-MD-RLK are not well-studied. Most of them are designated as Brassinosteroid-Signaling Kinase 3-Interacting RLKs (BSRs; Xu et al., 2014). LIK1 (LysM RLK1-Interacting Kinase; AT3G14840) was shown to be phosphorylated by CERK1, and *lik1* mutants exhibited different resistance levels against hemibiotrophic or necrotrophic pathogens (Le et al., 2014). It is also likely to perceive LPS (Hussan et al., 2020). *RKF1* (*Receptor-Like Kinase*

In Flowers 1; AT1G29720) was found to be involved in regulating pollen hydration for proper pollen tube growth at the early stages (Lee and Goring, 2021). *LMK1* (*Leucine-Rich Repeat Receptor-Like Kinase With Extracellular Malectin-Like Domain 1*; At1g07650) was involved in sensing carbon/nitrogen stress, and overexpression of *LMK1* induced cell death in leaf (Li et al., 2020).

Although these MD-RLKs, MLD-RLPs and MLD-RLKs possess the potential saccharide binding domain, apart from *FER* which was shown to bind to pectin, none of them has been experimentally demonstrated to be a receptor for saccharides (Tang et al., 2022). WAK1 (Cell Wall-Associated Kinase 1) is the only receptor so far identified to bind to polysaccharide, although it possesses a epidermal growth factor (EGF) domain instead of MD/MLD (Brutus et al., 2010; Kohorn and Kohorn, 2012).

Therefore, *CORK1* is the first LRR-MD-RLK demonstrated to perceive sugars (Manuscript 5, Figure 1 – Figure 4). The importance of MD in sugar perception was further demonstrated by mutation in the two conserved phenylalanine residues in the MD (Manuscript 5, Figure 6). However, *CORK1* should not be the only receptor for sugars, as various sugars have been show to elicit calcium signaling and ROS production in plants. The uncharacterized LRR-MD-RLKs might be potential candidates.

6.12 Conclusion and future perspectives

This thesis exemplifies effects of PGPMs and their chemical mediators on model plants. The study identified novel mediators and perception systems, which extends our knowledge on plant-microbe interaction.

The new *Trichoderma* strain has potential for commercial use. However, it is important to note that it may not be suitable for all kinds of environments. This strain can solubilize P to provide plants and can rescue salt stress, but if the environmental stress is too harsh, the benefit from the fungal colonization may be reduced, and could possibly harm plants in the field. Therefore, field studies under various conditions should be carried out to determine when and where this strain can be applied. Similarly, for the development of other bacterial or fungal strains, environmental factors should always be taken into account. A single strain can not always provide benefit to plants under all circumstances. Furthermore, the interaction with other microbes in the rhizosphere should also be considered. For example, although aggressive towards pathogens, the new *Trichoderma* strain did not affect AM formation. Testing the compatibility of new PGPMs with each other is important, so they can have synergistic effect to provide crops with maximum benefit.

The characterized *Trichoderma* strain appears to communicate with the roots via new chemical elicitors in their cell wall, however, whether and how they influence plant growth and defence or phytohormone distribution should be further examined.

I demonstrated that volatile compounds can provide nutrition and promote plant growth. However, complete understanding of the mechanism of TMTM incorporation would provide us with better ideas of how plants utilize atmospheric S. As proposed by Loreto and D'Auria (2021), there could be a group of specific proteins which perceive TMTM. Isotope labelling experiments and metabolomics should be helpful to elucidate the metabolic pathway. Even if the hypothesis proposed here is not supported by future studies, metabolomic experiments will provide important information on how TMTM reacts with cellular components. Future research should focus on the role of the GSH/GSSG system, since previous findings also showed the incorporation of GSH into DADS. Moreover, in Manuscript 4, the reduction of GSH is less than GSLs, indicating a possible replenishment of GSH by TMTM, while GSLs needed to be converted from other S-containing compounds. The connection between these S-containing metabolites may be altered by TMTM.

Finally, the identification of the COM-receptor CORK1 opens a new gateway to explore sugar perception in plants. As discussed, none of the MD/MLD-RLKs has been shown to be involved in sugar binding. Therefore, looking into other members that belongs to the same clade as *CORK1* could elucidate the perception system of other cell wall sugars. The mechanism of how malectin binds to sugars can also be studied. One way is to isolate the MDs/MLDs from different candidates and apply different sugars on them for isothermal titration calorimetry (ITC) or surface plasmon resonance (SPR) assays. Different mutations can be introduced at the conserved residues to see if the interaction is influenced (Manuscript 5, Figure 6). Computer modelling or crystallization with sugar ligands can demonstrate which sugar can bind and which of the conserved amino acid residues participate in binding. Most importantly, with knock-out/over-expression mutants, the function of these MD-RLKs in plant growth and development or in plant-microbe interaction can be analyzed. As *cork1* mutants did not show noticeable phenotype under optimal lab growth conditions, it is likely that other members participate in sugar sensing.

In the near future, not only more PGPMs will be discovered, but how they interact with plants will also be clarified through these important chemical mediators and delicate mechanisms. This will definitely reinforce our knowledge to manipulate plant growth, and provide a better sustainable way for future agriculture.

7. References

- Aarabi, F. et al.** (2016). Sulfur deficiency–induced repressor proteins optimize glucosinolate biosynthesis in plants. *Sci. Adv.* **2**: e1601087.
- Akum, F.N., Steinbrenner, J., Biedenkopf, D., Imani, J., and Kogel, K.-H.** (2015). The *Piriformospora indica* effector PIIN_08944 promotes the mutualistic Sebacinalean symbiosis. *Front. Plant Sci.* **6**: 906.
- Ameztoy, K. et al.** (2019). Plant responses to fungal volatiles involve global posttranslational thiol redox proteome changes that affect photosynthesis. *Plant Cell Environ.* **42**: 2627–2644.
- Anderson-Prouty, A.J. and Albersheim, P.** (1975). Host-pathogen interactions: VIII. Isolation of a pathogen-synthesized fraction rich in glucan that elicits a defense response in the pathogen's host. *Plant Physiol.* **56**: 286–291.
- Ané, J.-M. et al.** (2002). Genetic and cytogenetic mapping of DMI1, DMI2, and DMI3 genes of *Medicago truncatula* involved in Nod factor transduction, nodulation, and mycorrhization. *Mol. Plant-Microbe Interact.* **15**: 1108–1118.
- Antolín-Llovera, M., Petutsching, E.K., Ried, M.K., Lipka, V., Nürnberger, T., Robatzek, S., and Parniske, M.** (2014a). Knowing your friends and foes--plant receptor-like kinases as initiators of symbiosis or defence. *New Phytol.* **204**: 791–802.
- Antolín-Llovera, M., Ried, M.K., and Parniske, M.** (2014b). Cleavage of the SYMBIOSIS RECEPTOR-LIKE KINASE ectodomain promotes complex formation with Nod factor receptor 5. *Curr. Biol.* **24**: 422–427.
- Arora, N.K., Fatima, T., Mishra, I., and Verma, S.** (2020). Microbe-based Inoculants: Role in Next Green Revolution. In *Environmental Concerns and Sustainable Development: Volume 2: Biodiversity, Soil and Waste Management*, V. Shukla and N. Kumar, eds (Springer: Singapore), pp. 191–246.
- Arrighi, J.-F. et al.** (2006). The *Medicago truncatula* lysin motif-receptor-like kinase gene family includes NFP and new nodule-expressed genes. *Plant Physiol.* **142**: 265–279.
- Asai, T., Tena, G., Plotnikova, J., Willmann, M.R., Chiu, W.-L., Gomez-Gomez, L., Boller, T., Ausubel, F.M., and Sheen, J.** (2002). MAP kinase signalling cascade in *Arabidopsis* innate immunity. *Nature* **415**: 977–983.
- Atmodjo, M.A., Hao, Z., and Mohnen, D.** (2013). Evolving views of pectin biosynthesis. *Annu. Rev. Plant Biol.* **64**: 747–779.
- Baiyee, B., Pornsuriya, C., Ito, S., and Sunpapao, A.** (2019). *Trichoderma spirale* T76-1 displays biocontrol activity against leaf spot on lettuce (*Lactuca sativa* L.) caused by *Corynespora cassiicola* or *Curvularia aeria*. *Biol. Control* **129**: 195–200.

- Bakhtiari, M. and Rasmann, S.** (2020). Variation in below-to abovegrounds systemic induction of glucosinolates mediates plant fitness consequences under herbivore attack. *J. Chem. Ecol.* **46**: 317–329.
- Bakshi, M., Vahabi, K., Bhattacharya, S., Sherameti, I., Varma, A., Yeh, K.-W., Baldwin, I., Johri, A.K., and Oelmüller, R.** (2015). WRKY6 restricts *Piriformospora indica*-stimulated and phosphate-induced root development in *Arabidopsis*. *BMC Plant Biol.* **15**: 305.
- Balagué, C., Gouget, A., Bouchez, O., Souriac, C., Haget, N., Boutet-Mercey, S., Govers, F., Roby, D., and Canut, H.** (2017). The *Arabidopsis thaliana* lectin receptor kinase LecRK-I.9 is required for full resistance to *Pseudomonas syringae* and affects jasmonate signalling. *Mol. Plant Pathol.* **18**: 937–948.
- Baldi, E., Amadei, P., Pelliconi, F., and Tosell, M.** (2016). Use of *Trichoderma* spp. and arbuscular mycorrhizal fungi to increase soil beneficial population of bacteria in a nectarine commercial orchard: Effect on root growth, nutrient acquisition and replanting disease. *J. Plant Nutr.* **39**: 1147–1155.
- Bashan, Y. and de-Bashan, L.E.** (2010). How the Plant Growth-Promoting Bacterium *Azospirillum* Promotes Plant Growth—A Critical Assessment - ScienceDirect. In *Advances in Agronomy* (Academic Press), pp. 77–136.
- Bauer, J.T., Kleczewski, N.M., Bever, J.D., Clay, K., and Reynolds, H.L.** (2012). Nitrogen-fixing bacteria, arbuscular mycorrhizal fungi, and the productivity and structure of prairie grassland communities. *Oecologia* **170**: 1089–1098.
- Baum, C. and Hryniewicz, K.** (2006). Clonal and seasonal shifts in communities of saprotrophic microfungi and soil enzyme activities in the mycorrhizosphere of *Salix* spp. *J. Plant Nutr. Soil Sci.* **169**: 481–487.
- Beijerinck, M.W.** (1904). Phenomenes de reduction produits par les microbes. *Arch. Néerlandaises Sci. Exactes Nat. (Section 2)* **9**: 131–157.
- Bellande, K., Bono, J.-J., Savelli, B., Jamet, E., and Canut, H.** (2017). Plant lectins and lectin receptor-like Kinases: How do they sense the outside? *Int. J. Mol. Sci.* **18**: E1164.
- Bellenger, J.P., Darnajoux, R., Zhang, X., and Kraepiel, A.M.L.** (2020). Biological nitrogen fixation by alternative nitrogenases in terrestrial ecosystems: a review. *Biogeochemistry* **149**: 53–73.
- Birkinshaw, J.H. and Chaplen, P.** (1955). Biochemistry of the wood-rotting fungi. 8. Volatile metabolic products of *Daedalea juniperina* Murr. *Biochem. J.* **60**: 255–261.
- Bischof, R.H., Ramoni, J., and Seiboth, B.** (2016). Cellulases and beyond: the first 70 years of the enzyme producer *Trichoderma reesei*. *Microb. Cell Factories* **15**: 106.

- Blom, D., Fabbri, C., Connor, E.C., Schiestl, F.P., Klauser, D.R., Boller, T., Eberl, L., and Weisskopf, L.** (2011). Production of plant growth modulating volatiles is widespread among rhizosphere bacteria and strongly depends on culture conditions. *Environ. Microbiol.* **13**: 3047–3058.
- Boisson-Dernier, A., Roy, S., Kritsas, K., Grobei, M.A., Jaciubek, M., Schroeder, J.I., and Grossniklaus, U.** (2009). Disruption of the pollen-expressed FERONIA homologs ANXUR1 and ANXUR2 triggers pollen tube discharge. *Dev. Camb. Engl.* **136**: 3279–3288.
- Boleta, E.H.M., Shintate Galindo, F., Jalal, A., Santini, J.M.K., Rodrigues, W.L., Lima, B.H. de, Arf, O., Silva, M.R. da, Buzetti, S., and Teixeira Filho, M.C.M.** (2020). Inoculation with growth-promoting bacteria *Azospirillum brasilense* and its effects on productivity and nutritional accumulation of wheat cultivars. *Front. Sustain. Food Syst.* **4**: 265.
- Bolton, S.G., Cerda, M.M., Gilbert, A.K., and Pluth, M.D.** (2019). Effects of sulfane sulfur content in benzyl polysulfides on thiol-triggered H₂S release and cell proliferation. *Free Radic. Biol. Med.* **131**: 393–398.
- Bonfante, P. and Genre, A.** (2010). Mechanisms underlying beneficial plant–fungus interactions in mycorrhizal symbiosis. *Nat. Commun.* **1**: 1–11.
- Bononi, L., Chiaramonte, J.B., Pansa, C.C., Moitinho, M.A., and Melo, I.S.** (2020). Phosphorus-solubilizing *Trichoderma* spp. from Amazon soils improve soybean plant growth. *Sci. Rep.* **10**: 2858.
- Breia, R., Conde, A., Badim, H., Fortes, A.M., Gerós, H., and Granell, A.** (2021). Plant SWEETs: from sugar transport to plant-pathogen interaction and more unexpected physiological roles. *Plant Physiol.* **186**: 836–852.
- Brock, N.L., Tudzynski, B., and Dickschat, J.S.** (2011). Biosynthesis of sesqui- and diterpenes by the gibberellin producer *Fusarium fujikuroi*. *Chembiochem Eur. J. Chem. Biol.* **12**: 2667–2676.
- Brotman, Y., Briff, E., Viterbo, A., and Chet, I.** (2008). Role of swollenin, an expansin-like protein from *Trichoderma*, in plant root colonization. *Plant Physiol.* **147**: 779–789.
- Brotman, Y., Kapuganti, J.G., and Viterbo, A.** (2010). *Trichoderma*. *Curr. Biol.* **20**: R390-391.
- Brutus, A., Sicilia, F., Macone, A., Cervone, F., and De Lorenzo, G.** (2010). A domain swap approach reveals a role of the plant wall-associated kinase 1 (WAK1) as a receptor of oligogalacturonides. *Proc. Natl. Acad. Sci. U. S. A.* **107**: 9452–9457.
- Cai, Y.-R. and Hu, C.-H.** (2017). Computational study of H₂S release in reactions of diallyl polysulfides with thiols. *J. Phys. Chem. B* **121**: 6359–6366.

- Cao, Y., Liang, Y., Tanaka, K., Nguyen, C.T., Jedrzejczak, R.P., Joachimiak, A., and Stacey, G.** (2014). The kinase LYK5 is a major chitin receptor in *Arabidopsis* and forms a chitin-induced complex with related kinase CERK1. *eLife* **3**: e03766.
- Cartieaux, F., Thibaud, M.-C., Zimmerli, L., Lessard, P., Sarrobert, C., David, P., Gerbaud, A., Robaglia, C., Somerville, S., and Nussaume, L.** (2003). Transcriptome analysis of *Arabidopsis* colonized by a plant-growth promoting rhizobacterium reveals a general effect on disease resistance. *Plant J. Cell Mol. Biol.* **36**: 177–188.
- Cavagnaro, T.R., Jackson, L.E., Six, J., Ferris, H., Goyal, S., Asami, D., and Scow, K.M.** (2006). Arbuscular mycorrhizas, microbial communities, nutrient availability, and soil aggregates in organic tomato production. *Plant Soil* **282**: 209–225.
- Chandanie, W.A., Kubota, M., and Hyakumachi, M.** (2009). Interactions between the arbuscular mycorrhizal fungus *Glomus mosseae* and plant growth-promoting fungi and their significance for enhancing plant growth and suppressing damping-off of cucumber (*Cucumis sativus* L.). *Appl. Soil Ecol.* **41**: 336–341.
- Chaverri, P. and Samuels, G.J.** (2013). Evolution of habitat preference and nutrition mode in a cosmopolitan fungal genus with evidence of interkingdom host jumps and major shifts in ecology. *Evol. Int. J. Org. Evol.* **67**: 2823–2837.
- Chen, H.-Y., Huh, J.-H., Yu, Y.-C., Ho, L.-H., Chen, L.-Q., Tholl, D., Frommer, W.B., and Guo, W.-J.** (2015). The *Arabidopsis* vacuolar sugar transporter SWEET2 limits carbon sequestration from roots and restricts *Pythium* infection. *Plant J.* **83**: 1046–1058.
- Chen, J.-L., Sun, S.-Z., Miao, C.-P., Wu, K., Chen, Y.-W., Xu, L.-H., Guan, H.-L., and Zhao, L.-X.** (2016). Endophytic *Trichoderma gamsii* YIM PH30019: A promising biocontrol agent with hyperosmolar, mycoparasitism, and antagonistic activities of induced volatile organic compounds on root-rot pathogenic fungi of *Panax notoginseng*. *J. Ginseng Res.* **40**: 315–324.
- Chen, L.-Q. et al.** (2010). Sugar transporters for intercellular exchange and nutrition of pathogens. *Nature* **468**: 527–532.
- Chen, S., Ehrhardt, D.W., and Somerville, C.R.** (2010). Mutations of cellulose synthase (CESA1) phosphorylation sites modulate anisotropic cell expansion and bidirectional mobility of cellulose synthase. *Proc. Natl. Acad. Sci. U. S. A.* **107**: 17188–17193.
- Cheng, F., Ali, M., Liu, C., Deng, R., and Cheng, Z.** (2020). Garlic allelochemical diallyl disulfide alleviates autotoxicity in the root exudates caused by long-term continuous cropping of tomato. *J. Agric. Food Chem.* **68**: 11684–11693.
- Cheng, F., Cheng, Z.-H., and Meng, H.-W.** (2016). Transcriptomic insights into the allelopathic effects of the garlic allelochemical diallyl disulfide on tomato roots. *Sci. Rep.* **6**: 38902.

- Cheong, J.-J. and Choi, Y.D.** (2003). Methyl jasmonate as a vital substance in plants. *Trends Genet. TIG* **19**: 409–413.
- Chinchilla, D., Bauer, Z., Regenass, M., Boller, T., and Felix, G.** (2006). The *Arabidopsis* receptor kinase FLS2 binds flg22 and determines the specificity of flagellin perception. *Plant Cell* **18**: 465–476.
- Chinchilla, D., Bruisson, S., Meyer, S., Zühlke, D., Hirschfeld, C., Joller, C., L’Haridon, F., Mène-Saffrané, L., Riedel, K., and Weisskopf, L.** (2019). A sulfur-containing volatile emitted by potato-associated bacteria confers protection against late blight through direct anti-oomycete activity. *Sci. Rep.* **9**: 1–15.
- Chinchilla, D., Zipfel, C., Robatzek, S., Kemmerling, B., Nürnberger, T., Jones, J.D.G., Felix, G., and Boller, T.** (2007). A flagellin-induced complex of the receptor FLS2 and BAK1 initiates plant defence. *Nature* **448**: 497–500.
- Choi, G.-H., Ro, J.-H., Park, B.-J., Lee, D.-Y., Cheong, M.-S., Lee, D.-Y., Seo, W.-D., and Kim, J.H.** (2016). Benzaldehyde as a new class plant growth regulator on *Brassica campestris*. *J. Appl. Biol. Chem.* **59**: 159–164.
- Citron, C.A., Wickel, S.M., Schulz, B., Draeger, S., and Dickschat, J.S.** (2012). A diels–alder/retro-diels–alder approach for the enantioselective synthesis of microbial butenolides. *Eur. J. Org. Chem.* **2012**: 6636–6646.
- Claverie, J., Balacey, S., Lemaître-Guillier, C., Brulé, D., Chiltz, A., Granet, L., Noirot, E., Daire, X., Darblade, B., Héloir, M.-C., and Poinssot, B.** (2018). The cell wall-derived xyloglucan is a new DAMP triggering plant immunity in *Vitis vinifera* and *Arabidopsis thaliana*. *Front. Plant Sci.* **9**: 1725.
- Clay, N.K., Adio, A.M., Denoux, C., Jander, G., and Ausubel, F.M.** (2009). Glucosinolate metabolites required for an arabidopsis innate immune response. *Science* **323**: 95–101.
- Contreras-Cornejo, H.A., López-Bucio, J.S., Méndez-Bravo, A., Macías-Rodríguez, L., Ramos-Vega, M., Guevara-García, Á.A., and López-Bucio, J.** (2015). Mitogen-activated protein kinase 6 and Ethylene and auxin signaling pathways are involved in *Arabidopsis* root-system architecture alterations by *Trichoderma atroviride*. *Mol. Plant-Microbe Interact. MPMI* **28**: 701–710.
- Dangl, J.L. and Jones, J.D.G.** (2001). Plant pathogens and integrated defence responses to infection. *Nature* **411**: 826–833.
- Day, D.A., Kaiser, B.N., Thomson, R., Udvardi, M.K., Moreau, S., and Puppò, A.** (2001). Nutrient transport across symbiotic membranes from legume nodules. *Funct. Plant Biol.* **28**: 669–676.

- De Jaeger, N., Declerck, S., and de la Providencia, I.E.** (2010). Mycoparasitism of arbuscular mycorrhizal fungi: a pathway for the entry of saprotrophic fungi into roots. *FEMS Microbiol. Ecol.* **73**: 312–322.
- Dickschat, J.S.** (2017). Fungal volatiles – a survey from edible mushrooms to moulds. *Nat. Prod. Rep.* **34**: 310–328.
- Dobert, R.C., Rood, S.B., and Blevins, D.G.** (1992). Gibberellins and the Legume-Rhizobium Symbiosis : I. Endogenous Gibberellins of Lima Bean (*Phaseolus lunatus* L.) Stems and Nodules. *Plant Physiol.* **98**: 221–224.
- Druzhinina, I.S. et al.** (2018). Massive lateral transfer of genes encoding plant cell wall-degrading enzymes to the mycoparasitic fungus *Trichoderma* from its plant-associated hosts. *PLoS Genet.* **14**: e1007322.
- Duan, Q., Kita, D., Johnson, E.A., Aggarwal, M., Gates, L., Wu, H.-M., and Cheung, A.Y.** (2014). Reactive oxygen species mediate pollen tube rupture to release sperm for fertilization in *Arabidopsis*. *Nat. Commun.* **5**: 3129.
- Escobar-Restrepo, J.-M., Huck, N., Kessler, S., Gagliardini, V., Gheyselinck, J., Yang, W.-C., and Grossniklaus, U.** (2007). The FERONIA receptor-like kinase mediates male-female interactions during pollen tube reception. *Science* **317**: 656–660.
- Farias, G.C., Nunes, K.G., Soares, M.A., de Siqueira, K.A., Lima, W.C., Neves, A.L.R., de Lacerda, C.F., and Filho, E.G.** (2020). Dark septate endophytic fungi mitigate the effects of salt stress on cowpea plants. *Braz. J. Microbiol. Publ. Braz. Soc. Microbiol.* **51**: 243–253.
- Felix, G., Duran, J.D., Volko, S., and Boller, T.** (1999). Plants have a sensitive perception system for the most conserved domain of bacterial flagellin. *Plant J. Cell Mol. Biol.* **18**: 265–276.
- Felix, G., Regenass, M., and Boller, T.** (1993). Specific perception of subnanomolar concentrations of chitin fragments by tomato cells: induction of extracellular alkalization, changes in protein phosphorylation, and establishment of a refractory state. *Plant J.* **4**: 307–316.
- Feng, W. et al.** (2018). The FERONIA receptor kinase maintains cell-wall integrity during salt stress through Ca²⁺ signaling. *Curr. Biol.* **28**: 666-675.e5.
- Filho, M.C.M.T., ShintateGalindo, F., Buzetti, S., and Santini, J.M.K.** (2017). Inoculation with *Azospirillum brasilense* Improves Nutrition and Increases Wheat Yield in Association with Nitrogen Fertilization (IntechOpen).
- Fitzgerald, J.W.** (1976). Sulfate ester formation and hydrolysis: a potentially important yet often ignored aspect of the sulfur cycle of aerobic soils. *Bacteriol. Rev.* **40**: 698–721.
- Fliegmann, J. et al.** (2013). Lipo-chitooligosaccharidic symbiotic signals are recognized by LysM receptor-like kinase LYR3 in the legume *Medicago truncatula*. *ACS Chem. Biol.* **8**: 1900–1906.

- Flor, H.H.** (1942). Inheritance of pathogenicity in *Melampsora lini*. *Phytopathology*. **32**: 653–669.
- Floss, D.S., Levy, J.G., Lévesque-Tremblay, V., Pumplin, N., and Harrison, M.J.** (2013). DELLA proteins regulate arbuscule formation in arbuscular mycorrhizal symbiosis. *Proc. Natl. Acad. Sci.* **110**: E5025–E5034.
- Fones, H.N., Bebbler, D.P., Chaloner, T.M., Kay, W.T., Steinberg, G., and Gurr, S.J.** (2020). Threats to global food security from emerging fungal and oomycete crop pathogens. *Nat. Food* **1**: 332–342.
- Gaffney, T., Friedrich, L., Vernooij, B., Negrotto, D., Nye, G., Uknes, S., Ward, E., Kessmann, H., and Ryals, J.** (1993). Requirement of salicylic acid for the induction of systemic acquired resistance. *Science* **261**: 754–756.
- Galletti, R., Ferrari, S., and De Lorenzo, G.** (2011). *Arabidopsis* MPK3 and MPK6 play different roles in basal and oligogalacturonide- or flagellin-induced resistance against *Botrytis cinerea*. *Plant Physiol.* **157**: 804–814.
- Galli, C., Bernasconi, R., Soldà, T., Calanca, V., and Molinari, M.** (2011). Malectin participates in a backup glycoprotein quality control pathway in the mammalian ER. *PloS One* **6**: e16304.
- Gao, X., Guo, H., Zhang, Q., Guo, H., Zhang, L., Zhang, C., Gou, Z., Liu, Y., Wei, J., Chen, A., Chu, Z., and Zeng, F.** (2020). Arbuscular mycorrhizal fungi (AMF) enhanced the growth, yield, fiber quality and phosphorus regulation in upland cotton (*Gossypium hirsutum* L.). *Sci. Rep.* **10**: 2084.
- Gao, Y., Wu, Y., Du, J., Zhan, Y., Sun, D., Zhao, J., Zhang, S., Li, J., and He, K.** (2017). Both light-induced SA accumulation and ETI mediators contribute to the cell death regulated by BAK1 and BKK1. *Front. Plant Sci.* **8**: 622.
- Garcia de Salamone, I.E., Döbereiner, J., Urquiaga, S., and Boddey, R.M.** (1996). Biological nitrogen fixation in *Azospirillum* strain-maize genotype associations as evaluated by the ¹⁵N isotope dilution technique. *Biol. Fertil. Soils* **23**: 249–256.
- Ge, Z. et al.** (2017). *Arabidopsis* pollen tube integrity and sperm release are regulated by RALF-mediated signaling. *Science* **358**: 1596–1600.
- Gharbi, E., Martínez, J.-P., Benahmed, H., Lepoint, G., Vanpee, B., Quinet, M., and Lutts, S.** (2017). Inhibition of ethylene synthesis reduces salt-tolerance in tomato wild relative species *Solanum chilense*. *J. Plant Physiol.* **210**: 24–37.
- Gherbi, H., Markmann, K., Svistoonoff, S., Estevan, J., Autran, D., Giczey, G., Auguy, F., Péret, B., Laplaze, L., Franche, C., Parniske, M., and Bogusz, D.** (2008). SymRK defines a common genetic basis for plant root endosymbioses with arbuscular mycorrhiza fungi, rhizobia, and *Frankiabacteria*. *Proc. Natl. Acad. Sci.* **105**: 4928–4932.

- Gibson, L.J.** (2012). The hierarchical structure and mechanics of plant materials. *J. R. Soc. Interface* **9**: 2749–2766.
- Gigolashvili, T., Yatusevich, R., Berger, B., Müller, C., and Flügge, U.-I.** (2007). The R2R3-MYB transcription factor HAG1/MYB28 is a regulator of methionine-derived glucosinolate biosynthesis in *Arabidopsis thaliana*. *Plant J.* **51**: 247–261.
- Giordano, D., Facchiano, A., D’Auria, S., and Loreto, F.** (2021). A hypothesis on the capacity of plant odorant-binding proteins to bind volatile isoprenoids based on in silico evidences. *eLife* **10**: e66741.
- Giovannetti, M., Tolosano, M., Volpe, V., Kopriva, S., and Bonfante, P.** (2014). Identification and functional characterization of a sulfate transporter induced by both sulfur starvation and mycorrhiza formation in *Lotus japonicus*. *New Phytol.* **204**: 609–619.
- Godoy, F., Olivos-Hernández, K., Stange, C., and Handford, M.** (2021). Abiotic stress in crop species: Improving tolerance by applying plant metabolites. *Plants* **10**: 186.
- Gómez-Gómez, L., Bauer, Z., and Boller, T.** (2001). Both the extracellular leucine-rich repeat domain and the kinase activity of FLS2 are required for flagellin binding and signaling in *Arabidopsis*. *Plant Cell* **13**: 1155–1163.
- Gonneau, M. et al.** (2018). Receptor kinase THESEUS1 is a rapid alkalization factor 34 receptor in *Arabidopsis*. *Curr. Biol.* **28**: 2452-2458.e4.
- Gouda, S., Kerry, R.G., Das, G., Paramithiotis, S., Shin, H.-S., and Patra, J.K.** (2018). Revitalization of plant growth promoting rhizobacteria for sustainable development in agriculture. *Microbiol. Res.* **206**: 131–140.
- Gray, L.E. and Gerdemann, J.W.** (1973). Uptake of sulphur-35 by vesicular-arbuscular mycorrhizae. *Plant Soil* **39**: 687–689.
- Grosch, R., Lottmann, J., Rehn, V.N.C., Rehn, K.G., Mendonça-Hagler, L., Smalla, K., and Berg, G.** (2007). Analysis of antagonistic interactions between *Trichoderma* isolates from Brazilian weeds and the soil-borne pathogen *Rhizoctonia solani*. *J. Plant Dis. Prot.* **114**: 167–175.
- Güimil, S., Chang, H.-S., Zhu, T., Sesma, A., Osbourn, A., Roux, C., Ioannidis, V., Oakeley, E.J., Docquier, M., Descombes, P., Briggs, S.P., and Paszkowski, U.** (2005). Comparative transcriptomics of rice reveals an ancient pattern of response to microbial colonization. *Proc. Natl. Acad. Sci.* **102**: 8066–8070.
- Guo, W.-J., Nagy, R., Chen, H.-Y., Pfrunder, S., Yu, Y.-C., Santelia, D., Frommer, W.B., and Martinoia, E.** (2014). SWEET17, a facilitative transporter, mediates fructose transport across the tonoplast of *Arabidopsis* roots and leaves. *Plant Physiol.* **164**: 777–789.

- Gupta, S. and Pandey, S.** (2019). ACC deaminase producing bacteria with multifarious plant growth promoting traits alleviates salinity stress in french bean (*Phaseolus vulgaris*) Plants. *Front. Microbiol.* **10**: 1506.
- Gupta, V.V.S.R., Zhang, B., Penton, C.R., Yu, J., and Tiedje, J.M.** (2019). Diazotroph diversity and nitrogen fixation in summer active perennial grasses in a mediterranean region agricultural soil. *Front. Mol. Biosci.* **6**: 115.
- Gust, A.A., Biswas, R., Lenz, H.D., Rauhut, T., Ranf, S., Kemmerling, B., Götz, F., Glawischnig, E., Lee, J., Felix, G., and Nürnberger, T.** (2007). Bacteria-derived peptidoglycans constitute pathogen-associated molecular patterns triggering innate immunity in *Arabidopsis*. *J. Biol. Chem.* **282**: 32338–32348.
- Hailu Gunnabo, A., Geurts, R., Wolde-meskel, E., Degefu, T., E. Giller, K., and van Heerwaarden, J.** (2021). Phylogeographic distribution of rhizobia nodulating common bean (*Phaseolus vulgaris* L.) in Ethiopia. *FEMS Microbiol. Ecol.* **97**.
- Halkier, B.A. and Gershenzon, J.** (2006). Biology and biochemistry of glucosinolates. *Annu. Rev. Plant Biol.* **57**: 303–333.
- Harris, D.F., Lukoyanov, D.A., Kallas, H., Trncik, C., Yang, Z.-Y., Compton, P., Kelleher, N., Einsle, O., Dean, D.R., Hoffman, B.M., and Seefeldt, L.C.** (2019). Mo-, V-, and Fe-nitrogenases use a universal eight-electron reductive-elimination mechanism to achieve N₂ reduction. *Biochemistry* **58**: 3293–3301.
- Hashem, A., Tabassum, B., and Fathi Abd Allah, E.** (2019). *Bacillus subtilis*: A plant-growth promoting rhizobacterium that also impacts biotic stress. *Saudi J. Biol. Sci.* **26**: 1291–1297.
- Hématy, K., Sado, P.-E., Van Tuinen, A., Rochange, S., Desnos, T., Balzergue, S., Pelletier, S., Renou, J.-P., and Höfte, H.** (2007). A receptor-like kinase mediates the response of *Arabidopsis* cells to the inhibition of cellulose synthesis. *Curr. Biol.* **17**: 922–931.
- Herridge, D.F., Peoples, M.B., and Boddey, R.M.** (2008). Global inputs of biological nitrogen fixation in agricultural systems. *Plant Soil* **311**: 1–18.
- Hok, S. et al.** (2014). The receptor kinase IMPAIRED OOMYCETE SUSCEPTIBILITY1 attenuates abscisic acid responses in *Arabidopsis*. *Plant Physiol.* **166**: 1506–1518.
- Honma, M. and Shimomura, T.** (1978). Metabolism of 1-aminocyclopropane-1-carboxylic acid. *Agric. Biol. Chem.* **42**: 1825–1831.
- Horrigan, L., Lawrence, R.S., and Walker, P.** (2002). How sustainable agriculture can address the environmental and human health harms of industrial agriculture. *Environ. Health Perspect.* **110**: 445–456.

- Hu, X.Y., Neill, S.J., Cai, W.M., and Tang, Z.C.** (2004). Induction of defence gene expression by oligogalacturonic acid requires increases in both cytosolic calcium and hydrogen peroxide in *Arabidopsis thaliana*. *Cell Res.* **14**: 234–240.
- Huang, C., Yan, Y., Zhao, H., Ye, Y., and Cao, Y.** (2020). *Arabidopsis* CPK5 phosphorylates the chitin receptor LYK5 to regulate plant innate immunity. *Front. Plant Sci.* **11**: 702.
- Huang, P.-Y., Yeh, Y.-H., Liu, A.-C., Cheng, C.-P., and Zimmerli, L.** (2014). The *Arabidopsis* LecRK-VI.2 associates with the pattern-recognition receptor FLS2 and primes *Nicotiana benthamiana* pattern-triggered immunity. *Plant J.* **79**: 243–255.
- Hussan, R.H., Dubery, I.A., and Piater, L.A.** (2020). Identification of MAMP-responsive plasma membrane-associated proteins in *Arabidopsis thaliana* following challenge with different LPS chemotypes from *Xanthomonas campestris*. *Pathogens* **9**: 787.
- Jamieson, P.A., Shan, L., and He, P.** (2018). Plant cell surface molecular cypher: Receptor-like proteins and their roles in immunity and development. *Plant Sci. Int. J. Exp. Plant Biol.* **274**: 242–251.
- Jeena, G.S., Kumar, S., and Shukla, R.K.** (2019). Structure, evolution and diverse physiological roles of SWEET sugar transporters in plants. *Plant Mol. Biol.* **100**: 351–365.
- Jeschke, V. and Burow, M.** (2018). Glucosinolates. In *eLS* (John Wiley & Sons, Ltd), pp. 1–8.
- Jiang, Y., Tian, J., and Ge, F.** (2020). New insight into carboxylic acid metabolisms and pH regulations during insoluble phosphate solubilisation process by *Penicillium oxalicum* PSF-4. *Curr. Microbiol.* **77**: 4095–4103.
- Johnson, J.M. et al.** (2018). A poly(A) ribonuclease controls the cellobiose-based interaction between *Piriformospora indica* and its host *Arabidopsis*. *Plant Physiol.* **176**: 2496–2514.
- Johnson, J.M., Reichelt, M., Vadassery, J., Gershenzon, J., and Oelmüller, R.** (2014). An *Arabidopsis* mutant impaired in intracellular calcium elevation is sensitive to biotic and abiotic stress. *BMC Plant Biol.* **14**: 162.
- Jones, J.D.G. and Dangl, J.L.** (2006). The plant immune system. *Nature* **444**: 323–329.
- Júnior, J.Q. de O., Jesus, E. da C., Lisboa, F.J., Berbara, R.L.L., and Faria, S.M. de** (2017). Nitrogen-fixing bacteria and arbuscular mycorrhizal fungi in *Piptadenia gonoacantha* (Mart.) Macbr. *Braz. J. Microbiol.* **48**: 95–100.
- Kamiya, Y.** (2009). Plant hormones: Versatile regulators of plant growth and development. *Annu. Rev. Plant Biol.* **60**: 1.
- Kamle, M., Borah, R., Bora, H., Jaiswal, A.K., Singh, R.K., and Kumar, P.** (2020). Systemic Acquired Resistance (SAR) and Induced Systemic Resistance (ISR): Role and Mechanism of Action against Phytopathogens. In *Fungal Biotechnology and Bioengineering*, A.E.-L.

- Hesham, R.S. Upadhyay, G.D. Sharma, C. Manoharachary, and V.K. Gupta, eds, Fungal Biology. (Springer International Publishing: Cham), pp. 457–470.
- Keunen, E., Schellingen, K., Vangronsveld, J., and Cuypers, A.** (2016). Ethylene and metal stress: Small molecule, big impact. *Front. Plant Sci.* **7**: 23.
- Khan, N., Bano, A., Ali, S., and Babar, Md.A.** (2020). Crosstalk amongst phytohormones from planta and PGPR under biotic and abiotic stresses. *Plant Growth Regul.* **90**: 189–203.
- Kim, D., Abdelaziz, M.E., Ntui, V.O., Guo, X., and Al-Babili, S.** (2017). Colonization by the endophyte *Piriformospora indica* leads to early flowering in *Arabidopsis thaliana* likely by triggering gibberellin biosynthesis. *Biochem. Biophys. Res. Commun.* **490**: 1162–1167.
- Kobae, Y.** (2019). Dynamic phosphate uptake in arbuscular mycorrhizal roots under field conditions. *Front. Environ. Sci.* **6**: 159.
- Kohorn, B. and Kohorn, S.** (2012). The cell wall-associated kinases, WAKs, as pectin receptors. *Front. Plant Sci.* **3**: 88.
- Koukounaras, A., Siomos, A.S., and Sfakiotakis, E.** (2006). 1-Methylcyclopropene prevents ethylene induced yellowing of rocket leaves. *Postharvest Biol. Technol.* **1**: 109–111.
- Krueger, R.J. and Siegel, L.M.** (1982). Evidence for siroheme-Fe4S4 interaction in spinach ferredoxin-sulfite reductase. *Biochemistry* **21**: 2905–2909.
- Kumar Arora, N., Fatima, T., Mishra, J., Mishra, I., Verma, S., Verma, R., Verma, M., Bhattacharya, A., Verma, P., Mishra, P., and Bharti, C.** (2020). Halo-tolerant plant growth promoting rhizobacteria for improving productivity and remediation of saline soils. *J. Adv. Res.* **26**: 69–82.
- Kumar, M., Yadav, V., Kumar, H., Sharma, R., Singh, A., Tuteja, N., and Johri, A.K.** (2011). *Piriformospora indica* enhances plant growth by transferring phosphate. *Plant Signal. Behav.* **6**: 723–725.
- Kunze, G., Zipfel, C., Robatzek, S., Niehaus, K., Boller, T., and Felix, G.** (2004). The N terminus of bacterial elongation factor Tu elicits innate immunity in *Arabidopsis* Plants. *Plant Cell* **16**: 3496–3507.
- Lancaster, J.R., Vega, J.M., Kamin, H., Orme-Johnson, N.R., Orme-Johnson, W.H., Krueger, R.J., and Siegel, L.M.** (1979). Identification of the iron-sulfur center of spinach ferredoxin-nitrite reductase as a tetranuclear center, and preliminary EPR studies of mechanism. *J. Biol. Chem.* **254**: 1268–1272.
- Larsen, T.O.** (1998). Volatile flavour production by *Penicillium caseifulvum*. *Int. Dairy J.* **8**: 883–887.
- Le, M.H., Cao, Y., Zhang, X.-C., and Stacey, G.** (2014). LIK1, a CERK1-interacting kinase, regulates plant immune responses in *Arabidopsis*. *PloS One* **9**: e102245.

- Lee, H.K. and Goring, D.R.** (2021). Two subgroups of receptor-like kinases promote early compatible pollen responses in the *Arabidopsis thaliana* pistil. *J. Exp. Bot.* **72**: 1198–1211.
- Lee, Y.-C., Johnson, J.M., Chien, C.-T., Sun, C., Cai, D., Lou, B., Oelmüller, R., and Yeh, K.-W.** (2011). Growth promotion of Chinese cabbage and *Arabidopsis* by *Piriformospora indica* is not stimulated by mycelium-synthesized auxin. *Mol. Plant-Microbe Interact. MPMI* **24**: 421–431.
- Li, H., Chen, M., Duan, L., Zhang, T., Cao, Y., and Zhang, Z.** (2018a). Domain swap approach reveals the critical roles of different domains of SYMRK in root nodule symbiosis in *Lotus japonicus*. *Front. Plant Sci.* **9**: 697.
- Li, J., Meng, B., Chai, H., Yang, X., Song, W., Li, S., Lu, A., Zhang, T., and Sun, W.** (2019). Arbuscular mycorrhizal fungi alleviate drought stress in C3 (*Leymus chinensis*) and C4 (*Hemarthria altissima*) grasses via altering antioxidant enzyme activities and photosynthesis. *Front. Plant Sci.* **10**: 499.
- Li, S., Lei, L., Yingling, Y.G., and Gu, Y.** (2015). Microtubules and cellulose biosynthesis: the emergence of new players. *Curr. Opin. Plant Biol.* **28**: 76–82.
- Li, X. et al.** (2020). Protein phosphorylation dynamics under carbon/nitrogen-nutrient stress and identification of a cell death-related receptor-like kinase in *Arabidopsis*. *Front. Plant Sci.* **11**: 377.
- Li, Z.T., Janisiewicz, W.J., Liu, Z., Callahan, A.M., Evans, B.E., Jurick, W.M., and Dardick, C.** (2018b). Exposure in vitro to an environmentally isolated strain TC09 of *Cladosporium sphaerospermum* triggers plant growth promotion, early flowering, and fruit yield increase. *Front. Plant Sci.* **9**: 1959.
- Liang, D., Wu, H., Wong, M.W., and Huang, D.** (2015). Diallyl trisulfide is a fast H₂S donor, but diallyl disulfide is a slow one: The reaction pathways and intermediates of glutathione with polysulfides. *Org. Lett.* **17**: 4196–4199.
- Lindström, K. and Mousavi, S.A.** (2020). Effectiveness of nitrogen fixation in rhizobia. *Microb. Biotechnol.* **13**: 1314–1335.
- Lipman, J.G., Mclean, H.C., and Lint, H.C.** (1916). Sulfur oxidation in soils and its effect on the availability of mineral phosphates. *Soil Sci.* **2**: 499–538.
- Liu, C.-Y., Zhang, F., Zhang, D.-J., Srivastava, A.K., Wu, Q.-S., and Zou, Y.-N.** (2018). Mycorrhiza stimulates root-hair growth and IAA synthesis and transport in trifoliolate orange under drought stress. *Sci. Rep.* **8**: 1978.
- Lopes, M.J. dos S., Dias-Filho, M.B., and Gurgel, E.S.C.** (2021). Successful plant growth-promoting microbes: Inoculation methods and abiotic factors. *Front. Sustain. Food Syst.* **5**: 48.

- Loreto, F. and D'Auria, S.** (2021). How do plants sense volatiles sent by other plants? *Trends Plant Sci.*: S1360-1385(21)00220-X.
- Lucke, M., Correa, M.G., and Levy, A.** (2020). The role of secretion systems, effectors, and secondary metabolites of beneficial rhizobacteria in interactions with plants and microbes. *Front. Plant Sci.* **11**: 1718.
- Lv, Z., Hao, L., Ma, B., He, Z., Luo, Y., Xin, Y., and He, N.** (2021). *Ciboria carunculoides* suppresses mulberry immune responses through regulation of salicylic acid signaling. *Front. Plant Sci.* **12**: 658590.
- Martinez, A., Obertello, M., Pardo, A., Ocampo, J.A., and Godeas, A.** (2004). Interactions between *Trichoderma pseudokoningii* strains and the arbuscular mycorrhizal fungi *Glomus mosseae* and *Gigaspora rosea*. *Mycorrhiza* **14**: 79–84.
- Marzluf, G.A.** (1997). Molecular genetics of sulfur assimilation in filamentous fungi and yeast. *Annu. Rev. Microbiol.* **51**: 73–96.
- Matsushima, R., Fukao, Y., Nishimura, M., and Hara-Nishimura, I.** (2004). NAI1 gene encodes a basic-helix-loop-helix-type putative transcription factor that regulates the formation of an endoplasmic reticulum-derived structure, the ER body. *Plant Cell* **16**: 1536–1549.
- Matsushima, R., Kondo, M., Nishimura, M., and Hara-Nishimura, I.** (2003). A novel ER-derived compartment, the ER body, selectively accumulates a beta-glucosidase with an ER-retention signal in *Arabidopsis*. *Plant J. Cell Mol. Biol.* **33**: 493–502.
- Meena, R.S. et al.** (2020). Impact of agrochemicals on soil microbiota and management: A Review. *Land* **9**: 34.
- Meents, A.K., Furch, A.C.U., Almeida-Trapp, M., Özyürek, S., Scholz, S.S., Kirbis, A., Lenser, T., Theißen, G., Grabe, V., Hansson, B., Mithöfer, A., and Oelmüller, R.** (2019). Beneficial and pathogenic *Arabidopsis* root-interacting fungi differently affect auxin levels and responsive genes during early infection. *Front. Microbiol.* **10**: 380.
- Meldau, D.G., Meldau, S., Hoang, L.H., Underberg, S., Wunsche, H., and Baldwin, I.T.** (2013). Dimethyl disulfide produced by the naturally associated bacterium *Bacillus* sp B55 promotes *Nicotiana attenuata* growth by enhancing sulfur nutrition. *Plant Cell* **25**: 2731–2747.
- Mélida, H., Bacete, L., Ruprecht, C., Rebaque, D., del Hierro, I., López, G., Brunner, F., Pfrengle, F., and Molina, A.** (2020). Arabinoxylan-oligosaccharides act as damage associated molecular patterns in plants regulating disease resistance. *Front. Plant Sci.* **11**: 1210.
- Métraux, J.P., Signer, H., Ryals, J., Ward, E., Wyss-Benz, M., Gaudin, J., Raschdorf, K., Schmid, E., Blum, W., and Inverardi, B.** (1990). Increase in salicylic acid at the onset of systemic acquired resistance in cucumber. *Science* **250**: 1004–1006.

- Mikola, P.U.** (1986). Relationship between nitrogen fixation and mycorrhiza. *MIRCEN J. Appl. Microbiol. Biotechnol.* **2**: 275–282.
- Milne, R.J., Perroux, J.M., Rae, A.L., Reinders, A., Ward, J.M., Offler, C.E., Patrick, J.W., and Grof, C.P.L.** (2017). Sucrose transporter localization and function in phloem unloading in developing stems. *Plant Physiol.* **173**: 1330–1341.
- Mitra, D., Djebaili, R., Pellegrini, M., Mahakur, B., Sarker, A., Chaudhary, P., Khoshru, B., Gallo, M.D., Kitouni, M., Barik, D.P., Panneerselvam, P., and Mohapatra, P.K.D.** (2021). Arbuscular mycorrhizal symbiosis: plant growth improvement and induction of resistance under stressful conditions. *J. Plant Nutr.* **44**: 1993–2028.
- Miya, A., Albert, P., Shinya, T., Desaki, Y., Ichimura, K., Shirasu, K., Narusaka, Y., Kawakami, N., Kaku, H., and Shibuya, N.** (2007). CERK1, a LysM receptor kinase, is essential for chitin elicitor signaling in *Arabidopsis*. *Proc. Natl. Acad. Sci. U. S. A.* **104**: 19613–19618.
- Miyazaki, S., Murata, T., Sakurai-Ozato, N., Kubo, M., Demura, T., Fukuda, H., and Hasebe, M.** (2009). ANXUR1 and 2, sister genes to FERONIA/SIRENE, are male factors for coordinated fertilization. *Curr. Biol.* **19**: 1327–1331.
- Mohnen, D.** (2008). Pectin structure and biosynthesis. *Curr. Opin. Plant Biol.* **11**: 266–277.
- Mugford, S.G., Lee, B.-R., Koprivova, A., Matthewman, C., and Kopriva, S.** (2011). Control of sulfur partitioning between primary and secondary metabolism: Sulfur partitioning. *Plant J.* **65**: 96–105.
- Nadarajah, K.K.** (2020). ROS homeostasis in abiotic stress tolerance in plants. *Int. J. Mol. Sci.* **21**: 5208.
- Nadzieja, M., Kelly, S., Stougaard, J., and Reid, D.** (2018). Epidermal auxin biosynthesis facilitates rhizobial infection in *Lotus japonicus*. *Plant J.* **95**: 101–111.
- Nagashima, A., Higaki, T., Koeduka, T., Ishigami, K., Hosokawa, S., Watanabe, H., Matsui, K., Hasezawa, S., and Touhara, K.** (2019). Transcriptional regulators involved in responses to volatile organic compounds in plants. *J. Biol. Chem.* **294**: 2256–2266.
- Nannipieri, P., Giagnoni, L., Landi, L., and Renella, G.** (2011). Role of Phosphatase Enzymes in Soil. In *Phosphorus in Action: Biological Processes in Soil Phosphorus Cycling*, E. Bünemann, A. Oberson, and E. Frossard, eds, *Soil Biology*. (Springer: Berlin, Heidelberg), pp. 215–243.
- Nemcovic, M., Jakubíková, L., Viden, I., and Farkas, V.** (2008). Induction of conidiation by endogenous volatile compounds in *Trichoderma* spp. *FEMS Microbiol. Lett.* **284**: 231–236.
- Newman, M.A., Daniels, M.J., and Dow, J.M.** (1995). Lipopolysaccharide from *Xanthomonas campestris* induces defense-related gene expression in *Brassica campestris*. *Mol. Plant. Microbe Interact.* **8**: 778–780.

- Ngou, B.P.M., Ahn, H.-K., Ding, P., and Jones, J.D.G.** (2021). Mutual potentiation of plant immunity by cell-surface and intracellular receptors. *Nature* **592**: 110–115.
- Nouman, W., Basra, S.M.A., Yasmeen, A., Gull, T., Hussain, S.B., Zubair, M., and Gul, R.** (2014). Seed priming improves the emergence potential, growth and antioxidant system of *Moringa oleifera* under saline conditions. *Plant Growth Regul.* **73**: 267–278.
- Ogawa, M., Hanada, A., Yamauchi, Y., Kuwahara, A., Kamiya, Y., and Yamaguchi, S.** (2003). Gibberellin biosynthesis and response during *Arabidopsis* seed germination. *Plant Cell* **15**: 1591–1604.
- Omar, S.A. and Abd-Alla, M.H.** (2000). Physiological aspects of fungi isolated from root nodules of faba bean (*Vicia faba* L.). *Microbiol. Res.* **154**: 339–347.
- Orozco-Mosqueda, Ma. del C., Duan, J., DiBernardo, M., Zetter, E., Campos-García, J., Glick, B.R., and Santoyo, G.** (2019). The production of ACC deaminase and trehalose by the plant growth promoting bacterium *Pseudomonas* sp. UW4 synergistically protect tomato plants against salt stress. *Front. Microbiol.* **10**: 1392.
- Özgen, M., Park, S., and Palta, J.P.** (2005). Mitigation of ethylene-promoted leaf senescence by a natural lipid, lysophosphatidylethanolamine. *HortScience* **40**: 1166–1167.
- Pan, H., Stonoha-Arther, C., and Wang, D.** (2018). *Medicago* plants control nodulation by regulating proteolysis of the receptor-like kinase DMI2. *Plant Physiol.* **177**: 792–802.
- Pan, R., Xu, L., Wei, Q., Wu, C., Tang, W., Oelmüller, R., and Zhang, W.** (2017). *Piriformospora indica* promotes early flowering in *Arabidopsis* through regulation of the photoperiod and gibberellin pathways. *PLOS ONE* **12**: e0189791.
- Park, S.-W., Kaimoyo, E., Kumar, D., Mosher, S., and Klessig, D.F.** (2007). Methyl salicylate is a critical mobile signal for plant systemic acquired resistance. *Science* **318**: 113–116.
- Park, Y.-S., Dutta, S., Ann, M., Raaijmakers, J.M., and Park, K.** (2015). Promotion of plant growth by *Pseudomonas fluorescens* strain SS101 via novel volatile organic compounds. *Biochem. Biophys. Res. Commun.* **461**: 361–365.
- Paszkowski, U. and Gutjahr, C.** (2013). Multiple control levels of root system remodeling in arbuscular mycorrhizal symbiosis. *Front. Plant Sci.* **4**: 204.
- Peng, Y., van Wersch, R., and Zhang, Y.** (2018). Convergent and divergent signaling in PAMP-triggered immunity and effector-triggered immunity. *Mol. Plant-Microbe Interact. MPMI* **31**: 403–409.
- Peñuelas, J., Asensio, D., Tholl, D., Wenke, K., Rosenkranz, M., Piechulla, B., and Schnitzler, J.P.** (2014). Biogenic volatile emissions from the soil. *Plant Cell Environ.* **37**: 1866–1891.
- Pieterse, C.M.J., Leon-Reyes, A., Van der Ent, S., and Van Wees, S.C.M.** (2009). Networking by small-molecule hormones in plant immunity. *Nat. Chem. Biol.* **5**: 308–316.

- Plett, J.M., Daguerre, Y., Wittulsky, S., Vayssières, A., Deveau, A., Melton, S.J., Kohler, A., Morrell-Falvey, J.L., Brun, A., Veneault-Fourrey, C., and Martin, F.** (2014). Effector MiSSP7 of the mutualistic fungus *Laccaria bicolor* stabilizes the *Populus* JAZ6 protein and represses jasmonic acid (JA) responsive genes. *Proc. Natl. Acad. Sci.*
- Poveda, J., Abril-Urias, P., and Escobar, C.** (2020). Biological control of plant-parasitic nematodes by filamentous fungi inducers of resistance: *Trichoderma*, mycorrhizal and endophytic Fungi. *Front. Microbiol.* **11**: 992.
- Poveda, J., Hermosa, R., Monte, E., and Nicolás, C.** (2019). *Trichoderma harzianum* favours the access of arbuscular mycorrhizal fungi to non-host *Brassicaceae* roots and increases plant productivity. *Sci. Rep.* **9**: 11650.
- Pozo, M.J., López-Ráez, J.A., Azcón-Aguilar, C., and García-Garrido, J.M.** (2015). Phytohormones as integrators of environmental signals in the regulation of mycorrhizal symbioses. *New Phytol.* **205**: 1431–1436.
- Pozo, M.J., Van Der Ent, S., Van Loon, L.C., and Pieterse, C.M.J.** (2008). Transcription factor MYC2 is involved in priming for enhanced defense during rhizobacteria-induced systemic resistance in *Arabidopsis thaliana*. *New Phytol.* **180**: 511–523.
- Pršić, J. and Ongena, M.** (2020). Elicitors of plant immunity triggered by beneficial bacteria. *Front. Plant Sci.* **11**: 1675.
- Ranf, S., Gisch, N., Schäffer, M., Illig, T., Westphal, L., Knirel, Y.A., Sánchez-Carballo, P.M., Zähringer, U., Hückelhoven, R., Lee, J., and Scheel, D.** (2015). A lectin S-domain receptor kinase mediates lipopolysaccharide sensing in *Arabidopsis thaliana*. *Nat. Immunol.* **16**: 426–433.
- Raven, J.A., Evans, M.C.W., and Korb, R.E.** (1999). The role of trace metals in photosynthetic electron transport in O₂-evolving organisms. *Photosynth. Res.* **60**: 111–150.
- Raymond, J., Siefert, J.L., Staples, C.R., and Blankenship, R.E.** (2004). The natural history of nitrogen fixation. *Mol. Biol. Evol.* **21**: 541–554.
- Rebaque, D. et al.** (2021). Cell wall-derived mixed-linked β -1,3/1,4-glucans trigger immune responses and disease resistance in plants. *Plant J.* **106**: 601–615.
- Richard, M.M.S., Gratias, A., Meyers, B.C., and Geffroy, V.** (2018). Molecular mechanisms that limit the costs of NLR-mediated resistance in plants. *Mol. Plant Pathol.* **19**: 2516–2523.
- Rutten, P.J. and Poole, P.S.** (2019). Oxygen regulatory mechanisms of nitrogen fixation in rhizobia. *Adv. Microb. Physiol.* **75**: 325–389.
- Saidi, A. and Hajibarat, Z.** (2021). Phytohormones: Plant switchers in developmental and growth stages in potato. *J. Genet. Eng. Biotechnol.* **19**: 89.

- Saikia, J., Sarma, R.K., Dhandia, R., Yadav, A., Bharali, R., Gupta, V.K., and Saikia, R.** (2018). Alleviation of drought stress in pulse crops with ACC deaminase producing rhizobacteria isolated from acidic soil of Northeast India. *Sci. Rep.* **8**: 3560.
- Sánchez-Montesinos, B., Santos, M., Moreno-Gavira, A., Marín-Rodulfo, T., Gea, F.J., and Diáñez, F.** (2021). Biological control of fungal diseases by *Trichoderma aggressivum* f. *europaeum* and its compatibility with fungicides. *J. Fungi* **7**: 598.
- Sauer, N. and Stolz, J.** (1994). SUC1 and SUC2: Two sucrose transporters from *Arabidopsis thaliana*; expression and characterization in baker's yeast and identification of the histidine-tagged protein. *Plant J. Cell Mol. Biol.* **6**: 67–77.
- Savcı, S.** (2012). An agricultural pollutant: Chemical fertilizer. *Int. J. Environ. Sci. Dev.* **3**.
- Schalchli, H., Hormazabal, E., Becerra, J., Birkett, M., Alvear, M., Vidal, J., and Quiroz, A.** (2011). Antifungal activity of volatile metabolites emitted by mycelial cultures of saprophytic fungi. *Chem. Ecol.* **27**: 503–513.
- Schallus, T., Jaeckh, C., Fehér, K., Palma, A.S., Liu, Y., Simpson, J.C., Mackeen, M., Stier, G., Gibson, T.J., Feizi, T., Pieler, T., and Muhle-Goll, C.** (2008). Malectin: A novel carbohydrate-binding protein of the endoplasmic reticulum and a candidate player in the early steps of protein N-glycosylation. *Mol. Biol. Cell* **19**: 3404–3414.
- Scharnagl, K., Sanchez, V., and von Wettberg, E.** (2018). The impact of salinity on mycorrhizal colonization of a rare legume, *Galactia smallii*, in South Florida pine rocklands. *BMC Res. Notes* **11**: 2.
- Schauser, L., Roussis, A., Stiller, J., and Stougaard, J.** (1999). A plant regulator controlling development of symbiotic root nodules. *Nature* **402**: 191–195.
- Scheller, H.V. and Ulvskov, P.** (2010). Hemicelluloses. *Annu. Rev. Plant Biol.* **61**: 263–289.
- Schmidt, R., Cordovez, V., de Boer, W., Raaijmakers, J., and Garbeva, P.** (2015). Volatile affairs in microbial interactions. *ISME J.* **9**: 2329–2335.
- Schulz, S. and Dickschat, J.S.** (2007). Bacterial volatiles: The smell of small organisms. *Nat. Prod. Rep.* **24**: 814–842.
- Schulz-Bohm, K., Martín-Sánchez, L., and Garbeva, P.** (2017). Microbial volatiles: Small molecules with an important role in intra- and inter-kingdom interactions. *Front. Microbiol.* **8**: 2484.
- Seefeldt, L.C., Hoffman, B.M., and Dean, D.R.** (2009). Mechanism of Mo-dependent nitrogenase. *Annu. Rev. Biochem.* **78**: 701.
- Seifert, R.M. and King, A.D.** (1982). Identification of some volatile constituents of *Aspergillus clavatus*. *J. Agric. Food Chem.* **30**: 786–790.

- Sharma, S.B., Sayyed, R.Z., Trivedi, M.H., and Gobi, T.A.** (2013). Phosphate solubilizing microbes: Sustainable approach for managing phosphorus deficiency in agricultural soils. *SpringerPlus* **2**: 587.
- Sheard, L.B. et al.** (2010). Jasmonate perception by inositol-phosphate-potentiated COI1-JAZ co-receptor. *Nature* **468**: 400–405.
- Sherameti, I., Venus, Y., Drzewiecki, C., Tripathi, S., Dan, V.M., Nitz, I., Varma, A., Grundler, F.M., and Oelmüller, R.** (2008). PYK10, a beta-glucosidase located in the endoplasmatic reticulum, is crucial for the beneficial interaction between *Arabidopsis thaliana* and the endophytic fungus *Piriformospora indica*. *Plant J. Cell Mol. Biol.* **54**: 428–439.
- Shih, H.-W., Miller, N.D., Dai, C., Spalding, E.P., and Monshausen, G.B.** (2014). The receptor-like kinase FERONIA is required for mechanical signal transduction in *Arabidopsis* seedlings. *Curr. Biol.* **24**: 1887–1892.
- Shin, W., Islam, R., Benson, A., Joe, M.M., Kim, K., Gopal, S., Samaddar, S., Banerjee, S., and Sa, T.** (2016). Role of diazotrophic bacteria in biological nitrogen fixation and plant growth improvement. *Korean J. Soil Sci. Fertil.* **49**: 17–29.
- Shu, K., Liu, X.-D., Xie, Q., and He, Z.-H.** (2016). Two faces of one seed: Hormonal regulation of dormancy and germination. *Mol. Plant* **9**: 34–45.
- Singh, U.B., Malviya, D., Singh, S., Kumar, M., Sahu, P.K., Singh, H.V., Kumar, S., Roy, M., Imran, M., Rai, J.P., Sharma, A.K., and Saxena, A.K.** (2019). *Trichoderma harzianum*- and methyl jasmonate-induced resistance to *Bipolaris sorokiniana* through enhanced phenylpropanoid activities in bread wheat (*Triticum aestivum* L.). *Front. Microbiol.* **10**: 1697.
- Sirrenberg, A., Göbel, C., Grond, S., Czempinski, N., Ratzinger, A., Karlovsky, P., Santos, P., Feussner, I., and Pawlowski, K.** (2007). *Piriformospora indica* affects plant growth by auxin production. *Physiol. Plant.* **131**: 581–589.
- Souza, C. de A., Li, S., Lin, A.Z., Boutrot, F., Grossmann, G., Zipfel, C., and Somerville, S.C.** (2017). Cellulose-derived oligomers act as damage-associated molecular patterns and trigger defense-like responses. *Plant Physiol.* **173**: 2383–2398.
- de Souza, R., Ambrosini, A., and Passaglia, L.M.P.** (2015). Plant growth-promoting bacteria as inoculants in agricultural soils. *Genet. Mol. Biol.* **38**: 401–419.
- Splivallo, R., Novero, M., Berteà, C.M., Bossi, S., and Bonfante, P.** (2007). Truffle volatiles inhibit growth and induce an oxidative burst in *Arabidopsis thaliana*. *New Phytol.* **175**: 417–424.
- Stillmark, H.** (1888). Über Ricin ein giftiges Ferment aus den Samen von *Ricinus communis* L. und einige anderen Euphorbiaceen. MD Thesis, University of Dorpat, Dorpat, Estonia.

- Stracke, S., Kistner, C., Yoshida, S., Mulder, L., Sato, S., Kaneko, T., Tabata, S., Sandal, N., Stougaard, J., Szczyglowski, K., and Parniske, M.** (2002). A plant receptor-like kinase required for both bacterial and fungal symbiosis. *Nature* **417**: 959–962.
- Sultana, M.M., Hachiya, T., Dutta, A.K., Nishimura, K., Suzuki, T., Tanaka, A., and Nakagawa, T.** (2020). Expression analysis of genes encoding malectin-like domain (MLD)- and leucine-rich repeat (LRR)- containing proteins in *Arabidopsis thaliana*. *Biosci. Biotechnol. Biochem.* **84**: 154–158.
- Tanaka, S. and Kahmann, R.** (2021). Cell wall-associated effectors of plant-colonizing fungi. *Mycologia* **113**: 247–260.
- Tang W, Lin W, Zhou X, Guo J, Dang X, Li B, Lin D, Yang Z.** (2022) Mechano-transduction via the pectin-FERONIA complex activates ROP6 GTPase signaling in *Arabidopsis* pavement cell morphogenesis. *Curr. Biol.* **32**:508-517.e3.
- Tausz, M., Šircelj, H., and Grill, D.** (2004). The glutathione system as a stress marker in plant ecophysiology: is a stress-response concept valid? *J. Exp. Bot.* **55**: 1955–1962.
- Teixeira, M.A., Rajewski, A., He, J., Castaneda, O.G., Litt, A., and Kaloshian, I.** (2018). Classification and phylogenetic analyses of the *Arabidopsis* and tomato G-type lectin receptor kinases. *BMC Genomics* **19**: 239.
- Thomas, G., Withall, D., and Birkett, M.** (2020). Harnessing microbial volatiles to replace pesticides and fertilizers. *Microb. Biotechnol.* **13**: 1366–1376.
- Thorpe, G.W., Reodica, M., Davies, M.J., Heeren, G., Jarolim, S., Pillay, B., Breitenbach, M., Higgins, V.J., and Dawes, I.W.** (2013). Superoxide radicals have a protective role during H₂O₂ stress. *Mol. Biol. Cell* **24**: 2876–2884.
- Tian, J., Ge, F., Zhang, D., Deng, S., and Liu, X.** (2021). Roles of phosphate solubilizing microorganisms from managing soil phosphorus deficiency to mediating biogeochemical P cycle. *Biology* **10**: 158.
- Ting, H.-M., Cheah, B.H., Chen, Y.-C., Yeh, P.-M., Cheng, C.-P., Yeo, F.K.S., Vie, A.K., Rohloff, J., Winge, P., Bones, A.M., and Kissen, R.** (2020). The role of a glucosinolate-derived nitrile in plant immune responses. *Front. Plant Sci.* **11**.
- Tsaneva, M. and Van Damme, E.J.M.** (2020). 130 years of plant lectin research. *Glycoconj. J.* **37**: 533–551.
- Turan, M., Ataoğlu, N., and Şahin, F.** (2006). Evaluation of The capacity of phosphate solubilizing bacteria and fungi on different forms of phosphorus in liquid culture. *J. Sustain. Agric.* **28**: 99–108.

- Ubeda-Tomás, S., Swarup, R., Coates, J., Swarup, K., Laplaze, L., Beemster, G.T.S., Hedden, P., Bhalerao, R., and Bennett, M.J.** (2008). Root growth in *Arabidopsis* requires gibberellin/DELLA signalling in the endodermis. *Nat. Cell Biol.* **10**: 625–628.
- Vahabi, K., Camehl, I., Sherameti, I., and Oelmüller, R.** (2013). Growth of *Arabidopsis* seedlings on high fungal doses of *Piriformospora indica* has little effect on plant performance, stress, and defense gene expression in spite of elevated jasmonic acid and jasmonic acid-isoleucine levels in the roots. *Plant Signal. Behav.* **8**: e26301.
- Van Oosten, M.J., Pepe, O., De Pascale, S., Silletti, S., and Maggio, A.** (2017). The role of biostimulants and bioeffectors as alleviators of abiotic stress in crop plants. *Chem. Biol. Technol. Agric.* **4**: 5.
- Vasseur-Coronado, M., Vlassi, A., Boulois, H.D. du, Schuhmacher, R., Parich, A., Pertot, I., and Puopolo, G.** (2021). Ecological role of volatile organic compounds emitted by *Pantoea agglomerans* as interspecies and interkingdom signals. *Microorganisms* **9**: 1186.
- Veselova, M., Plyuta, V., and Khmel, I.** (2019). Volatile compounds of bacterial origin: Structure, biosynthesis, and biological activity. *Microbiology* **88**: 261–274.
- Vincent, D., Rafiqi, M., and Job, D.** (2020). The multiple facets of plant–fungal interactions revealed through plant and fungal secretomics. *Front. Plant Sci.* **10**: 1626.
- Vlot, A.C., Sales, J.H., Lenk, M., Bauer, K., Brambilla, A., Sommer, A., Chen, Y., Wenig, M., and Nayem, S.** (2021). Systemic propagation of immunity in plants. *New Phytol.* **229**: 1234–1250.
- Waksman, S.A. and Joffe, J.S.** (1922). Microorganisms concerned in the oxidation of sulfur in the soil: II. *Thiobacillus Thiooxidans*, a new sulfur-oxidizing organism isolated from the soil. *J. Bacteriol.* **7**: 239–256.
- Wan, J., Zhang, X.-C., Neece, D., Ramonell, K.M., Clough, S., Kim, S.-Y., Stacey, M.G., and Stacey, G.** (2008). A LysM receptor-like kinase plays a critical role in chitin signaling and fungal resistance in *Arabidopsis*. *Plant Cell* **20**: 471–481.
- Wang, Y., Zhang, W., Liu, W., Ahammed, G.J., Wen, W., Guo, S., Shu, S., and Sun, J.** (2021). Auxin is involved in arbuscular mycorrhizal fungi-promoted tomato growth and NADP-malic enzymes expression in continuous cropping substrates. *BMC Plant Biol.* **21**: 48.
- Wekesa, C.S., Furch, A.C.U., and Oelmüller, R.** (2021). Isolation and characterization of high-efficiency rhizobia from western Kenya nodulating with common bean. *Front. Microbiol.* **12**: 2548.
- van Wersch, S. and Li, X.** (2019). Stronger when together: Clustering of plant NLR disease resistance genes. *Trends Plant Sci.* **24**: 688–699.

- Willmann, R. et al.** (2011). *Arabidopsis* lysin-motif proteins LYM1 LYM3 CERK1 mediate bacterial peptidoglycan sensing and immunity to bacterial infection. *Proc. Natl. Acad. Sci.* **108**: 19824–19829.
- Wittstock, U., Kurzbach, E., Herfurth, A.-M., and Stauber, E.J.** (2016). Chapter Six - Glucosinolate Breakdown. In *Advances in Botanical Research*, S. Kopriva, ed, Glucosinolates. (Academic Press), pp. 125–169.
- Woo, S.L., Ruocco, M., Vinale, F., Nigro, M., Marra, R., Lombardi, N., Pascale, A., Lanzuise, S., Manganiello, G., and Lorito, M.** (2014). *Trichoderma*-based products and their widespread use in agriculture. *Open Mycol. J.* **8**.
- Xian, L., Yu, G., Wei, Y., Rufian, J.S., Li, Y., Zhuang, H., Xue, H., Morcillo, R.J.L., and Macho, A.P.** (2020). A bacterial effector protein hijacks plant metabolism to support pathogen nutrition. *Cell Host Microbe* **28**: 548-557.e7.
- Xu, F. et al.** (2021). Coordination of root auxin with the fungus *Piriformospora indica* and bacterium *Bacillus cereus* enhances rice rhizosphere formation under soil drying. *ISME J.*
- Xu, P., Xu, S.-L., Li, Z.-J., Tang, W., Burlingame, A.L., and Wang, Z.-Y.** (2014). A brassinosteroid-signaling kinase interacts with multiple receptor-like kinases in *Arabidopsis*. *Mol. Plant* **7**: 441–444.
- Xue, H., Lozano-Durán, R., and Macho, A.P.** (2020). Insights into the root invasion by the plant pathogenic bacterium *Ralstonia solanacearum*. *Plants* **9**: 516.
- Yamada, K. et al.** (2016). The *Arabidopsis* CERK1-associated kinase PBL27 connects chitin perception to MAPK activation. *EMBO J.* **35**: 2468–2483.
- Yamada, K., Hara-Nishimura, I., and Nishimura, M.** (2011). Unique defense strategy by the endoplasmic reticulum body in plants. *Plant Cell Physiol.* **52**: 2039–2049.
- Yamada, K., Yamaguchi, K., Yoshimura, S., Terauchi, A., and Kawasaki, T.** (2017). Conservation of chitin-induced MAPK signaling pathways in rice and *Arabidopsis*. *Plant Cell Physiol.* **58**: 993–1002.
- Yamamoto, Y., Negi, J., Wang, C., Isogai, Y., Schroeder, J.I., and Iba, K.** (2016). The transmembrane region of guard cell SLAC1 channels perceives CO₂ signals via an ABA-independent pathway in *Arabidopsis*. *Plant Cell* **28**: 557–567.
- Yang, C., Liu, R., Pang, J., Ren, B., Zhou, H., Wang, G., Wang, E., and Liu, J.** (2021a). Poaceae-specific cell wall-derived oligosaccharides activate plant immunity via OsCERK1 during *Magnaporthe oryzae* infection in rice. *Nat. Commun.* **12**: 2178.
- Yang, F., Liu, X., Wang, H., Deng, R., Yu, H., and Cheng, Z.** (2019). Identification and allelopathy of green garlic (*Allium sativum* L.) volatiles on scavenging of cucumber (*Cucumis sativus* L.) reactive oxygen species. *Mol. Basel Switz.* **24**.

- Yang, H., Wang, D., Guo, L., Pan, H., Yvon, R., Garman, S., Wu, H.-M., and Cheung, A.Y.** (2021b). Malectin/malectin-like domain-containing proteins: A repertoire of cell surface molecules with broad functional potential. *Cell Surf. Amst. Neth.* **7**: 100056.
- Yanni, Y.G. et al.** (2001). The beneficial plant growth-promoting association of *Rhizobium leguminosarum* bv. trifolii with rice roots. *Funct. Plant Biol.* **28**: 845–870.
- Yeh, Y.-H., Panzeri, D., Kadota, Y., Huang, Y.-C., Huang, P.-Y., Tao, C.-N., Roux, M., Chien, H.-C., Chin, T.-C., Chu, P.-W., Zipfel, C., and Zimmerli, L.** (2016). The *Arabidopsis* malectin-like/LRR-RLK IOS1 is critical for BAK1-dependent and BAK1-independent pattern-triggered immunity. *Plant Cell* **28**: 1701–1721.
- Yu, N. et al.** (2014). A DELLA protein complex controls the arbuscular mycorrhizal symbiosis in plants. *Cell Res.* **24**: 130–133.
- Yu, X., Feng, B., He, P., and Shan, L.** (2017). From chaos to harmony: Responses and signaling upon microbial pattern recognition. *Annu. Rev. Phytopathol.* **55**: 109–137.
- Yuan, M., Jiang, Z., Bi, G., Nomura, K., Liu, M., Wang, Y., Cai, B., Zhou, J.-M., He, S.Y., and Xin, X.-F.** (2021). Pattern-recognition receptors are required for NLR-mediated plant immunity. *Nature* **592**: 105–109.
- Zaidi, A., Ahemad, M., Oves, M., Ahmad, E., and Khan, M.S.** (2010). Role of Phosphate-Solubilizing Bacteria in Legume Improvement. In *Microbes for Legume Improvement*, M.S. Khan, J. Musarrat, and A. Zaidi, eds (Springer: Vienna), pp. 273–292.
- Zavaliev, R., Mohan, R., Chen, T., and Dong, X.** (2020). Formation of NPR1 condensates promotes cell survival during the plant immune response. *Cell* **182**: 1093-1108.e18.
- Zelensky, A.N. and Gready, J.E.** (2005). The C-type lectin-like domain superfamily. *FEBS J.* **272**: 6179–6217.
- Zhang, H., Kim, M.-S., Krishnamachari, V., Payton, P., Sun, Y., Grimson, M., Farag, M.A., Ryu, C.-M., Allen, R., Melo, I.S., and Paré, P.W.** (2007). Rhizobacterial volatile emissions regulate auxin homeostasis and cell expansion in *Arabidopsis*. *Planta* **226**: 839–851.
- Zhang, H., Sun, Y., Xie, X., Kim, M.-S., Dowd, S.E., and Paré, P.W.** (2009). A soil bacterium regulates plant acquisition of iron via deficiency-inducible mechanisms. *Plant J. Cell Mol. Biol.* **58**: 568–577.
- Zhang, H., Xie, X., Kim, M.-S., Korniyev, D.A., Holaday, S., and Paré, P.W.** (2008). Soil bacteria augment *Arabidopsis* photosynthesis by decreasing glucose sensing and abscisic acid levels in planta. *Plant J. Cell Mol. Biol.* **56**: 264–273.
- Zhang, J., Wang, N., Miao, Y., Hauser, F., McCammon, J.A., Rappel, W.-J., and Schroeder, J.I.** (2018a). Identification of SLAC1 anion channel residues required for CO₂/bicarbonate

sensing and regulation of stomatal movements. *Proc. Natl. Acad. Sci. U. S. A.* **115**: 11129–11137.

- Zhang, L., Shi, N., Fan, J., Wang, F., George, T.S., and Feng, G.** (2018b). Arbuscular mycorrhizal fungi stimulate organic phosphate mobilization associated with changing bacterial community structure under field conditions. *Environ. Microbiol.* **20**: 2639–2651.
- Zhang, S., Gan, Y., and Xu, B.** (2019). Mechanisms of the IAA and ACC-deaminase producing strain of *Trichoderma longibrachiatum* T6 in enhancing wheat seedling tolerance to NaCl stress. *BMC Plant Biol.* **19**: 22.
- Zhang, X., Yang, Z., Wu, D., and Yu, F.** (2020). RALF-FERONIA signaling: Linking plant immune response with cell growth. *Plant Commun.* **1**: 100084.
- Zhao, K. et al.** (2019). TesG is a type I secretion effector of *Pseudomonas aeruginosa* that suppresses the host immune response during chronic infection. *Nat. Microbiol.* **4**: 459–469.
- Zhao, K., Penttinen, P., Zhang, X., Ao, X., Liu, M., Yu, X., and Chen, Q.** (2014). Maize rhizosphere in Sichuan, China, hosts plant growth promoting *Burkholderia cepacia* with phosphate solubilizing and antifungal abilities. *Microbiol. Res.* **169**: 76–82.
- Zhou, J.-M. and Chai, J.** (2008). Plant pathogenic bacterial type III effectors subdue host responses. *Curr. Opin. Microbiol.* **11**: 179–185.
- Zipfel, C. and Rathjen, J.P.** (2008). Plant immunity: AvrPto targets the frontline. *Curr. Biol.* **18**: R218-220.: R218-220.

8. Curriculum Vitae

Personal information

Name: Yu-Heng Tseng

Date of birth: 15.10.1991

Place of birth: Kaohsiung, Taiwan

Address: Dornburger Straße 159, 07743 Jena

E-mail: yu.tseng@uni-jena.de

Phone: +49 176 2878 0272

Education professional experiences

June 2018 – present

Ph. D student

Department of Plant Physiology, Matthias Schleiden Institute of Genetics, Bioinformatics and Molecular Botany, Friedrich-Schiller-University Jena, Jena, Germany

International Max Planck Research School (IMPRS)
"Chemical Communication in Ecological Systems"

Topic: Characterization of mutualistic plant-fungus interactions and the participating fungal chemical mediators

Supervisors: Prof. Dr. R. Oelmüller, PD Dr. Axel Mithöfer

December 2017 – May 2018

Assistant Scientist

Asclepiumm Taiwan Co., Ltd., Taipei, Taiwan

Topic: Development of a new peptide drug targeting wet macular degeneration

June 2014 – September 2016

MSc, in Genome and Systems Biology

Institute of Molecular Biology, Academia Sinica, Taipei, Taiwan

National Taiwan University, Taipei, Taiwan

Topic: Characterization of auxin influx carriers in rice
(*Oryza sativa* L.)

Supervisors: Dr. Su-May Yu

September 2011 – June 2014

BSc. in Life Sciences

National Tsing Hua University, Hsinchu, Taiwan

Topic: Identification of HSP27 interacting proteins for
longevity and starvation resistance in *Drosophila*

Supervisors: Prof. Dr. Horng-Dar Wang

Publications

Rouina, H., **Tseng, Y. H.**, Nataraja, K. N., Uma Shaanker, R., Krüger, R., Kniemeyer, O., Brakhage, A. Oelmüller, R. (2021). Comparative secretome analyses of *Trichoderma/Arabidopsis* co-cultures identify proteins for salt stress, plant growth promotion, and root colonization. *Frontiers in Ecology and Evolution*, 9:808430. Doi: 10.3389/fevo.2021.808430

Rouina, H., **Tseng, Y. H.**, Nataraja, K. N., Uma Shaanker, R., Oelmüller, R. (2021). *Arabidopsis* restricts sugar loss to a colonizing *Trichoderma harzianum* train by downregulating SWEET11 and -12 and upregulation of SUC1 and SWEET2 in the roots. *Microorganisms*, 9, 1246. Doi: 10.3390/microorganisms9061246

Tseng, Y. H., Rouina, H., Groten, K., Rajani, P., Furch, A., Reichelt, M., Baldwin, I. T., Nataraja, K. N., Uma Shaanker, R., Oelmüller, R. (2020). An endophytic *Trichoderma* strain promotes growth of its hosts and defends against pathogen attack. *Frontiers in Plant Science*, 11, 573670. Doi: 10.3389/fpls.2020.573670

Kang, M. L., Chen, Y. C., Chen, S. F., Lin, H. C., **Tseng, Y. H.**, Wang, H. D. (2014). The prerequisite of nuclear localization for heat shock protein 27 in modulation of starvation adaptation and longevity in *Drosophila*. *Adaptive Medicine*, 6(3):118-123. Doi: 10.4247/AM.2014.ABE083

Oral Presentations

Tseng, Y. H., Scholz, S., Fliegmann, J., Oelmüller, R. (2021). CORK1, a LRR receptor kinase for celooligomer perception in *Arabidopsis*. *Talk presented at 20th IMPRS Symposium, MPI for Chemical Ecology, Online, Germany*

Tseng, Y. H. (2021). Life sciences-life or science? My experiences as a researcher. *Guest speaker for career planning talk series, National Chaochou Senior High School, Taiwan*

Tseng, Y. H., and Oelmüller, R. (2020). *Arabidopsis* response to a S-containing fungal volatile from *M. hyalina* under sulfur deficiency. *Talk presented at 19th IMPRS Symposium, MPI for Chemical Ecology, Online, Germany*

Tseng, Y. H., Mithöfer, A., Oelmüller, R. (2020). *Arabidopsis thaliana* Respond to A Sulfur-Containing Volatile Produced by *Mortierella hyalina* under Sulfur-Deficient Condition. *Talk presented at Mitteldeutsche Pflanzenphysiologie-Tagung 2020, Jena, Germany*

Tseng, Y. H., Mithöfer, A., Oelmüller, R. (2019). Characterization of new plant interacting fungi growing with *Arabidopsis* roots. *Talk presented at Mitteldeutsche Pflanzenphysiologie-Tagung 2019, Leipzig, Germany*

Tseng, Y. H., and Oelmüller, R. (2019). Characterization of the symbiotic interaction of unusual root-colonizing fungal isolates conferring salt- and heat-stress tolerance to plants including *Arabidopsis thaliana*. *Talk presented at 3rd International Conference “Challenges in Biotechnological and Environmental Approaches”, Tirana, Albania*

Poster Presentations

Tseng, Y. H., Scholz, S., Mithöfer, A., Oelmüller, R. (2019). Who's there? Chemical perception of microbes by the *Arabidopsis* root. *Poster presented at ChemBioSys Retreat 2019, Masserberg, Germany*

Tseng, Y. H., Scholz, S., Mithöfer, A., Oelmüller, R. (2019). Who's there? Chemical perception of microbes by the *Arabidopsis* root. *Poster presented at 18th IMPRS Symposium, MPI for Chemical Ecology, Dornburg, Germany*

9. Acknowledgenemt

Doing PhD is a long process, but close to the end, it seems like I just started it yesterday. I still remember it was a chilly December night in Taipei when I first met my supervisor Professor Dr. Ralf Oelmüller. I am very grateful that he was willing to recruit me to his lab and providing me this wonderful chance to do my PhD research here in Jena. Thanks for his immense support and help not only for my study, but also for my daily life in Germany.

Thanks to my second supervisor PD Dr. Axel Mithöfer. Your advice inspired me a lot for all my projects. It is always wonderful to talk to you to get updated with the things going on at the MPI-CE. Thanks also for your patience too, for the volatile project was sometimes difficult to carry out.

Thanks to Dr. Irena Sherameti, who helped me deal with all the German bureaucracy every student need to go through. Without you, I might never be solve all the difficulties to stay in Germany. I am also appreciated to be invited to your country, not just to share science to your people but also explore the wonderful country.

Thanks to Dr. Sandra Scholz for your (almost daily) help on everything. You are always there for me when I need help with my experiments or with the university. Without you, my research might not go as smooth as it was.

Thanks to Dr. Michael Reichelt and Dr. Stefan Bartram from MPI-CE. You are always efficient and helpful for all my samples. Thanks to Dr. Karin Groten for helping me out with your tobacco plants. Your ideas are invaluable. Thanks to Dr. Judith Fliegmann, Dr. Thomas Krüger, Dr. Olaf Kniemeyer and Prof. Dr. Axel Brakhage for your great effort on the last manuscript. Special thanks to Andreas Weber and the green house team at the MPI-CE. It would not be possible for me to finish the plant transformation without your good care of my plants.

Thanks to Dr. Claudia Voelckel for your support on all my IMPRS activities.

Thanks to our secretories, Carmen Galambos, Steffen Langbein an Akina Türk. It is always interesting to practice my German with all of you, and thanks for your assistance with my contract.

Thanks to Claudia Röppischer, Sarah Mußbach, Christin Weilandt and Sacha Janster for excellent technical assistance. Special thanks to Sacha who also improved my driving skills.

Thanks to all my lab members and friends Dr. Alexandra Furch, Dr. Matthias Zimmermann, Anja Meents, Dr. Vincensius Oetama, Sedef Özyürek, Parijat Barman, Hamid Rouina, Clabe Wekesa and your family, Keziah Omenge, and our recent new members Akanksha Gandhi, Liza Zhyr and Priya Reddy. Thanks for all your daily support and the broad topics we chatted about. I will miss the BBQ party, the board game nights and all the things we did together.

Lastly, I would like to thank my family. 感謝爸媽多年來的栽培與支持，讓我能夠接受這個機會來德國做研究。感謝哥哥，在許多週末陪我聊天，以及邀請我去高中分享科學，讓我學習了不少。感謝珮蓉，謝謝妳這多年來耐心的陪伴與支持，還有跟我一起在歐洲各地探險。

10. Eigenständigkeitserklärung

Hiermit erkläre ich, dass mir die geltende Promotionsordnung der Fakultät für Biowissenschaften der Friedrich-Schiller-Universität Jena vom 23.09.2019 bekannt ist. Ich habe die vorliegende Dissertation mit dem Titel „Characterization of mutualistic plant-fungus interactions and the participating fungal chemical mediators“ selbstständig und ohne unerlaubte Hilfe (gemäß § 5 Abschnitt 4 der oben genannten Promotionsordnung) angefertigt und keine Textabschnitte eines Dritten oder eigener Prüfungsarbeiten ohne Kennzeichnung übernommen. Alle verwendeten Hilfsmittel und Quellen sind in der Dissertation bzw. in den entsprechenden Manuskripten eindeutig aufgeführt und wörtlich oder inhaltlich entnommene Stellen angegeben. Alle Beiträge von Personen, die durch Experimente, Auswertung und Erstellung der Manuskripte mitgewirkt haben, sind an den entsprechenden Stellen deutlich und umfänglich benannt. Des Weiteren versichere ich, dass ich weder die Hilfe eines Promotionsberaters oder einer kommerziellen Promotionsvermittlung in Anspruch genommen habe und dass Dritte weder unmittelbar noch mittelbar geldwerte Leistungen von mir im Zusammenhang mit Inhalten dieser Dissertation erhalten haben. Die vorliegende Dissertation oder eine in wesentlichen Teilen ähnliche Abhandlung wurde zu keinem früheren Zeitpunkt an einer anderen Hochschule oder Fakultät als Dissertation eingereicht.

Ort, Datum

Unterschrift